

1-1-2013

Minimization of Noise and Vibration Related to Driveline Imbalance using Robust Design Processes

Omar Alhubailat

Follow this and additional works at: <https://scholarsjunction.msstate.edu/td>

Recommended Citation

Alhubailat, Omar, "Minimization of Noise and Vibration Related to Driveline Imbalance using Robust Design Processes" (2013). *Theses and Dissertations*. 3110.
<https://scholarsjunction.msstate.edu/td/3110>

This Dissertation - Open Access is brought to you for free and open access by the Theses and Dissertations at Scholars Junction. It has been accepted for inclusion in Theses and Dissertations by an authorized administrator of Scholars Junction. For more information, please contact scholcomm@msstate.libanswers.com.

Minimization of noise and vibration related to driveline imbalance using robust
design processes

By

Omar Al-Shubailat

A Dissertation
Submitted to the Faculty of
Mississippi State University
in Partial Fulfillment of the Requirements
for the Degree of Doctor of Philosophy
in Computational Engineering
in the Department of Computational Engineering

Mississippi State, Mississippi

August 2013

Copyright by
Omar Al-Shubailat
2013

Minimization of noise and vibration related to driveline imbalance using robust design
processes

By

Omar Al-Shubailat

Approved:

Roger L. King,
Professor and Graduate Coordinator
Computational Engineering
(Major Professor)

Mohamad Qatu,
Professor
Central Michigan University
(Director of Dissertation)

Clayton T. Walden,
Research Professor
Industrial and Systems Engineering
(Minor Professor)

Ioana Banicescu,
Professor
Computer Science and Engineering
(Committee Member)

Youssef Hammi,
Assistant Research Professor
Mechanical Engineering
(Committee Member)

Jerome A. Gilbert,
Interim Dean of the Bagley College of
Engineering

Name: Omar Al-Shubailat

Date of Degree: August 17, 2013

Institution: Mississippi State University

Major Field: Computational Engineering

Major Professor: Roger L. King

Director of Dissertation: Mohammad Qatu

Title of Study: Minimization of noise and vibration related to driveline imbalance using robust design processes

Pages in Study: 164

Candidate for Degree of Doctor of Philosophy

Variation in vehicle noise, vibration and harshness (NVH) response can be caused by variability in design (e.g. tolerance), material, manufacturing, or other sources of variation. Such variation in the vehicle response causes a higher percentage of produced vehicles to have higher levels (out of specifications) of NVH leading to higher number of warranty claims and loss of customer satisfaction, which are proven costly. Measures must be taken to ensure less warranty claims and higher levels of customer satisfactions. As a result, original equipment manufacturers (OEMs) have implemented design for variation in the design process to secure an acceptable (or within specification) response. The focus here will be on aspects of design variations that should be considered in the design process of drivelines. Variations due to imbalance in rotating components can be unavoidable or costly to control. Some of the major components in the vehicle that are known to have imbalance and traditionally cause NVH issues and concerns include the crankshaft, the drivetrain components (transmission, driveline, half shafts, etc.), and

wheels. The purpose is to assess NVH as a result of driveline imbalance variations and develop a tool to help design a more robust system to such variations.

DEDICATION

To my beloved parents: my late father and my mother- I am because of you.

To my beloved wife who suffered a lot with me: Zubaida.

To my daughters: Jena and Haya. Also the new comer: Abdullah.

To my siblings: Rawda, Taghreed, Khoulood, Ala' and Ammar.

To Zubaida's family: especially my father and mother in law.

To my friends everywhere who help and support me always.

To my extended family in Jordan and United States.

To all my mentors and colleagues everywhere.

To my beloved country, Jordan, who has all the beautiful people who helped carving me to what I am today.

ACKNOWLEDGEMENTS

I thank first and last our Lord, almighty God. He placed in my heart the patience and perseverance to stay my course and finish my work. I ask Him to help me improve myself and pay back my debts to all those whom He placed in my path to help and support me.

I have so many people to thank; many beautiful souls whom I'm indebted for until I die. I'd like to start by mentioning all my mentors throughout my life, starting with my late father and my beloved mother, may God bless them both.

I was blessed to have wise and patient mentors throughout my life; while I was in Jordan early on in my life and in United States when I moved in 2000.

Dr. Mohamad Qatu has been my mentor since 2009 when I started working under him on NVH in automotive industry. Dr. Roger L. King, who has been my principal mentor and facilitator for couple of years; especially after Dr. Qatu moved in mid 2011 up to Central Michigan University. Dr. King has been generous to share with me his insights while supporting my decisions.

I'd like to thank other committee members for their help and support.

The Center for Advanced Vehicular Systems (CAVS) has been my second home for the past 3 years. I spent in it many hours daily and conducted all my research there. I'd like to thank the Dr. Roger King again in his capacity as director of CAVS, my fellow researchers, staff and employees for their kind support.

Nissan North America Incorporation and its management and staff have helped and supported me throughout my research, as they supplied me with the needed information, vehicles and expertise.

All thanks to my colleagues everywhere who supported my work and helped when I asked them to help.

I'd like also to thank all the great minds throughout the history and until today for their hard and ingenious work, through it I managed to learn and improve myself.

I'd like to cite the great mind Nikola Tesla on frequency and vibration: "If you want to find the secrets of the universe, think in terms of energy, frequency and vibration."

Omar Shubailat

Starkville-Mississippi

June 2013

TABLE OF CONTENTS

DEDICATION	ii
ACKNOWLEDGEMENTS	iii
LIST OF TABLES	viii
LIST OF FIGURES	ix
CHAPTER	
I. INTRODUCTION	1
The Technical Approach.....	3
System Variations	8
Scope	13
Assumptions.....	14
Contributions.....	15
II. LITERATURE REVIEW	17
Driveline NVH: Investigation and Studies	17
Six Sigma Utilized in NVH Challenges.....	19
III. EXPERIMENTAL SET UP.....	21
Technical approach.....	21
Channels and sensors	27
Apparatus and Testing Equipment.....	28
Testing Procedures.....	30
IV. EXPERIMENTAL SENSITIVITY FUNCTIONS.....	41
Sensitivity Curves	52
Rear Driveshaft and Rear Axle Plane	53
Two Wheel Drive (2WD)-Run up (RU) Sensitivity Calculations:.....	54
Two Wheel Drive (2WD)-Run down (RD) Sensitivity Calculations:	58
Four Wheel Drive (4WD)-Run up (RU) Sensitivity Calculations:.....	62

	Four Wheel Drive (4WD)-Run down (RD) Sensitivity Calculations:	66
V.	SIMULATING NVH VARIATION	70
	Generating Imbalance Probability Distributions	71
	Simulating NVH Due to Imbalance through a Developed Tool.....	77
VI.	CONCLUSIONS.....	84
	Contributions.....	86
	Future Work	86
	REFERENCES	89
APPENDIX		
A.	SENSITIVITY CURVES FOR PLANES: A, B AND C	92
	Plane A sensitivity curves.....	93
	Two Wheel Drive (2WD)-Run up (RU) Sensitivity Calculations:	93
	Two Wheel Drive (2WD)-Run down (RD) Sensitivity Calculations:	97
	Four Wheel Drive (4WD)-Run up (RU) Sensitivity Calculations:.....	101
	Four Wheel Drive (4WD)-Run down (RD) Sensitivity Calculations:	105
	Plane B sensitivity curves	109
	Two Wheel Drive (2WD)-Run up (RU) Sensitivity Calculations:	109
	Two Wheel Drive (2WD)-Run down (RD) Sensitivity Calculations:	113
	Four Wheel Drive (4WD)-Run up (RU) Sensitivity Calculations:.....	117
	Four Wheel Drive (4WD)-Run down (RD) Sensitivity Calculations:	121
	Plane C sensitivity curves	125
	Two Wheel Drive (2WD)-Run up (RU) Sensitivity Calculations:	125
	Two Wheel Drive (2WD)-Run down (RD) Sensitivity Calculations:	129
	Four Wheel Drive (4WD)-Run up (RU) Sensitivity Calculations:.....	133
	Four Wheel Drive (4WD)-Run down (RD) Sensitivity Calculations:	137
B.	SIMULATION RUN OUTPUT CASES	141
	Simulation run output curves for 2WD-RU.....	142
	Simulation run output curves for 2WD-RD.....	145
	Simulation run output curves for 4WD-RU.....	148
	Simulation run output curves for 4WD-RD.....	151

C.	MANUAL FOR THE DEVELOPED SIMULATION PROGRAM	154
	Using the developed simulation Java program	155

LIST OF TABLES

3.1	Plane name and location.....	24
3.2	Shaft information (approx.).....	25
3.3	Imbalance introduced for each plan	27
5.1	Front driveshaft statistical parameters for collected measurements.....	73
5.2	Rear driveshaft statistical parameters for collected measurements.....	74
5.3	Parameters of the fitted probability distributions from empirical data points	77

LIST OF FIGURES

1.1	The Possible Root Causes of driveline NVH	6
1.2	Left: AWD configuration for an East-West engine. Right: RWD configuration for a North-South engine	9
1.3	Typical statistical imbalances for an interface plane.....	10
1.4	Typical Sensitivity Function to Driveline Imbalance at a Certain Plane	12
3.1	Optimizing Vehicle NVH Characteristics for Driveline Integration [15]	22
3.2	truck with two drive shafts [23].	23
3.3	A typical light-duty four-wheel-drive pick-up truck driveline and the corresponding planes of imbalance[17]	24
3.4	Plane A with a tachometer and reflecting strip is set as 0° angle.....	26
3.5	Channels ID, type and direction (if applicable)	31
3.6	Testing plan and data acquisition	32
3.7	Front and rear drivelines, from underneath the truck.....	33
3.8	Front driveline axle plane with tachometer and reflective tape	34
3.9	Front driveline axle plane with a tri-axial accelerometer.....	35
3.10	Seat track tri-axial accelerometer	36
3.11	Front-end data acquisition hardware	36
3.12	Truck tested on dynamometer	37
3.13	Monitoring data collection live	37
3.14	In-board and Outboard microphones- front view.....	38
3.15	microphones- back view.....	38

3.16	Tachometers hardware and frontend	39
3.17	Tri-axial accelerometer attached to steering wheel	39
3.18	Tachometer and imbalance mass attached at the front driveshaft	40
3.19	Front-axle plane and the tri-axial accelerometer position is pointed out	40
4.1	The commercial software Test.Lab's signature testing	43
4.2	Selecting runs to be averaged	44
4.3	Calculating average for each run and part of a run (i.e., RU or RD)	44
4.4	X-axis alignment by arranging equidistance points	45
4.5	Microsoft Excel 2010 used for further sensitivity calculations	45
4.6	Copied data into the spreadsheet	46
4.7	Amplitude and phase curves of the collected data	47
4.8	Data points rearranged	48
4.9	Phasors represented in real and imaginary format	49
4.10	Phasors averaged in real and imaginary format.	50
4.11	Sensitivity represented in complex numbers' format	51
4.12	Sensitivity in magnitude and modulus.	51
4.13	LTI system representations in time and frequency domains[29]	53
4.14	Sensitivity and phase Seat-Track-Z-Axis Rear-Axle 2WD RU	54
4.15	Sensitivity and phase Seat-Track-X-Axis Rear-Axle 2WD RU	54
4.16	Sensitivity and phase Seat-Track-Y-Axis Rear-Axle 2WD RU	55
4.17	Sensitivity and phase Steering Wheel-Z-Axis Rear-Axle 2WD RU	55
4.18	Sensitivity and phase Steering Wheel-X-Axis Rear-Axle 2WD RU	56
4.19	Sensitivity and phase Steering Wheel-Y-Axis Rear-Axle 2WD RU	56
4.20	Sensitivity and phase F_{sOe} Rear-Axle 2WD RU	57
4.21	Sensitivity and phase F_{sie} Rear-Axle 2WD RU	57

4.22	Sensitivity and phase Seat Track -Z-Axis Rear-Axle 2WD RD	58
4.23	Sensitivity and phase Seat Track -X-Axis Rear-Axle 2WD RD	58
4.24	Sensitivity and phase Seat Track -Y-Axis Rear-Axle 2WD RD	59
4.25	Sensitivity and phase Steering Wheel-Z-Axis Rear-Axle 2WD RD	59
4.26	Sensitivity and phase Steering Wheel-X-Axis Rear-Axle 2WD RD	60
4.27	Sensitivity and phase Steering Wheel-Y-Axis Rear-Axle 2WD RD	60
4.28	Sensitivity and phase FsOe Rear-Axle 2WD RD	61
4.29	Sensitivity and phase Fsie Rear-Axle 2WD RD	61
4.30	Sensitivity and phase Seat-Track-Z-Axis Rear-Axle 4WD RU	62
4.31	Sensitivity and phase Seat-Track-X-Axis Rear-Axle 4WD RU	62
4.32	Sensitivity and phase Seat-Track-Y-Axis Rear-Axle 4WD RU	63
4.33	Sensitivity and phase Steering Wheel-Z-Axis Rear-Axle 4WD RU	63
4.34	Sensitivity and phase Steering Wheel-X-Axis Rear-Axle 4WD RU	64
4.35	Sensitivity and phase Steering Wheel-Y-Axis Rear-Axle 4WD RU	64
4.36	Sensitivity and phase FsOe Rear-Axle 4WD RU	65
4.37	Sensitivity and phase Fsie Rear-Axle 4WD RU	65
4.38	Sensitivity and phase Seat Track -Z-Axis Rear-Axle 4WD RD	66
4.39	Sensitivity and phase Seat Track -X-Axis Rear-Axle 4WD RD	66
4.40	Sensitivity and phase Seat Track -Y-Axis Rear-Axle 4WD RD	67
4.41	Sensitivity and phase Steering Wheel-Z-Axis Rear-Axle 4WD RD	67
4.42	Sensitivity and phase Steering Wheel-X-Axis Rear-Axle 4WD RD	68
4.43	Sensitivity and phase Steering Wheel-Y-Axis Rear-Axle 4WD RD	68
4.44	Sensitivity and phase FsOe Rear-Axle 4WD RD	69
4.45	Sensitivity and phase Fsie Rear-Axle 4WD RD	69
5.1	Front driveshaft	73

5.2	Rear driveshaft	74
5.3	Typical statistical imbalance for an interface plane	75
5.4	Distribution fitting steps.....	76
5.5	Preparing sensitivity curves	78
5.6	Produced sensitivity curves per plane	79
5.7	Simulation run per plane	80
5.8	Calculated vibration with data point from final balancing empirical data	81
5.9	Calculated vibration with data point from initial balancing empirical data	82
5.10	Simulation run output (mean and 6σ) for Seat Track z-axis 2WD-RU.....	83
A.1	Sensitivity and phase Seat-Track-Z-Axis Front-Axle 2WD RU	93
A.2	Sensitivity and phase Seat-Track-X-Axis Front-Axle 2WD RU	93
A.3	Sensitivity and phase Seat-Track-Y-Axis Front-Axle 2WD RU	94
A.4	Sensitivity and phase Steering Wheel-Z-Axis Front-Axle 2WD RU	94
A.5	Sensitivity and phase Steering Wheel-X-Axis Front-Axle 2WD RU.....	95
A.6	Sensitivity and phase Steering Wheel-Y-Axis Front-Axle 2WD RU.....	95
A.7	Sensitivity and phase F_{sOe} Front-Axle 2WD RU	96
A.8	Sensitivity and phase F_{sie} Front-Axle 2WD RU.....	96
A.9	Sensitivity and phase Seat Track -Z-Axis Front-Axle 2WD RD.....	97
A.10	Sensitivity and phase Seat Track -X-Axis Front-Axle 2WD RD	97
A.11	Sensitivity and phase Seat Track -Y-Axis Front-Axle 2WD RD	98
A.12	Sensitivity and phase Steering Wheel-Z-Axis Front-Axle 2WD RD	98
A.13	Sensitivity and phase Steering Wheel-X-Axis Front-Axle 2WD RD.....	99
A.14	Sensitivity and phase Steering Wheel-Y-Axis Front-Axle 2WD RD.....	99
A.15	Sensitivity and phase F_{sOe} Front-Axle 2WD RD.....	100

A.16	Sensitivity and phase F_{sie} Front-Axle 2WD RD.....	100
A.17	Sensitivity and phase Seat-Track-Z-Axis Front-Axle 4WD RU	101
A.18	Sensitivity and phase Seat-Track-X-Axis Front-Axle 4WD RU	101
A.19	Sensitivity and phase Seat-Track-Y-Axis Front-Axle 4WD RU.....	102
A.20	Sensitivity and phase Steering Wheel-Z-Axis Front-Axle 4WD RU	102
A.21	Sensitivity and phase Steering Wheel-X-Axis Front-Axle 4WD RU.....	103
A.22	Sensitivity and phase Steering Wheel-Y-Axis Front-Axle 4WD RU.....	103
A.23	Sensitivity and phase F_{sOe} Front-Axle 4WD RU	104
A.24	Sensitivity and phase F_{sie} Front-Axle 4WD RU	104
A.25	Sensitivity and phase Seat Track -Z-Axis Front-Axle 4WD RD.....	105
A.26	Sensitivity and phase Seat Track -X-Axis Front-Axle 4WD RD	105
A.27	Sensitivity and phase Seat Track -Y-Axis Front-Axle 4WD RD	106
A.28	Sensitivity and phase Steering Wheel-Z-Axis Front-Axle 4WD RD	106
A.29	Sensitivity and phase Steering Wheel-X-Axis Front-Axle 4WD RD.....	107
A.30	Sensitivity and phase Steering Wheel-Y-Axis Front-Axle 4WD RD.....	107
A.31	Sensitivity and phase F_{sOe} Front-Axle 4WD RD	108
A.32	Sensitivity and phase F_{sie} Front-Axle 4WD RD.....	108
A.33	Sensitivity and phase Seat-Track-Z-Axis Front-TC 2WD RU	109
A.34	Sensitivity and phase Seat-Track-X-Axis Front-TC 2WD RU.....	109
A.35	Sensitivity and phase Seat-Track-Y-Axis Front-TC 2WD RU.....	110
A.36	Sensitivity and phase Steering Wheel-Z-Axis Front-TC 2WD RU.....	110
A.37	Sensitivity and phase Steering Wheel-X-Axis Front-TC 2WD RU	111
A.38	Sensitivity and phase Steering Wheel-Y-Axis Front-TC 2WD RU	111
A.39	Sensitivity and phase F_{sOe} Front-TC 2WD RU.....	112
A.40	Sensitivity and phase F_{sie} Front-TC 2WD RU.....	112

A.41	Sensitivity and phase Seat Track -Z-Axis Front-TC 2WD RD	113
A.42	Sensitivity and phase Seat Track -X-Axis Front-TC 2WD RD	113
A.43	Sensitivity and phase Seat Track -Y-Axis Front-TC 2WD RD	114
A.44	Sensitivity and phase Steering Wheel-Z-Axis Front-TC 2WD RD.....	114
A.45	Sensitivity and phase Steering Wheel-X-Axis Front-TC 2WD RD	115
A.46	Sensitivity and phase Steering Wheel-Y-Axis Front-TC 2WD RD	115
A.47	Sensitivity and phase FsOe Front-TC 2WD RD.....	116
A.48	Sensitivity and phase Fsie Front-TC 2WD RD.....	116
A.49	Sensitivity and phase Seat-Track-Z-Axis Front-TC 4WD RU	117
A.50	Sensitivity and phase Seat-Track-X-Axis Front-TC 4WD RU.....	117
A.51	Sensitivity and phase Seat-Track-Y-Axis Front-TC 4WD RU.....	118
A.52	Sensitivity and phase Steering Wheel-Z-Axis Front-TC 4WD RU.....	118
A.53	Sensitivity and phase Steering Wheel-X-Axis Front-TC 4WD RU	119
A.54	Sensitivity and phase Steering Wheel-Y-Axis Front-TC 4WD RU	119
A.55	Sensitivity and phase FsOe Front-TC 4WD RU.....	120
A.56	Sensitivity and phase Fsie Front-TC 4WD RU.....	120
A.57	Sensitivity and phase Seat Track -Z-Axis Front-TC 4WD RD	121
A.58	Sensitivity and phase Seat Track -X-Axis Front-TC 4WD RD.....	121
A.59	Sensitivity and phase Seat Track -Y-Axis Front-TC 4WD RD.....	122
A.60	Sensitivity and phase Steering Wheel-Z-Axis Front-TC 4WD RD.....	122
A.61	Sensitivity and phase Steering Wheel-X-Axis Front-TC 4WD RD	123
A.62	Sensitivity and phase Steering Wheel-Y-Axis Front-TC 4WD RD	123
A.63	Sensitivity and phase FsOe Front-TC 4WD RD.....	124
A.64	Sensitivity and phase Fsie Front-TC 4WD RD.....	124
A.65	Sensitivity and phase Seat-Track-Z-Axis Rear-TC 2WD RU	125

A.66	Sensitivity and phase Seat-Track-X-Axis Rear-TC 2WD RU.....	125
A.67	Sensitivity and phase Seat-Track-Y-Axis Rear-TC 2WD RU.....	126
A.68	Sensitivity and phase Steering Wheel-Z-Axis Rear-TC 2WD RU.....	126
A.69	Sensitivity and phase Steering Wheel-X-Axis Rear-TC 2WD RU.....	127
A.70	Sensitivity and phase Steering Wheel-Y-Axis Rear-TC 2WD RU.....	127
A.71	Sensitivity and phase FsOe Rear-TC 2WD RU.....	128
A.72	Sensitivity and phase Fsie Rear-TC 2WD RU.....	128
A.73	Sensitivity and phase Seat Track -Z-Axis Rear-TC 2WD RD.....	129
A.74	Sensitivity and phase Seat Track -X-Axis Rear-TC 2WD RD.....	129
A.75	Sensitivity and phase Seat Track -Y-Axis Rear-TC 2WD RD.....	130
A.76	Sensitivity and phase Steering Wheel-Z-Axis Rear-TC 2WD RD.....	130
A.77	Sensitivity and phase Steering Wheel-X-Axis Rear-TC 2WD RD.....	131
A.78	Sensitivity and phase Steering Wheel-Y-Axis Rear-TC 2WD RD.....	131
A.79	Sensitivity and phase FsOe Rear-TC 2WD RD.....	132
A.80	Sensitivity and phase Fsie Rear-TC 2WD RD.....	132
A.81	Sensitivity and phase Seat-Track-Z-Axis Rear-TC 4WD RU.....	133
A.82	Sensitivity and phvase Seat-Track-X-Axis Rear-TC 4WD RU.....	133
A.83	Sensitivity and phase Seat-Track-Y-Axis Rear-TC 4WD RU.....	134
A.84	Sensitivity and phase Steering Wheel-Z-Axis Rear-TC 4WD RU.....	134
A.85	Sensitivity and phase Steering Wheel-X-Axis Rear-TC 4WD RU.....	135
A.86	Sensitivity and phase Steering Wheel-Y-Axis Rear-TC 4WD RU.....	135
A.87	Sensitivity and phase FsOe Rear-TC 4WD RU.....	136
A.88	Sensitivity and phase Fsie Rear-TC 4WD RU.....	136
A.89	Sensitivity and phase Seat Track -Z-Axis Rear-TC 4WD RD.....	137
A.90	Sensitivity and phase Seat Track -X-Axis Rear-TC 4WD RD.....	137

A.91	Sensitivity and phase Seat Track -Y-Axis Rear-TC 4WD RD	138
A.92	Sensitivity and phase Steering Wheel-Z-Axis Rear-TC 4WD RD	138
A.93	Sensitivity and phase Steering Wheel-X-Axis Rear-TC 4WD RD	139
A.94	Sensitivity and phase Steering Wheel-Y-Axis Rear-TC 4WD RD	139
A.95	Sensitivity and phase FsOe Rear-TC 4WD RD.....	140
A.96	Sensitivity and phase Fsie Rear-TC 4WD RD.....	140
B.1	Simulation run output (mean and 6σ) for Seat Track z-axis 2WD-RU.....	142
B.2	Simulation run output (mean and 6σ) for Seat Track x-axis 2WD-RU	142
B.3	Simulation run output (mean and 6σ) for Seat Track y-axis 2WD-RU	143
B.4	Simulation run output (mean and 6σ) for Steering Wheel z-axis 2WD- RU	143
B.5	Simulation run output (mean and 6σ) for Steering Wheel x-axis 2WD- RU	144
B.6	Simulation run output (mean and 6σ) for Steering Wheel y-axis 2WD- RU	144
B.7	Simulation run output (mean and 6σ) for Seat Track z-axis 2WD-RD.....	145
B.8	Simulation run output (mean and 6σ) for Seat Track x-axis 2WD-RD	145
B.9	Simulation run output (mean and 6σ) for Seat Track y-axis 2WD-RD	146
B.10	Simulation run output (mean and 6σ) for Steering Wheel z-axis 2WD- RD	146
B.11	Simulation run output (mean and 6σ) for Steering Wheel x-axis 2WD- RD	147
B.12	Simulation run output (mean and 6σ) for Steering Wheel y-axis 2WD- RD	147
B.13	Simulation run output (mean and 6σ) for Seat Track z-axis 4WD-RU.....	148
B.14	Simulation run output (mean and 6σ) for Seat Track x-axis 4WD-RU	148
B.15	Simulation run output (mean and 6σ) for Seat Track y-axis 4WD-RU	149

B.16	Simulation run output (mean and 6σ) for Steering Wheel z-axis 4WD- RU	149
B.17	Simulation run output (mean and 6σ) for Steering Wheel x-axis 4WD- RU	150
B.18	Simulation run output (mean and 6σ) for Steering Wheel y-axis 4WD- RU	150
B.19	Simulation run output (mean and 6σ) for Seat Track z-axis 4WD-RD.....	151
B.20	Simulation run output (mean and 6σ) for Seat Track x-axis 4WD-RD	151
B.21	Simulation run output (mean and 6σ) for Seat Track y-axis 4WD-RD	152
B.22	Simulation run output (mean and 6σ) for Steering Wheel z-axis 4WD- RD	152
B.23	Simulation run output (mean and 6σ) for Steering Wheel x-axis 4WD- RD	153
B.24	Simulation run output (mean and 6σ) for Steering Wheel y-axis 4WD- RD	153
C.1	The batch file name.	156
C.2	After launching the batch program with the Command Prompt Screen.	156
C.3	Probability distribution default parameters.	157
C.4	User specific probability distribution parameters' entering option.....	158
C.5	Normal distribution and the.....	159
C.6	The options after choosing the proper probability distribution.....	160
C.7	The program is locking on the right sensitivity curve through a series of questions.....	161
C.8	Three folder available for the user	162
C.9	Three output files with coded name to help identify the simulation run.....	163
C.10	Output file	163

CHAPTER I

INTRODUCTION

Vibration effects are ubiquitous, filling all mediums around and within us. In the contemporary world of vehicle design, researchers try to understand vibrations better in order to limit the vibrations' undesirable and harmful attributes. Especially important in the research of vibration effects on vehicles is the study of noise, vibration and harshness (NVH). NVH is an important field with a dedicated community working continuously from different walks of knowledge and expertise; industry, research and academia are collaborating in order to gain a deeper understanding and eventually overcome the challenges in the NVH field. Today, we have a better understanding of the contributors (sources), paths, and structure modal parameters of vibrations in different vehicle systems as well as how they interact; however, there remains a great deal more to explore and reveal in regards to the complex interactions and better predicting NVH issues as a result of interaction and departure between assumed models and real life models, without complicating the issue by taking in to account non-linear realms; all of these challenges, as well as many others, are still ongoing concerns in the NVH field.

Variations in vehicle noise, vibration, and harshness (NVH) response from one vehicle to the next can have significant impact on the company's profile and profitability. Variation can be caused by variability in design (e.g., tolerance stack-up), material (e.g., stiffness properties), manufacturing (e.g., locations of part-to-part assembly, welding),

customer usage, environmental conditions, or other sources of variation. Such variation in the vehicle response causes a higher percentage of produced vehicles to go out of specification in terms of their NVH response. This has been found to be a major component of warranty claims; there is evidence that more than one-fourth of warranty claims are first detected through excessive noise and vibration levels [1]. Furthermore, variations in vehicle NVH response can cause a loss in customer satisfaction, which has been proven to be even more costly to the company's profitability than the warranty claims.

Measures must be taken to ensure reduced warranty claims and higher levels of customer satisfaction. Excessive variations in vehicle response cause manufacturers to improve the target mean-value (in order to lessen the number of vehicles that can go above specification limits). This approach is costly, and it does not guarantee satisfactory results if a high level of variation is encountered. Instead, research must necessarily be performed in order to understand and control the root cause of variation in the vehicle NVH response. As a result, original equipment manufacturers (OEM) have implemented variations in the design process in an attempt to secure a response that remains within specifications.

Variations are caused by a vast array of factors. For example, variations can be caused by disparities in the design process such as tolerance stack-up, the wide-variety of materials that are used, and the many different manufacturing processes. Certain materials (e.g., rubber) have variation in stiffness that is either unavoidable or costly if tighter control is desired. Rubber materials are used as engine mounts, sub-frame mounts, exhaust hangers, tires, and a variety of other components. Furthermore, differences in

vehicle usage and environmental conditions are often uncontrolled factors. In addition, variations of particular interest in the case of rotating components are due to imbalance.

Driveline-induced NVH can be felt by the customer at many Customer Touch Points (CTPs). The CTPs that are typically considered include:

- a. Vibration at the steering wheel.
- b. Vibration in the seat. To avoid the complexity of adding the seat dynamics into the analysis, the vibration at the seat track will be assessed. It should be noted here that this particular assessment may require the acceleration (or velocity) to be measured in all three directions.
- c. Audible noise. This is measured either at the driver's in-board ear, the driver's out-board ear, or both.

There are many types of CTPs that should be taken into account. Vibration of the floor pan can also be assessed. In addition, there are other possible CTPs such as the seat track of other seats in the vehicle, the arm-rest areas for the passengers, and the transmission lever of the vehicle. Attention to these areas of CTPs can be deemed less significant than the others, as customers encounter them less often.

The Technical Approach

Noise and vibration energy are inevitably born at a source. In almost all the cases studied, the source is a structural or mechanical element. The noise and/or vibration energy is then transferred through the vehicle's structure and enclosures to a receiving point, which is often referred to as the path. The receiving point (a customer touch point) is, in turn, referred to as the receiver. If the path of the noise and/or vibration energy includes an energy transfer through air, the NVH energy is referred to as airborne.

Examples of airborne noise include pump whine, transmission whine, alternator whine, as well as many others. It should be emphasized that although we refer to this as airborne noise, the actual energy is necessarily born at a structure (usually the housing of the pump, transmission, or alternator that is transmitting such energy). If all the NVH energy is going through a structural path, the NVH concern is referred to structureborne noise. In general, structureborne vibration concerns are of low to medium frequency nature. This is the case because of two main reasons [1]:

- a. Higher frequency energy is usually dampened in the structural path through possibly various levels of isolation.
- b. Customers are less sensitive (or even not sensitive) to vibration energy at higher frequencies (above 150 Hz). Higher frequency energy is usually picked up by customers as sound.

Figure 1.1 shows a typical diagram that demonstrates the warranty claim that is generally referred to as “vehicle vibrates while driving” as perceived by the customer. The figure shows how this issue has to first be translated into values measured objectively at CTPs (seat track, steering wheel, and possibly others). While this may seem trivial, experience shows that it may actually be a challenging step. Challenges may arise in trying to duplicate the customer complaints that occur both at the dealer with the actual vehicle in which the customer experienced the concern or in a similar setting with a similar vehicle. In many cases, the concern may appear in certain conditions that are not easily reproducible even with the same vehicle. It should be kept in mind that variations at this level may occur.

These variations can be due to:

- a. Variations in customer perception of the NVH phenomenon. What is unacceptable to some customers may be admissible, or even unperceived, to the remaining customer base.
- b. Variations in the customer usage conditions; this refers to variations in the habits of different drivers. For example, certain resonances may not be excited unless the vehicle accelerates slowly (under partial throttle conditions).
- c. Variations in the environmental surrounding; this includes variations in altitude, humidity, temperature and others.

The second challenge that is faced is to find the actual metric that can be used for measurement as well as the measurement's location. In the case of driveline imbalance-related NVH issues, these are concerns that are both audible and sensible, such as vibration energy. Historically, contentions have been raised among researchers regarding the locations of vibration sensors (e.g. the steering wheel, seat track, arm rest, floor pan, brake or gas pedal, or other possible CTPs) and audible sensors (driver's outboard ear, driver's inboard ear, passenger sound, and others). Standard procedures should be adopted in order to ensure repeatability and reproducibility of the NVH concern.

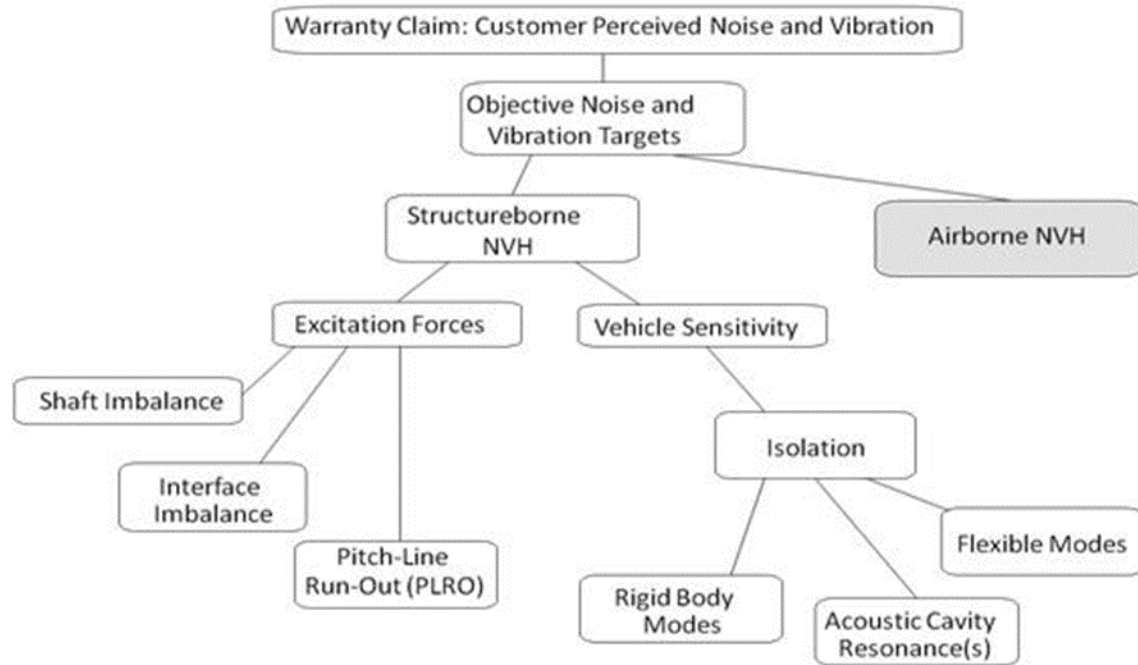


Figure 1.1 The Possible Root Causes of driveline NVH

The third challenge is to determine the levels at which such measurements become a customer complaint (leading to a warranty claim, loss of customer satisfaction, or both) that simply cannot be ignored based on the manufacturer's objective. Because the driveline concern at hand can be both a noise and a vibration concern, both noise and vibration data will be needed. As mentioned earlier, the noise portion is actually transferred through the structure and is thus a structureborne noise. It should be noted that there are other driveline NVH concerns such as driveline boom or clunk that manifest themselves as audible noise; thus, an airborne path is needed. However, this is not considered here.

There are two main components that manifest themselves to the vibration and noise levels felt by the customer. The first of these is the source of the vibration energy.

Vibration can be excited at the driveline assembly, even when driven on a smooth road. It is important to emphasize the separation between imbalance induced NVH and other NVH (e.g., friction, etc ...). The driveline assembly will include the shaft, center bearing(s), brackets, and joints. Driveline is the source or force for this NVH energy.

The second is the transfer path. Before a detailed study is conducted on how to assess total vibration at CTPs, it is important to understand the vibration transfer mechanism from the driveline assembly to the vehicle's main frame. The vibration is induced at the driveline assembly. This can be due to many factors: driveline imbalance, run-out, and frictional joints as well as other malformations such as bad bearings, joints, half shafts, etc.

Each of these sources can result in vibration being transferred to the vehicle's main frame through attachment points (i.e., struts). Relating the in-vehicle NVH to the root cause is usually done through tracking the frequency of the NVH phenomenon. Imbalance related vibrations are of first order (as compared with the driveline speed in revolution per minute (rpm)). A dynamic model is needed for any of the above mechanisms to predict vibration levels at any of the attachment points with the main frame of the vehicle, or CTPs, as a result of a vibration born at the source. Alternatively, and particularly in an assembly plant setting, such a transfer function can be determined experimentally. The emphasis of this work will be on driveline imbalance. A transfer function that relates imbalance value to the customer concern (e.g., vibration acceleration level or others) is determined at each of these touch points. This function is directly related to the input parameters of imbalance (measured in gr-cm). The function is

developed in the frequency domain. When this is developed experimentally, special care is needed to isolate the sources of vibrations mentioned above in an experimental setting.

System Variations

The variations expected in the sources of vibration (part-to-part variation) should be recognized and accounted for. These variations are not designed in the system; instead, they are an outcome of certain manufacturing and control processes. Having a tighter control is often achievable (e.g. balancing all shafts used in the driveline), but this may be proven unnecessary or even costly. This work will allow the engineer to conduct parametric optimization where all design parameters can be considered to achieve the acceptable NVH levels with certain reliability in mind.

The forcing function (i.e. imbalance) at the attachment point needs to be determined first. For a driveline vibration with one central bearing, three interface points are observed along with the rest of the vehicle structure. The first is either the attachment to the power-take-off unit (PTU) in an all-wheel drive (AWD) assembly with an east-west engine configuration see left side of Figure 1.2 or the attachment between the driveline itself and the transmission in a rear wheel drive vehicle (RWD) of a north-south engine configuration see right side of Figure 1.2. The second attachment is at the center bearing. The third attachment is with the rear axle. Total assembly of an as-installed imbalance needs to be assessed at these three attachments (or planes). For each of these attachments or planes, a static distribution of imbalance (characterized usually by a Weibull distribution) needs to be known and well understood.

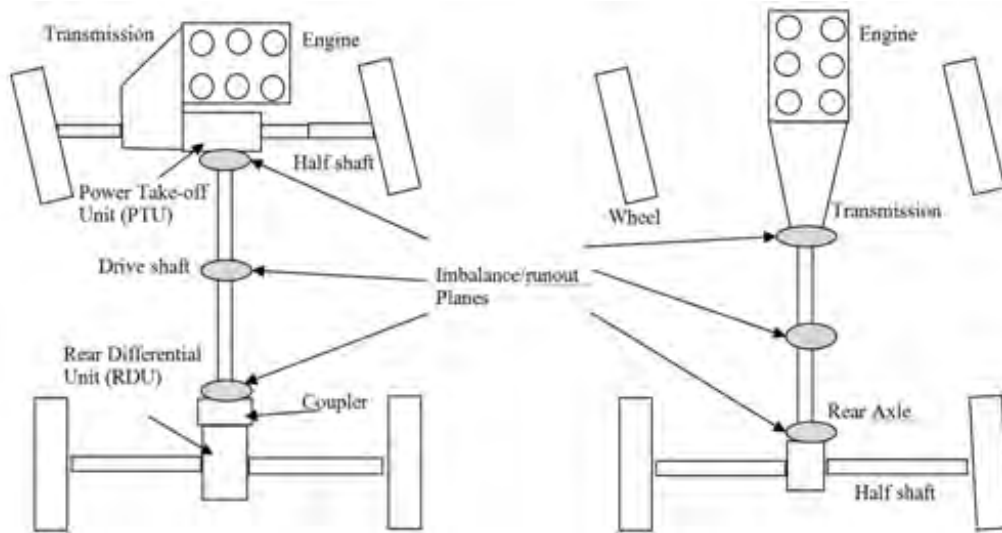


Figure 1.2 Left: AWD configuration for an East-West engine. Right: RWD configuration for a North-South engine

A proper procedure needs to be implemented when the components (drive shafts, joints ...) are assembled together. Variations in each of these planes need to be properly added together to determine the total variation at each of the planes. This can be done using the Monte Carlo process. It should be noted that the results may follow a Weibull distribution instead of a normal distribution. A typical statistical imbalance for each of the planes is shown in Figure 1.3.

It is important to understand the transfer mechanism of this vibration energy to the CTPs. This mechanism is frequently referred to as vehicle sensitivity[1]. It should be mentioned here that several vehicle sensitivity functions (depending on the number of attachment points with the source and the CTPs considered in the analysis) are to be determined. Vehicle sensitivity functions can be determined analytically by developing the transfer function from the attachment point(s) (or planes) and the CTPs. The determination of such transfer function can be made using existing models of the main

frame of the vehicle in order to conduct a proper finite element analysis (FEA).

Additionally, the transfer function can also be determined experimentally. Both methods for finding the transfer function may prove to be necessary. The experimental approach for determining the transfer function can be valuable in order to:

- a. Determine variations in the transfer function itself (part to part variation) as a result of possible variations in the main frame, welding or other sources.
- b. Correlate the analytical model using FEA.

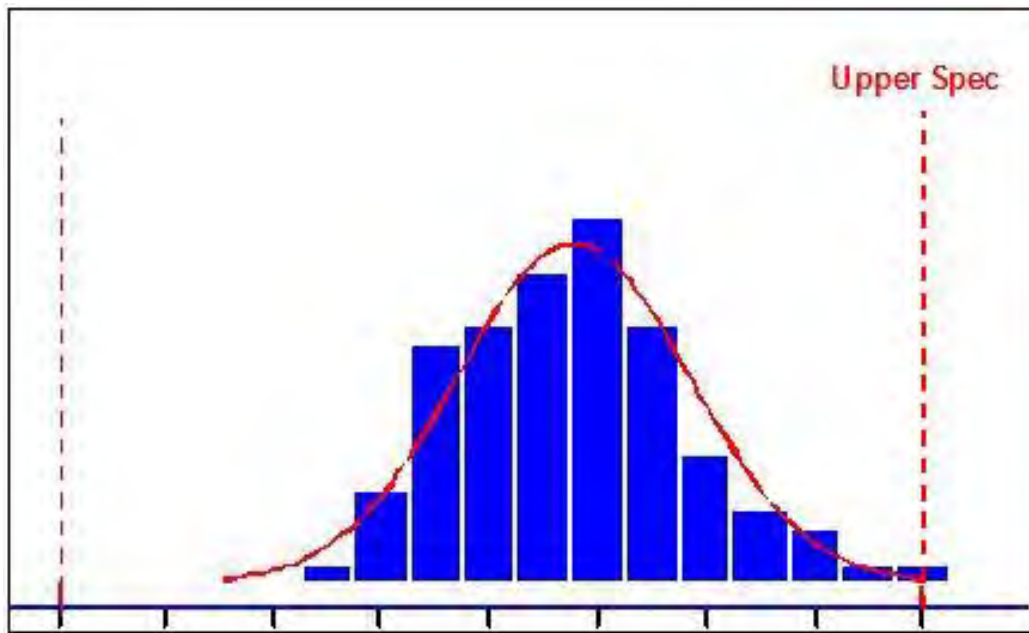


Figure 1.3 Typical statistical imbalances for an interface plane

If concern is felt by the customer at both the steering wheel and seat track as well as interior sound levels (as is typically the case), a transfer function needs to be added from each of these planes to each of the customer points. If the steering wheel vibration is

measured in one direction and the seat track is measured in three directions, as sound levels are measured in one location (driver's outboard ear (DOE)), a total of 15 transfer functions need to be determined. In other words, five transfer functions need to be determined for each of the planes. The five transfer functions refer to one for the steering wheel, three for the seat track, and one sound pressure level measurement. Vehicle sensitivity for DOE is usually referenced as the following mathematical equation (2.1):

$$\text{Vehicle sensitivity} = \left(\frac{P}{F} \right)_{DOE,i} \quad (2.1)$$

Forcing function at each plane is referred to as (F)_i, where i refers to the plane at which imbalance is assessed. (P)_{DOE} is the output; in this case, it is sound pressure level (SPL); thus, it is measured in decibel (dB). In case of vibration, the output may be measured as acceleration, in mm/s² or velocity in mm/s or displacement in mm for each CTP understudy equation (2.2).

$$\begin{aligned} \text{In vehicle levels} &= \text{Vehicle sensitivity} \times \text{forcing function} \\ P_{i,DOE} &= \left(\frac{P}{F} \right)_i \times (F)_i \end{aligned} \quad (2.2)$$

Figure 1.4 shows typical sensitivity functions for several vehicles. The RSS value refers to a root of sums squared. This is used when a tri-accelerometer is used to assess vibration levels at a certain location. This is the general practice for the seat track vibration level measurement.

The total vibration or noise at the CTPs is assessed as the product of the forcing function at the attachment and the transfer function. This is to be done in the frequency domain. It should be noted again that due to part-to-part variations of vibration sources,

and possibly experimentally assessed variations in vehicle sensitivity, a Monte Carlo process is an integral part of this work.

Total in-vehicle sound or vibration levels are found by adding all NVH data coming from each of the planes, equation (2.3):

$$P)_{DOE} = \sum_i P_i)_{DOE} \quad (2.3)$$

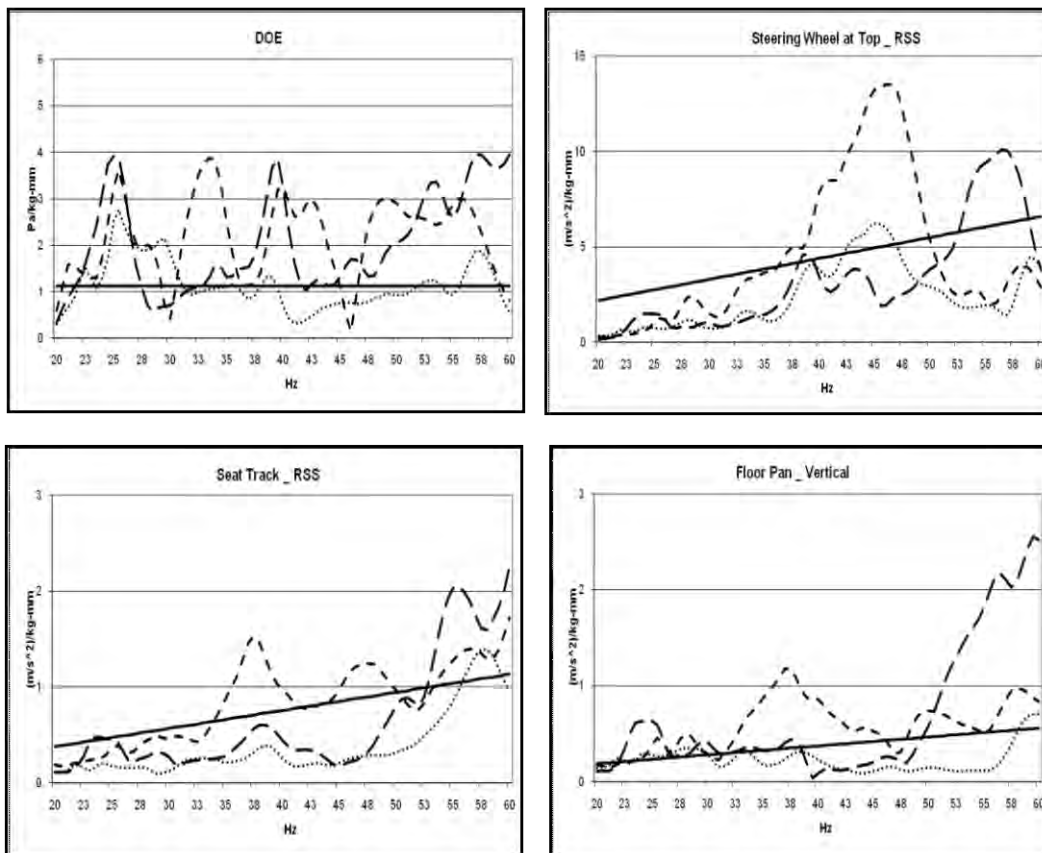


Figure 1.4 Typical Sensitivity Function to Driveline Imbalance at a Certain Plane

This optimization process often gives the engineer the choice of whether to request a more stringent control of some of these imbalance variations or design the system to be robust to them (i.e. improve vehicle sensitivity). A computational tool can be developed to help the engineer decide the better approach (i.e., the most economical approach) in the attempt to achieve acceptable interior NVH levels and their variations; this will lead to a more predictable number of failures that is acceptable to the company depending on its objective, the brand at hand (e.g. luxury), and the impact of the failures. This will lead to software and optimization tools for the design engineer to determine the most appropriate approach to handle objectionable interior vibration levels induced by sources at the driveline assembly. This model can then be used with the well-established statistical Monte Carlo process to determine the imbalance levels needed at each plane to achieve the desired in-vehicle NVH response and reliability.

Scope

The scope of this research is to study the noise, vibration and harshness (NVH) variations from the customer's (driver's) point of view by measuring NVH at customer touch points (CTP's) when controlled changes to driveshaft imbalance are applied. The vehicle considered is a 2011 Nissan Titan crew truck. The frequency range under study is in the low to medium range in the neighborhood of 10 to 55 Hz.

The focus of this research will be on part-time four-wheel drive (4WD), i.e. with a front-rear locking transfer case, automatic transmission, short wheelbase (SWB) light-duty vehicle (truck). Many different combinations of engine location and driven wheels are found in practice. The methodology utilized throughout this research should be able to be applied to different body styles with little to no adjustments. This methodology may

be expanded to strictly two-wheel drive (2WD) vehicles, e.g. front-wheel drive (FWD) or rear-wheel drive (RWD) vehicles. In regard to all-wheel drive (AWD) or 4WD without a locked mode vehicles from the same category, it was determined some adjustments will be required for the preliminary data collection stage in order to distinguish contributing forces relative to each driveline segment (front and rear); this is because it will be nearly impossible to conduct testing with proper repeatability due to phasing considerations, as both driveshaft segments will be rotating at the same speed with no phase relationship. Furthermore, wheel order interfering may occur if the axle ratio is close to an integer. Both cases will require special adjustments to overcome such challenges; however, the stages afterward in utilizing the methodology and developing the tools should be the same.

Assumptions

Experimental modal analysis answers important questions when utilized properly. Significant factors such as damping, critical frequencies, and modal shapes are all addressed. When researchers use such tools, they usually make assumptions in order to draw correct visualization of the captured system(s) responses. The main assumptions of this work are linearity (superposition and scaling), time invariant, reciprocity, and observability:

- a. Linearity is assumed throughout this research; specifically, the superposition property will be a result of such assumption: the resultant response of multiple stimuli at a given place and time will be equal to the sum of the response of each stimulus individually, bearing in mind that responses are not scalar quantities; rather, they are vectors or phasors.

- b. Time invariant systems; the response (output) of a transfer function (system function) depends on the stimuli (input) and not time on the time. If multiple stimuli excite a system at different points of time, the resultant should be the same each time.
- c. Reciprocity is assumed here and supported by previous assumptions. Response (R_{ab}) at location (a) excited by a stimulus at location (b) will be equal to a response (R_{ba}) measured at location (b) excited by an exciter (R_{ab}) at location (a).
- d. Observable: “that is, the input/ output measurements that are made contain enough information to generate an adequate behavioral model of the structure.”[2]

Contributions

Noise, vibration and harshness (NVH) is a born physical phenomenon that presents itself strongly in contemporary vehicles since the modern mechanical vehicle’s conceptualization and production.

Prediction of the behavior of different systems and parts of the vehicle before assembly and after assembly under different circumstances is critical to the design process. This challenge to designers is in addition to inherent design challenges, which we have discussed earlier in the introduction, regarding variations within specified tolerance limits of the physical shape, material properties, manufacturing processes, and the stack-up and operating environment. All of these variations will have direct effect on NVH responses and sensitivities; another variable to these challenges is an NVH inherent

challenge related to the customer's perception of what is considered uncomfortable or objectionable.

The mindset is to develop a tool towards a robust design for driveline NVH which enables the design engineer to better understand the effect of driveline imbalance on the customer touch points (CTP's), especially after reviewing published materials in this matter and getting to the conclusion that there is a lack in design tools to study vehicle sensitivity to driveline imbalance. This study will result in the following contributions:

- Establishing an NVH baseline case for a Nissan truck at predetermined CTPs with specific driving and sweeping styles.
- Designing, developing, and validating a testing methodology for inducing driveline imbalance at predetermined planes.
- Developing a novel transfer function for driveline imbalance.
- Developing a unique set of verifiable sensitivity to imbalance graphs dedicated to each plane in each specific driving and sweeping style.
- Developing a procedure through which OEMs can realistically assess the broad sensitivity to imbalance, improving product and process design process including setting up specifications.

CHAPTER II

LITERATURE REVIEW

Driveline NVH: Investigation and Studies

Driveshaft assemblies can be a source of first order vibrations (one excitation per revolution) and second order vibrations (two excitations per revolution). Driveline imbalance and runout will introduce a resultant force once every rotation on the joining planes. In our case, where we are studying two drivelines with a transfer case, we are primarily concerned with the axle planes for both front and rear drivelines beside the planes that connect drivelines with the transfer case. When u-joints' (Cardan or Universal joints) angles are out of their operating angle values, a second order vibration will take place due to the torsional forces acting twice on each rotation. Another second order vibration is related to the bending moments in the driveline which manifest themselves as torque transmitted from a u-joint at the operating angles; these are called secondary couples. The secondary couples will fluctuate at a frequency corresponding to the second (driveline) order [3].

Extensive research has been done on Driveline NVH by numerous studies. For example, the Universal Joint and Driveshaft Design Manual includes a comprehensive overview of automotive noise and vibration that includes a focus on powertrain and driveline NVH [4]. More recently, Iqbal et al [5, 6] has shown a significant interest in the subject of driveline NVH. Specifically, the researchers discuss optimization of

frequencies of a two-span shaft system joined with a hinge. In addition, Qatu and Iqbal [5] study the transverse vibration of a two-segment cross-ply composite shaft with a lumped mass. Iqbal et al [6] expands upon this research by investigating transverse vibration of a three-piece shaft system joined with multiple hinges. Robustness of powertrain mount systems for noise, vibration and harshness at idle has been the subject of several studies [7], and robustness of axle mount systems for driveline NVH was also considered [8]. Optimization studies on driveline systems have been the subject of other studies. Optimization of the high frequency torsional vibration of vehicle driveline systems using genetic algorithms has been carried out by leading researchers [9]. Noise, vibration, and harshness levels have been given a significant amount of attention from various researchers due to its importance in the vehicular economy (i.e., its impact on driving experience and customer brand appreciation, which drives bottom line profits).

In 2011, Qatu et al [10, 11] discussed some of the main methodologies of this research. It is based upon utilizing stochastic methodology to predict NVH response relative to customers (drivers). Using the science of probability and statistics in NVH experimentation and testing field is not new. In a survey by Lalor and Priebisch [12], the authors refer to several sources in which NVH is studied with the following terms in mind: variation, prediction, variability, shifting, interaction, optimization, and statistical variability. All mentioned terms are related to the uncertainty and stochastic science. In the same paper, the authors discuss variability in vehicles with reference to several resources of conducted studies on variations among manufactured vehicles of the same platform, year, and in the same manufacturing facility.

Variability in large structures such as bridges, commercial airplanes, large marine vessels, or large buildings is a nonissue because extensive individual studies are made on each project using computer aided engineering (CAE) and testing; this is due to the amount of investment and elevated risks in case of failure. The automotive industry is a mature industry with millions of vehicles manufactured on a yearly basis. For example, in 2012, sixty million cars [13] were manufactured worldwide (“car” being defined as a light passenger vehicle with 4 wheels and no more than 8 seats). This large number of annually manufactured vehicles makes it infeasible to run extensive NVH testing on each finished product; for this reason, many researchers have utilized stochastic approaches to address NVH challenges in such a large population. Several studies of interest to us have been mentioned in the survey papers by Lalor and Priebisch [12, 14, 15]. Extensive research has focused on the factors leading to such variability in the past 40 years.

The study of imbalance and induced NVH in vehicle driveline has been discussed by several researchers [16-19]. Several key aspects of these studies should be highlighted as we review their research, which we would like to enhance:

- Details regarding the experimental testing approach were not discussed with elaboration. For example, introducing imbalance to the driveline was not discussed in detail in any of the studied papers.
- Taking a deterministic approach to study the matter. This research is considering variability in introduced imbalance.

Six Sigma Utilized in NVH Challenges

The main goal to be achieved by most commercially driven Six Sigma projects is translated into the bottom line cost in one way or another. Ulrich and Eppinger define

five dimensions that characterize a successful product development process: product quality, product cost, development time, development cost and development capabilities[20]. All mentioned dimensions can be translated easily into bottom line profit to the commercial institute. We may go a further step and talk about the effects of a substandard quality product to the society; “Quality Loss” which has been defined by Taguchi and Elsayed as: “the loss a product costs society from the time it is released for shipment [21].”

The noise, vibration and harshness (NVH) community members have embraced the Six Sigma philosophy and methodology. This is manifested in the number of NVH published papers addressing NVH related challenges that utilize Six Sigma methodology. Six Sigma methodologies target to achieve its bottom line goal by improving efficiency and effectiveness while reducing performance variation; from the later target its name was coined.

The tools and methodology of Six Sigma are not new to the NVH field; the deployment of such tools requires methodical plans and determination. This research has utilized a Six Sigma tool to validate and define the scope of the research in concern while taking into account the expected savings brought to the original equipment manufacturers (OEM) and their suppliers by utilizing the developed tool, which utilizes Monte Carlo (MC) statistical approach to model physical system with complex inputs and outputs. MC allows for large system outputs to be sampled in a number of random configurations; in turn, this data can be used to describe the system as a whole. MC is a good tool, whenever you need to make an estimate, forecast or decide where there is significant uncertainty.

CHAPTER III

EXPERIMENTAL SET UP

The major challenges preventing a fully simulated product development process are effectively discussed by H. Van der Auweraer and J. Leuridan when they explain why we are not developing new products that depend solely on simulation and Computer Aided Engineering (CAE): “Insufficient calculation speed and performance of solvers is only part of the explanation, since important breakthroughs in terms of computing power, parallel processing, and optimized algorithms have been made. Missing knowledge on exact material parameters, lack of appropriate models for complex connections, or insufficiently accurate model formulations for some parameters remain major bottlenecks [22].”

Technical approach

When utilized properly, experimental modal analysis addresses important issues such as damping factors, critical frequencies, and mode shapes. When researchers use such tools, they always make assumptions in order to draw correct visualization of the captured system(s) responses. The main assumptions of this research are the following: linearity (superposition), time invariant, reciprocity, and observability.

Driveline systems pose objectionable vibrations over several frequencies while operating a vehicle; please see Figure 3.1 for frequencies and the NVH accompanying it.

From the farthest left side (low frequency) shuffle (i.e., quick changes in the vehicle's load such as pedal tip-in/out) can result in an objectionable vehicle shuffle response, which is connected to the first natural frequency of the driveline and is usually in the 2 Hz – 8 Hz frequency range (depending on the selected gear)[18], may take place. Other types of objectionable NVH and manifestation frequency ranges are shown.

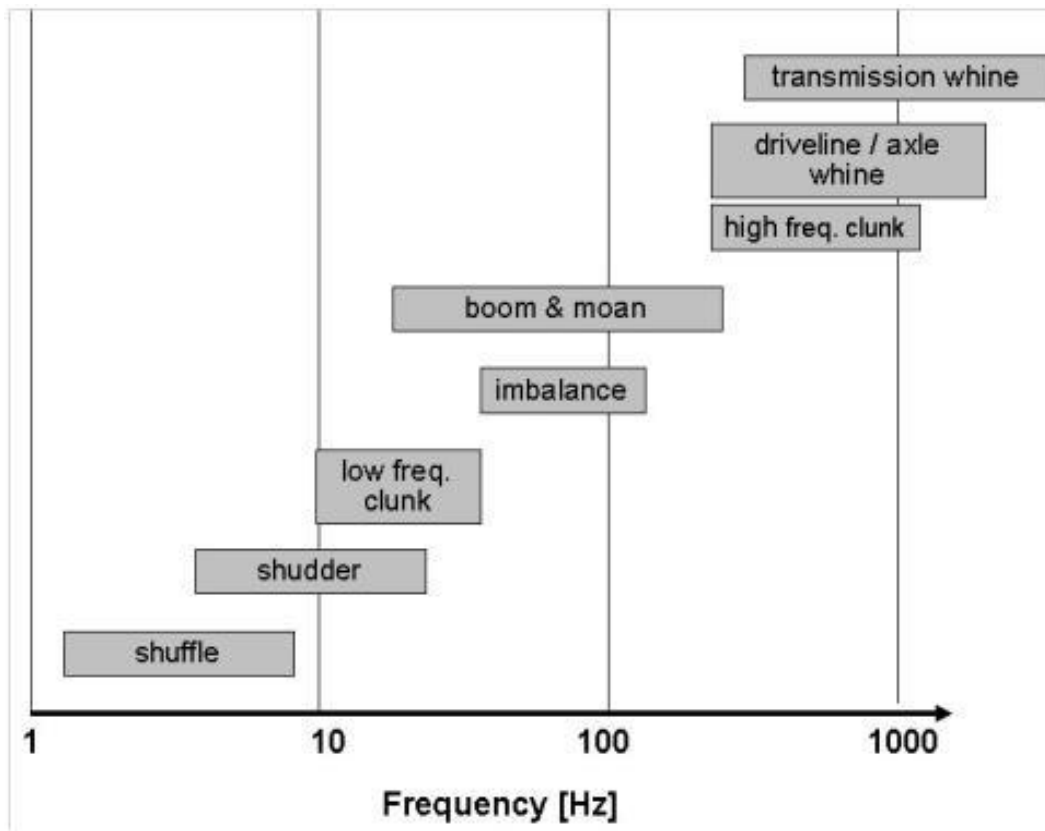


Figure 3.1 Optimizing Vehicle NVH Characteristics for Driveline Integration [15]

Although this innovation has implications in any vehicle design platform, this research has implemented a light part-time four-wheel-drive (4WD) truck with a transfer case providing High- 4WD and Low- 4WD; the truck runs rear wheel drive (RWD)

constantly with the front wheels only engaging when the 4WD switch is engaged see Figure 3.2.

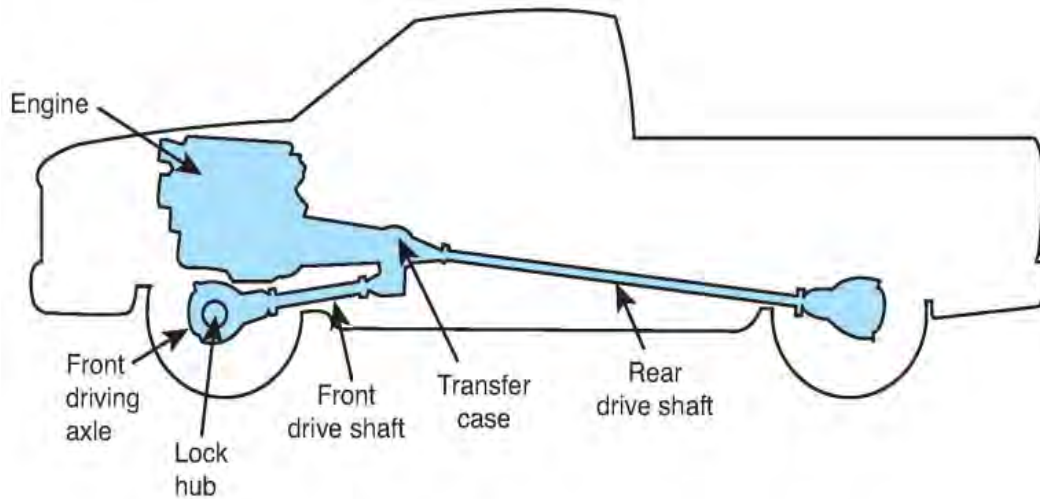


Figure 3.2 truck with two drive shafts [23].

We are interested in 4 planes; Figure 3 and Table 1 discuss each plane's location and identifying symbol.

When a rotating imbalance is present, the resultant input force to the system is given by equation (3.1):

$$F_j = U_j \omega^2 \quad (3.1)$$

Where F_j is the force at “jth” plane, U_j is the imbalance (i.e., mass multiplied by eccentricity) at each plane (for plane name and location, see Figure 3.3 and Table 3.1). ω is the angular velocity for the component.

Table 3.1 Plane name and location

	Front Axle (FA)	Transfer Case (TC)	Rear Axle (RA)
Front shaft	A	B	
Rear shaft		C	D

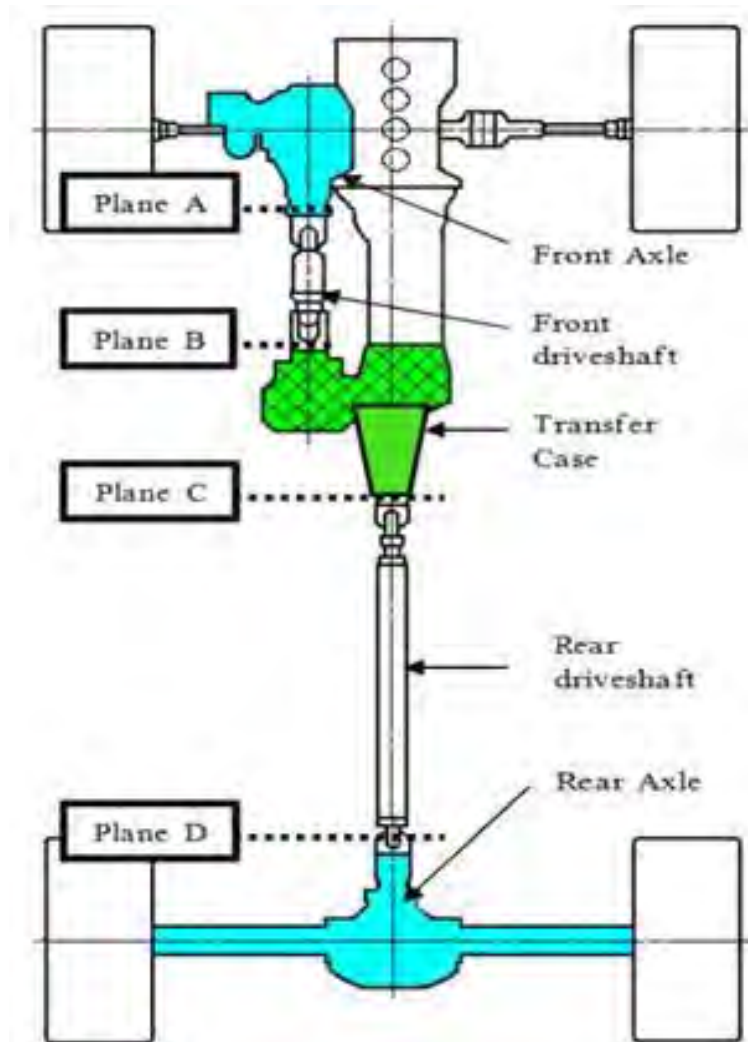


Figure 3.3 A typical light-duty four-wheel-drive pick-up truck driveline and the corresponding planes of imbalance[17]

Front and rear shafts' physical specifications (Table 3.2) will help in calculating imbalance at each plane by providing important dimensions at each plane.

Table 3.2 Shaft information (approx.)

Shaft Type	Φ (mm)	Mass (kg)	Mat.	Length (mm)
Front shaft	63.5	7.3	Steel	786.4
Rear shaft (TC end)	105.6	9.4	Alum.	1875.3
Rear shaft (RA end)	127.6	-		

To mark up angles on each plane, it is necessary to start from a reference point; the leading edge of the tachometer's reflecting strip was chosen. From this point, a 360° line was measured around the circumference in alignment with the vehicle's forward rotation of the driveshaft was marked up (Figure 3.4), in which the different angles for plane A were marked (the front driveshaft and front axle plane). The same process was applied for other planes as shown in Figure 3.3.



Figure 3.4 Plane A with a tachometer and reflecting strip is set as 0° angle

The tests involve attaching masses at specified angles to each plane in order to induce imbalance at each specific plane. Calculating imbalance is a straightforward calculation; the amount of added mass is multiplied by the distance from the center of rotation, equation (3.2):

$$U_j (\text{imbalance at plane } j) = \text{mass (gm)} \times \text{eccentricity (cm)} \quad (3.2)$$

Where, cm: centimeters, gm: grams.

Table 3.3 shows the imbalance calculated at each plane.

Table 3.3 Imbalance introduced for each plan

Plane	Imbalance introduced (gr.cm)
A: FA(Front Axle)-front shaft	25 gm@ 37.75* mm = 94.4 gm.cm
B: front shaft-TC (Transfer-Case)	25 gm@ 37.75* mm = 94.4 gm.cm
C: TC-rear shaft	28 gm@ 60.8** mm = 170.4 gm.cm 25 gm@ 66.8** mm = 167.0 gm.cm Total imbalance = 337.1 gm.cm
D: rear shaft-RA (Rear Axle)	28 gm@ 65.8** mm = 184.2 gm.cm 25 gm@ 71.8** mm = 179.5.0 gm.cm Total imbalance = 363.7 gm.cm

* Only two hose clamps were used; imbalance mass comes from the hex screw and shell of each hose clamp. The center of mass is measured at 6 mm from the shaft surface, and the mass is 12.5 gm/ Ea.

** Extra mass used: 28 gram at 2 mm center of mass above the shaft surface. Two hose clamps were used on top of the added mass. The new center of mass for the hose clamp hex screw and shell will become 10 mm (4 mm thickness of added mass) above the shaft surface, with no change in their total mass (i.e., 12.5 gm/ Ea).

Channels and sensors

Selected CTPs instrumentation will serve as objective and numerical measurement points to evaluate the effect of imbalance due to mass distribution change from the baseline case; in turn, this will serve as the plateau state of the system of the driveshaft to the introduced cases of imbalance at each plane at different angles. For the truck under study and consideration, we have a single-piece front driveshaft and rear driveshaft; both are connected to the transfer case, and each one in turn is connected to the front or rear half shafts through a differential. As is mentioned in the introduction, in order to monitor the imbalance effect on the occupants, we used accelerometers and

microphones on CTPs. Throughout the experiment, eight CTPs' input channels (six accelerometer channels and two microphone channels)[24] were selected to qualify effects of changes in the imbalance mass at different planes and angles; in addition, 12 channels (accelerometer channels only) were deployed on each plane for three directions: X, Y, and Z; these added channels served two purposes:

- Monitoring the vibration at all times in order to prevent unsafe operation of the vehicle under introduced imbalance conditions.
- Functioning as reference in case further analysis is needed.

Apparatus and Testing Equipment

- Truck general specifications:
 - 5.6-liter Dual-Over-Head Cam (DOHC) 32-valve V8 engine.
 - 317 hp @ 5,200 rpm.
 - 385 lb-ft of torque @ 3,400 rpm.
 - Continuously Variable Valve Timing Control System (CVTCS) on intake valves
 - Switch-operated 2-speed transfer case 4-wheel drive (4WD high – 1.000; 4WD low – 2.596).
 - Final gear ratio (2.94:1 – similar to a 4-speed automatic 3.73:1).
 - 5-speed automatic transmission.
 - Lower final gear ratio (3.36:1 – similar to a 4-speed automatic 4.10:1).
 - Electronic locking rear differential.
 - Independent double-wishbone front suspension with stabilizer bar.
 - Multi-leaf rear suspension.

- Wheelbase 139.8 in
- Curb weight: 5,549 lb.
- Digital Signal Processing settings:
 - Acquisition parameters:
 - Fixed sampling.
 - Bandwidth: 2048 Hz.
 - Resolution: 0.25 Hz.
 - Frequency lines: 8192.
 - Static bandwidth: 128 Hz.
 - Trigger settings: Free Run.
 - Viewing settings:
 - Function: Time.
 - Window: Hanning.
 - Spectrum format: RMS.
 - Tracking settings:
 - Tachometer: rear driveshaft
 - Minimum: 600 rpm.
 - Maximum: 3100 rpm.
 - Increment 25 rpm.
- Testing was conducted on chassis dynamometer with the following general specifications:
 - 4WD, 48" Center Mounted Chassis Dynamometer.
 - Vehicle types: Cars and commercial vehicles.

- Vehicle wheelbase range: 2.1-4.7 m (82.68-185.04 inch).
- Maximum vehicle axle loading: 4,536 kg (10,000 lb.).
- Speed range (continuous): 0-200 km/h (0-124 MPH).
- Maximum absorption tractive effort (continuous): 4500 N from 0-120 km/h.
- Maximum absorption power (continuous): 150 kW from 120-200 km/h.
- Maximum motoring tractive effort (continuous): 4500 N (0-120 km/h).
- Maximum motoring power (continuous): 150 kW from 120-200 km/h.
- Nominal inertia of each machine (approx.): 1400 kg m² (Each A.C. machine /Pair of Rollers).
- Equivalent vehicle mass (approx.): 3760 kg (Each A.C. machine /Pair of Rollers).
- Method of inertia simulation: Electrical
- Operational testing conditions:
 - Run-up: 600 - 3100 rpm (rear shaft)
 - Run-down: 3100-600 rpm (rear shaft)

Testing Procedures

One of the main focuses during experimentation was the achievement of testing goals in a safe manner. In order to monitor levels of vibrations induced when driveline imbalance was introduced, we added more accelerometers on all planes of interest. These accelerometers served well during the process of selecting the amount of imbalance to be introduced at each plane. We tried several imbalance masses and then swept with run up and run down (RU, RD) to find the amount of vibration introduced.

There were a total of eighteen vibration monitoring channels through accelerometers, two acoustic channels with microphones, and three CAN-BUS channels drawing data from built-in tachometers (see Figure 3.5 for the list of channels). Two external tachometers were installed on the rear shaft (Tacho 1) and front shaft (Tacho 2). Tachometer 1 from the rear shaft and the voltage input was used as the reference for all waterfall calculations, as this is a part-time 4WD truck with full-time RWD.

PhysicalChannelId	Point	ChannelGroupId	Direction
Tacho1	Tacho1	Tacho	None
Tacho2	Tacho2	Tacho	None
Input1	Rear(+X)Axle	Vibration	+X
Input2	Rear(+Y)Axle	Vibration	+Y
Input3	Rear(-Z)Axle	Vibration	-Z
Input4	TC(-X)RearShaft	Vibration	-X
Input5	TC(-Y)RearShaft	Vibration	-Y
Input6	TC(-Z)RearShaft	Vibration	-Z
Input7	TC(-X)FrontShaft	Vibration	-X
Input8	TC(-Y)FrontShaft	Vibration	-Y
Input9	TC(-Z)FrontShaft	Vibration	-Z
Input10	Front(+Z)Axle	Vibration	+Z
Input11	Front(+Y)Axle	Vibration	+Y
Input12	Front(-X)Axle	Vibration	-X
Input13	SeatTrack	Vibration	+X
Input14	SeatTrack	Vibration	+Y
Input15	SeatTrack	Vibration	-Z
Input16	SteeringWheel	Vibration	+Y
Input17	SteeringWheel	Vibration	+X
Input18	SteeringWheel	Vibration	+Z
Input19	FsOe	Acoustic	S
Input20	Fsie	Acoustic	S
Input21	Tacho1_Voltage	Other	None
Input22	Tacho2_Voltage	Other	None
Input73	XSI 1::ATMSG2::TBNREV	Static	None
Input74	XSI 1::ATMSG2::OUTREV	Static	None
Input75	XSI 1::ECCMSG0::TACHO	Static	None

Figure 3.5 Channels ID, type and direction (if applicable)

In order to achieve best levels of gage repeatability and reproducibility, tests were conducted with timers for run up and run down. It is understood that there will be variation due to the human factor in running an un-automated test; in order to minimize such inherent variation in the run up and run down testing, six tests were conducted for each case and averaged to obtain a mean for each study case. The plan of testing is shown below (see Figure 3.6).

The baseline cases (i.e., no mass added in RWD and 4WD-High) were conducted in the same setup and under same conditions. In addition, for the same reasons previously mentioned, average runs from six runs of run up and run down were deduced for each baseline case.

Run Up & Down							
Plane		Runs after Weights added /Angle				Number of runs	
		0 deg	90 deg	180 deg	270 deg		
2WD	Rear Driveshaft	TC	6	6	6	6	24
		RA	6	6	6	6	24
Front Driveshaft		FA	6	6	6	6	24
		TC	6	6	6	6	24
						Total	96 Runs
Plane		Runs after Weights added /Angle				Number of runs	
		0 deg	90 deg	180 deg	270 deg		
4WD-H	Rear Driveshaft	TC	6	6	6	6	24
		RA	6	6	6	6	24
Front Driveshaft		FA	6	6	6	6	24
		TC	6	6	6	6	24
						Total	96 Runs

Figure 3.6 Testing plan and data acquisition

Certain measures were taken during the testing in order to minimize sources of variation. For example, the truck was warmed up while on the dynamometer for 15

minutes before each testing session in order to minimize variations due to change in tire temperature, truck, and dynamometer apparatuses. Furthermore, the indoor testing (on a dynamometer) helped minimize source of variations among tests. In addition, each set of tests were taken together, and the testing process was planned to adhere to this requirement; therefore, testing necessarily took place over several days.

The tested truck is pictured from underneath in Figure 3.7, showing the front and rear drivelines (the closest being the front driveline and the farthest being the rear driveline).



Figure 3.7 Front and rear drivelines, from underneath the truck.

Each driveline setup was positioned to have the reflective tape represent the Zero angle, Figure 3.8, for introduced imbalance. The next marked-angle 90 degrees was marked by turning the driveline forward 90 degrees using an angle measuring device. This process continued to mark the position for the 180 degrees and 270 degrees.



Figure 3.8 Front driveline axle plane with tachometer and reflective tape

Figure 3.9 shows a wider picture for the same plane, seen before with a tri-axial accelerometer attached in proximity to capture the vibrations at that plane. The accelerometer is placed there, as well as for other planes, for reference as well as to monitor any excessive vibration that plane or other major planes may see when unsuitable imbalance is introduced to the driveline.



Figure 3.9 Front driveline axle plane with a tri-axial accelerometer.

Figure 3.10 to Figure 3.19 depict the tested vehicle, dynamometer, measuring devices, and measurement locations.



Figure 3.10 Seat track tri-axial accelerometer

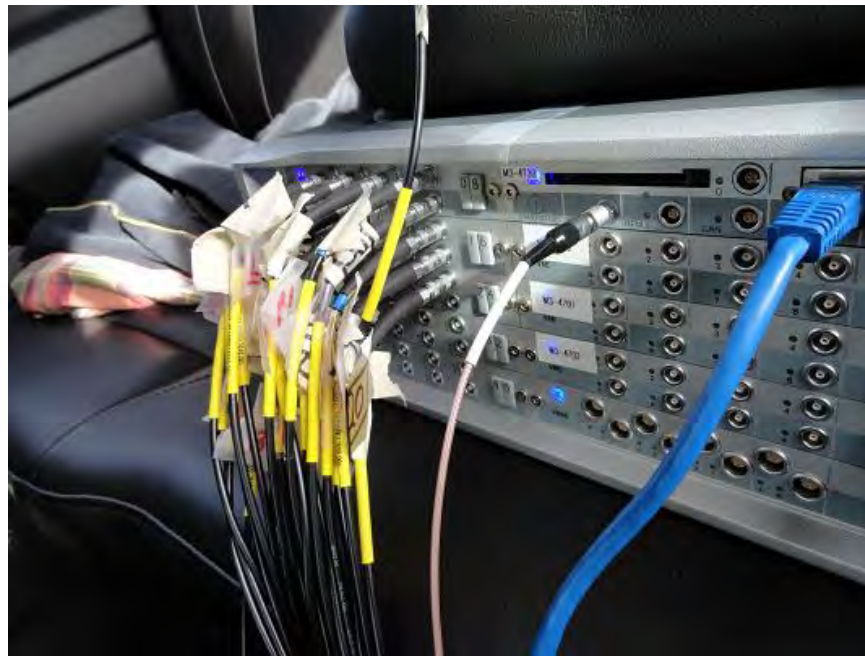


Figure 3.11 Front-end data acquisition hardware



Figure 3.12 Truck tested on dynamometer

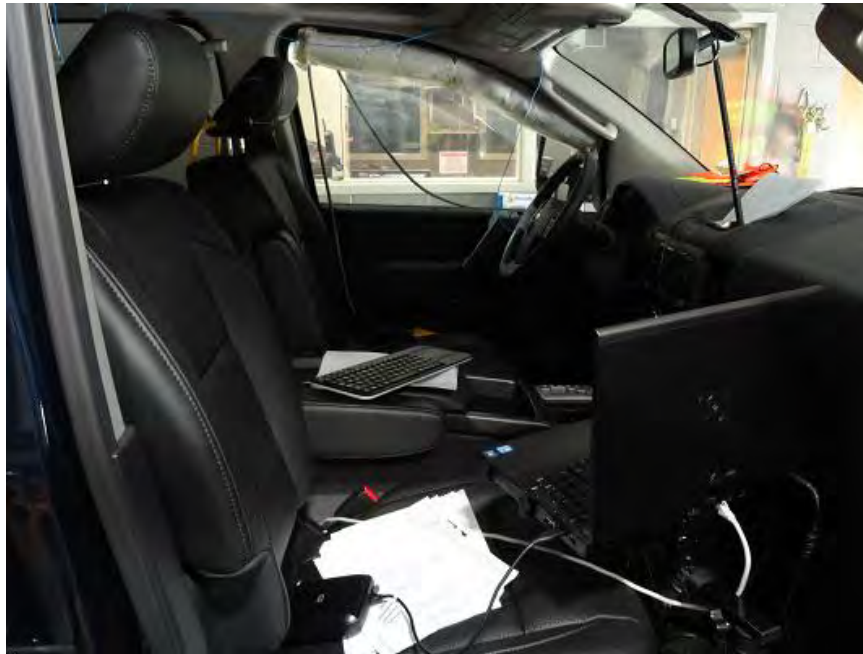


Figure 3.13 Monitoring data collection live



Figure 3.14 In-board and Outboard microphones- front view

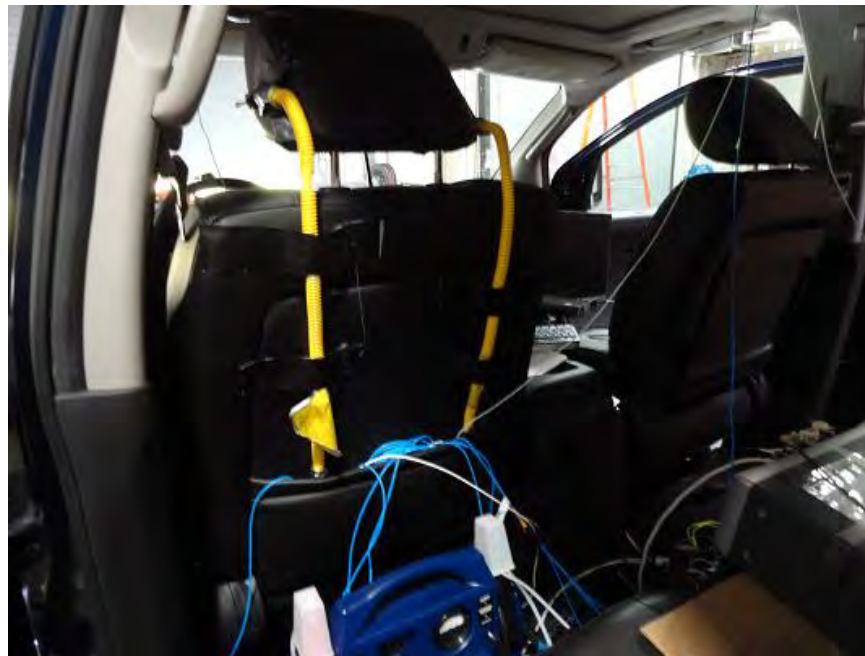


Figure 3.15 microphones- back view

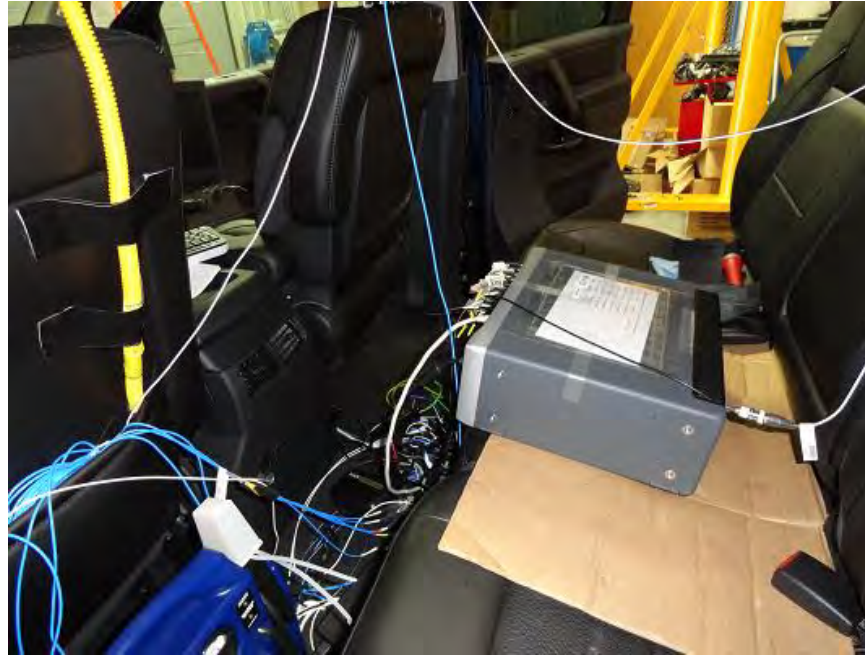


Figure 3.16 Tachometers hardware and frontend



Figure 3.17 Tri-axial accelerometer attached to steering wheel



Figure 3.18 Tachometer and imbalance mass attached at the front driveshaft



Figure 3.19 Front-axle plane and the tri-axial accelerometer position is pointed out

CHAPTER IV

EXPERIMENTAL SENSITIVITY FUNCTIONS

Vehicles are moving structures[4]; specifically, automotive vehicles are a type of vehicle that move both people and goods on road or off road. NVH is a resultant of the many different forces on the vehicle while in operation. For example, wind force is one major cause of vehicle NVH. In addition, other factors may affect the vehicle structure such as pure-engine forces; other forces may also cause NVH as power is transmitted through rotating parts like the transmission case, transfer case, drivelines, axles, wheel and tire assemblies, and other connected parts. NVH can be introduced through force(s) at predetermined planes; this leads to various levels of NVH at different receiving points depending on the position of the introduced force, its direction, and its amplitude. Other factors like NVH transfer path and its inherent attributes beside frequency levels play an important role over the resultant NVH measured at the CTPs of interest.

In order to study vehicle's sensitivity to imbalance forces at planes of interest, an imbalance was introduced to the drivelines on these planes. As expected, introducing imbalance forces at specific planes led to higher NVH levels in the truck. The collected data from all channels supported the subjective feedback of increased NVH at the driver's CTP's, which agrees with the theoretical expectation of a higher level of NVH due to the introduced imbalance.

Calculating sensitivity at specific locations [24] was straight forward after taking into consideration few needed conversions. The first step was taking raw data from accelerometers and microphones through dedicated channels and then obtaining an average of multiple runs. Dynamic systems in interactive environment will have uncontrollable factors that may affect the levels of NVH randomly; in order to mitigate such noise while testing; six runs were conducted for each case and then averaged.

Multiple testing runs are broken into the following main groups:

- 4WD engaged
- 2WD (disengaging 4WD)

Each group is broken into a subgroup based on the time during the run:

- Run up-RU (sweeping up by increasing the speed from standstill).
- Run down-RD (sweeping down by decreasing speed from the high reached speed).

The commercial software Test.Lab's signature testing (Figure 4.1) created and maintained by LMS International states, "MS Test.Lab Signature Testing offers online and off-line harmonic analyses based on narrow-band waterfall spectra and color maps, measured on rotating equipment in any operating condition [25]."



Figure 4.1 The commercial software Test.Lab's signature testing

Calculating averages for each testing setup was conducted utilizing Test.Lab because it possesses many tools that can manipulate and process data (see Figure 4.2 and Figure 4.3).

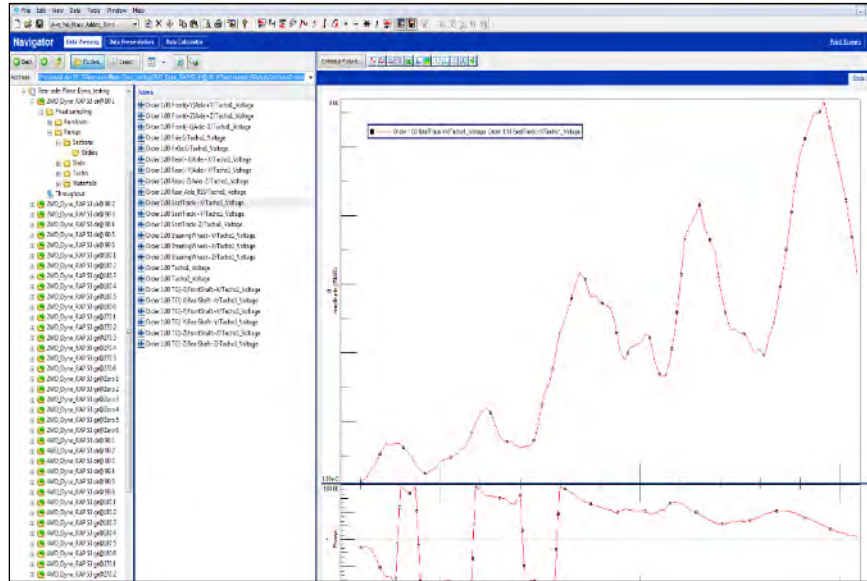


Figure 4.2 Selecting runs to be averaged

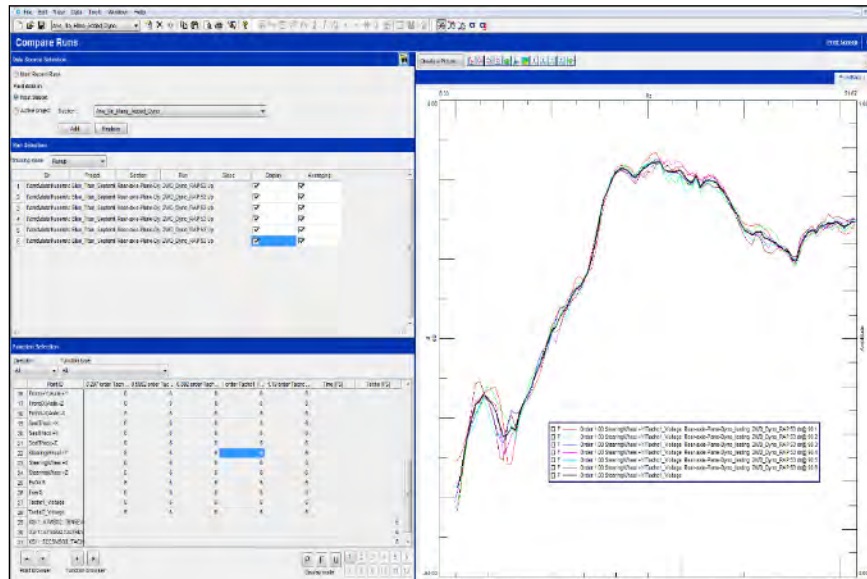


Figure 4.3 Calculating average for each run and part of a run (i.e., RU or RD)

In order to consider data points at specific rpm speed, the data has to be rearranged with equidistant x-axis points (i.e., rpm specified points). The points were

taken from 600-3100 rpm at every 5 rpm speed up or speed down. The previous software was utilized to conduct this calculation, as seen in Figure 4.4

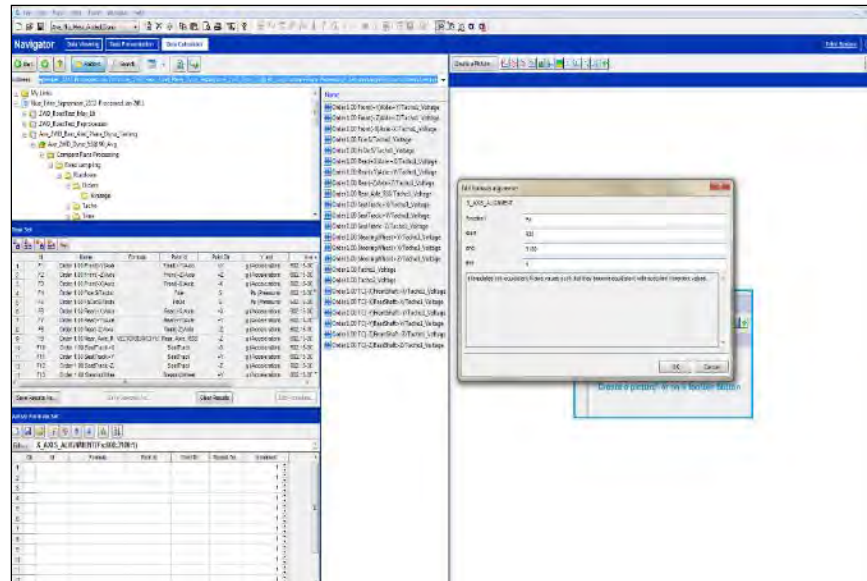


Figure 4.4 X-axis alignment by arranging equidistance points

After this point, all data from each channel of each run (i.e., 2WD or 4WD), run-up or rundown, was transferred to a spreadsheet in order to conduct further calculations. The number of points for each channel in each run was 500 points with 5 rpm increments. Microsoft Excel 2010 product was used to calculate sensitivity, as seen in Figure 4.5.

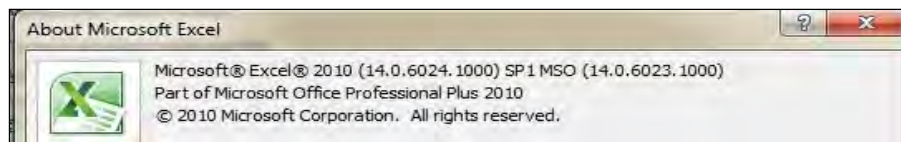


Figure 4.5 Microsoft Excel 2010 used for further sensitivity calculations

A snapshot of the copied data to the spreadsheet from the data acquisition software Test.Lab, before any manipulation or calculation conducted, is shown in Figure 4.6.

@90			@180			@270			@Zero			As Is 2WD (No Mass Added)		
rpm	m/s ²	°	rpm	m/s ²	°	rpm	m/s ²	°	rpm	m/s ²	°	rpm	m/s ²	°
Linear	Amplitude	Phase	Linear	Amplitude	Phase	Linear	Amplitude	Phase	Linear	Amplitude	Phase	Linear	Amplitude (RM)	Phase
600.00	0.00	0.00	600.00	0.02	15.40	600.00	0.02	-96.99	600.00	0.03	-167.82	600.00	0.02	-169.81
605.00	0.00	0.00	605.00	0.02	15.57	605.00	0.02	-97.94	605.00	0.03	-169.03	605.00	0.02	-172.45
610.00	0.03	123.52	610.00	0.02	15.92	610.00	0.02	-99.81	610.00	0.03	-171.34	610.00	0.02	-176.64
615.00	0.03	121.83	615.00	0.02	16.28	615.00	0.02	-101.67	615.00	0.03	-173.66	615.00	0.02	179.18
620.00	0.03	119.96	620.00	0.02	16.63	620.00	0.02	-103.54	620.00	0.03	-175.97	620.00	0.01	174.99
625.00	0.03	118.45	625.00	0.02	16.99	625.00	0.02	-105.46	625.00	0.03	-178.26	625.00	0.01	170.65
630.00	0.03	117.44	630.00	0.02	17.19	630.00	0.02	-107.71	630.00	0.03	179.52	630.00	0.01	166.03
635.00	0.03	116.41	635.00	0.02	17.38	635.00	0.02	-109.73	635.00	0.03	177.31	635.00	0.01	162.59
640.00	0.03	115.27	640.00	0.02	17.57	640.00	0.02	-111.74	640.00	0.03	175.10	640.00	0.01	159.53
645.00	0.03	114.12	645.00	0.02	17.76	645.00	0.02	-113.76	645.00	0.03	172.89	645.00	0.01	156.47
650.00	0.03	113.37	650.00	0.02	18.60	650.00	0.02	-115.34	650.00	0.03	171.13	650.00	0.01	153.46
655.00	0.03	114.14	655.00	0.02	21.12	655.00	0.02	-114.86	655.00	0.03	171.70	655.00	0.01	151.76
660.00	0.03	114.98	660.00	0.02	23.64	660.00	0.02	-113.91	660.00	0.03	172.28	660.00	0.01	149.92
665.00	0.03	115.83	665.00	0.02	26.17	665.00	0.02	-112.95	665.00	0.03	172.85	665.00	0.01	148.08
670.00	0.03	116.68	670.00	0.02	28.69	670.00	0.02	-111.99	670.00	0.03	173.43	670.00	0.01	146.85
675.00	0.03	116.72	675.00	0.02	30.30	675.00	0.02	-109.71	675.00	0.03	173.77	675.00	0.01	147.49
680.00	0.03	114.23	680.00	0.02	30.00	680.00	0.02	-104.61	680.00	0.03	173.07	680.00	0.01	152.83
685.00	0.03	111.70	685.00	0.02	29.70	685.00	0.02	-99.22	685.00	0.03	172.38	685.00	0.02	158.17
690.00	0.03	109.17	690.00	0.02	29.40	690.00	0.02	-93.82	690.00	0.03	171.69	690.00	0.02	163.52
695.00	0.03	106.64	695.00	0.02	29.10	695.00	0.02	-88.43	695.00	0.03	170.99	695.00	0.02	169.65
700.00	0.03	103.58	700.00	0.03	26.50	700.00	0.02	-84.16	700.00	0.03	170.37	700.00	0.02	175.95
705.00	0.03	101.18	705.00	0.03	19.96	705.00	0.02	-88.75	705.00	0.03	168.24	705.00	0.02	163.95

Figure 4.6 Copied data into the spreadsheet

Data points shown in Figure 4.6 present three columns, repeated five times, representing the four angles on the each pre-specified plane. The case represented here pertains to the rear-driveshaft-axle plane, while the measurement runs are for 2WD and run-up (RU). Each column holds the following data type from left to right: speed (rpm), acceleration amplitude (m/s²), and phase angle (degrees). The imbalance was introduced at four different angles: Zero, 90, 180 and 270 degrees. The base or as-is case with no imbalance introduced is the last set of columns, three columns, to the right in Figure 6 and the lowest curve line in Figure 4.7. The curves above the base case in Figure 4.7

represent the acceleration amplitudes after introducing imbalance into the rear driveshaft axle plane at different angles; the acceleration measurements at the seat track Y direction, in this case, grows higher as rotational speed of the driveline increases. The base case in cyan looks flat; this is because the driveline of the truck has been balanced in the most effective manner the production process allows in a manufacturing setting by the OEM

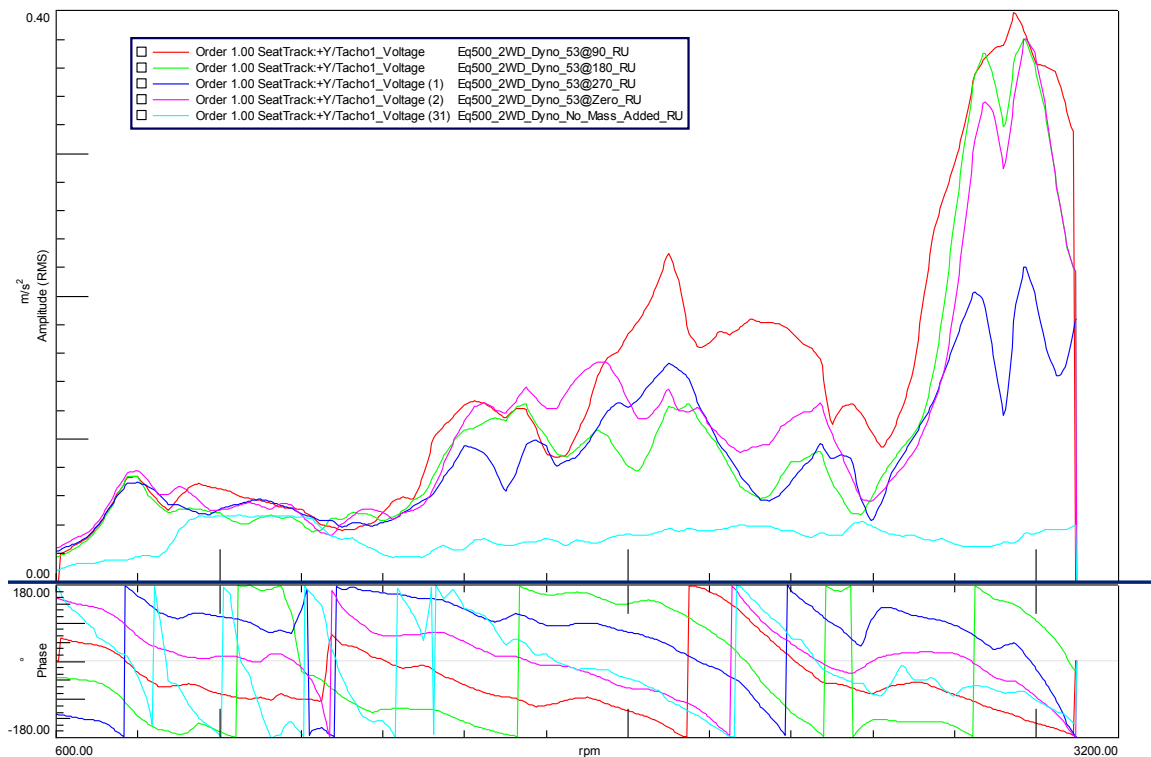


Figure 4.7 Amplitude and phase curves of the collected data

Data acquisition software represents phasor values in a manner that needs to be addressed and normalized in order to be used for the intended calculations. Phase angles are measured from the positive x-axis clockwise and then again counterclockwise from zero to 180 degrees; this is how the phase's values come out when transitioned into the

spreadsheet. Changing phase value into one system (i.e., counterclockwise from positive x-axes) required some manipulation. In addition, the amplitude at each rpm speed was transformed into speed by dividing acceleration values by the rotation speed, as seen in Figure 4.8.

@90			@180			@270			@Zero			As Is 2WD (No Mass Added)		
rpm	mm/s	°	rpm	mm/s	°	rpm	mm/s	°	rpm	mm/s	°	rpm	mm/s	°
Linear	Amplitude	Phase	Linear	Amplitude	Phase	Linear	Amplitude	Phase	Linear	Amplitude	Phase	Linear	Amplitude	Phase
600.00	0.00	-90.00	600.00	0.33	-74.60	600.00	0.35	173.01	600.00	0.43	102.18	600.00	0.28	100.19
605.00	0.00	-90.00	605.00	0.33	-74.43	605.00	0.35	172.06	605.00	0.43	100.97	605.00	0.27	97.55
610.00	0.43	33.52	610.00	0.32	-74.08	610.00	0.34	170.19	610.00	0.43	98.66	610.00	0.26	93.36
615.00	0.43	31.83	615.00	0.31	-73.72	615.00	0.33	168.33	615.00	0.42	96.34	615.00	0.24	89.18
620.00	0.42	29.96	620.00	0.31	-73.37	620.00	0.32	166.46	620.00	0.42	94.03	620.00	0.23	84.99
625.00	0.42	28.45	625.00	0.30	-73.01	625.00	0.32	164.54	625.00	0.42	91.74	625.00	0.21	80.65
630.00	0.41	27.44	630.00	0.29	-72.81	630.00	0.31	162.29	630.00	0.41	89.52	630.00	0.21	76.03
635.00	0.41	26.41	635.00	0.28	-72.62	635.00	0.30	160.27	635.00	0.41	87.31	635.00	0.20	72.59
640.00	0.41	25.27	640.00	0.28	-72.43	640.00	0.29	158.26	640.00	0.40	85.10	640.00	0.19	69.53
645.00	0.40	24.12	645.00	0.27	-72.24	645.00	0.28	156.24	645.00	0.40	82.89	645.00	0.19	66.47
650.00	0.40	23.37	650.00	0.26	-71.40	650.00	0.27	154.66	650.00	0.40	81.13	650.00	0.18	63.46
655.00	0.40	24.14	655.00	0.26	-68.88	655.00	0.26	155.14	655.00	0.39	81.70	655.00	0.18	61.76
660.00	0.40	24.98	660.00	0.26	-66.36	660.00	0.26	156.09	660.00	0.39	82.28	660.00	0.19	59.92
665.00	0.41	25.83	665.00	0.26	-63.83	665.00	0.25	157.05	665.00	0.39	82.85	665.00	0.19	58.08
670.00	0.41	26.68	670.00	0.26	-61.31	670.00	0.24	158.01	670.00	0.38	83.43	670.00	0.19	56.85
675.00	0.41	26.72	675.00	0.27	-59.70	675.00	0.24	160.29	675.00	0.38	83.77	675.00	0.19	57.49
680.00	0.42	24.23	680.00	0.28	-60.00	680.00	0.25	165.39	680.00	0.39	83.07	680.00	0.21	62.83
685.00	0.43	21.70	685.00	0.30	-60.30	685.00	0.26	170.78	685.00	0.40	82.38	685.00	0.22	68.17
690.00	0.44	19.17	690.00	0.32	-60.60	690.00	0.28	176.18	690.00	0.42	81.69	690.00	0.23	73.52
695.00	0.46	16.64	695.00	0.34	-60.90	695.00	0.29	-178.43	695.00	0.43	80.99	695.00	0.25	79.65
700.00	0.46	13.58	700.00	0.36	-63.50	700.00	0.30	-174.16	700.00	0.44	80.37	700.00	0.26	85.95

Figure 4.8 Data points rearranged

The next step is to construct a table of previously manipulated data points in both real and imaginary formats. In order to prepare for further manipulations in the future, each acceleration vector was transformed into its basic elements: real and imaginary parts, as seen in Figure 4.9.

rpm	@90		@180		@270		@Zero		As Is 2WD (No Mass Added)		
	mm/s		mm/s		mm/s		mm/s		rpm	mm/s	
	Real	Imaginary	Real	Imaginary	Real	Imaginary	Real	Imaginary	Linear	Real	Imaginary
600.00	0.00	0.00	0.09	-0.32	-0.35	0.04	-0.09	0.42	600	-0.05	0.28
605.00	0.00	0.00	0.09	-0.31	-0.34	0.05	-0.08	0.42	605	-0.04	0.27
610.00	0.36	0.24	0.09	-0.31	-0.34	0.06	-0.06	0.42	610	-0.01	0.25
615.00	0.36	0.22	0.09	-0.30	-0.33	0.07	-0.05	0.42	615	0.00	0.24
620.00	0.36	0.21	0.09	-0.29	-0.32	0.08	-0.03	0.42	620	0.02	0.23
625.00	0.37	0.20	0.09	-0.28	-0.31	0.08	-0.01	0.42	625	0.03	0.21
630.00	0.37	0.19	0.09	-0.28	-0.29	0.09	0.00	0.41	630	0.05	0.20
635.00	0.37	0.18	0.08	-0.27	-0.28	0.10	0.02	0.41	635	0.06	0.19
640.00	0.37	0.17	0.08	-0.26	-0.27	0.11	0.03	0.40	640	0.07	0.18
645.00	0.37	0.17	0.08	-0.26	-0.26	0.11	0.05	0.40	645	0.07	0.17
650.00	0.37	0.16	0.08	-0.25	-0.25	0.12	0.06	0.39	650	0.08	0.16
655.00	0.37	0.16	0.10	-0.25	-0.24	0.11	0.06	0.39	655	0.09	0.16
660.00	0.37	0.17	0.11	-0.24	-0.24	0.10	0.05	0.39	660	0.09	0.16
665.00	0.37	0.18	0.12	-0.24	-0.23	0.10	0.05	0.38	665	0.10	0.16
670.00	0.36	0.18	0.13	-0.23	-0.23	0.09	0.04	0.38	670	0.10	0.16
675.00	0.37	0.19	0.14	-0.23	-0.23	0.08	0.04	0.38	675	0.10	0.16
680.00	0.39	0.17	0.14	-0.25	-0.24	0.06	0.05	0.39	680	0.09	0.18
685.00	0.40	0.16	0.15	-0.26	-0.26	0.04	0.05	0.40	685	0.08	0.20
690.00	0.42	0.15	0.16	-0.28	-0.28	0.02	0.06	0.41	690	0.07	0.22
695.00	0.44	0.13	0.17	-0.30	-0.29	-0.01	0.07	0.42	695	0.04	0.24
700.00	0.45	0.11	0.16	-0.32	-0.30	-0.03	0.07	0.44	700	0.02	0.26

Figure 4.9 Phasors represented in real and imaginary format

Then, all imbalance directions were averaged into one vector using the real values, as shown in Figure 4.10.

rpm	Average of all directions	
	Real	Imaginary
600	-0.08878503	0.03719444
605	-0.08487463	0.03930532
610	0.01140287	0.10273677
615	0.01909686	0.10341524
620	0.02674933	0.10341577
625	0.03387729	0.10398787
630	0.04106235	0.10504502
635	0.04782146	0.10535695
640	0.05443483	0.10512583
645	0.06087924	0.10459465
650	0.06674645	0.10416466
655	0.06977630	0.10447083
660	0.07237511	0.10464803
665	0.07490594	0.10501628
670	0.07736308	0.10557043
675	0.07974651	0.10331517
680	0.08294012	0.09492067
685	0.08638464	0.08513463
690	0.09029355	0.07422922
695	0.09474114	0.06218575
700	0.09572353	0.04775561

Figure 4.10 Phasors averaged in real and imaginary format.

The baseline case was then subtracted from the calculated average (i.e., all four introduced imbalance directions) into one value that represents the average increase in NVH after introducing imbalance from the baseline case. This is followed by dividing the result by the imbalance introduced at each plane. Imbalance units are in gram-centimeter (gm-cm), as seen in Figure 4.11; this is the sensitivity. Standard format is represented in amplitude and phase angle Figure 4.12.

Sensitivity		
rpm	(mm/s)/(gm-cm)	
Linear	Real	Imaginary
600	-0.00033216	0.00120429
605	-0.00062897	0.00100020
610	-0.00087270	0.00047994
615	-0.00074771	-0.00003053
620	-0.00035376	-0.00030461
625	0.00003181	-0.00026355
630	-0.00011941	-0.00029564
635	-0.00015673	-0.00026693
640	-0.00019030	-0.00022678
645	-0.00021760	-0.00017425
650	-0.00023083	-0.00010933
655	-0.00022795	-0.00007414
660	-0.00029471	-0.00004111
665	-0.00036740	0.00000101
670	-0.00044610	0.00005348
675	-0.00053044	0.00011745
680	-0.00056322	0.00012333
685	-0.00054015	0.00009760
690	-0.00051958	0.00007110
695	-0.00050148	0.00004396
700	-0.00048600	0.00001629

Figure 4.11 Sensitivity represented in complex numbers' format.

rpm	Calculated Sensitivity	
	Amplitude	Phase
Linear	(mm/s)/(gm-cm)	deg
600	0.001249256479	-15.42
605	0.001181528941	-32.16
610	0.000995963545	-61.19
615	0.000748333987	87.66
620	0.000466829002	49.27
625	0.000265463473	-6.88
630	0.000318849821	21.99
635	0.000309542699	30.42
640	0.000296046617	40.00
645	0.000278772290	51.31
650	0.000255414580	64.66
655	0.000239706233	71.98
660	0.000297567660	82.06
665	0.000367398720	-89.84
670	0.000449293320	-83.16
675	0.000543288677	-77.51
680	0.000576563395	-77.65
685	0.000548901166	-79.76
690	0.000524418568	-82.21
695	0.000503399523	-84.99
700	0.000486276215	-88.08

Figure 4.12 Sensitivity in magnitude and modulus.

Each plane of the four studied planes with imbalance leads to 32 distinct sensitivity calculated graphs. This is due to the number of channels representing CTPs (i.e., eight) multiplied by driveline engagement (i.e., 4WD or 2WD), which is then multiplied by driving condition option (i.e., run-up (RU) or rundown (RD)).

Sensitivity Curves

A system can be viewed as a black box which one or more inputs will cause one or more outputs[26]. In an LTI system (i.e., linear Time Invariant system) is a system can be described by linear differential equations. I particular interest in time invariant systems in which all parameters are independent of time can be a good approximation of many physical systems. The system, viewed as a black box, which relates inputs and outputs which are caused by the inputs. The sensitivity curves are adapted to show the output per unit input over a spectrum of selected frequencies, in our case it is a non-stationary input signal[27] which has been processed using scan analysis with a window function. Utilizing mathematical tools like Fourier[28] and Laplace transformers are common to transform time domain systems into frequency domain systems. Such transformation tools help ease the mathematical calculations such as convolutions and trig identity representation and manipulation.

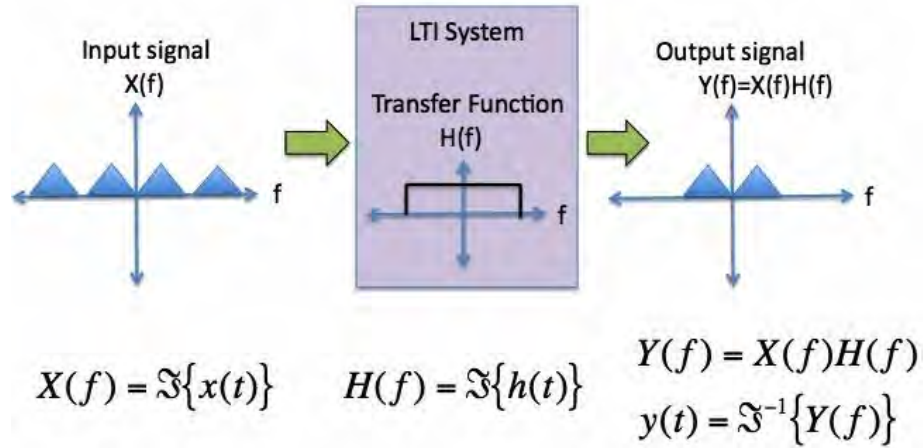


Figure 4.13 LTI system representations in time and frequency domains[29]

Rear Driveshaft and Rear Axle Plane

On this plane, sensitivity calculations were conducted as described earlier, calculating sensitivity curves for the different driveline engagement modes; (i.e., 2WD and 4WD) and different driving modes; (i.e., run up and run down). The others planes' sensitivity curves can be found in APPENDIX A.

Two Wheel Drive (2WD)-Run up (RU) Sensitivity Calculations:

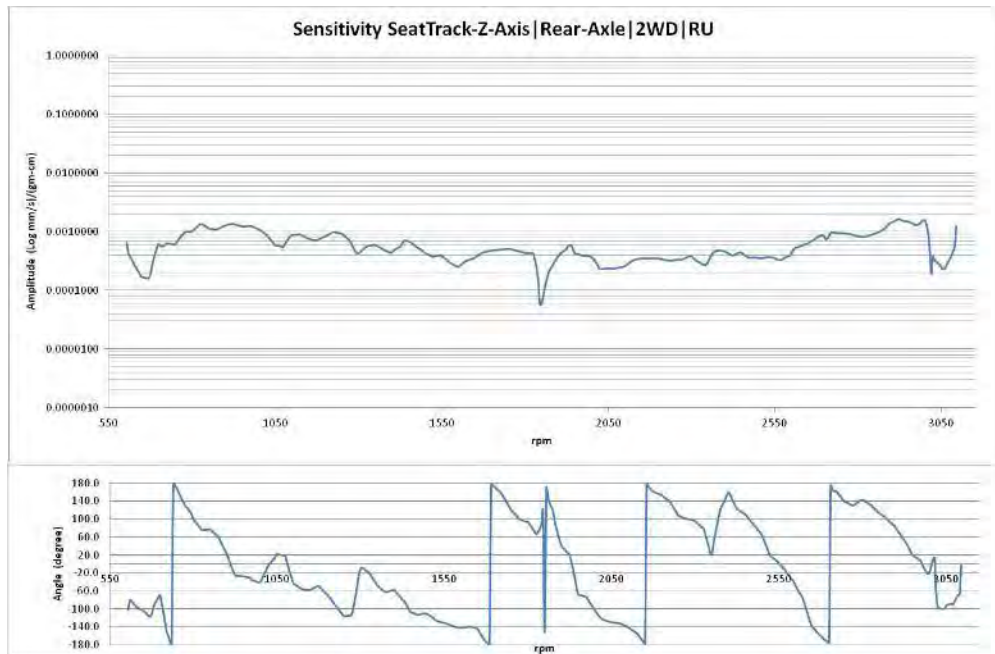


Figure 4.14 Sensitivity and phase Seat-Track-Z-Axis | Rear-Axle | 2WD |RU

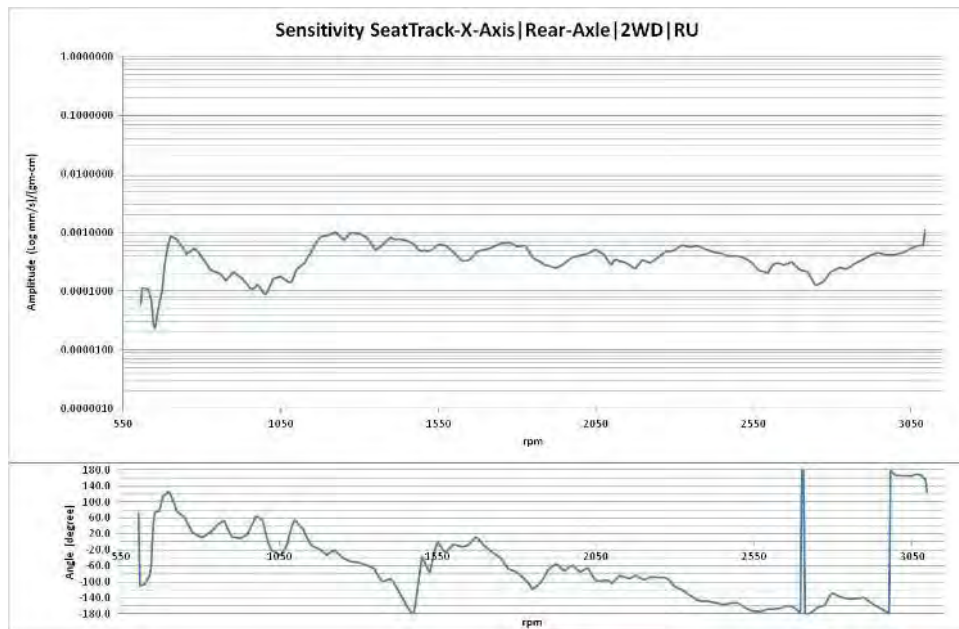


Figure 4.15 Sensitivity and phase Seat-Track-X-Axis | Rear-Axle | 2WD |RU

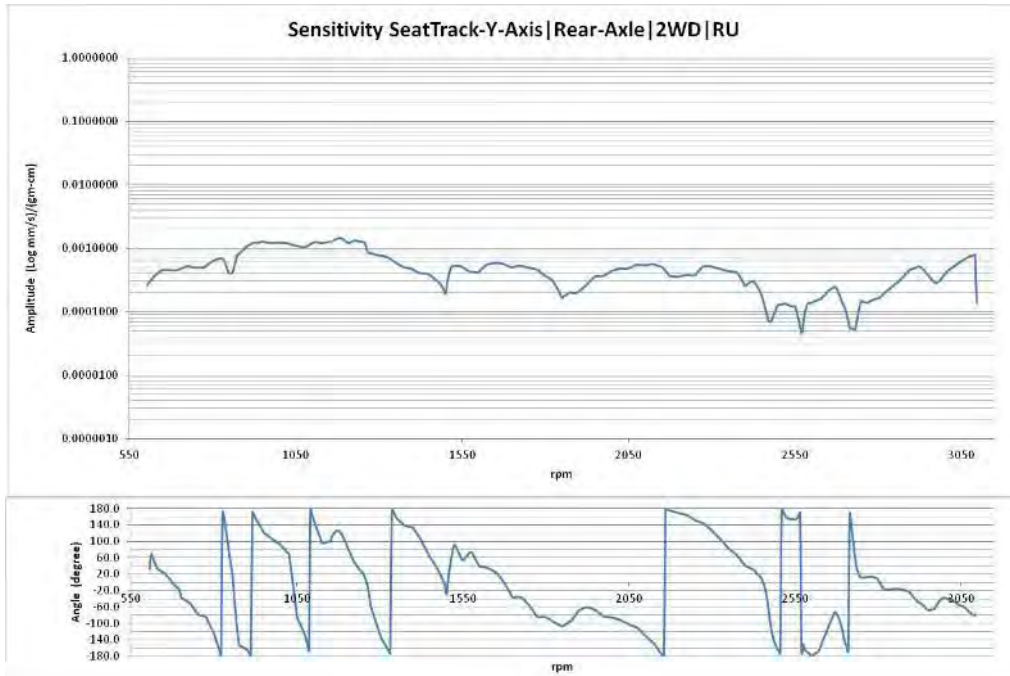


Figure 4.16 Sensitivity and phase Seat-Track-Y-Axis | Rear-Axle | 2WD |RU

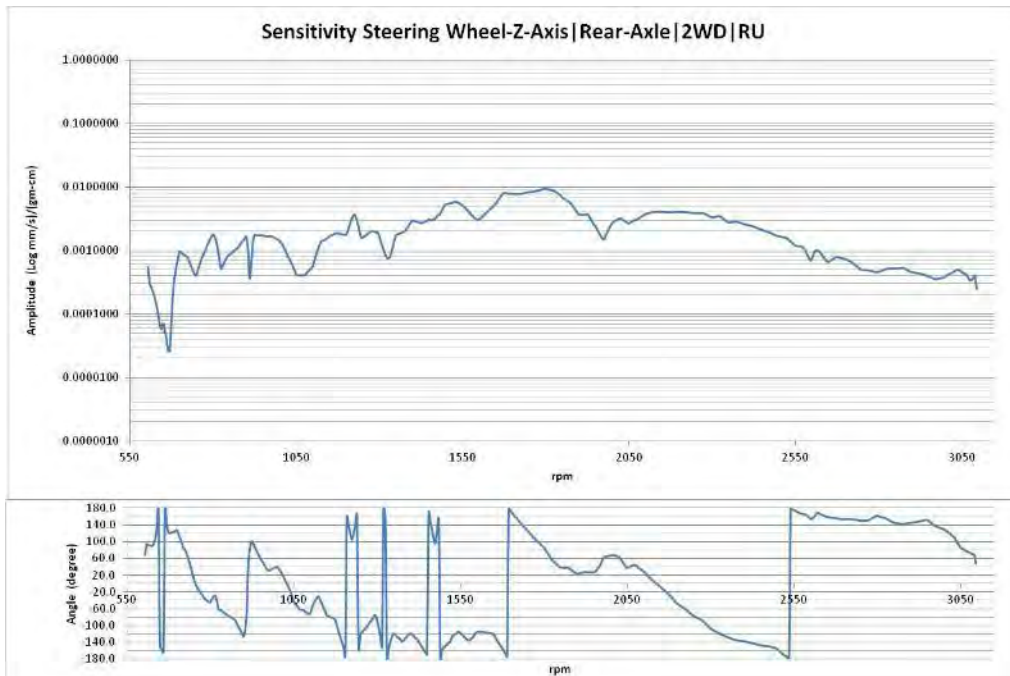


Figure 4.17 Sensitivity and phase Steering Wheel-Z-Axis | Rear-Axle | 2WD |RU

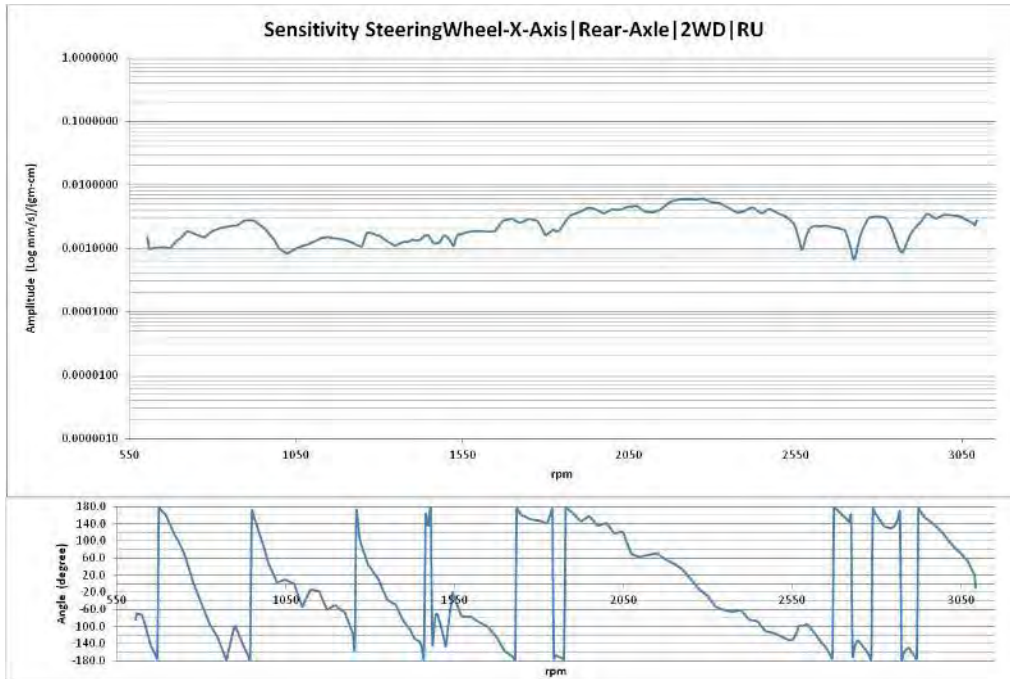


Figure 4.18 Sensitivity and phase Steering Wheel-X-Axis | Rear-Axle | 2WD |RU

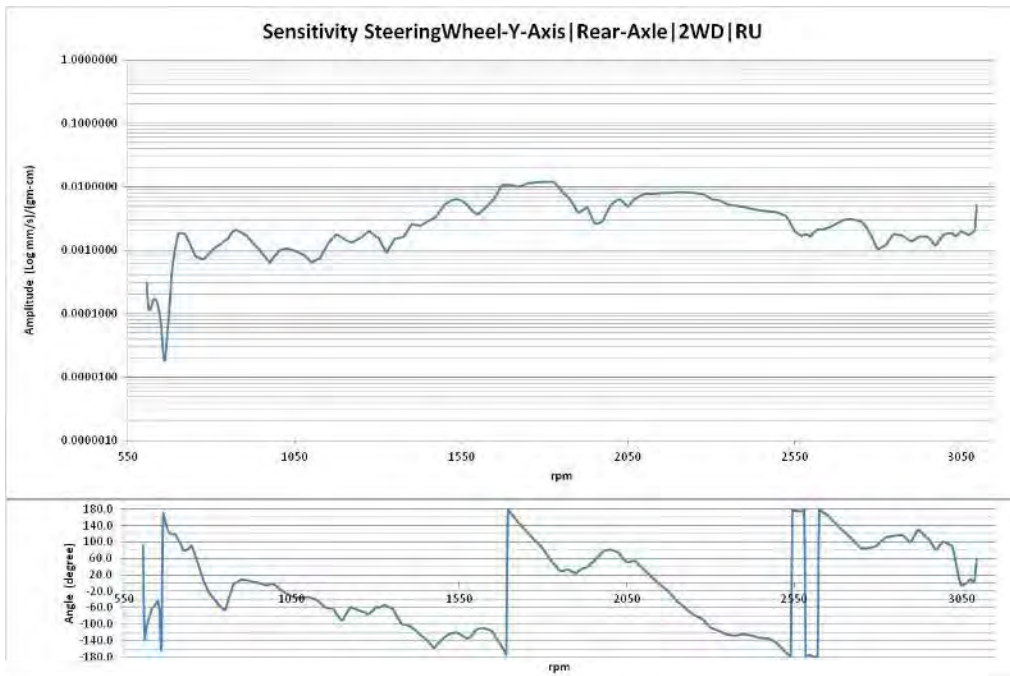


Figure 4.19 Sensitivity and phase Steering Wheel-Y-Axis | Rear-Axle | 2WD |RU

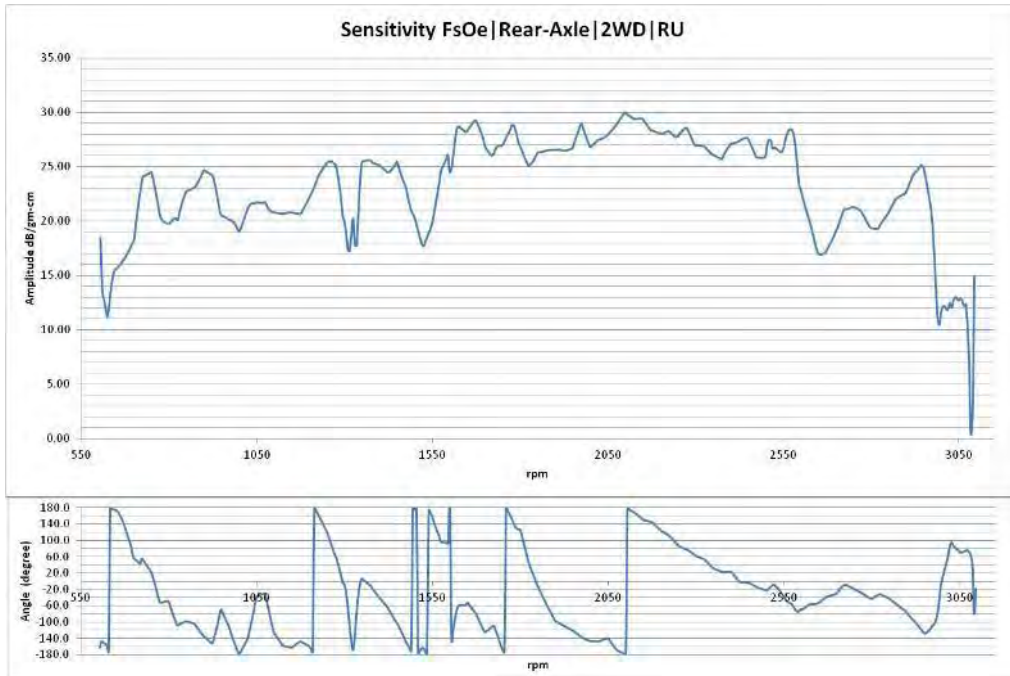


Figure 4.20 Sensitivity and phase FsOe | Rear-Axle | 2WD | RU

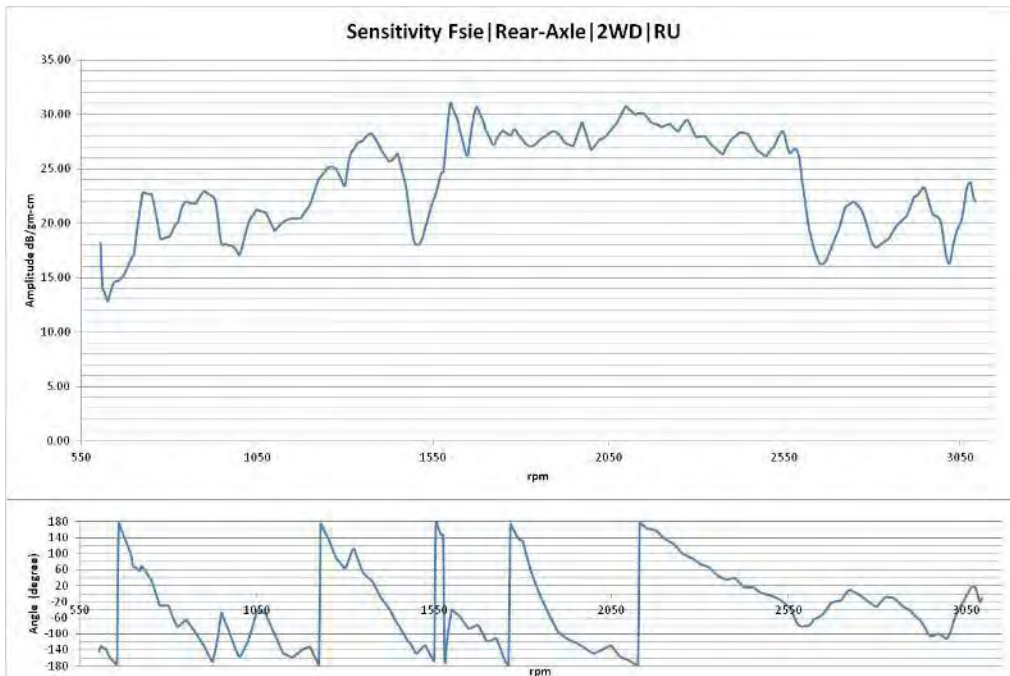


Figure 4.21 Sensitivity and phase Fsie | Rear-Axle | 2WD | RU

Two Wheel Drive (2WD)-Run down (RD) Sensitivity Calculations:

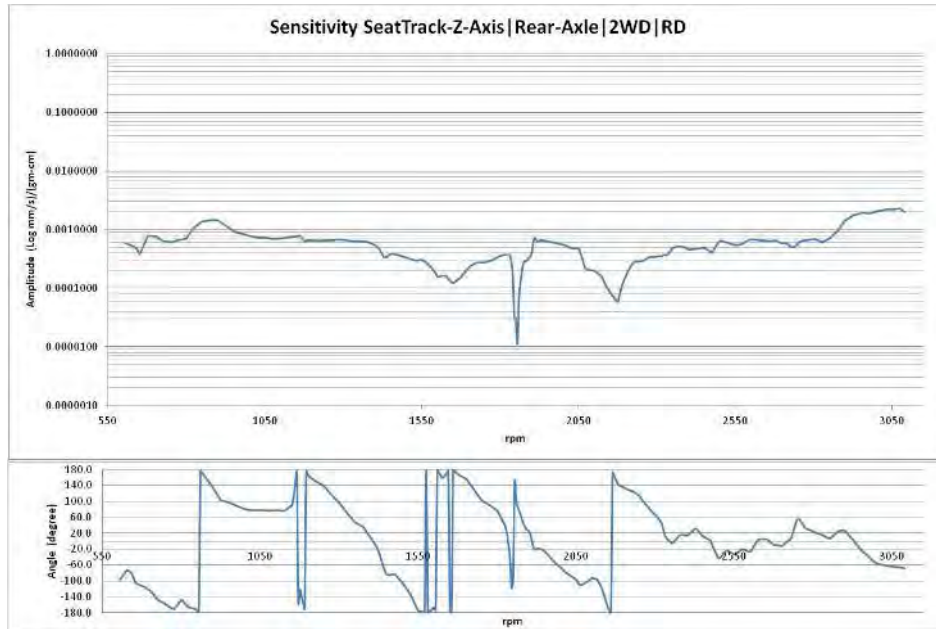


Figure 4.22 Sensitivity and phase Seat Track -Z-Axis | Rear-Axle | 2WD | RD

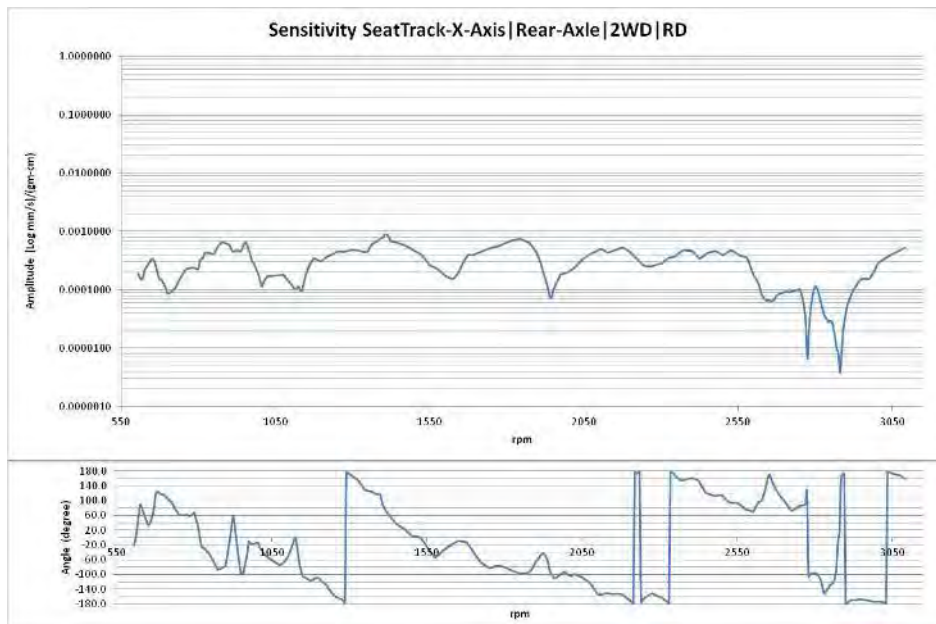


Figure 4.23 Sensitivity and phase Seat Track -X-Axis | Rear-Axle | 2WD | RD

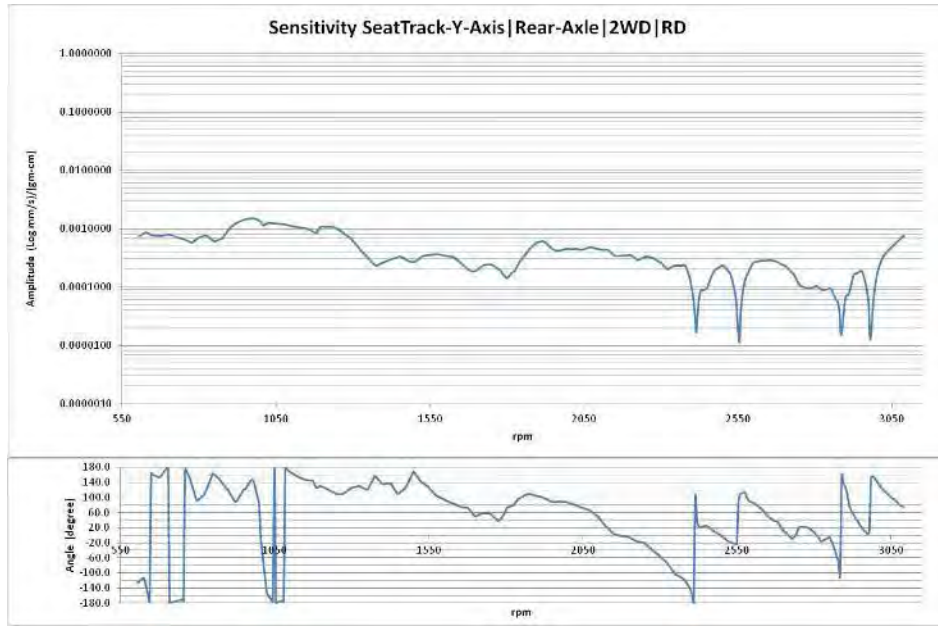


Figure 4.24 Sensitivity and phase Seat Track -Y-Axis| Rear-Axle | 2WD |RD

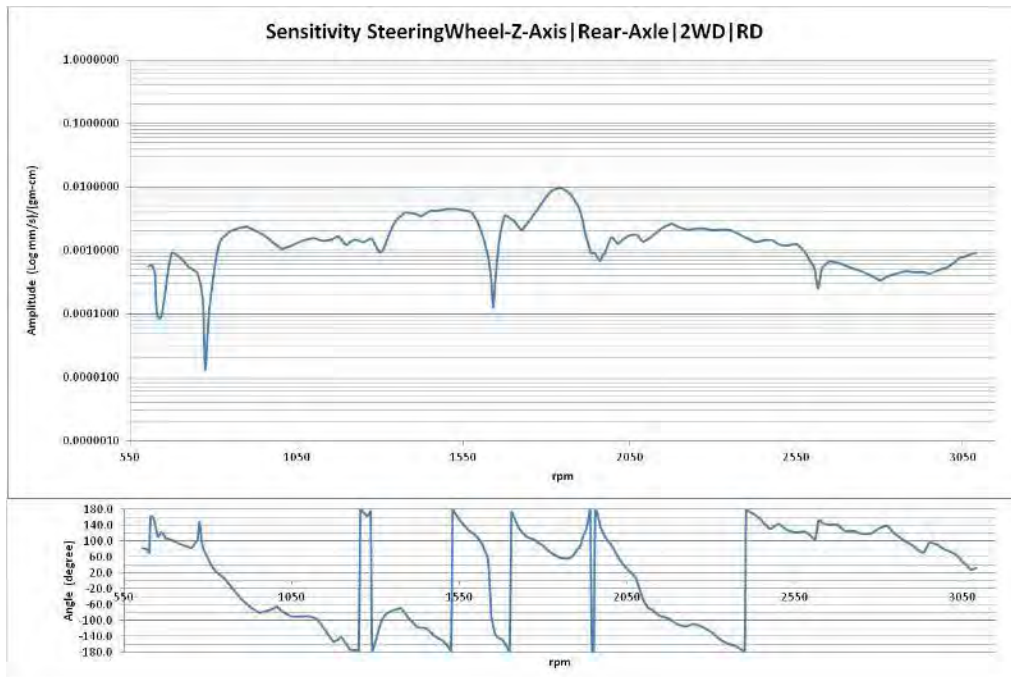


Figure 4.25 Sensitivity and phase Steering Wheel-Z-Axis| Rear-Axle | 2WD |RD

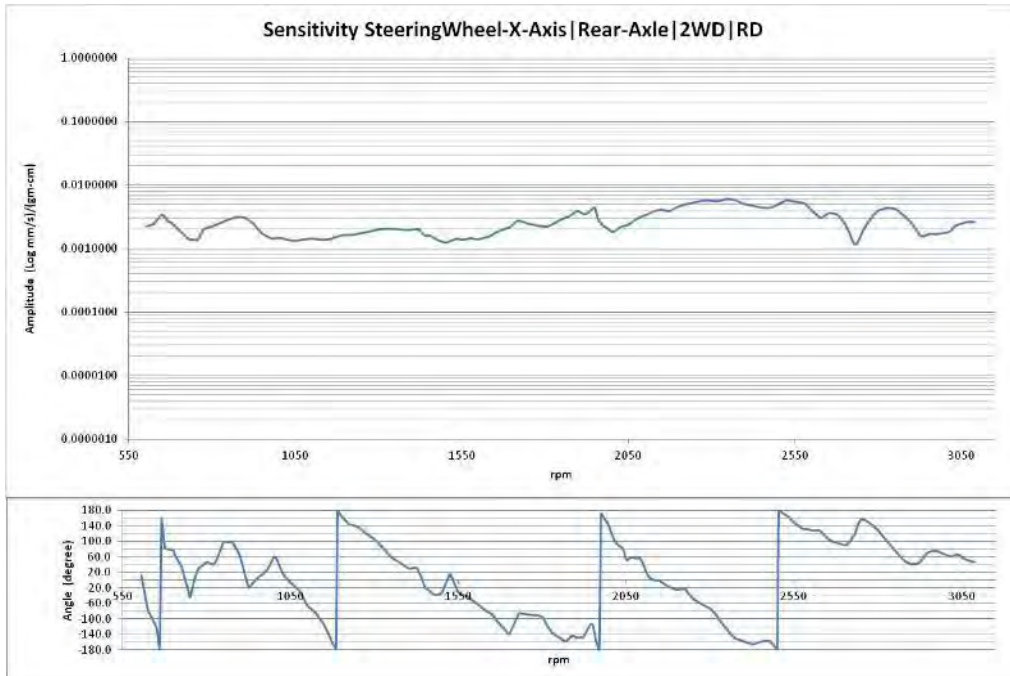


Figure 4.26 Sensitivity and phase Steering Wheel-X-Axis| Rear-Axle | 2WD |RD

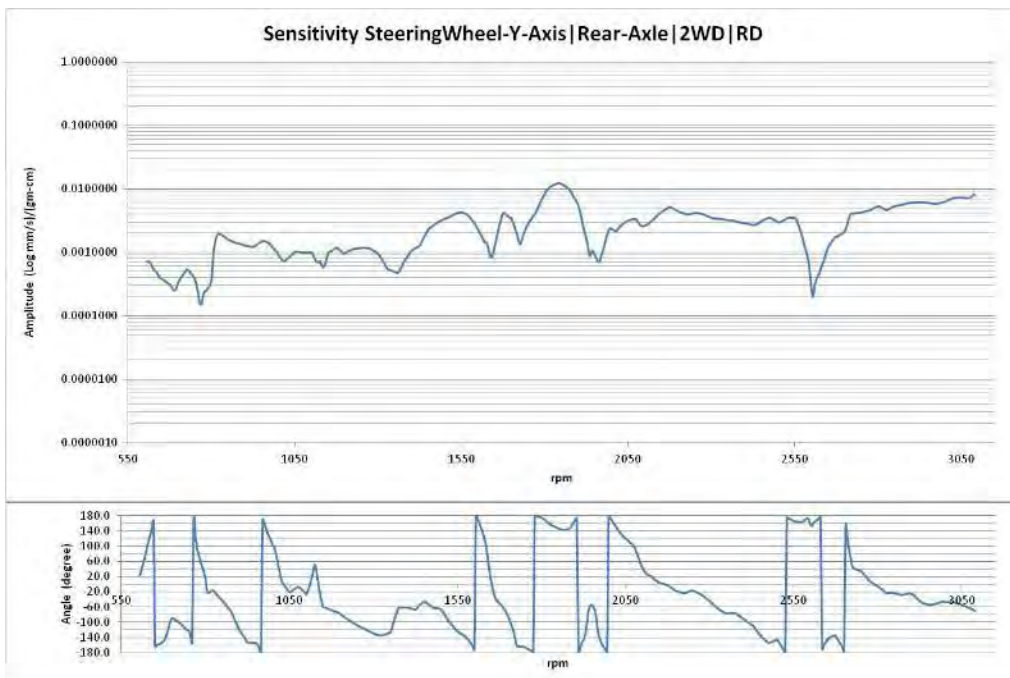


Figure 4.27 Sensitivity and phase Steering Wheel-Y-Axis| Rear-Axle | 2WD |RD

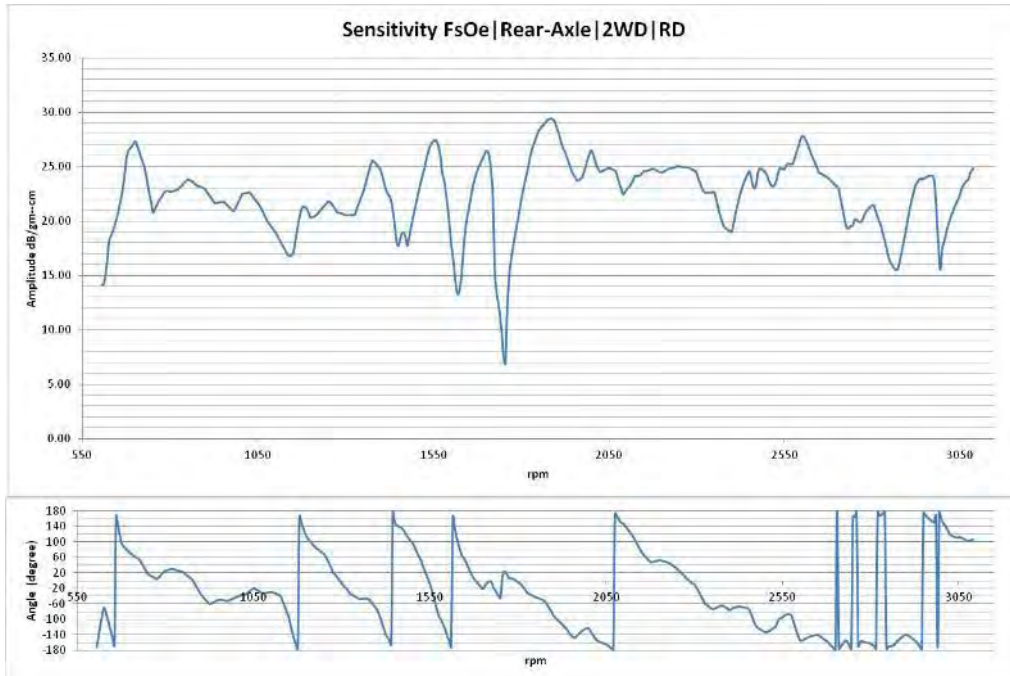


Figure 4.28 Sensitivity and phase FsOe | Rear-Axle | 2WD |RD

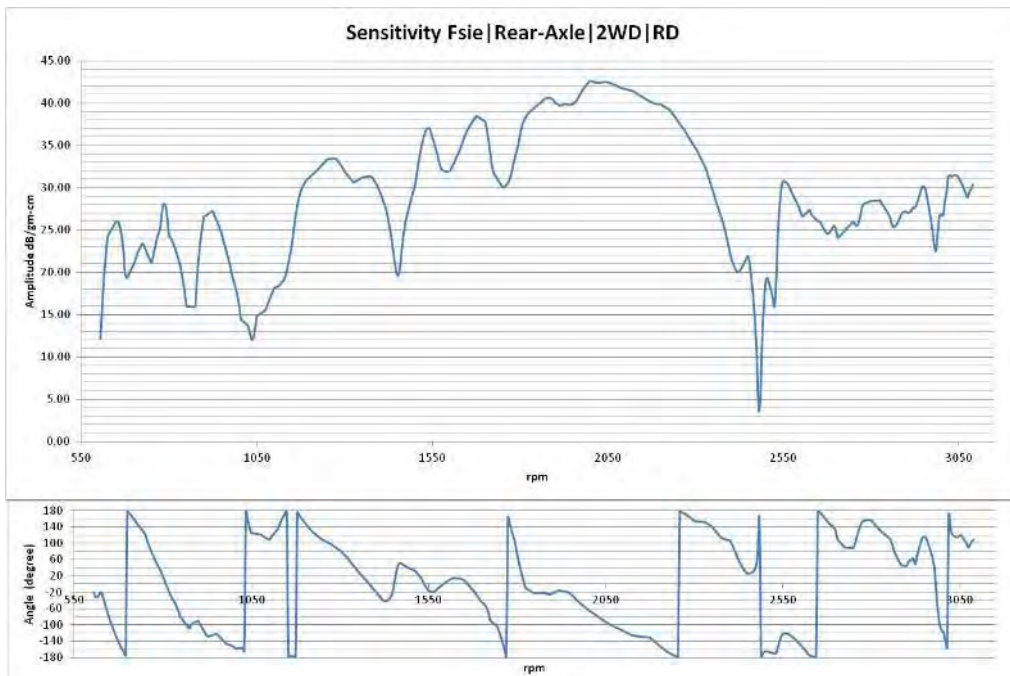


Figure 4.29 Sensitivity and phase Fsie | Rear-Axle | 2WD |RD

Four Wheel Drive (4WD)-Run up (RU) Sensitivity Calculations:

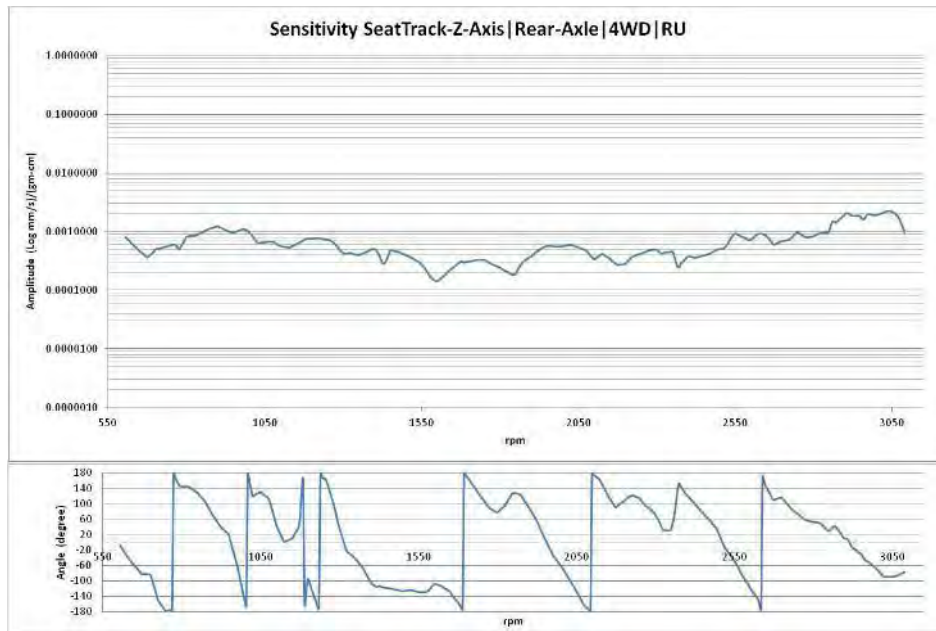


Figure 4.30 Sensitivity and phase Seat-Track-Z-Axis | Rear-Axle | 4WD |RU

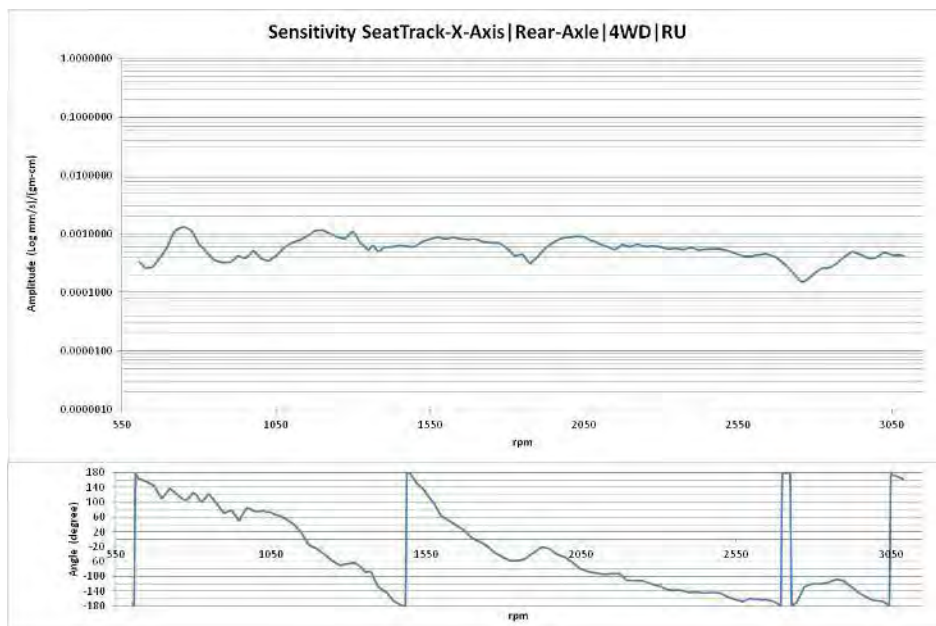


Figure 4.31 Sensitivity and phase Seat-Track-X-Axis | Rear-Axle | 4WD |RU

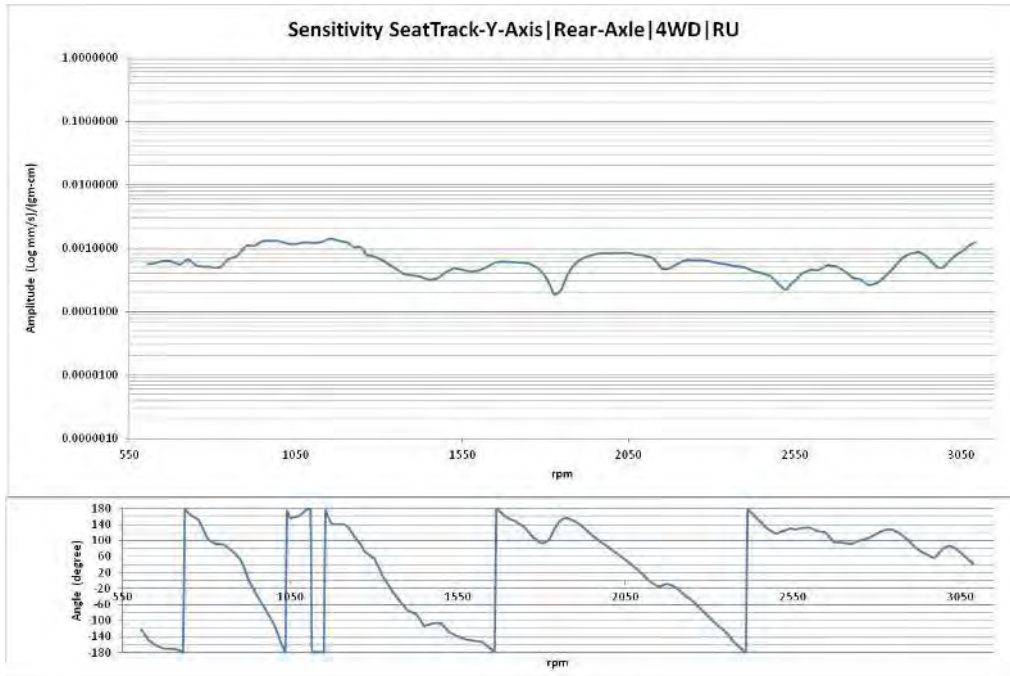


Figure 4.32 Sensitivity and phase Seat-Track-Y-Axis | Rear-Axle | 4WD | RU

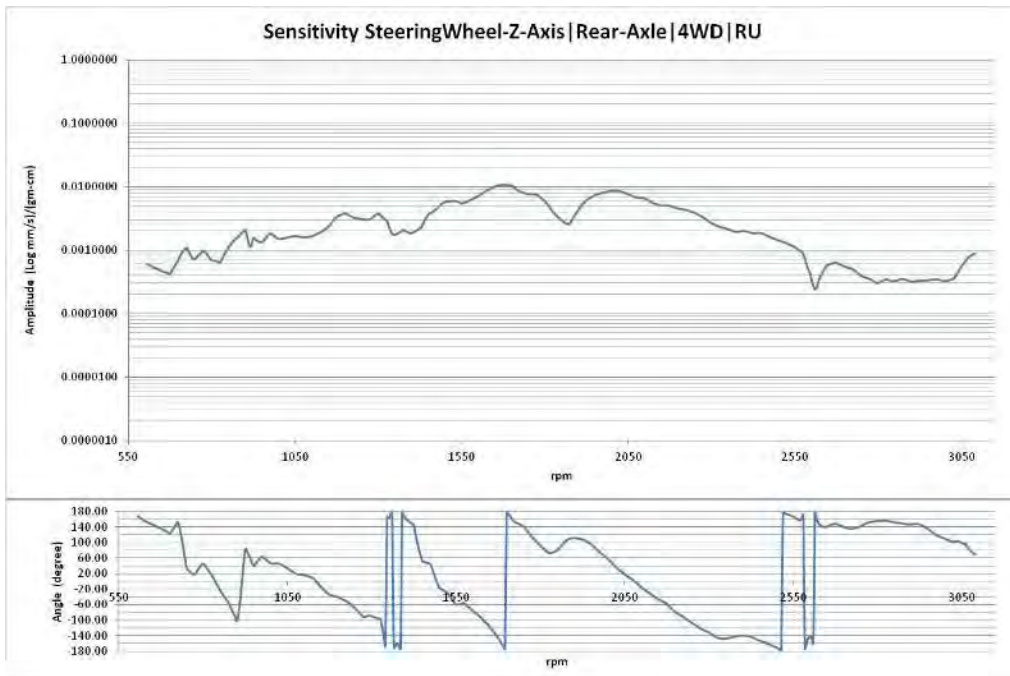


Figure 4.33 Sensitivity and phase Steering Wheel-Z-Axis | Rear-Axle | 4WD | RU

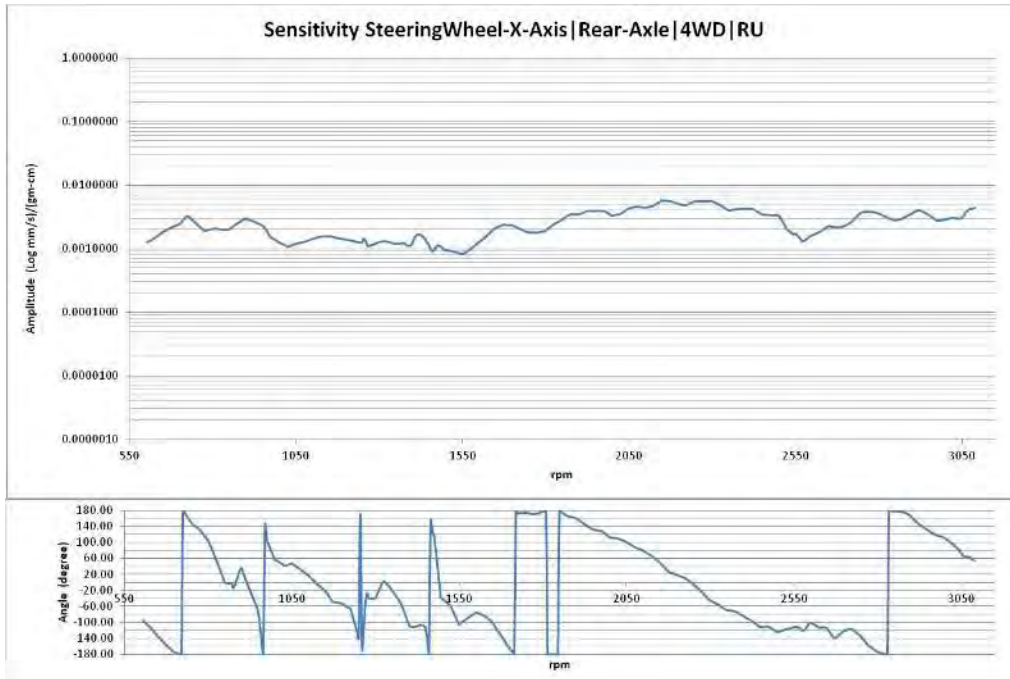


Figure 4.34 Sensitivity and phase Steering Wheel-X-Axis | Rear-Axle | 4WD |RU

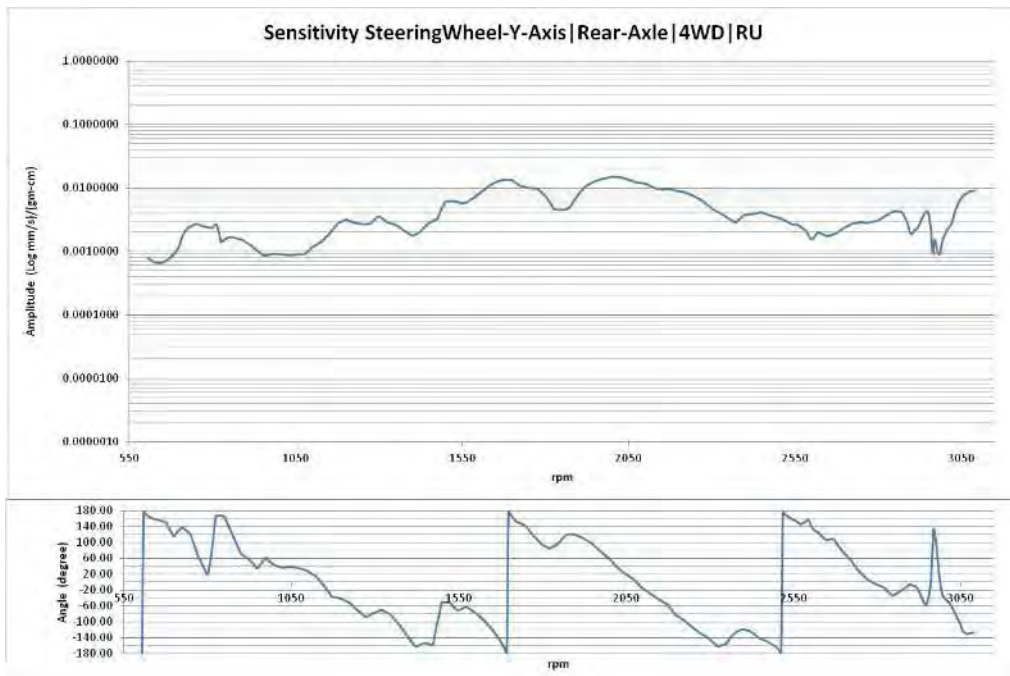


Figure 4.35 Sensitivity and phase Steering Wheel-Y-Axis | Rear-Axle | 4WD |RU

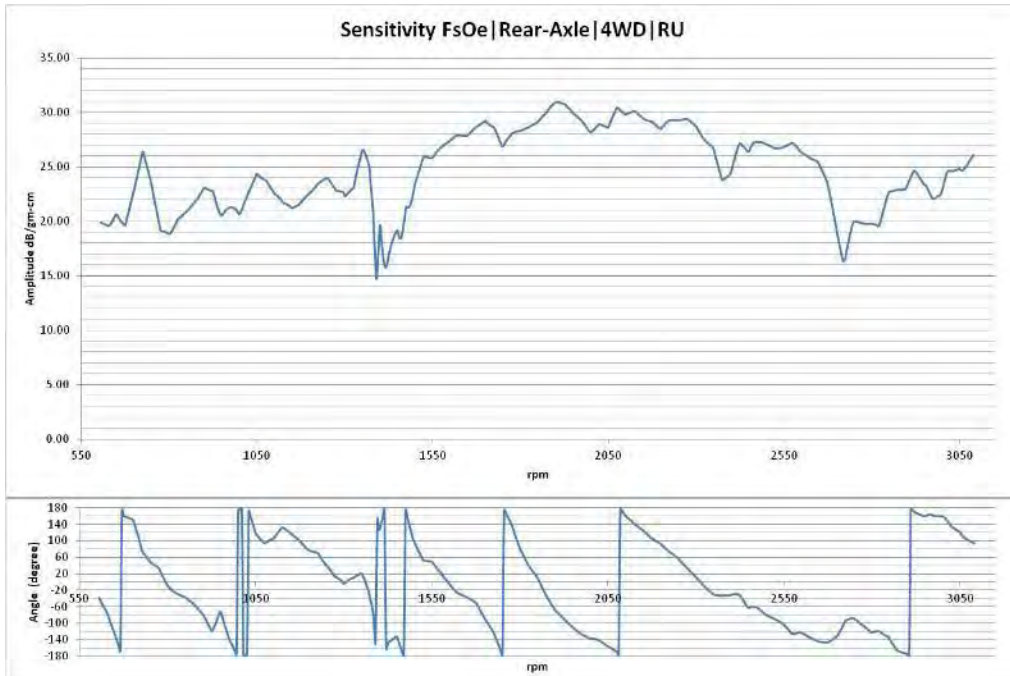


Figure 4.36 Sensitivity and phase FsOe | Rear-Axle | 4WD | RU

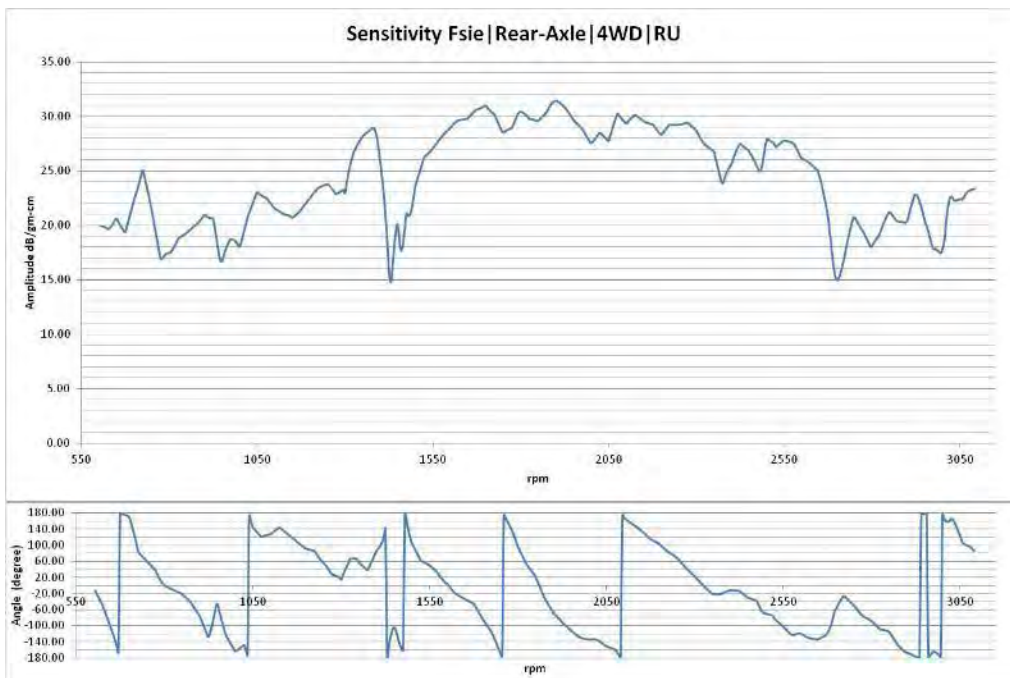


Figure 4.37 Sensitivity and phase Fsie | Rear-Axle | 4WD | RU

Four Wheel Drive (4WD)-Run down (RD) Sensitivity Calculations:

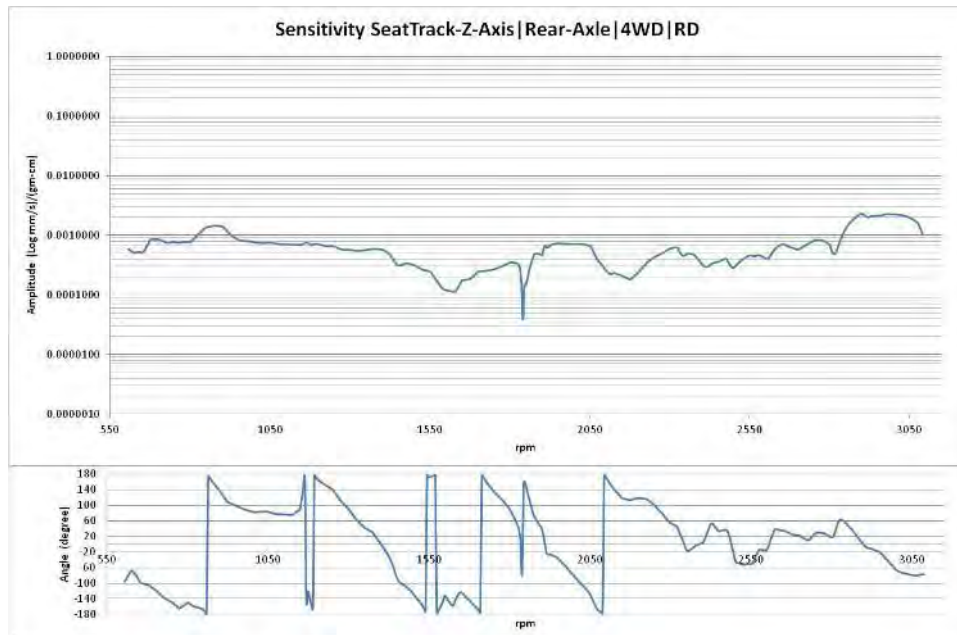


Figure 4.38 Sensitivity and phase Seat Track -Z-Axis| Rear-Axle | 4WD |RD

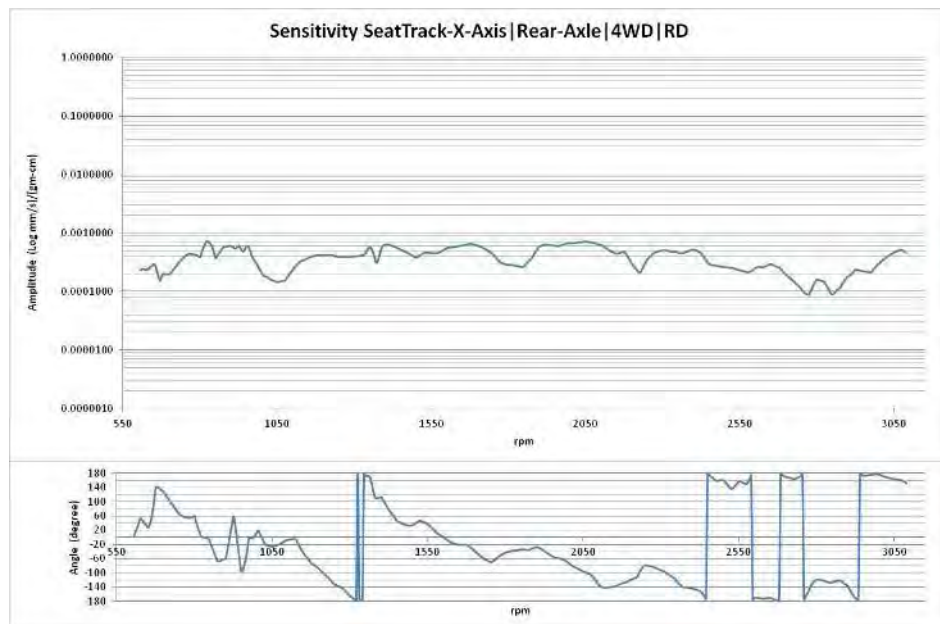


Figure 4.39 Sensitivity and phase Seat Track -X-Axis| Rear-Axle | 4WD |RD

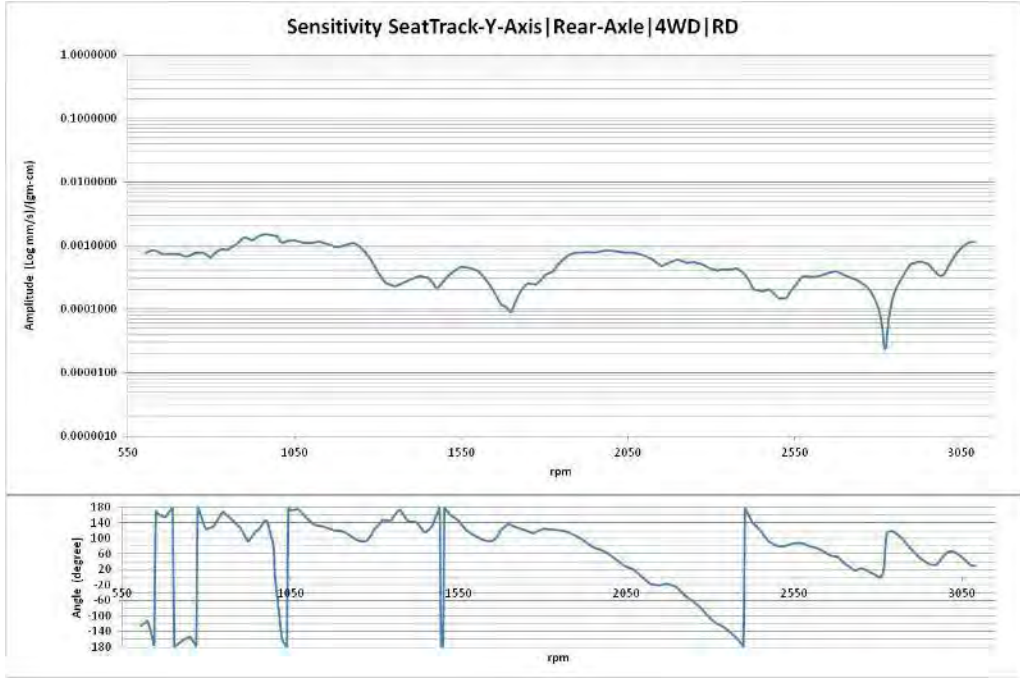


Figure 4.40 Sensitivity and phase Seat Track -Y-Axis| Rear-Axle | 4WD |RD

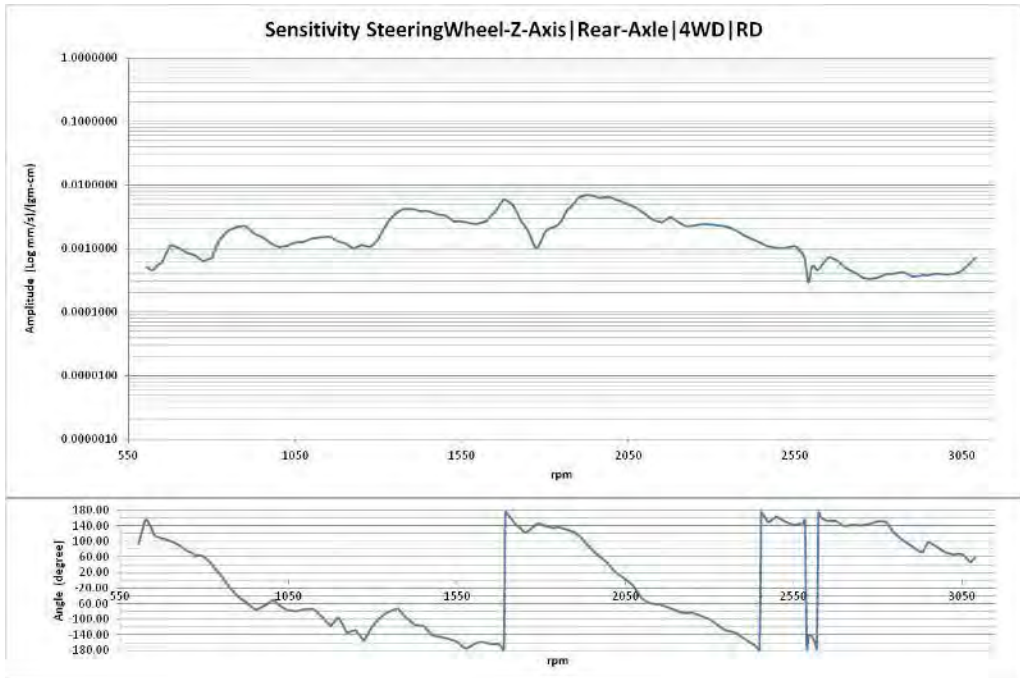


Figure 4.41 Sensitivity and phase Steering Wheel-Z-Axis| Rear-Axle | 4WD |RD

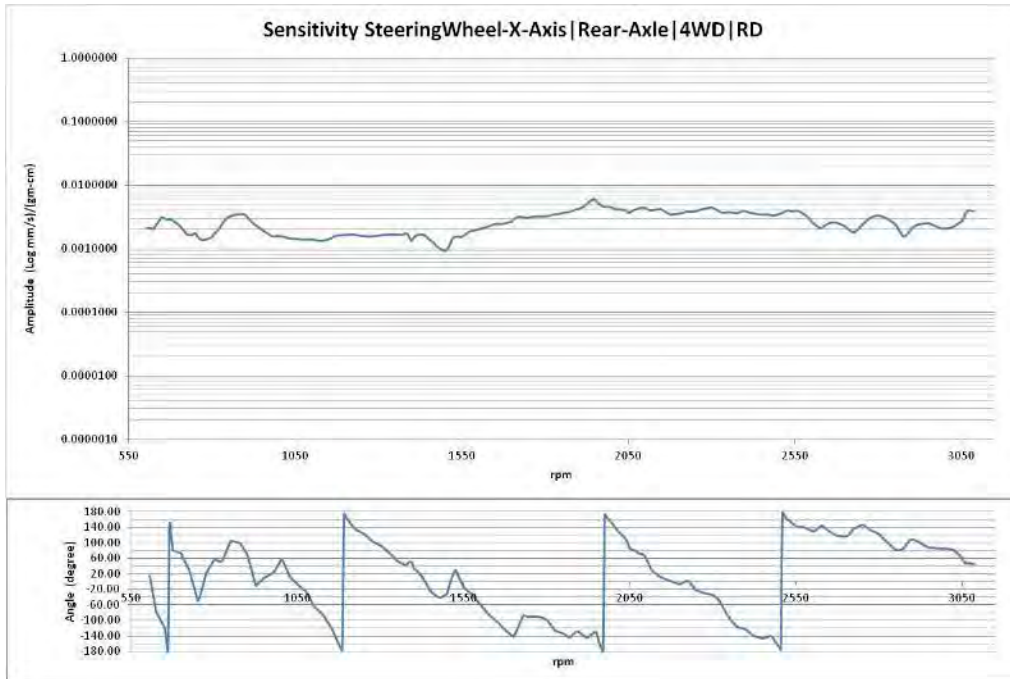


Figure 4.42 Sensitivity and phase Steering Wheel-X-Axis | Rear-Axle | 4WD | RD

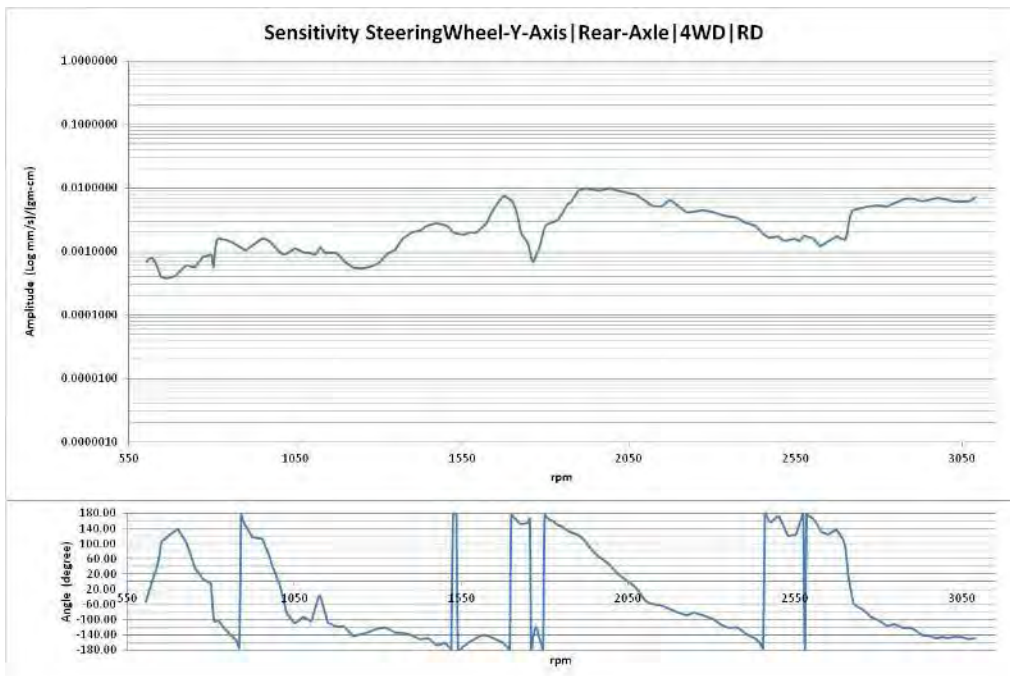


Figure 4.43 Sensitivity and phase Steering Wheel-Y-Axis | Rear-Axle | 4WD | RD

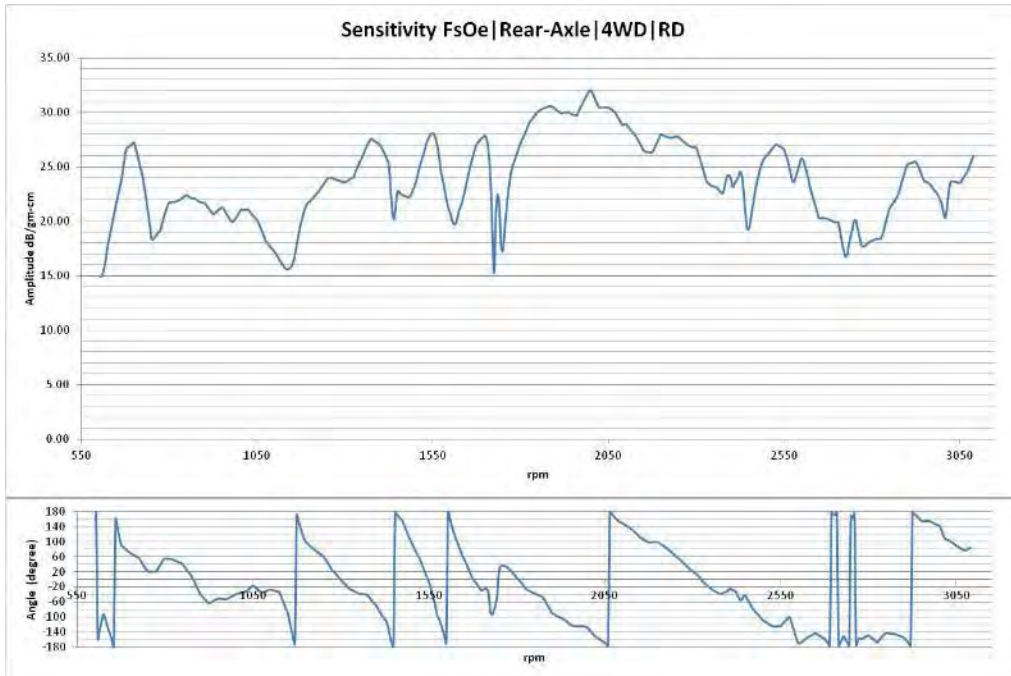


Figure 4.44 Sensitivity and phase FsOe | Rear-Axle | 4WD | RD

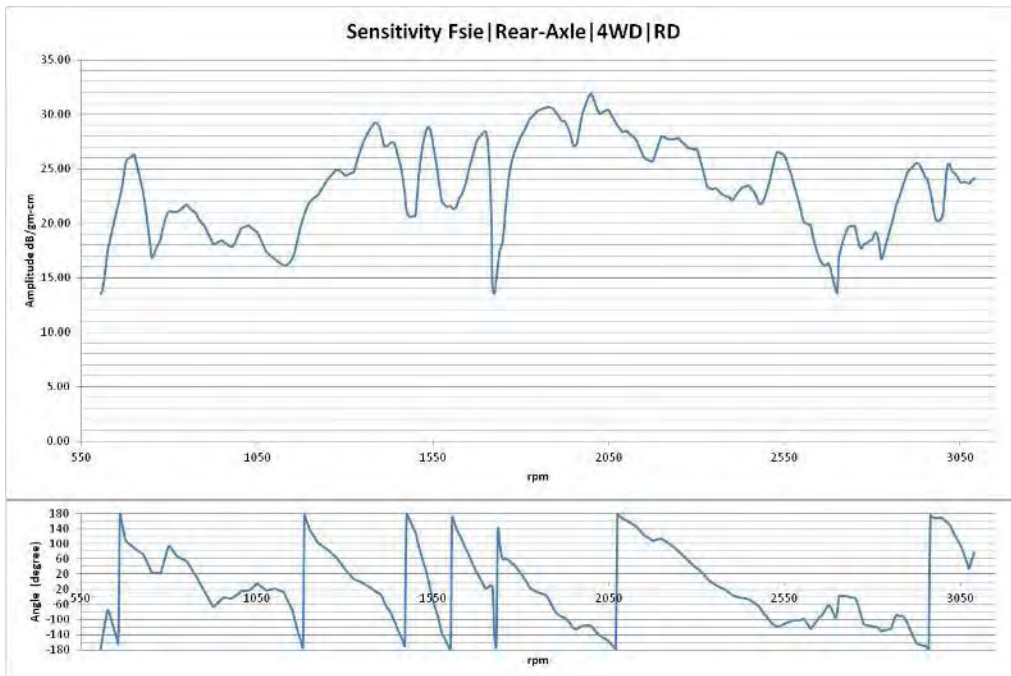


Figure 4.45 Sensitivity and phase Fsie | Rear-Axle | 4WD | RD

CHAPTER V

SIMULATING NVH VARIATION

Because imbalance values vary from vehicle to vehicle, a simulation tool will help designers and quality assurance team members to estimate NVH levels at the selected CTPs by mimicking real production line variation in driveline imbalance. The process involves acquiring empirical sample sets of driveshaft imbalance at different planes, fitting a probability distribution function (pdf) at each plane, and finally using produced functions to simulate for NVH levels at the elected frequency points.

The designer will be able to run simulations of imbalance from both single and multiple planes. In addition, the tool will allow switching to the use of a specific imbalance value rather than simply using probability distributions. The objective is to fit a probability distribution function for all driveshaft planes from which the simulation tool can generate imbalance values that mimic actual driveline imbalance values of manufactured trucks on a wide scale.

For each of the randomly selected imbalance levels at the four driveline planes, the tool will simultaneously simulate NVH responses at each of the eight CTPs. If the total number of iterations is 1000 (as it has been chosen), at the end of the simulation there will be 500,000 NVH response vectors, which is repeated for all eight preselected CTPs; this number is generated by multiplying the 500 frequency points of the frequency spectrum by the 1000 simulation iterations. The output of a single iteration at a CTP of a

preselected frequency level will be the phasor sum of NVH responses due to imbalance forces at each driveline plane. The summation, as mentioned before, will be a complex number. The output will provide a simulated check to assess if the current production process is resulting in a level of vehicle NVH that is acceptable when compared to company expectations, competitive market products, and prior experience with the customer base; a decision can then be made on what steps should be taken to remedy any possible problems. Steps the company may chose to do typically includes:

- a. Implementing tighter control of imbalance for each of the planes. This can be don by requiring the driveline manufacturer to deliver balanced shafts before assembly. Better control can also be achieved by implementing methods like yellow-dotting, where shafts are matched at opposite imbalance directions.
- b. Improving vehicle sensitivity by careful experimental and/or computational analyses of the transfer path of the vibration energy. This may involve detailed design changes to the architecture of the vehicle, its frame or various mounting schemes (powertrain mounts, axle mounts, sub-frame mounts and others.)

Generating Imbalance Probability Distributions

This research has utilized parts of EPA guidelines in order to fit empirical data points into probability distributions [30]. Fitting distributions consists of finding a mathematical function that best represents a statistical variable. Statisticians are often faced with the following problem: several observations of a quantitative character (e.g., x_1, x_2, \dots, x_n), being of a sample of an unknown population, must be tested to see if they

belong to a population with a pdf (probability density function) $f(x,q)$, where q is a vector of parameters to estimate with available data. To fit data points to a distribution, the following steps can be followed:

- 1) Model/function choice: hypothesize families of distributions
- 2) Estimate parameters
- 3) Evaluate quality of fit
- 4) Goodness of fit statistical tests

An important step in the Monte Carlo analysis (MCA) is the selection of the most appropriate distributions that represent the factors which have a strong influence on the risk estimates. This step in the development of a Monte Carlo model can be both challenging and resource intensive. Often, more than one probability distribution may appear to be suitable for characterizing a random variable. Certain probability distributions may be developed to characterize variability or uncertainty.

The distributions can be selected based on both the knowledge regarding the mechanisms that result in variability and the information already available for determining point estimates. Distributions may be specified in order to characterize variability or uncertainty. Often, a Monte Carlo simulation of variability will focus on describing differences between individual vehicles in a population.

Distributions are generated from representative sample populations in order to make inferences about the target population. Ideally, a sampled population should be a subset of a target population; the sampled population should be selected for measurement to provide accurate and representative information about the exposure factor being studied. However, defining representative samples is a matter of interpretation. A

probability distribution can be referred to as a type of model in the sense that it is an approximation: a simplified representation of variability or uncertainty that combines both data and judgment.

It is important to consider whether there are plausible bounds or limits for a variable. For example, in driveline imbalance, imbalance numbers are not perceived as negative; instead, imbalance is a non-negative scalar value expressed in gram-centimeter (gm-cm). Furthermore, the expected maximum value will be within realistic limits. For example, if a normal distribution is used to generate random numbers, there will be a minute chance that it will result an unreasonably large number. Therefore, distributions will generally be truncated at a minimum of zero; also, a probability distribution that is theoretically bounded at a nonzero value may be specified.

The following statistical parameters have been produced for front and rear driveshaft, the figure shows the planes on the drive shaft and the table shows the calculated mean and standard deviation (σ), see Table 5.1 and Figure 5.1.

Table 5.1 Front driveshaft statistical parameters for collected measurements

	Plane B Mean	Plane A Mean	Plane B Std	Plane A Std
Initial Balancing	78.64	43.99	40.11	22.85
Final Balancing	10.36	8.41	4.78	4.64

Data in gr-cm
1000 measured driveshafts



Figure 5.1 Front driveshaft

Statistical parameters (mean and sample standard deviation) for rear driveshaft are located in Table 5.2 and Figure 5.2.

Table 5.2 Rear driveshaft statistical parameters for collected measurements

	Plane D Mean	Plane C Mean	Plane D Std	Plane C Std
Initial Balancing	48.32	70.21	27.68	39.37
Final Balancing	6.55	6.52	2.68	2.97

Data in gm-cm
597 measured driveshafts



Figure 5.2 Rear driveshaft

The randomly collected imbalance data points represent actual imbalance values at studied planes of produced driveshaft. In order to have a visual understanding of the imbalance data points at one of the used drive shafts at a specific plane, this research used a frequency graph for specific chosen bins of values (i.e., 0-19, 20-39... gr-cm); afterwards, the process involved aggregating the number of points that fell in each bin.

Figure 5.3 represents a graph with imbalance points after initial balancing.

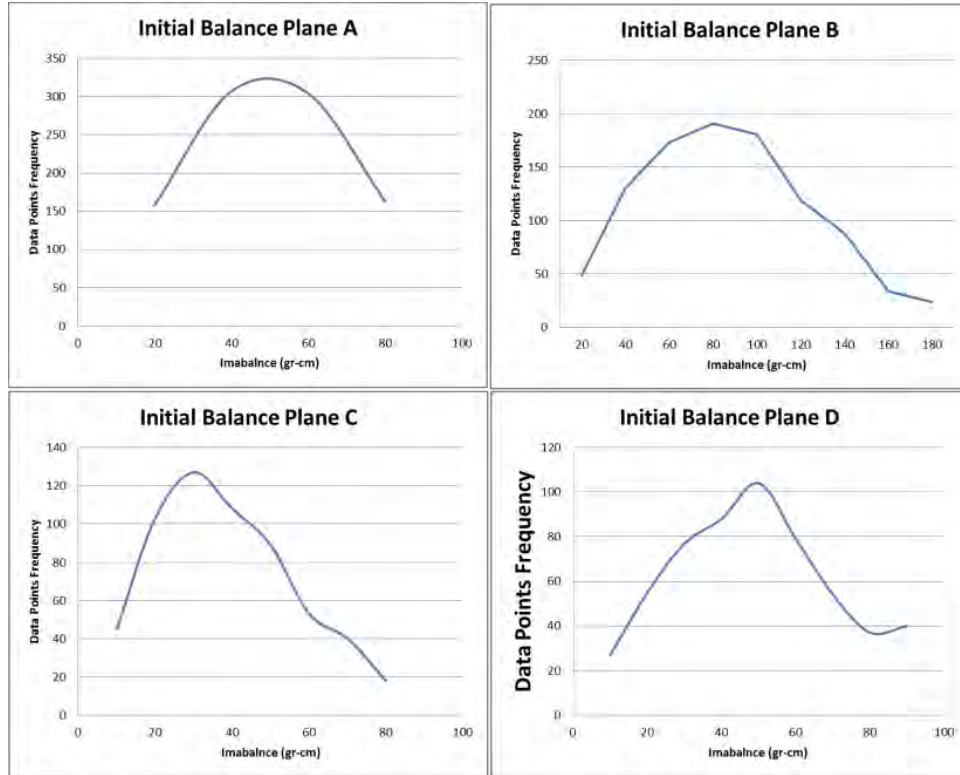


Figure 5.3 Typical statistical imbalance for an interface plane

The main steps followed to fit the probability distributions are mapped out with a flow diagram in Figure 5.4.

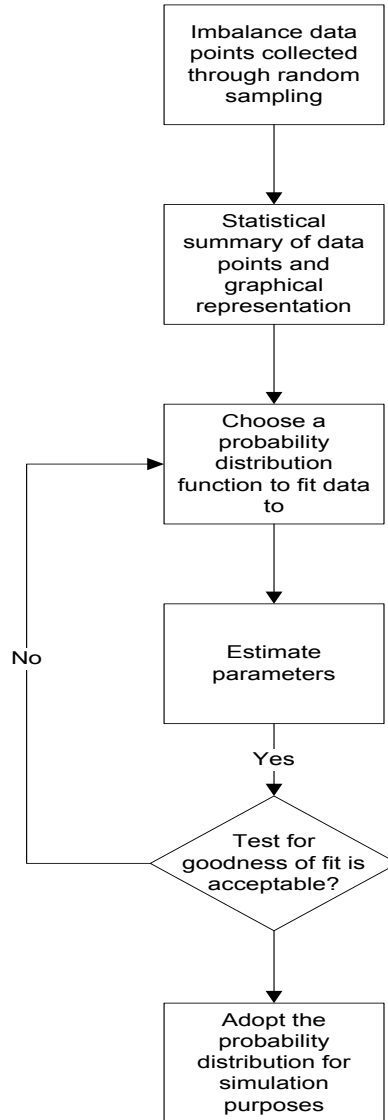


Figure 5.4 Distribution fitting steps

A Gamma distribution was proven to be the best fitted probability density function for the imbalance data.

The corresponding density function in the shape-rate parameterization is represented by equation (5.1):

$$g(x; \alpha, \beta) = \beta^\alpha \frac{1}{\Gamma(\alpha)} x^{\alpha-1} e^{-\beta x} \quad \text{for } x \geq 0 \text{ and } \alpha, \beta > 0 \quad (5.1)$$

The parameters are positive, real numbers. Table 5.3 shows the fitted pdf parameters of the probability distribution:

Table 5.3 Parameters of the fitted probability distributions from empirical data points

Balancing phase	Plane	Alpha	Beta	Notes
Initial	A	3.0394	14.4734	MLE: Maximum likelihood estimate
	B	3.1289	25.1331	MLE: Maximum likelihood estimate
	C	2.7464	25.5661	MLE: Maximum likelihood estimate
	D	2.8195	17.1300	MLE: Maximum likelihood estimate
Final	A	3.2877	2.5568	MOM: Methods of moments
	B	3.5694	2.9013	MLE: Maximum likelihood estimate
	C	3.6410	1.7895	MLE: Maximum likelihood estimate
	D	4.6740	1.4102	MLE: Maximum likelihood estimate

The distribution fitting was conducted through Matlab software version 7.12.0.635-R2011A with statistical package version 7.5-R2011

Simulating NVH Due to Imbalance through a Developed Tool

The impulse transfer function NVH output measured at each CTP has been proved to be directly related to imbalance forces at each studied driveline plane. The difference between baseline cases (i.e., no mass introduced at a plane) compared with cases after introducing masses at each plane revealed the direct relationship between imbalance force at driveline and NVH at selected CTPs. Deducing sensitivity curves at preselected frequency levels will aid in the process of simulating for introduced imbalance forces at each plane. Furthermore, the summation of NVH responses at each CTP can be conducted due to the fact that the process involves a linear time invariant system (LTI), see Figure 5.5.

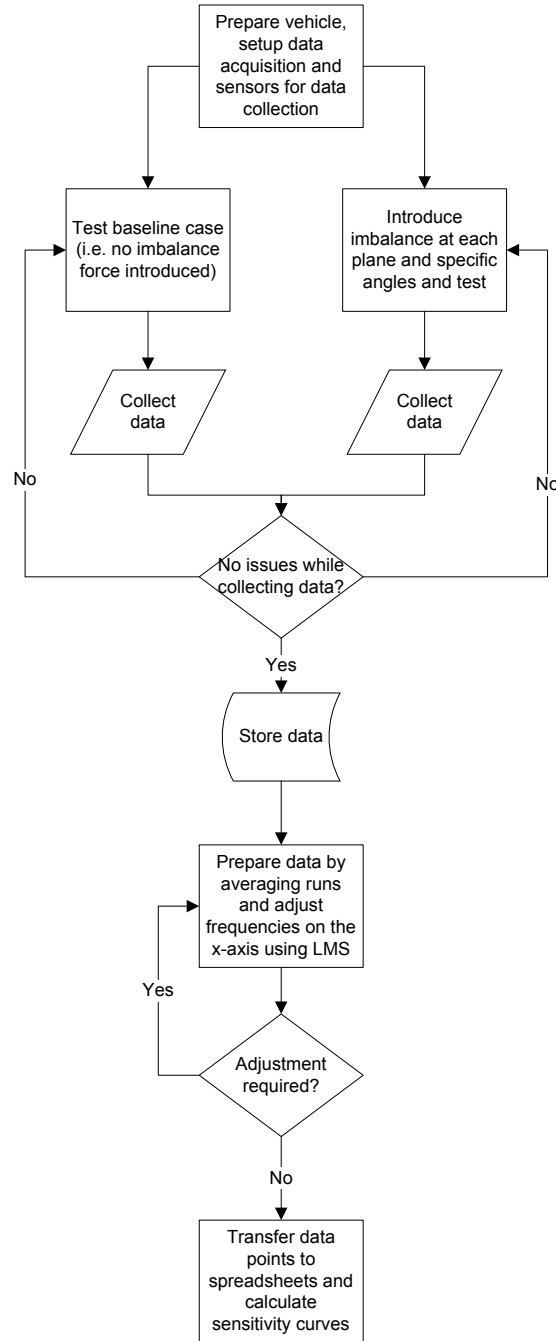


Figure 5.5 Preparing sensitivity curves

The sensitivity curves produced for each plane, drive-wheel engagement (i.e., 2WD or 4WD), and engine engagement (i.e., RU or RD) are the points of variability for

imbalance NVH calculations at each CTP and direction. Each plane will produce 32 sensitivity curves; Figure 5.6 shows the breakdown of sensitivity curves for plane A. The same number of sensitivity curves must be produced for other planes (i.e., planes B, C, and D).

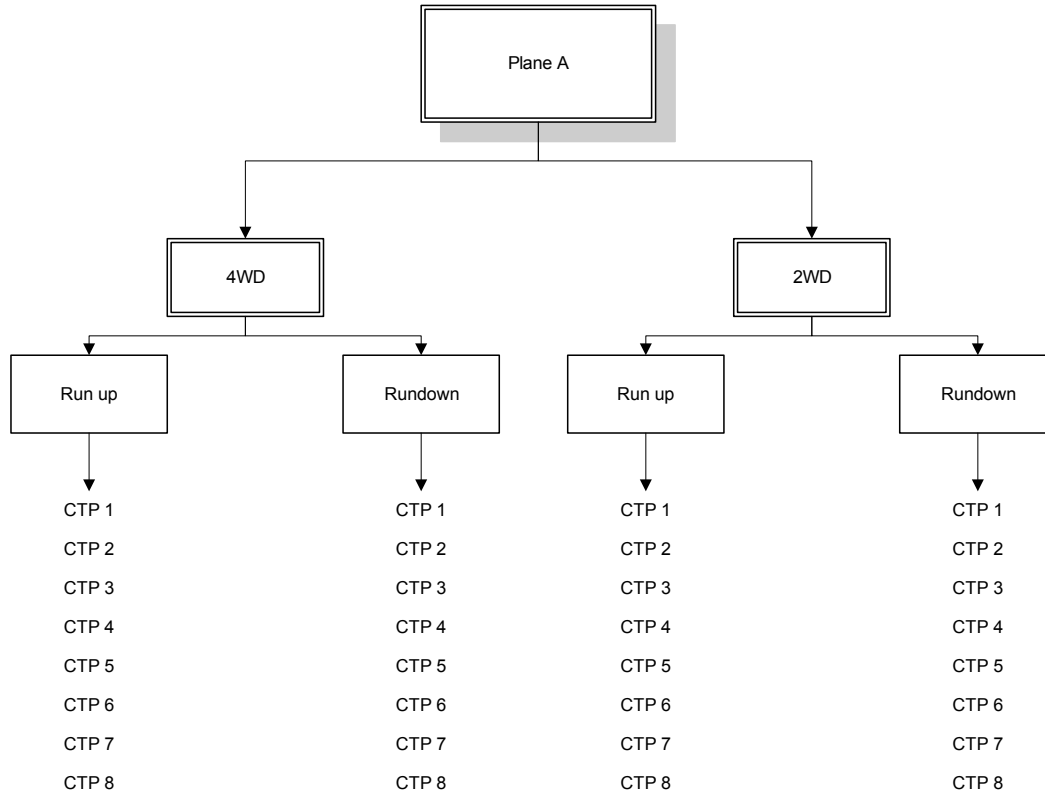


Figure 5.6 Produced sensitivity curves per plane

New computational power is becoming a driving force that encourages more rigorous and accurate simulation, which implies a paradigm shift in respect to the significance of statistics[31]. A program in Java programming language has been developed to be able to accommodate for complexity of handling the different sensitivity

curves and possible combinations for each case from each plane. The summation of NVH response at each CTP has to be handled by the corresponding sensitivity curves. For example, the case of 4WD and run up (RU) has to be used for all planes if input imbalance forcing is to be summed properly. In addition, the program also generates the imbalance random value at each plane. The probability distribution used to draw random imbalance values is distinctive for each plane, as is discussed in the previous section. The output will be eight spreadsheets, one for each CTP; in each spread sheet, there will be 1000 iterations with two columns per iteration, as seen in Figure 5.7

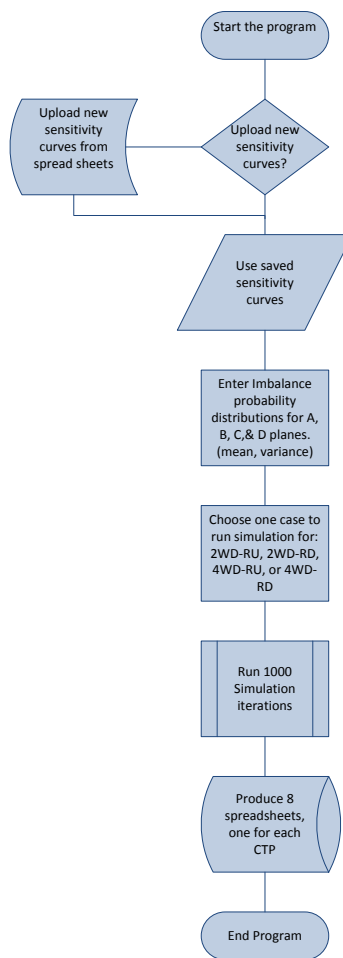


Figure 5.7 Simulation run per plane

Each plane will produce 32 sensitivity curves with eight CTPs at four different driving styles (i.e., 4WD, 2WD, RU, or RD). The developed tool will help to simulate NVH at each CTP for different imbalance levels based on the actual production imbalance levels. In order to demonstrate how the software works, a couple of cases with actual imbalance levels will be used to simulate NVH levels inside the vehicle at selected CTPs.

The two cases of NVH at Seat Track-Z direction have been calculated using random empirical data for after initial balancing, as seen Figure 5.8, and also after final balancing, as seen in Figure 5.9.

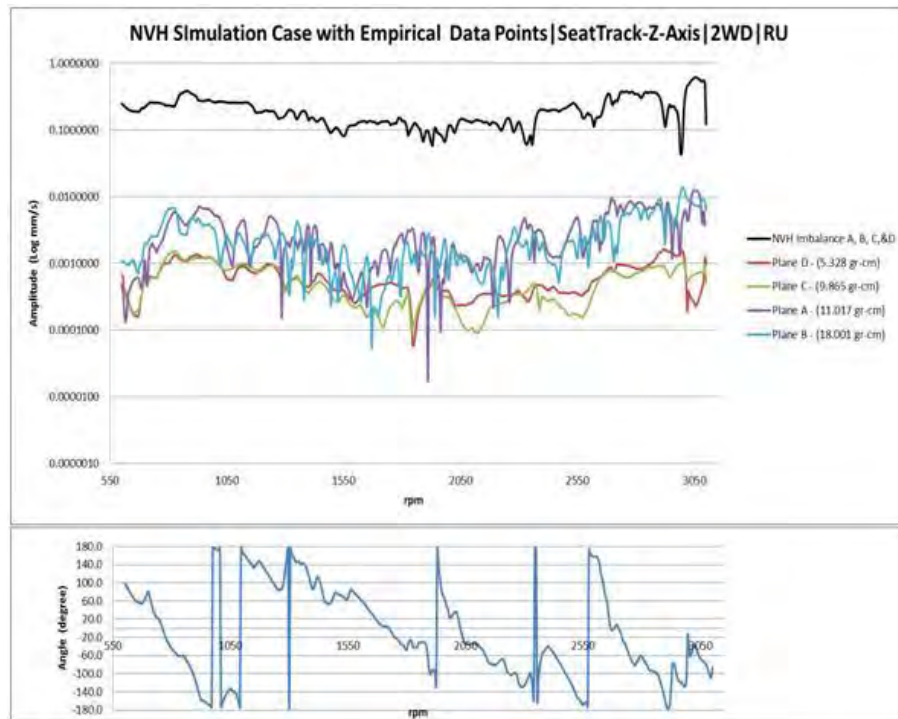


Figure 5.8 Calculated vibration with data point from final balancing empirical data

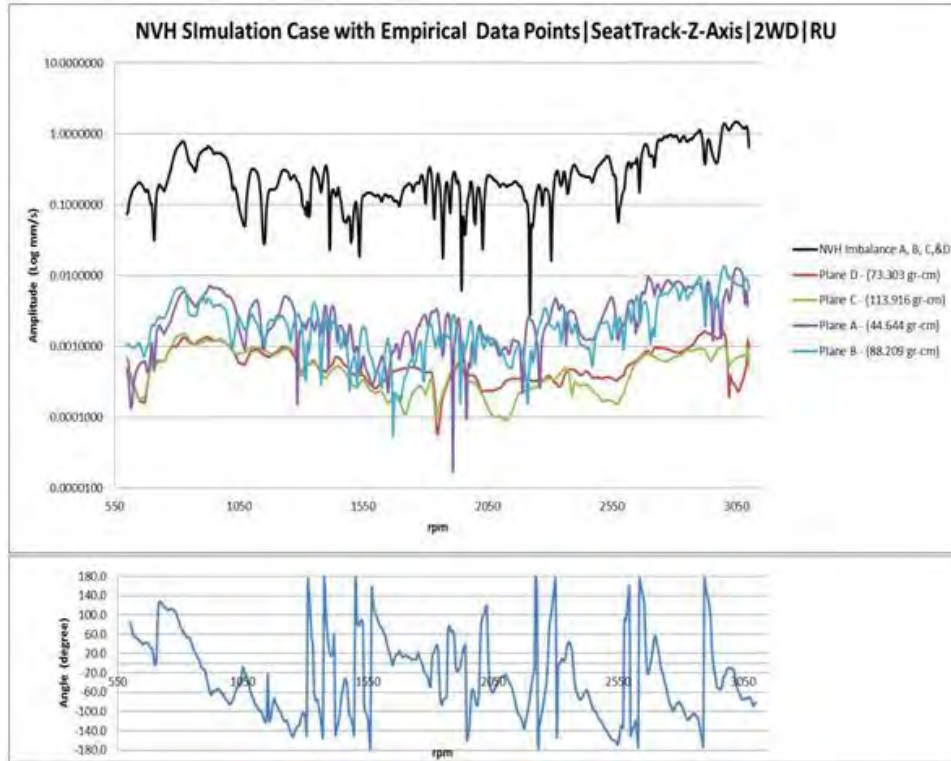


Figure 5.9 Calculated vibration with data point from initial balancing empirical data

The simulation runs will produce a representative sample of NVH points that can be used to produce a mean (μ) and a sample standard deviation (σ). Figure 8 is a graph of the mean of amplitudes and six times the standard deviation (i.e., sigma) for each frequency level of the spectrum; the simulation tool ran 1000 iterations.

The simulation for all CTPs with different driving modes; (i.e., driveline engagement: 2WD or 4WD and engine engagement: run up or rundown) can be found in APPENDIX B.

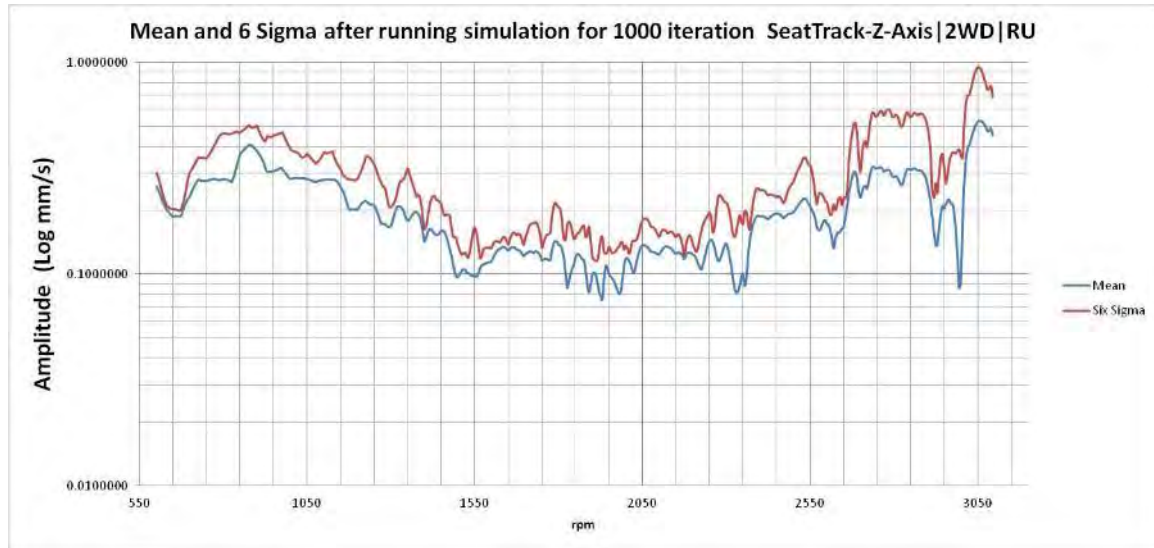


Figure 5.10 Simulation run output (mean and 6σ) for Seat Track z-axis 2WD-RU

Finally the output from the simulation will be used to calculate the NVH capability of expected produced truck. The capability study of one-sided specification was introduced by Kane [32], equation (5.2):

$$C_{PU} = \frac{USL - \mu}{6\sigma} \quad (5.2)$$

One-sided process capability index C_{PU} of the upper specification limit (USL) is calculated using the process mean μ and process standard deviation σ . In our case, the industry will have an USL specified for design and quality assurance teams in order to adhere to.

CHAPTER VI

CONCLUSIONS

A simulation tool that estimates NVH in projected vehicle platform production has been developed; this tool has been used to predict imbalance related NVH levels at Customer Touch Points (CTPs) of interest, see APPENDIX C.

Through assuming linear time invariant (LTI) system throughout the research and the simulation tool development, NVH to imbalance sensitivity curves have been produced for the selected CTPs. These imbalance sensitivity curves give NVH signatures that are due to input imbalance force at major driveline planes. Various sensitivity curves have been developed experimentally for different drive-wheel engagements (i.e., 2WD or 4WD), and engine engagement (i.e., RU or RD). By concentrating on specific frequency levels of the spectrum, sensitivity to imbalance curve has been produced for each case.

The study resulted in the following major conclusions:

- Driveline imbalance at each plane contributes significantly to vehicle interior NVH.
- The level of NVH contribution will increase as the imbalance increases at each plane.

- The combined (summation) NVH levels from multiple imbalance input forces at each level will not always increase NVH; rather, it will sometimes reduce total NVH level at CTPs.

The summation is taking place in complex numbers; thus, the phasor amount and phase angle will affect the final resulting NVH level at each CTP. This level will vary with each variation in the amplitude and phase angle from the imbalance input force. This is why the developed tool will help in calculating expected levels of NVH in response to variation in amplitude and phase of the randomly generated imbalance values at the studied driveline planes.

The imbalance variation due to production, material, and assembly variations can be captured at the driveline level by collecting actual imbalance values at each plane, then fitting probability distributions to be used later as a random number generator of possible imbalance values at each plane. The fitted distributions from the actual data were approximated to Gama probability distribution.

The developed tool simulated NVH representing produced vehicles. This tool can help designers to draw an approximate picture of the possibility of having defective vehicles (i.e., objectionable customer NVH level), which can be expressed in the form of defects per million opportunities (DPMO) or in a capability study as discussed in chapter five. These indicators will help designers and manufacturers learn about the vehicles' sensitivity to driveline induced NVH that will aid the manufacturers in anticipating and preparing for warranty recalls due to driveline NVH.

Contributions

The purpose is to develop a tool towards a robust design for driveline NVH, which enables the design engineer to better understand the effect of driveline imbalance on the CTPs. Several other contributions include:

- Establishing an NVH baseline case for a Nissan truck at predetermined CTPs with specific driving and sweeping styles.
- Designing, developing, and validating a testing methodology for inducing driveline imbalance at predetermined planes.
- Developing a novel transfer function for driveline imbalance.
- Developing a unique set of verifiable sensitivity to imbalance graphs dedicated to each plane in each specific driving and sweeping style.
- Developing a procedure through which OEMs can realistically assess the broad sensitivity to imbalance that results in an improvement in product and process design process, including setting up specifications.

Future Work

This simulation program is a powerful tool, as it utilizes an important dynamic system property at a certain region of operation and framework: linear time invariant (LTI) property of dynamic systems at a region of operation. This tool can be expanded to several sources of NVH in the automotive industry, especially those related to rotating or reciprocating systems; furthermore, it can be utilized to simulate for variation in engineering and designing specifications that may lead to different levels of NVH. The necessity for the use of this tool will usually stem from the need to assess an issue from warranty history information or to anticipate for issues, through brainstorming, while in

the designing stage. Afterwards, selecting a specific NVH source (i.e., imbalance, runout, non-uniformity, or other parameters), the steps followed in this research to develop a simulating tool can be then implemented.

When producing sensitivity curves, it is imperative to be aware of possible interferences that may result in the inaccuracy of results due to several factors while prepping for NVH testing, such as rotating systems at the same rpm with the same orders.

There are many possibilities in expanding this tool; it can be used in a variety of fields such as multiple vehicular systems, machinery, appliances, and other industries.

The tool itself may also be improved. For example, improvement can be made in the future by adding capabilities that allow it to accept empirical data points of any design or engineering aspect that is being studied in order to fit these points into probability distributions; in turn, these probability distributions can be used to simulate for variation of design or engineering parameters. Furthermore, another improvement can be made to the frontend of the tool by preparing universal interfaces which will take care of averaging, phasor addition in complex numbers, and x-axis equidistance readjustment.

Generating imbalance at each plane randomly after fitting a probability distribution may produce different types of probability distribution types; (i.e., Gamma, Norma, and others); the current developed program will only allow 2 variations of probability distributions to generate random imbalance levels at each plane, namely: Gamma distribution and Normal distribution. Future work may involve allowing more probability distributions to be used.

Also current tool won't allow for a mixed types of probability distributions to be used when generating imbalance values; (i.e., when choosing one of the two available

distributions; the chosen distribution must be used for all planes at the same time, rather it allows for different parameters to be entered). Future work will include allowing mixing and matching different types of types of probability distributions to be used at different planes for the same simulation run.

Also Noise calculations need to be revised and verified as the use of decibel requires special rules to add them as they are in logarithmic format. Future work will allow having the simulation add the noise output from each plane properly.

Also the developed program output can be enhanced to allow for graphing directly after running the simulation. As of now the graphing is conducted manually with the help of spreadsheets.

REFERENCES

- [1] M. Hashioka, and I. Kido, "An Application Technique of Transfer Path Analysis for Automotive Body Vibration," *Noise and vibration*. pp. 2007-01-2334.
- [2] A. G. Piersol, and T. L. Paez, *HARRIS' SHOCK AND VIBRATION HANDBOOK*: New York : McGraw-Hill, c2010. 6th ed., 2010.
- [3] *Universal joint and driveshaft design manual*: SAE, Second Printing, 1991.
- [4] M. S. Qatu, M. K. Abdelhamid, P. Jian *et al.*, "Overview of automotive noise and vibration," *International Journal of Vehicle Noise & Vibration*, vol. 5, no. 1/2, pp. 1-35, 2009.
- [5] S. Q. Mohamad, and I. Javed, "Transverse vibration of a two-segment cross-ply composite shafts with a lumped mass," *Composite Structures*, vol. 92, pp. 1126-1131, 2010.
- [6] J. Iqbal, A. Rohilla, Q. Ahmed *et al.*, "Improving powerplant and powertrain bending in East-West engine configurations," *INTERNATIONAL JOURNAL OF VEHICLE NOISE AND VIBRATION*, vol. 1, no. 3/4, pp. 358-367, 2005.
- [7] M. Qatu, M. Sirafi, and F. Johns, "Robustness of powertrain mount system for noise, vibration and harshness at idle," *Proceedings of the Institution of Mechanical Engineers -- Part D -- Journal of Automobile Engineering (Professional Engineering Publishing)*, vol. 216, no. 10, pp. 805, 2002.
- [8] J. Iqbal, and M. Qatu, "Robustness of Axle Mount System for Driveline NVH," *Noise & vibration conference*. p. 1485.
- [9] A. Farshidianfar, M. Ebrahimi, H. Rahnejat *et al.*, "- Optimization of the high-frequency torsional vibration of vehicle driveline systems using genetic algorithms," vol. - 216, no. - 3, pp. - 262, 2002.
- [10] M. S. Qatu, R. King, R. Wheeler *et al.*, "Vehicle Design for Robust Driveline NVH Due to Imbalance and Runout Using a Monte Carlo Process," *SAE Int. J. Passeng. Cars – Mech. Syst.*, vol. 4, no. 2, August 2011, 2011.
- [11] M. S. Qatu, R. King, O. Shubailat *et al.*, "Determination of Interior NVH Levels from Tire/Wheel Variations using a Monte Carlo Process," *Noise and vibration conference; SAE 2011*. pp. 2011-01-1580.

- [12] N. Lalor, and H. H. Priebsch, "The prediction of low- and mid-frequency internal road vehicle noise: a literature survey," *Proceedings of the Institution of Mechanical Engineers -- Part D -- Journal of Automobile Engineering (Professional Engineering Publishing)*, vol. 221, no. 3, pp. 245, 2007.
- [13] "Number of Manufactured Cars," <http://www.worldometers.info/cars/>.
- [14] B. Gaerdhagen, and J. Plunt, "Variation of Vehicle NVH Properties due to Component Eigenfrequency Shifting. Basic Limits of Predictability," *SAE TRANSACTIONS*, vol. 104, no. 6/PT2, pp. 2258-2267, 1996.
- [15] T. Wellmann, K. Govindswamy, E. Braun *et al.*, "2007-01-2246 Aspects of Driveline Integration for Optimized Vehicle NVH Characteristics," *SAE TRANSACTIONS*, vol. 116, pp. 1790-1800, 2008.
- [16] N. N. Verichev, "Chaotic torsional vibration of imbalanced shaft driven by a limited power supply," *Journal of Sound and Vibration*, vol. 331, pp. 384-393.
- [17] G. Meinhardt, Sun, Z., Steyer, G., and sengupta, S, "'An Application of Variation Simulation - Predicting Interior Driveline Vibration Based on Production Variation of Imbalance and Runout,'" in SAE 2011 Noise and Vibration Conference and Exhibition, Grand Rapids-MI, 2011.
- [18] W. Braun, G. Meinhardt, F. Walter *et al.*, "- Driveline Imbalance Sensitivity Testing Methodology," 2005.
- [19] P. Zavala, M. Moraes, G. F. d. Jesus *et al.*, "Driveline Induced Vibration Investigation," *Noise and vibration*. pp. 2006-01-2883.
- [20] K. T. Ulrich, and S. D. Eppinger, *Product design and development / Karl T. Ulrich, Steven D. Eppinger*: Boston : McGraw-Hill Higher Education, c2008. 4th ed., 2008.
- [21] G. Taguchi, E. A. Elsayed, and T. Hsiang, *Quality Engineering in Production Systems*: McGraw-Hill, New York, NY., 1989.
- [22] H. Van der Auweraer, and J. Leuridan, "A new testing paradigm for today's product development process - part 1," *Ein neues Test Paradigma für heutige Produktentwicklungsprozesse - Teil 1*, no. 9, pp. 14, 2006.
- [23] J. Erjavec, "Ch:6 Drive Shafts and Universal Joints," *Manual transmissions & transaxles*, figure 6-5, Delmar Cengage Learning, 2011.
- [24] Nissan, "Basic noise and vibration measuring points," *NISSAN ENGINEERING MANUAL*, KD2-50101 [8], Nissan, 2009, pp. 4, 11 & 12.

- [25] LMS, "Signature Testing with Test.Lab," March 6, 2013.
- [26] A. Brandt, *Noise and Vibration Analysis: Signal Analysis and Experimental Procedures*: Wiley, 2011.
- [27] R. B. Randall, *Frequency analysis*: Brüel & Kjaer, 1987.
- [28] J. P. Den Hartog, *Mechanical Vibrations*: DOVER PUBN Incorporated, 1985.
- [29] "Fourier Transform," 2013; <http://www.thefouriertransform.com/>.
- [30] US-EPA, "Risk Assessment Guidance for Superfund (RAGS) -: Process for Conducting Probabilistic Risk Assessment ", 2001.
- [31] B. A. Berg, *Markov chain Monte Carlo simulations and their statistical analysis : with web-based Fortran code / Bernd A. Berg*: Hackensack, NJ : World Scientific, c2004., 2004.
- [32] V. E. Kane, "Process capability indices," *Journal of Quality Technology*, vol. 18, no. 1, pp. 41-52, 1986.

APPENDIX A

SENSITIVITY CURVES FOR PLANES: A, B AND C

Plane A sensitivity curves

Two Wheel Drive (2WD)-Run up (RU) Sensitivity Calculations:

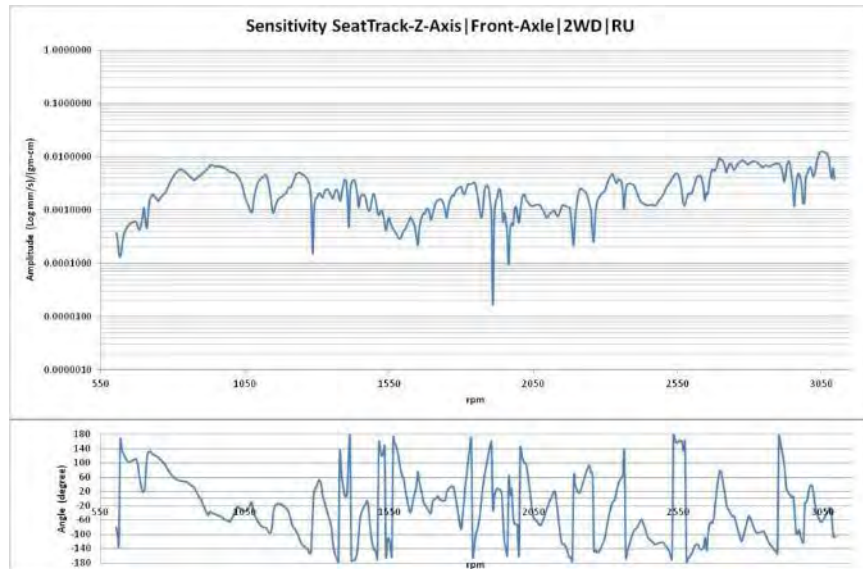


Figure A.1 Sensitivity and phase Seat-Track-Z-Axis | Front-Axle | 2WD |RU

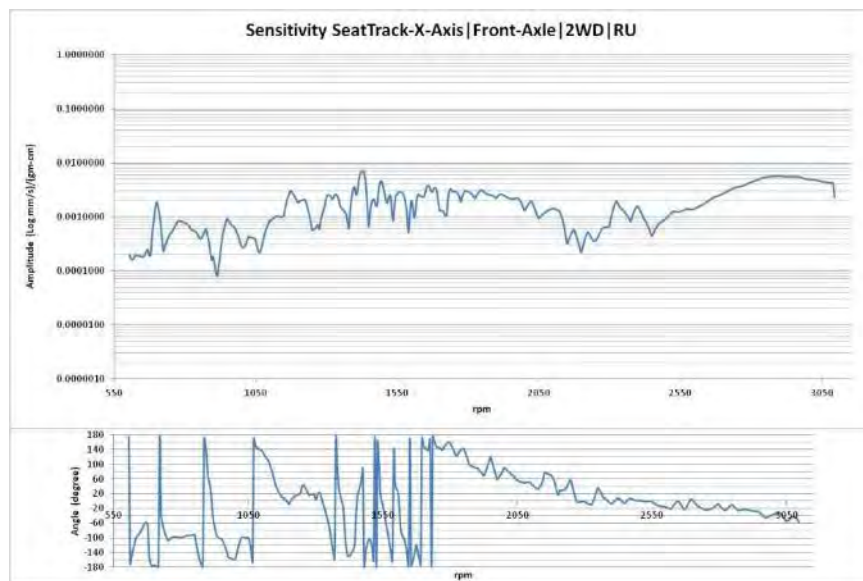


Figure A.2 Sensitivity and phase Seat-Track-X-Axis | Front-Axle | 2WD |RU

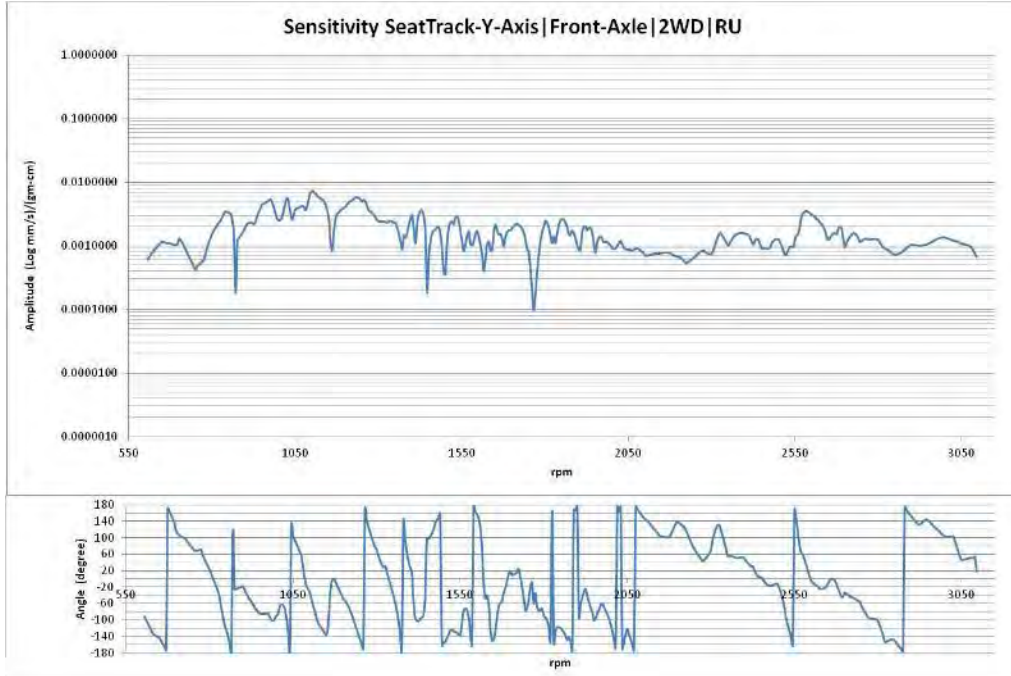


Figure A.3 Sensitivity and phase Seat-Track-Y-Axis| Front-Axle | 2WD |RU

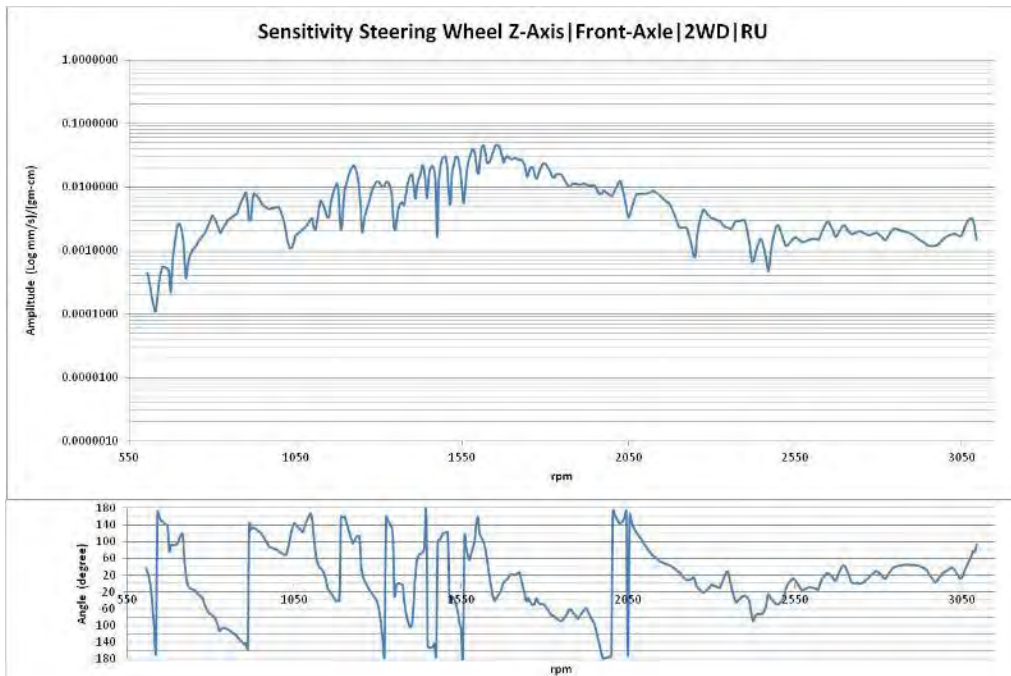


Figure A.4 Sensitivity and phase Steering Wheel-Z-Axis| Front-Axle | 2WD |RU

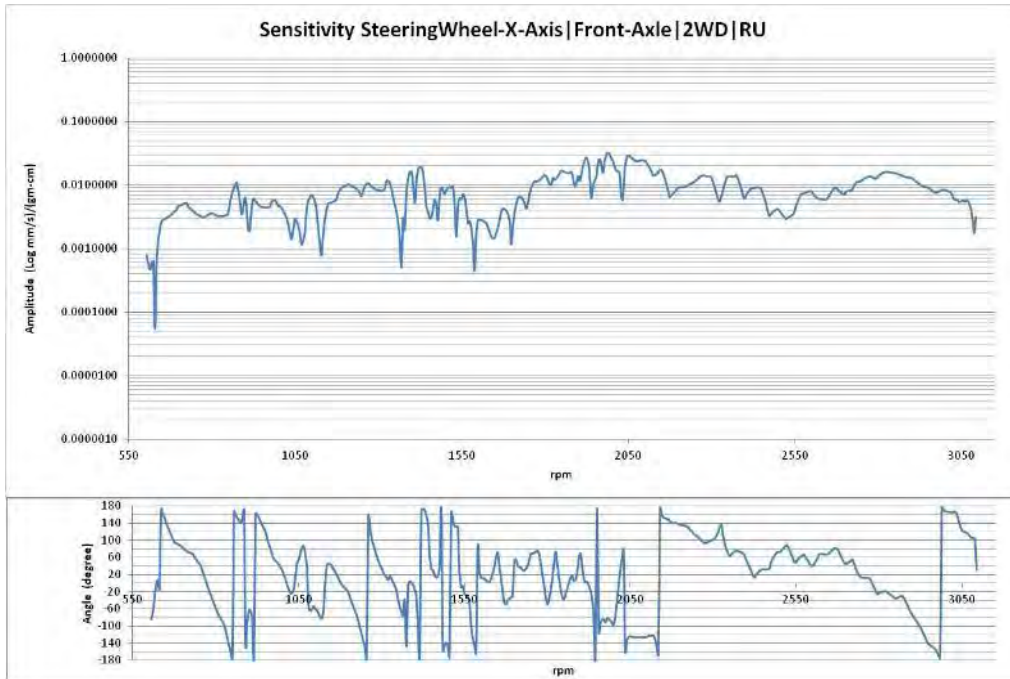


Figure A.5 Sensitivity and phase Steering Wheel-X-Axis| Front-Axle | 2WD |RU

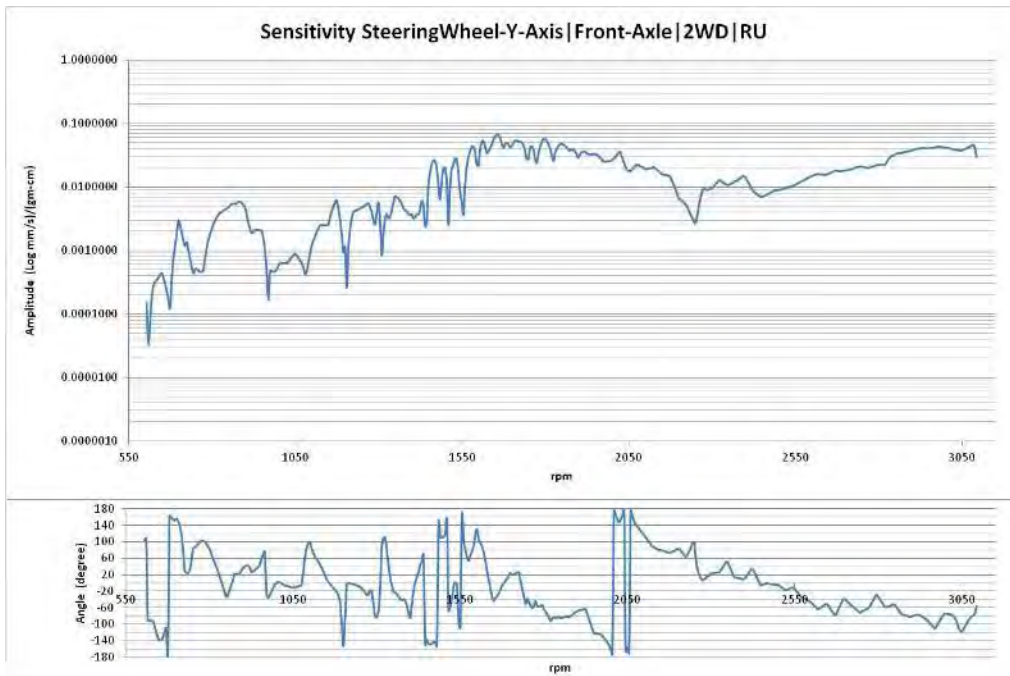


Figure A.6 Sensitivity and phase Steering Wheel-Y-Axis| Front-Axle | 2WD |RU

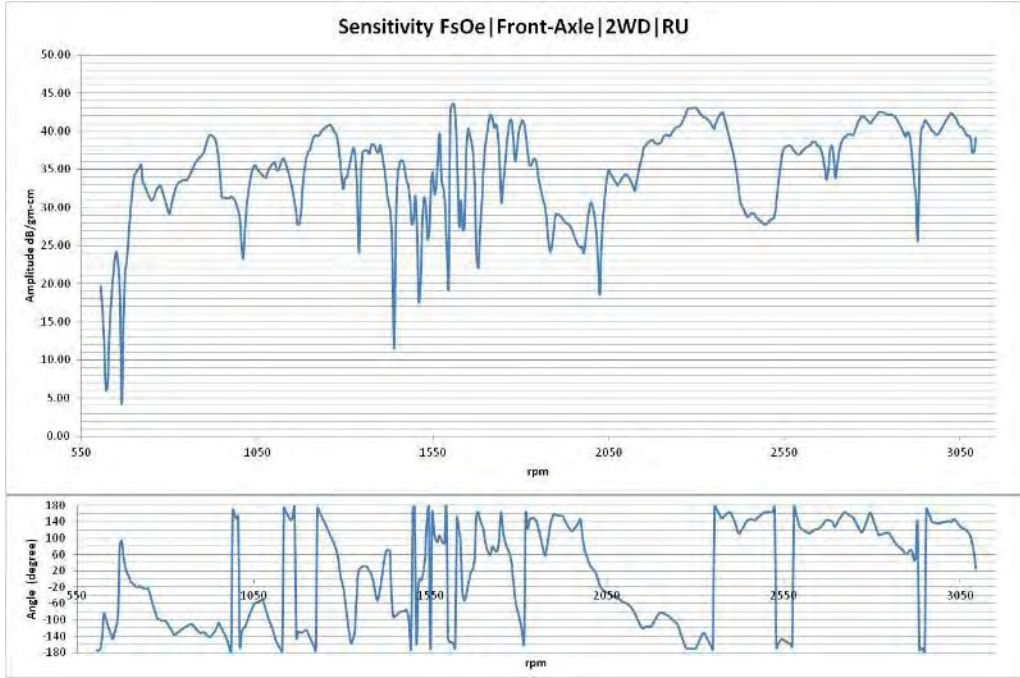


Figure A.7 Sensitivity and phase FsOe | Front-Axle | 2WD | RU

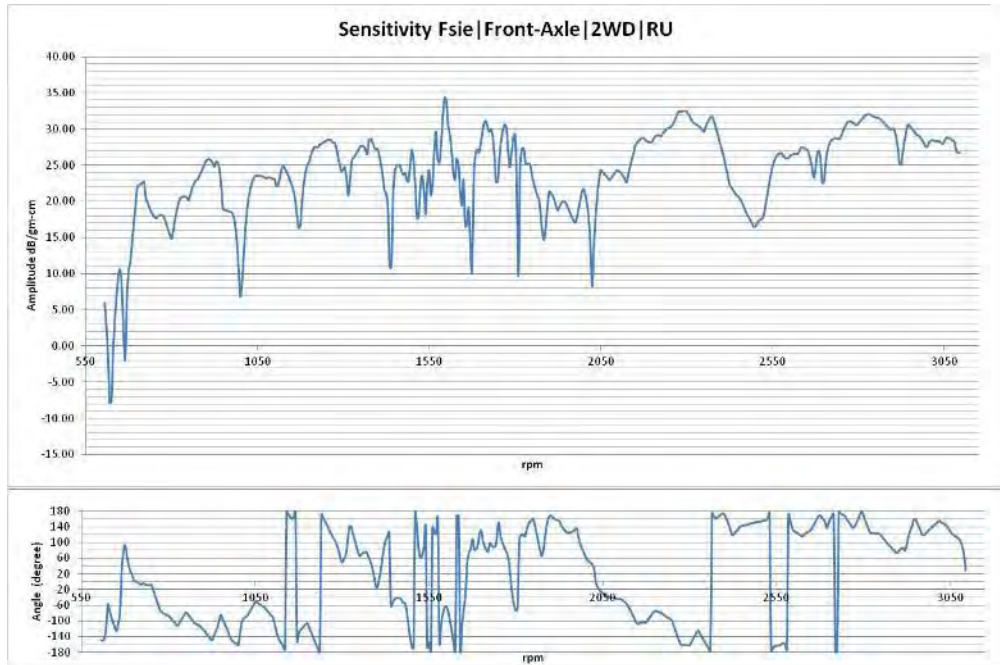


Figure A.8 Sensitivity and phase Fsie | Front-Axle | 2WD | RU

Two Wheel Drive (2WD)-Run down (RD) Sensitivity Calculations:

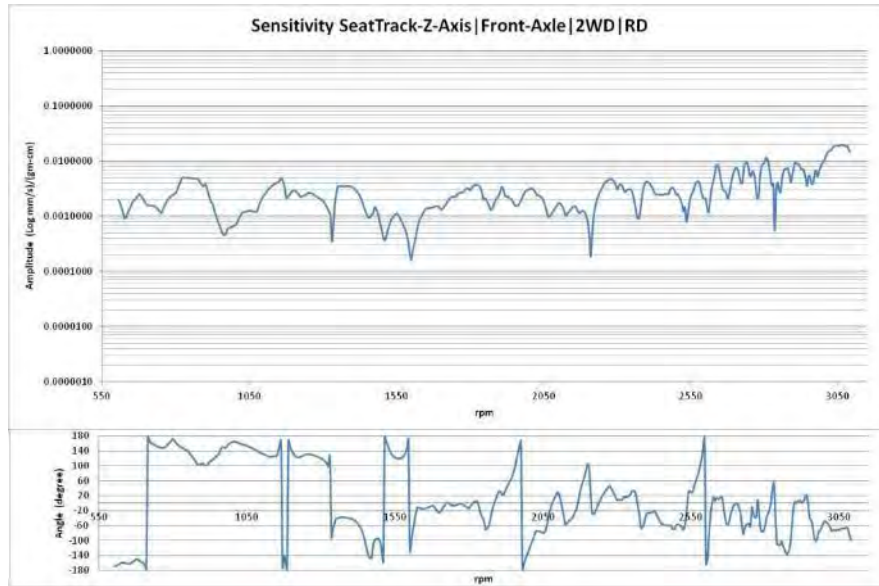


Figure A.9 Sensitivity and phase Seat Track -Z-Axis| Front-Axle | 2WD |RD

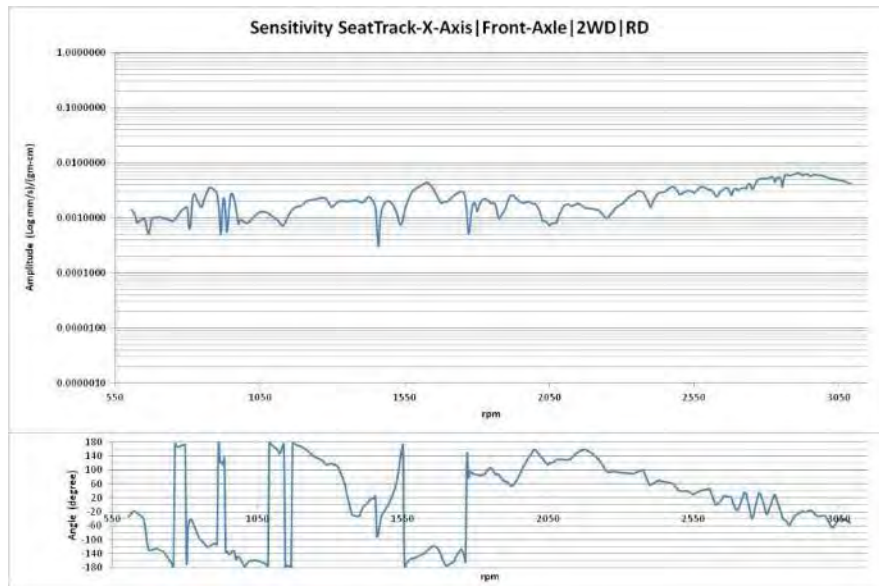


Figure A.10 Sensitivity and phase Seat Track -X-Axis| Front-Axle | 2WD |RD

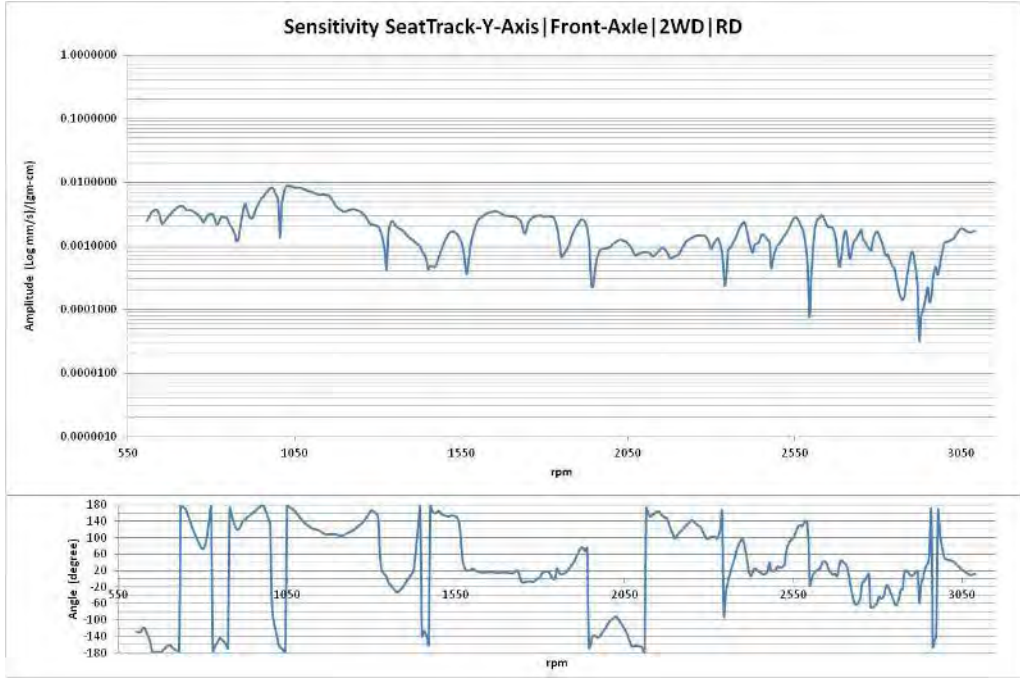


Figure A.11 Sensitivity and phase Seat Track -Y-Axis| Front-Axle | 2WD |RD

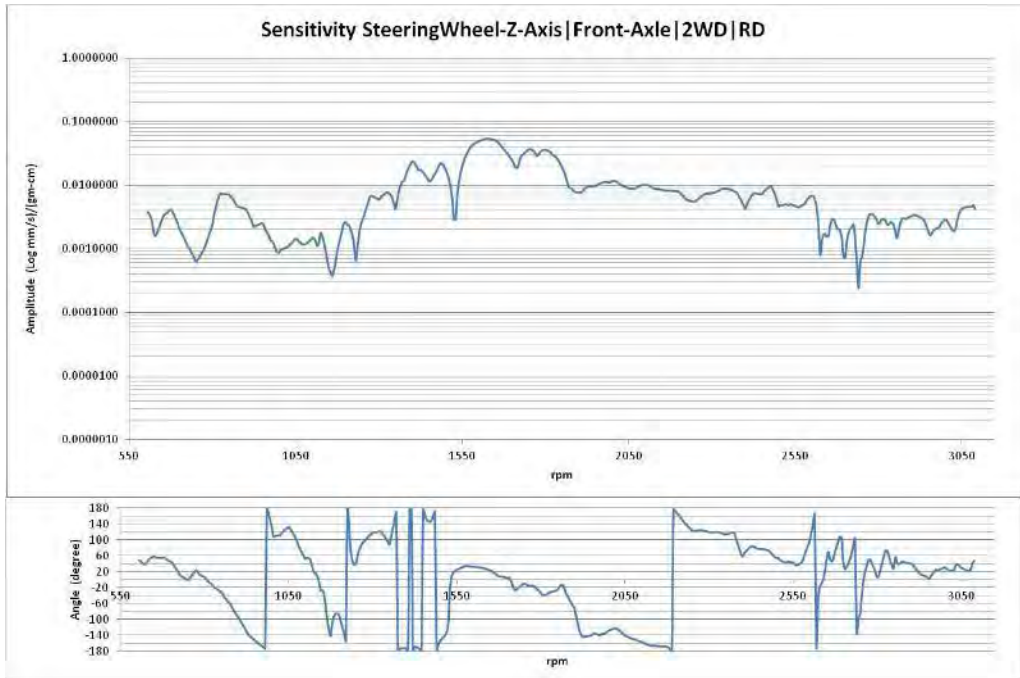


Figure A.12 Sensitivity and phase Steering Wheel-Z-Axis| Front-Axle | 2WD |RD

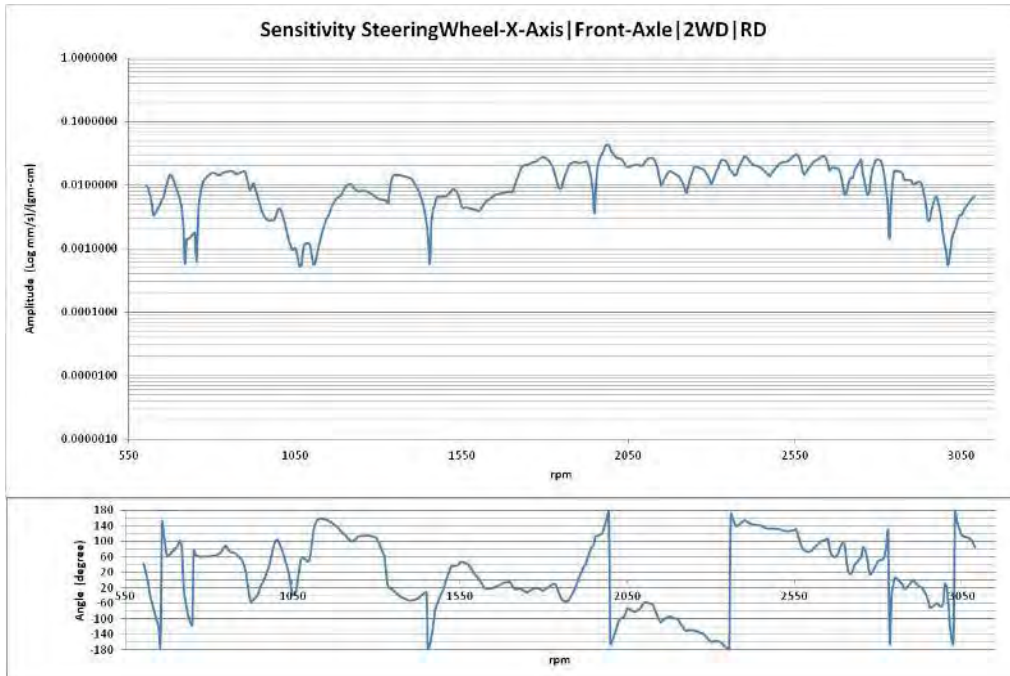


Figure A.13 Sensitivity and phase Steering Wheel-X-Axis | Front-Axle | 2WD | RD

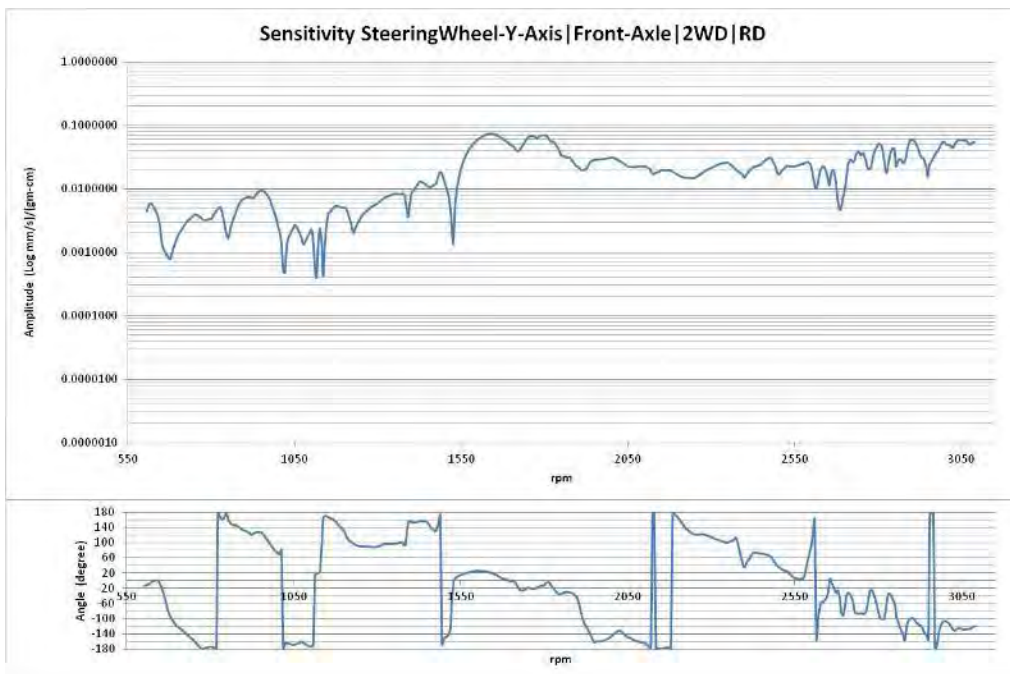


Figure A.14 Sensitivity and phase Steering Wheel-Y-Axis | Front-Axle | 2WD | RD

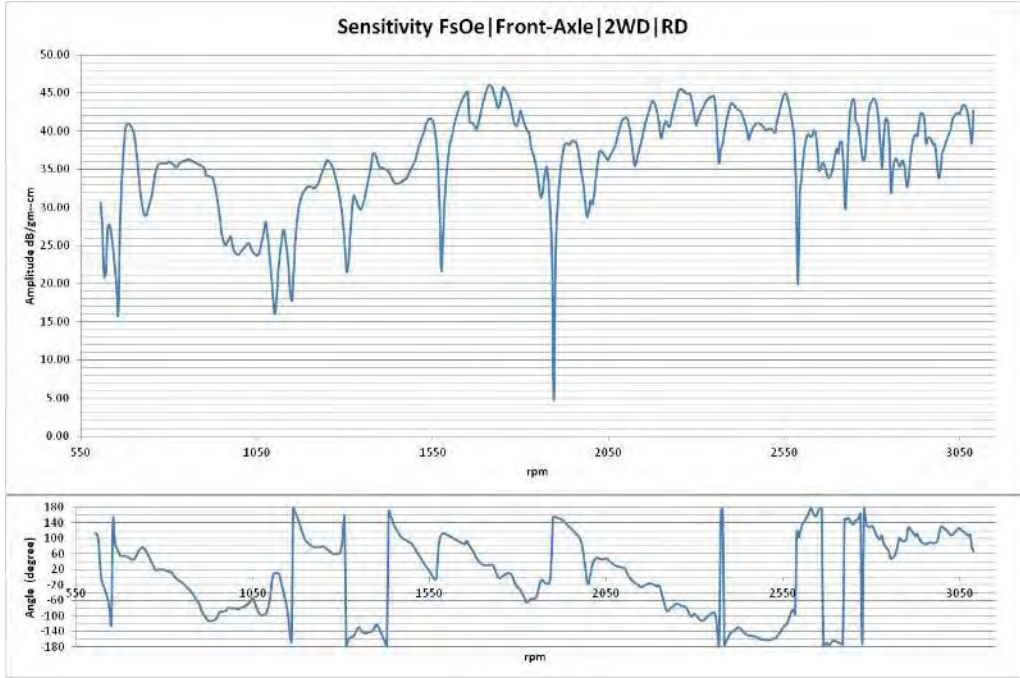


Figure A.15 Sensitivity and phase FsOe | Front-Axle | 2WD | RD

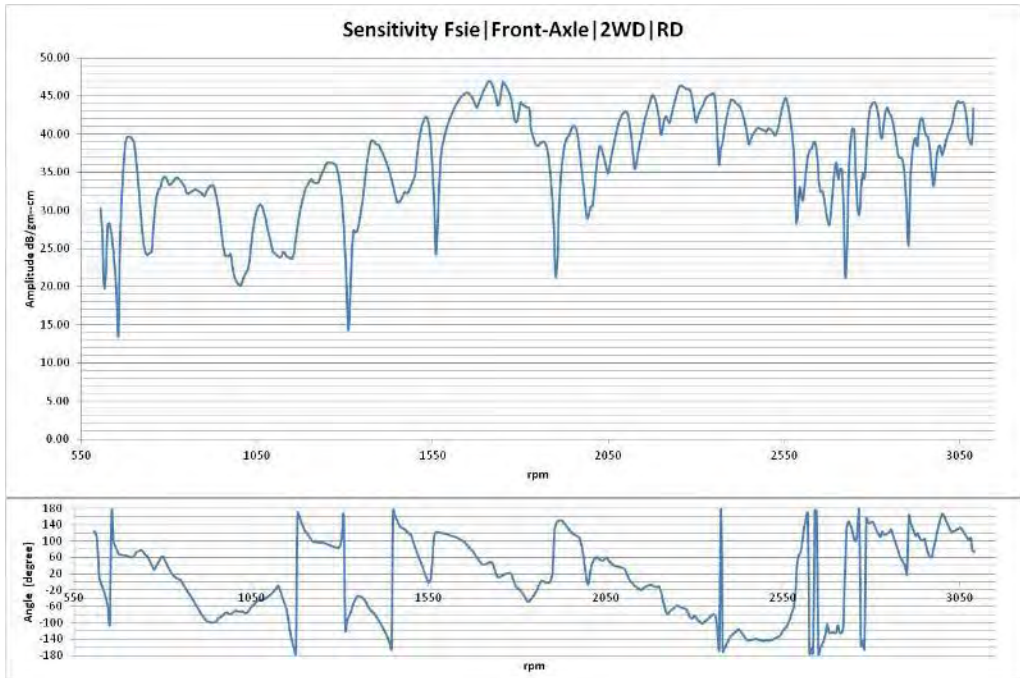


Figure A.16 Sensitivity and phase Fsie | Front-Axle | 2WD | RD

Four Wheel Drive (4WD)-Run up (RU) Sensitivity Calculations:

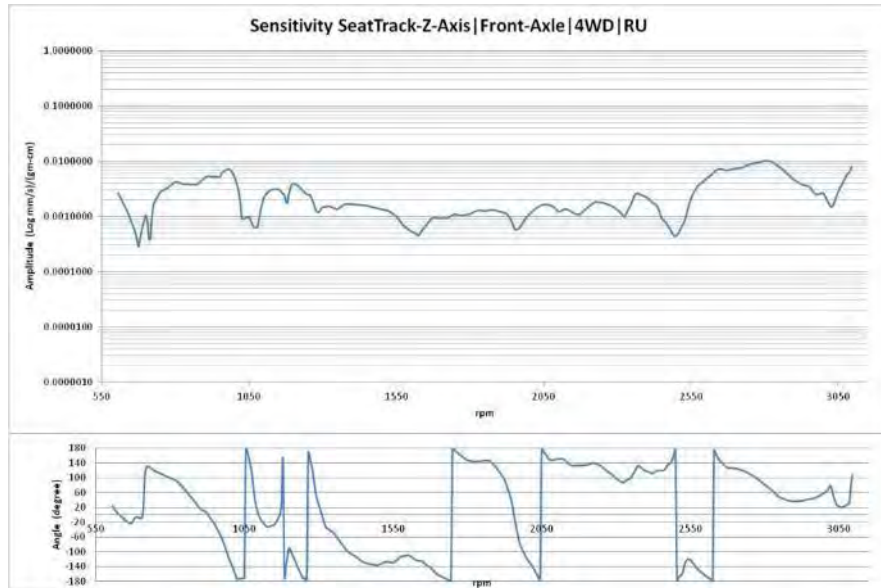


Figure A.17 Sensitivity and phase Seat-Track-Z-Axis | Front-Axle | 4WD |RU

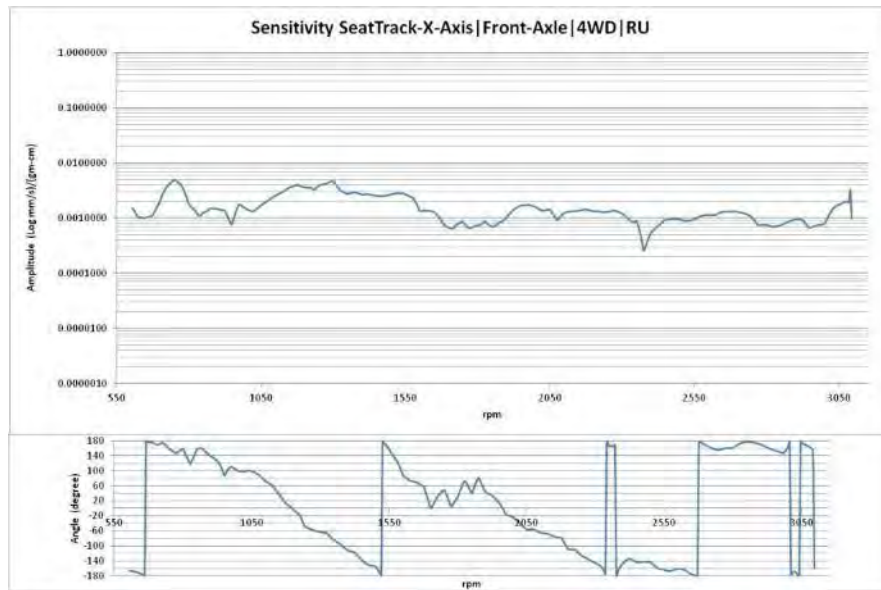


Figure A.18 Sensitivity and phase Seat-Track-X-Axis | Front-Axle | 4WD |RU

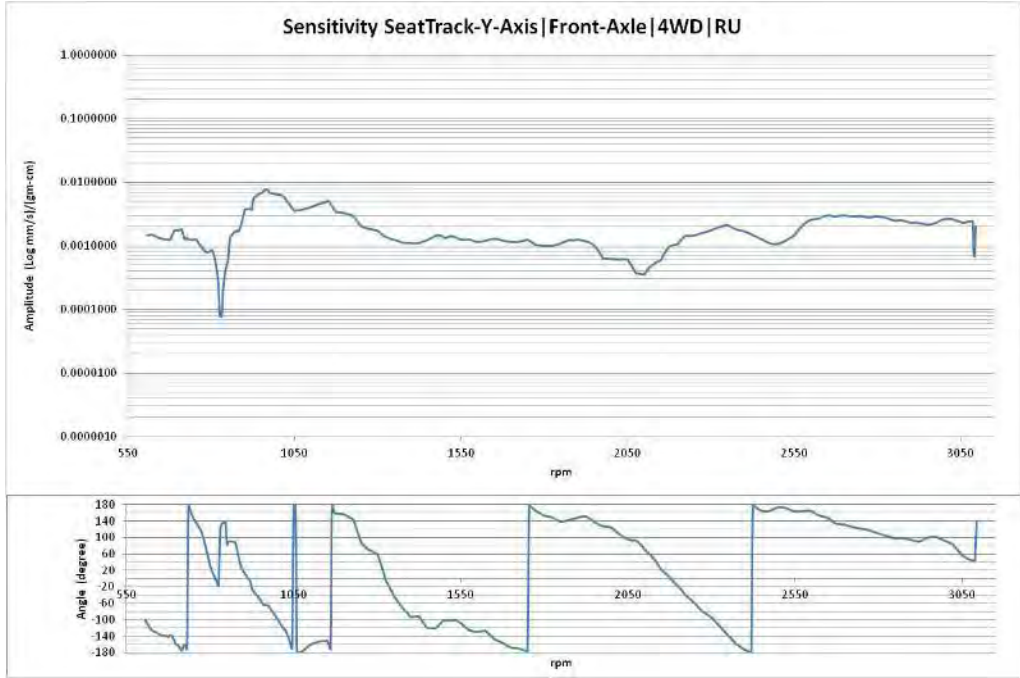


Figure A.19 Sensitivity and phase Seat-Track-Y-Axis| Front-Axle | 4WD |RU

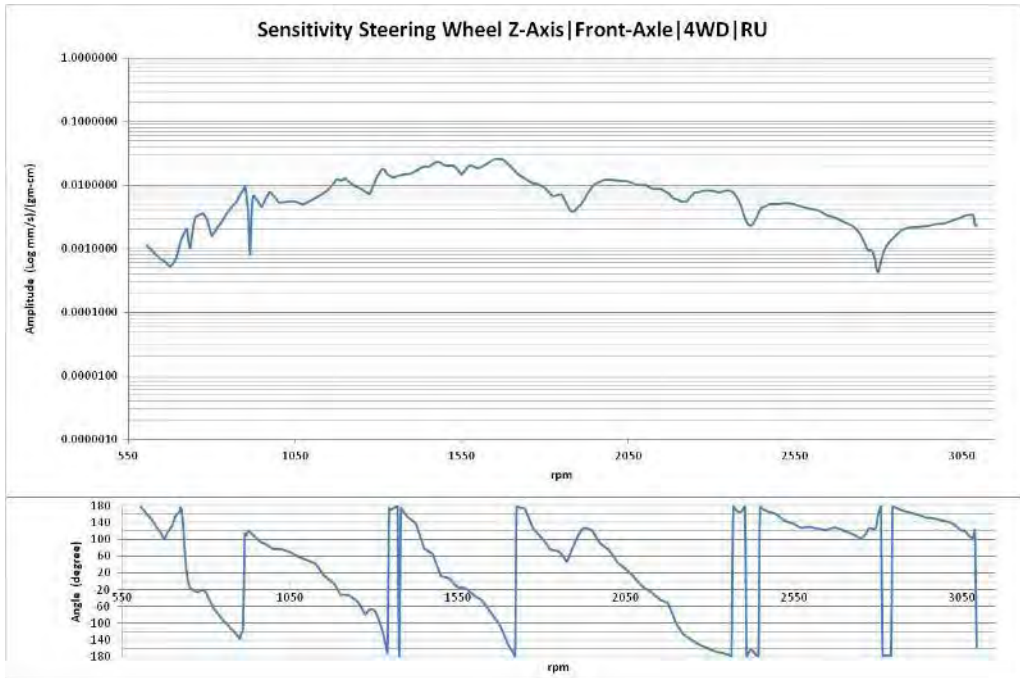


Figure A.20 Sensitivity and phase Steering Wheel-Z-Axis| Front-Axle | 4WD |RU

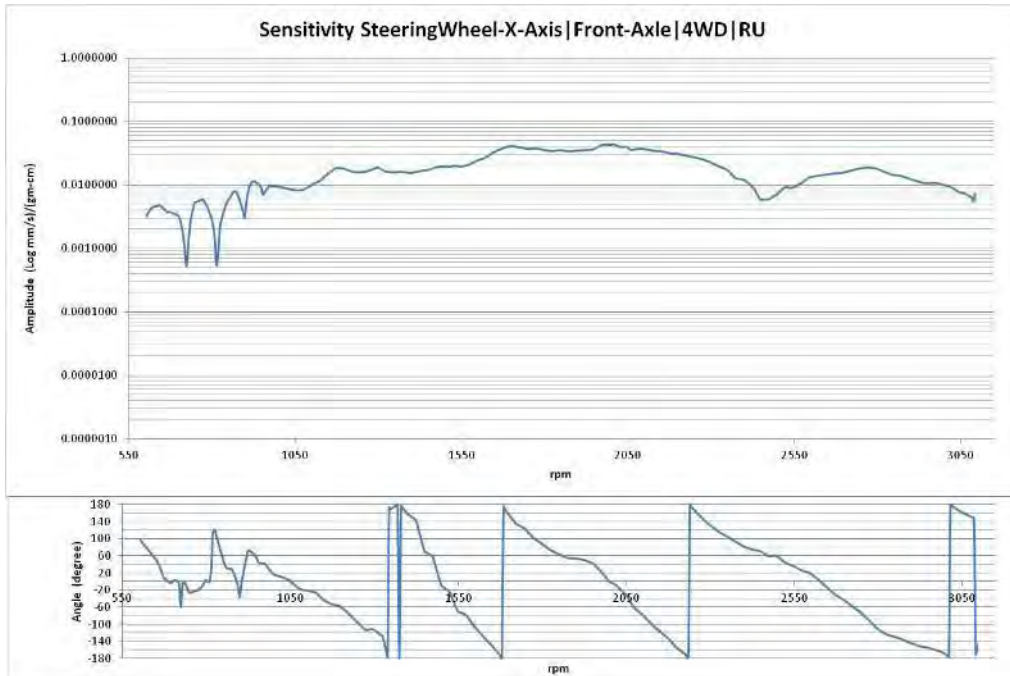


Figure A.21 Sensitivity and phase Steering Wheel-X-Axis| Front-Axle | 4WD |RU

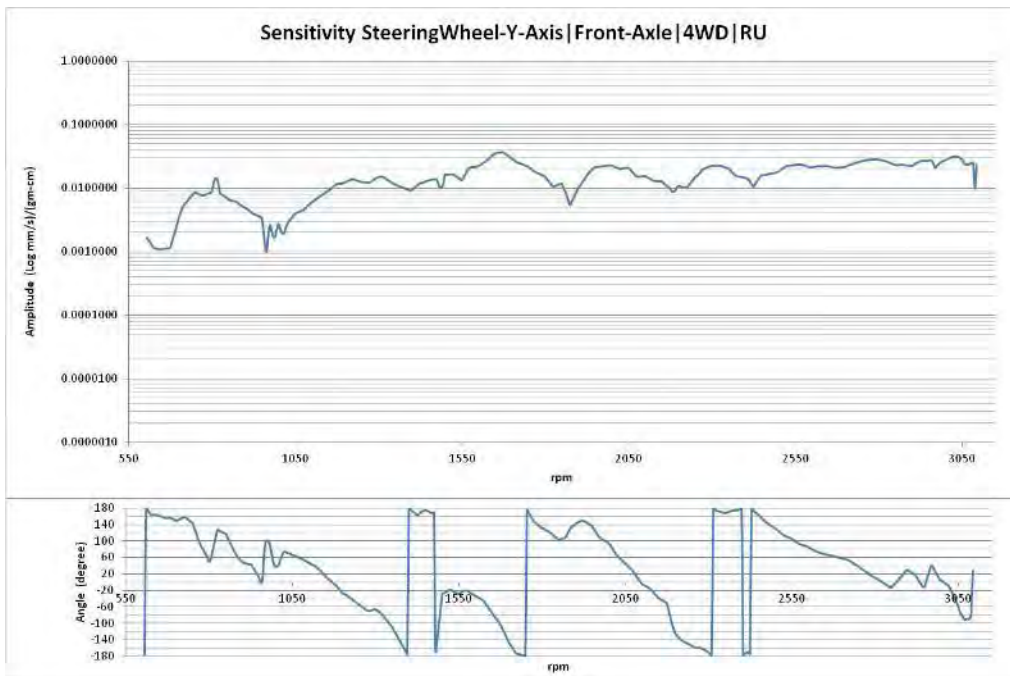


Figure A.22 Sensitivity and phase Steering Wheel-Y-Axis| Front-Axle | 4WD |RU

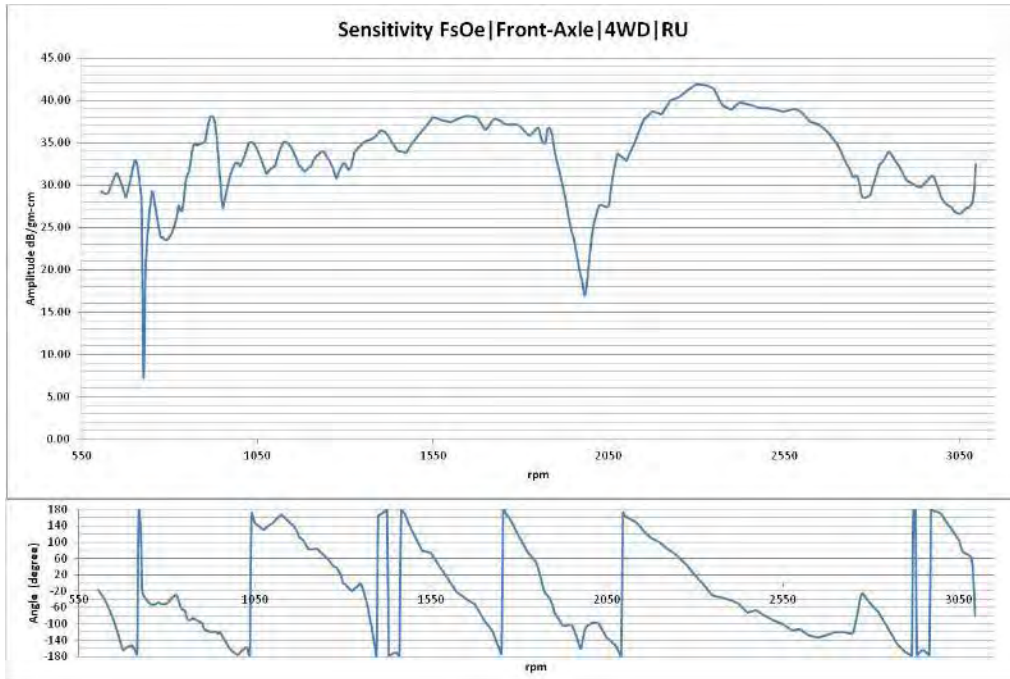


Figure A.23 Sensitivity and phase FsOe | Front-Axle | 4WD | RU

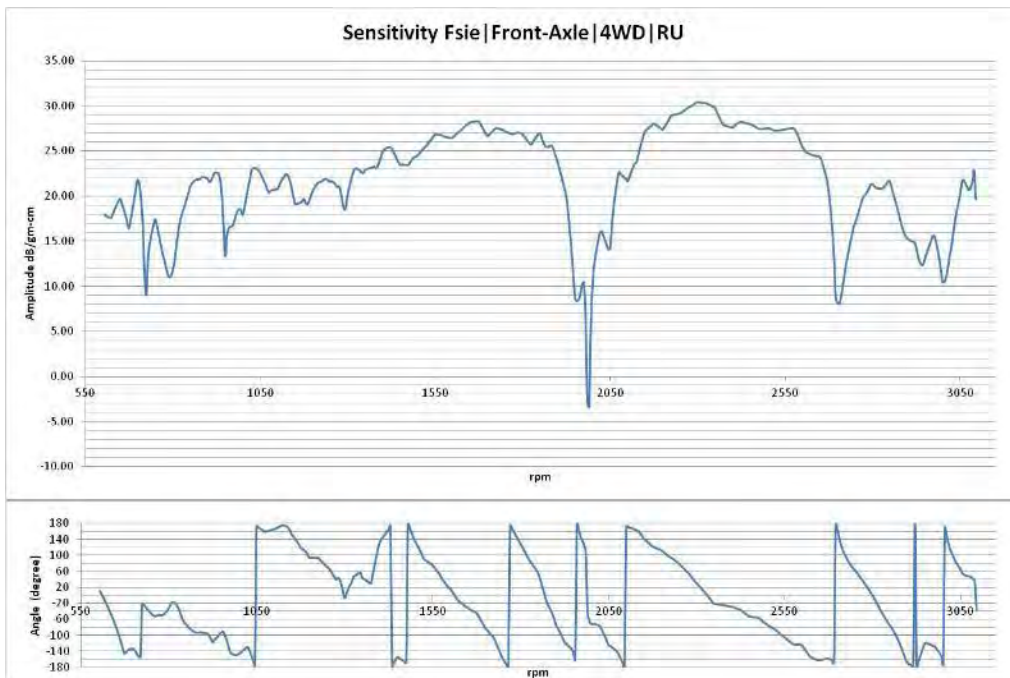


Figure A.24 Sensitivity and phase Fsie | Front-Axle | 4WD | RU

Four Wheel Drive (4WD)-Run down (RD) Sensitivity Calculations:

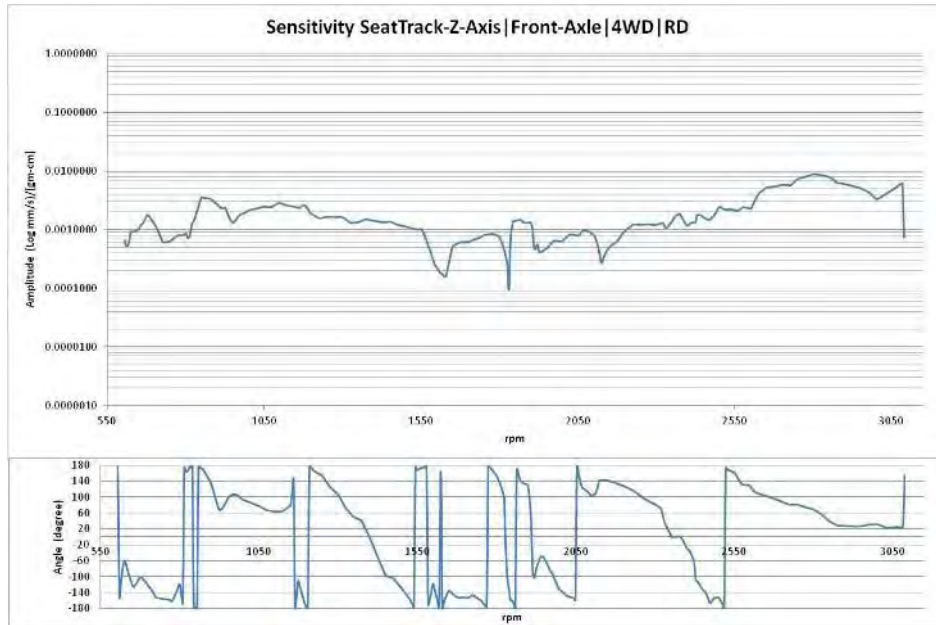


Figure A.25 Sensitivity and phase Seat Track -Z-Axis | Front-Axle | 4WD | RD

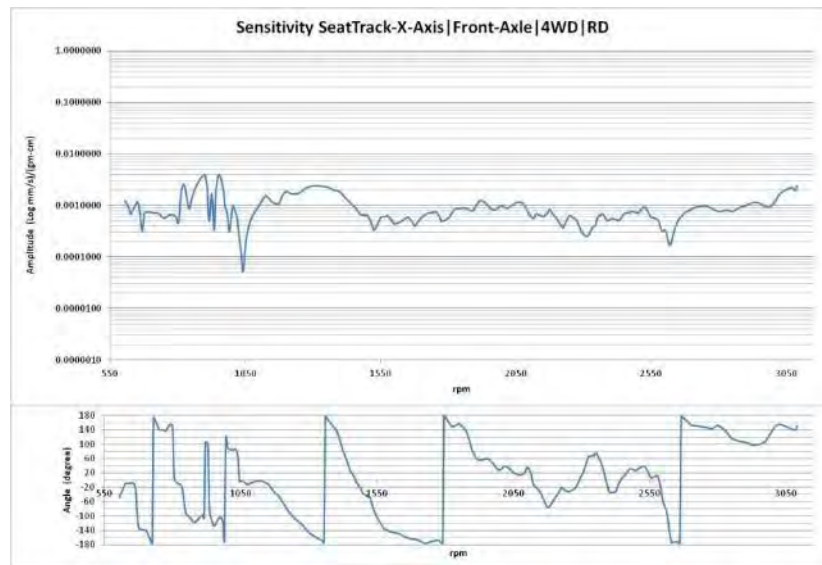


Figure A.26 Sensitivity and phase Seat Track -X-Axis | Front-Axle | 4WD | RD

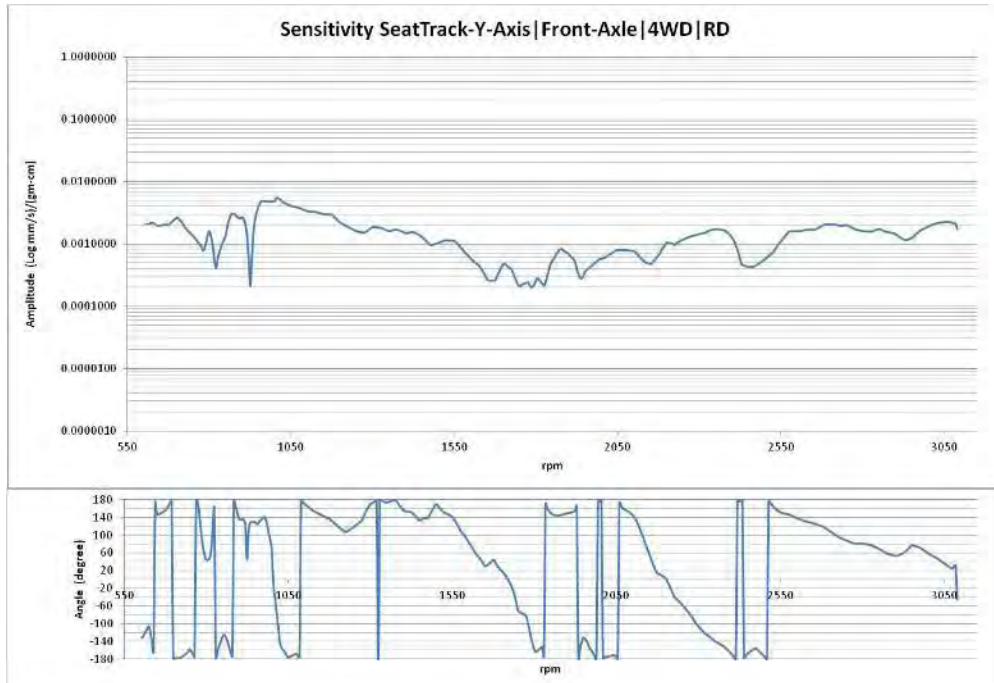


Figure A.27 Sensitivity and phase Seat Track -Y-Axis| Front-Axle | 4WD |RD

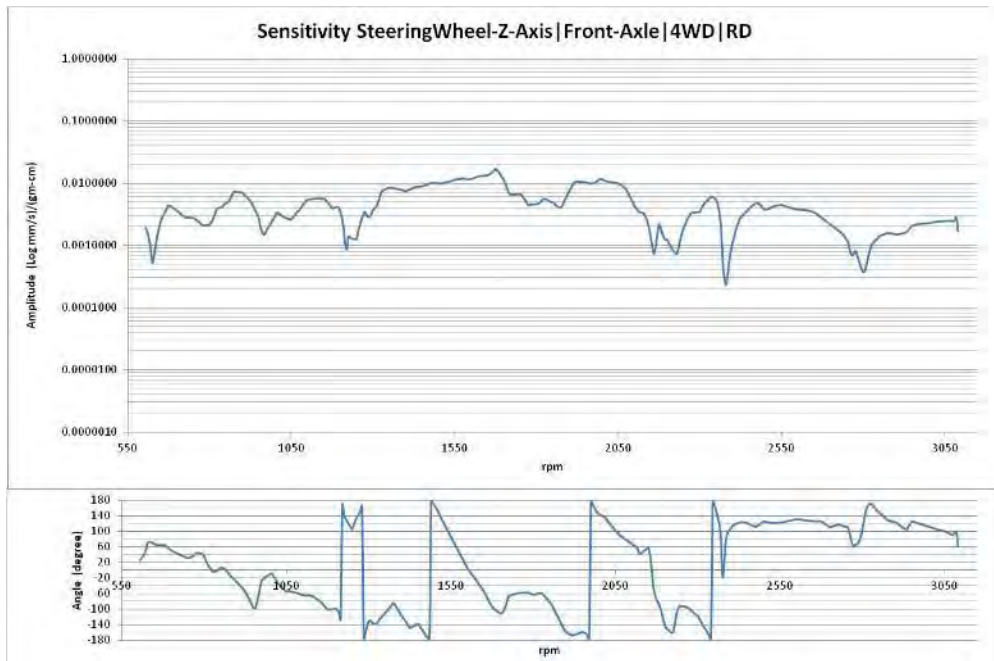


Figure A.28 Sensitivity and phase Steering Wheel-Z-Axis| Front-Axle | 4WD |RD

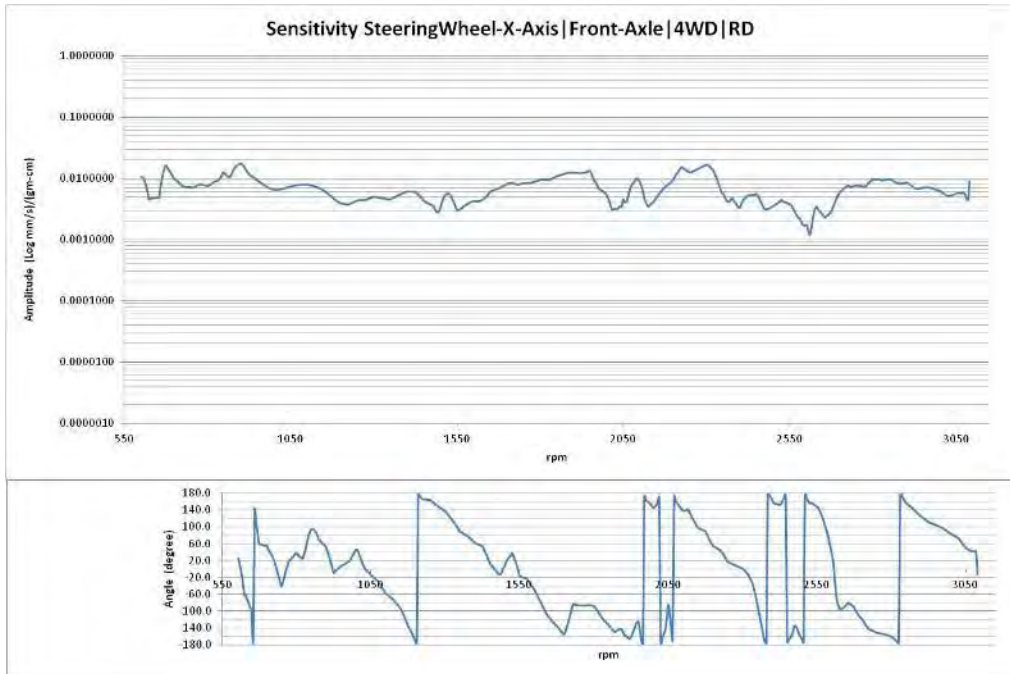


Figure A.29 Sensitivity and phase Steering Wheel-X-Axis | Front-Axle | 4WD | RD

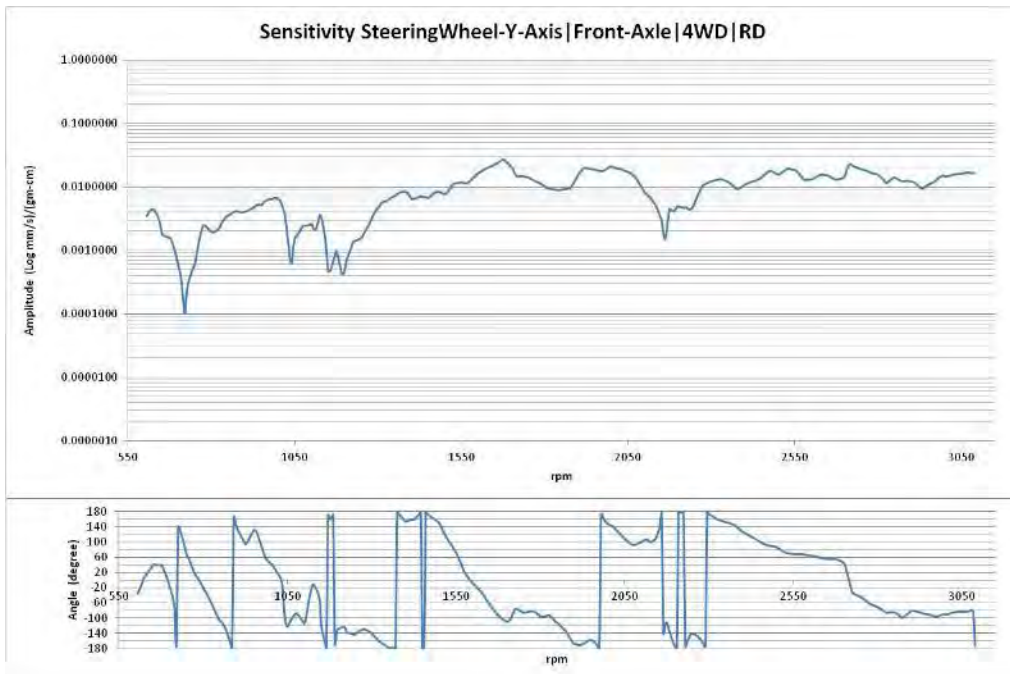


Figure A.30 Sensitivity and phase Steering Wheel-Y-Axis | Front-Axle | 4WD | RD

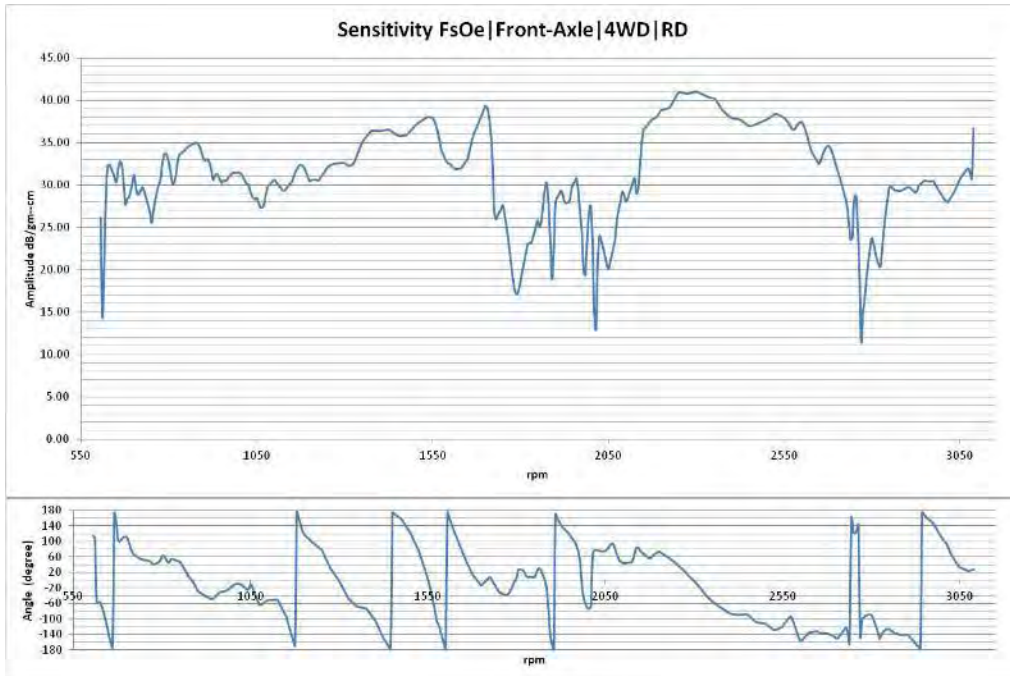


Figure A.31 Sensitivity and phase FsOe | Front-Axle | 4WD | RD

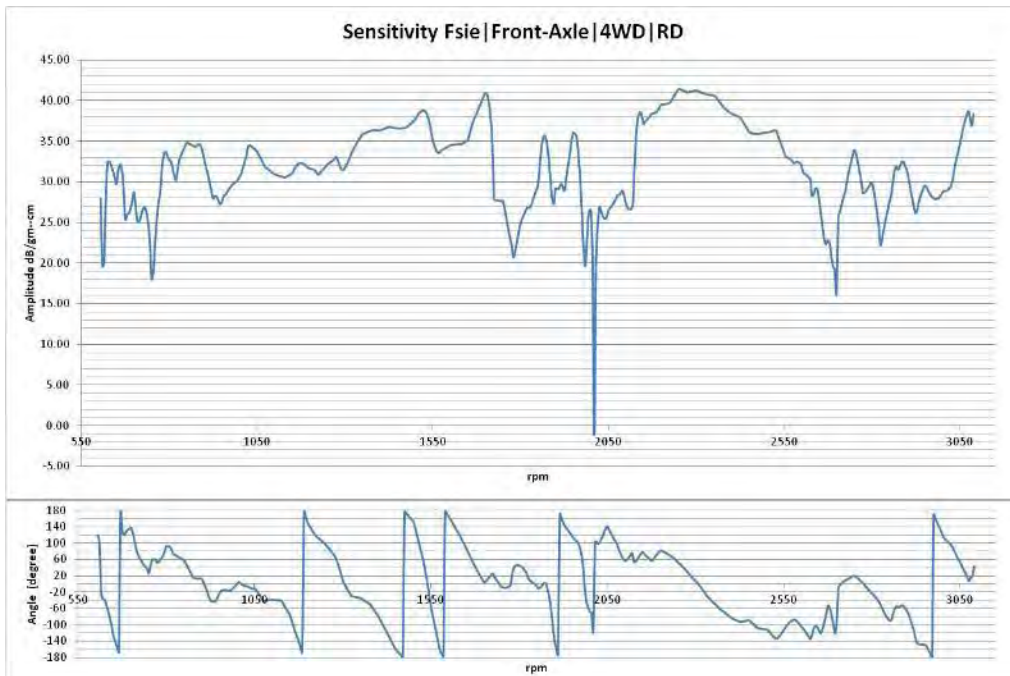


Figure A.32 Sensitivity and phase Fsie | Front-Axle | 4WD | RD

Plane B sensitivity curves

Two Wheel Drive (2WD)-Run up (RU) Sensitivity Calculations:

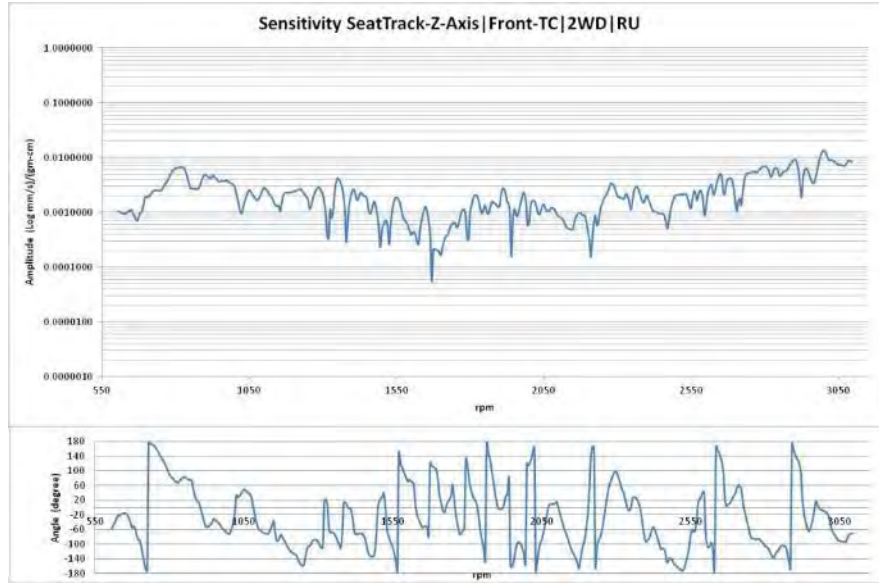


Figure A.33 Sensitivity and phase Seat-Track-Z-Axis| Front-TC | 2WD |RU

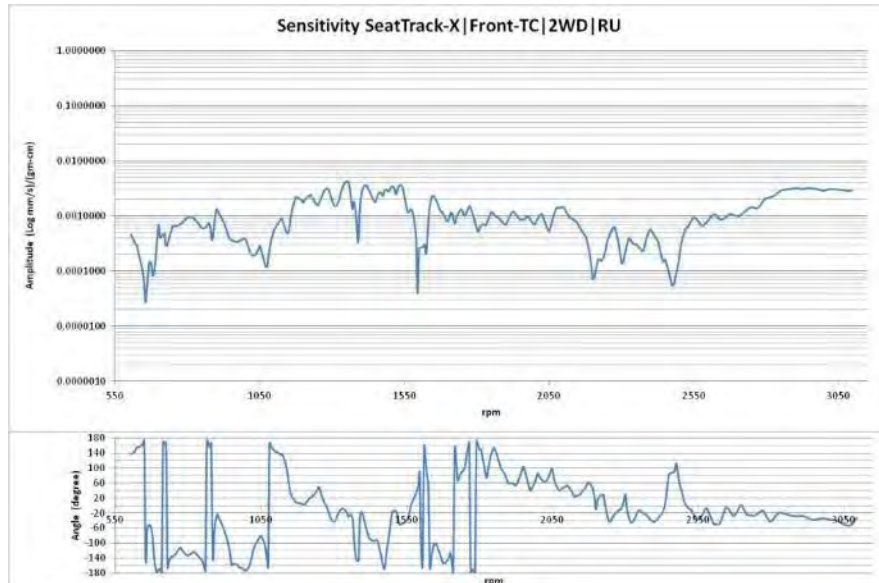


Figure A.34 Sensitivity and phase Seat-Track-X-Axis| Front-TC | 2WD |RU

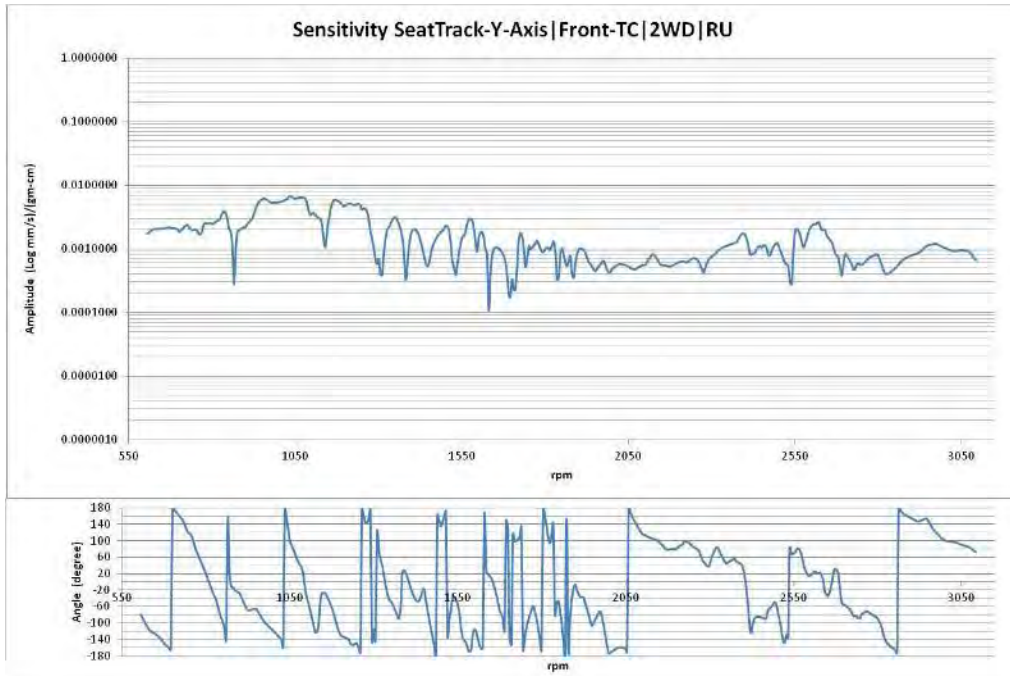


Figure A.35 Sensitivity and phase Seat-Track-Y-Axis| Front-TC | 2WD |RU

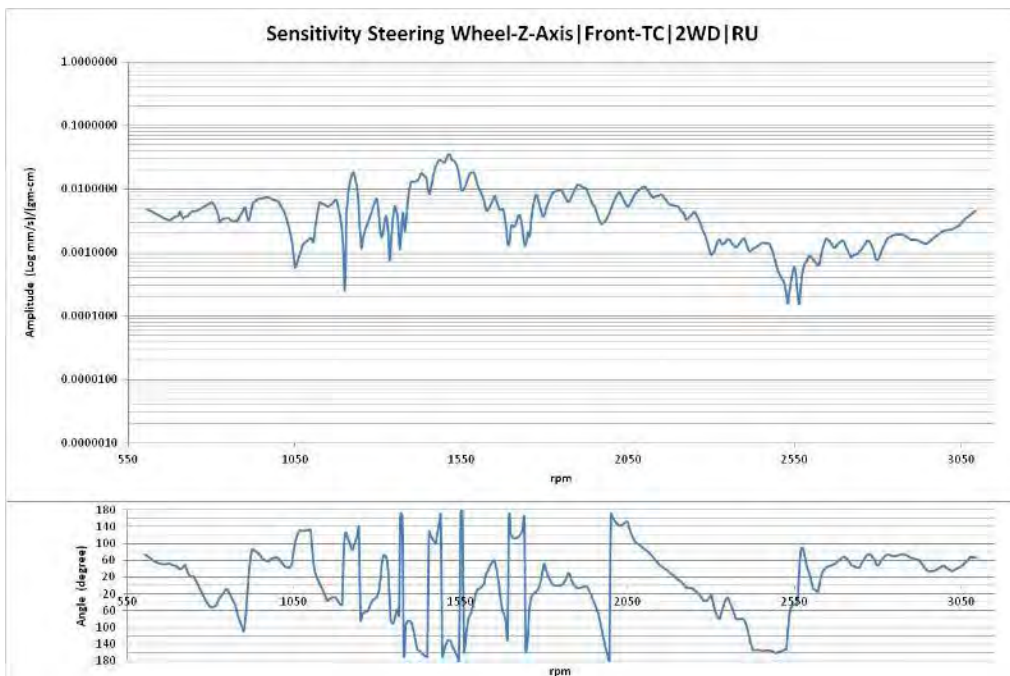


Figure A.36 Sensitivity and phase Steering Wheel-Z-Axis| Front-TC | 2WD |RU

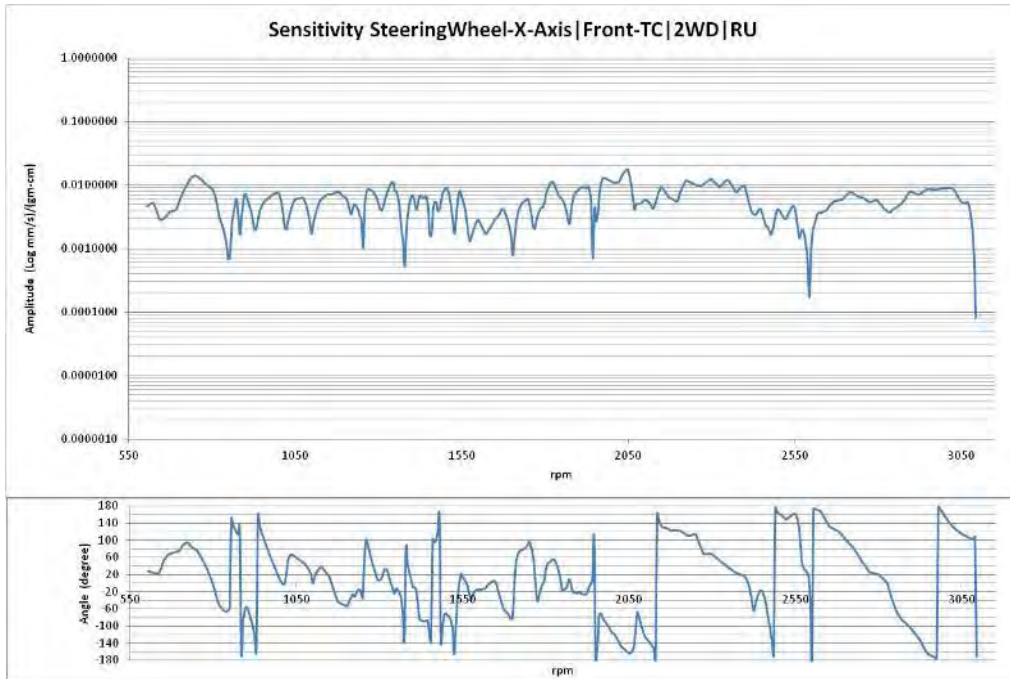


Figure A.37 Sensitivity and phase Steering Wheel-X-Axis| Front-TC | 2WD |RU

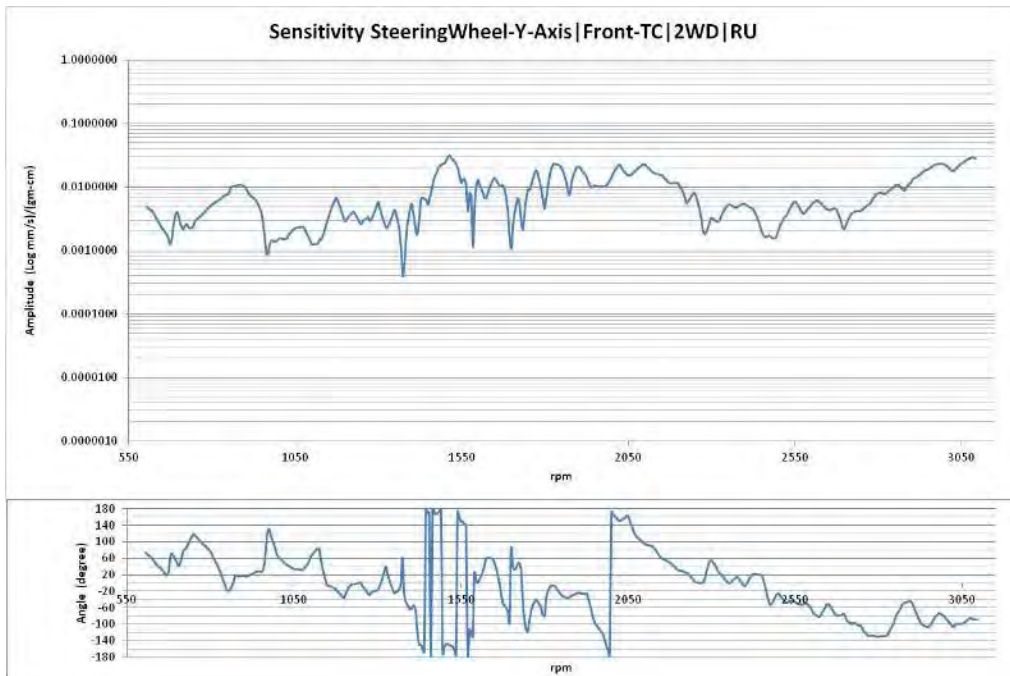


Figure A.38 Sensitivity and phase Steering Wheel-Y-Axis| Front-TC | 2WD |RU

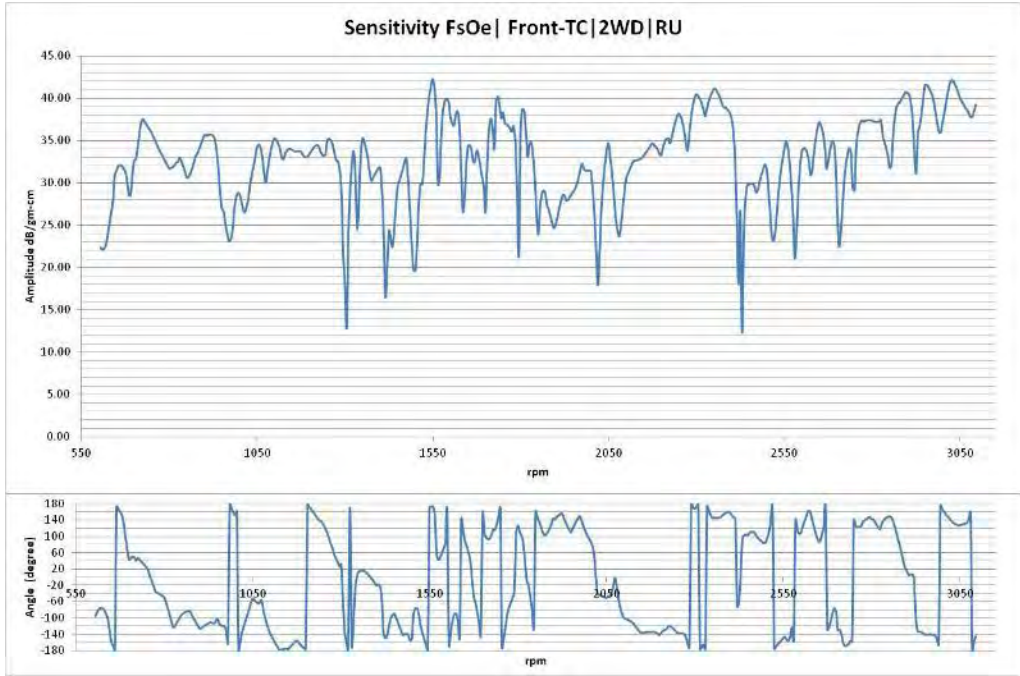


Figure A.39 Sensitivity and phase FsOe | Front-TC | 2WD | RU

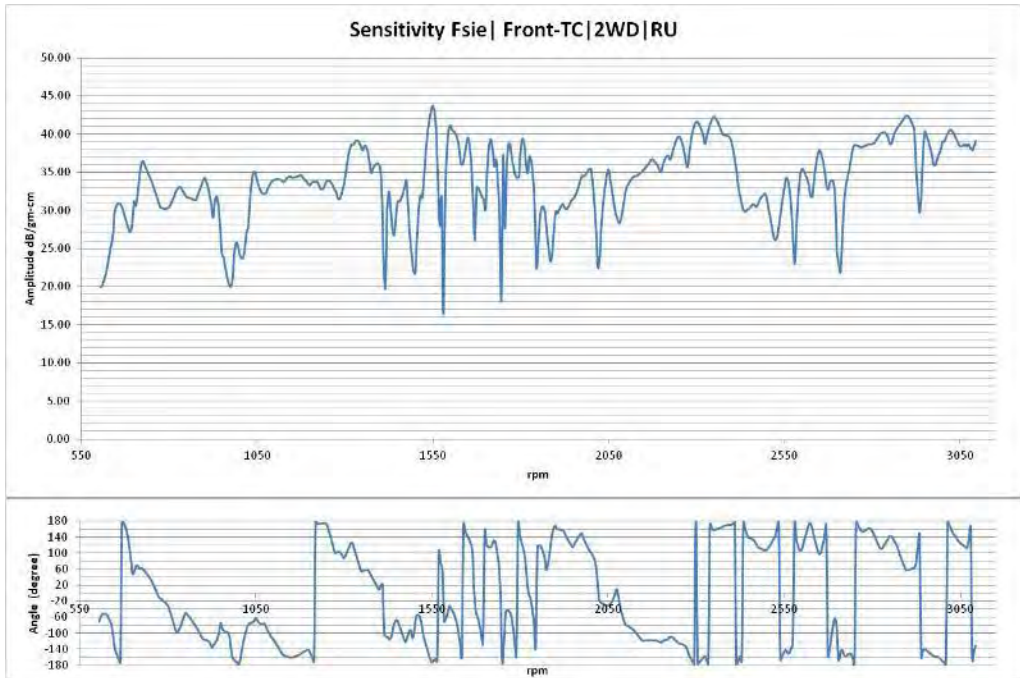


Figure A.40 Sensitivity and phase Fsie | Front-TC | 2WD | RU

Two Wheel Drive (2WD)-Run down (RD) Sensitivity Calculations:

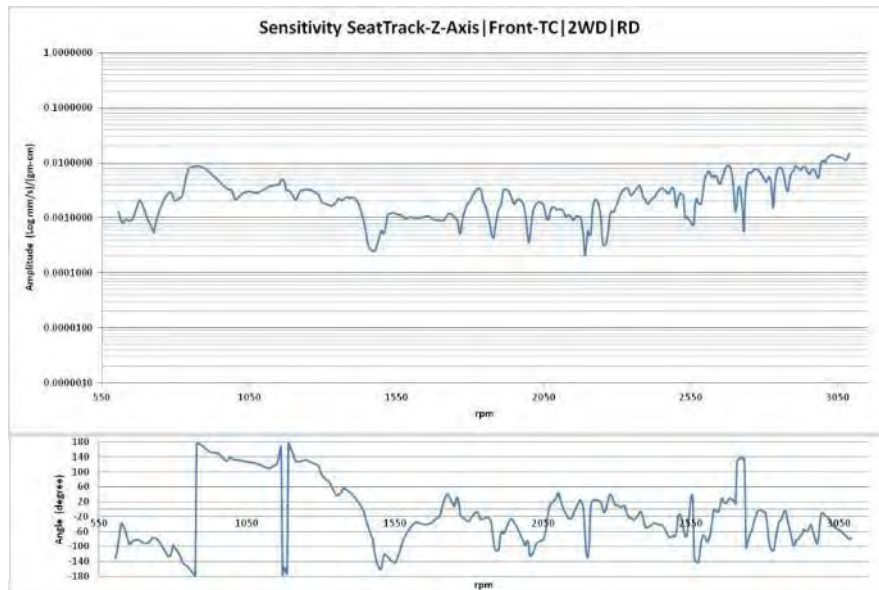


Figure A.41 Sensitivity and phase Seat Track -Z-Axis| Front-TC | 2WD |RD

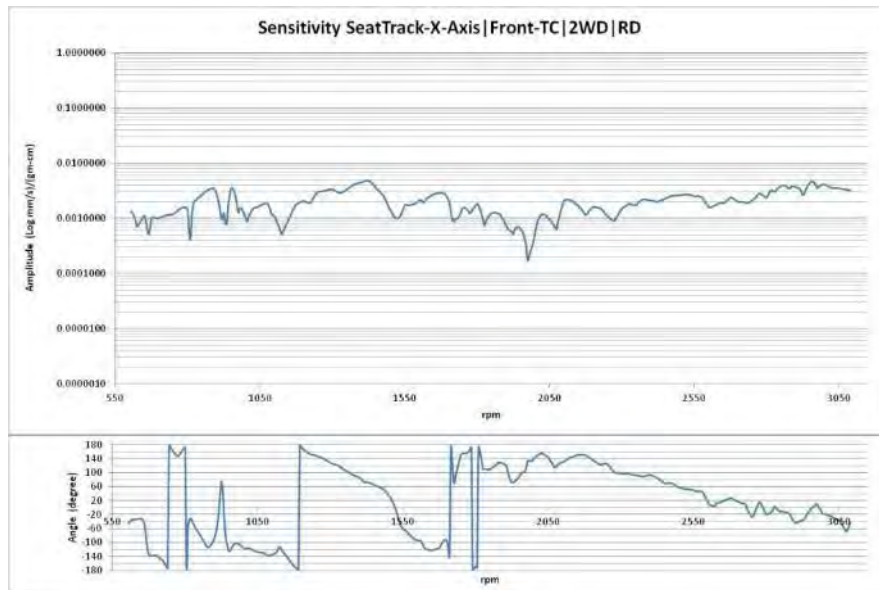


Figure A.42 Sensitivity and phase Seat Track -X-Axis| Front-TC | 2WD |RD

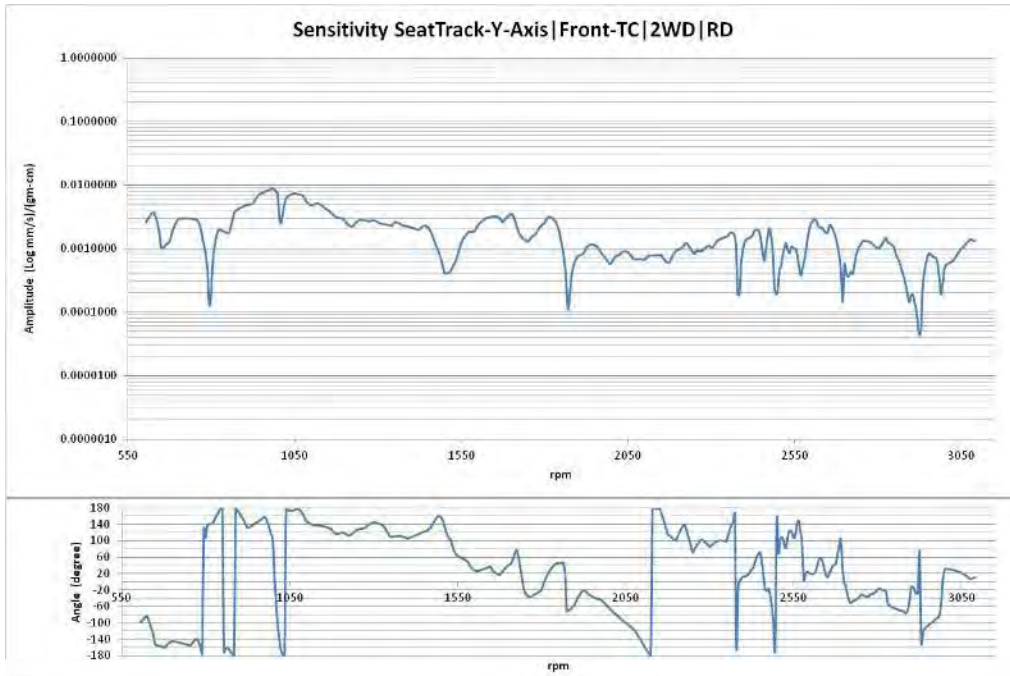


Figure A.43 Sensitivity and phase Seat Track -Y-Axis| Front-TC | 2WD |RD

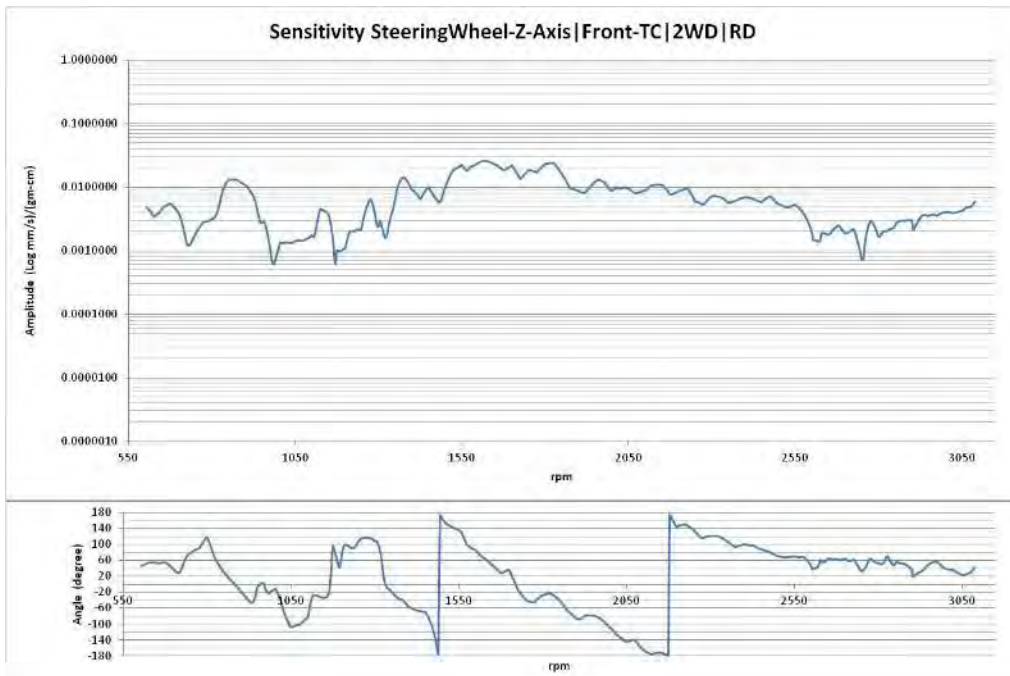


Figure A.44 Sensitivity and phase Steering Wheel-Z-Axis| Front-TC | 2WD |RD

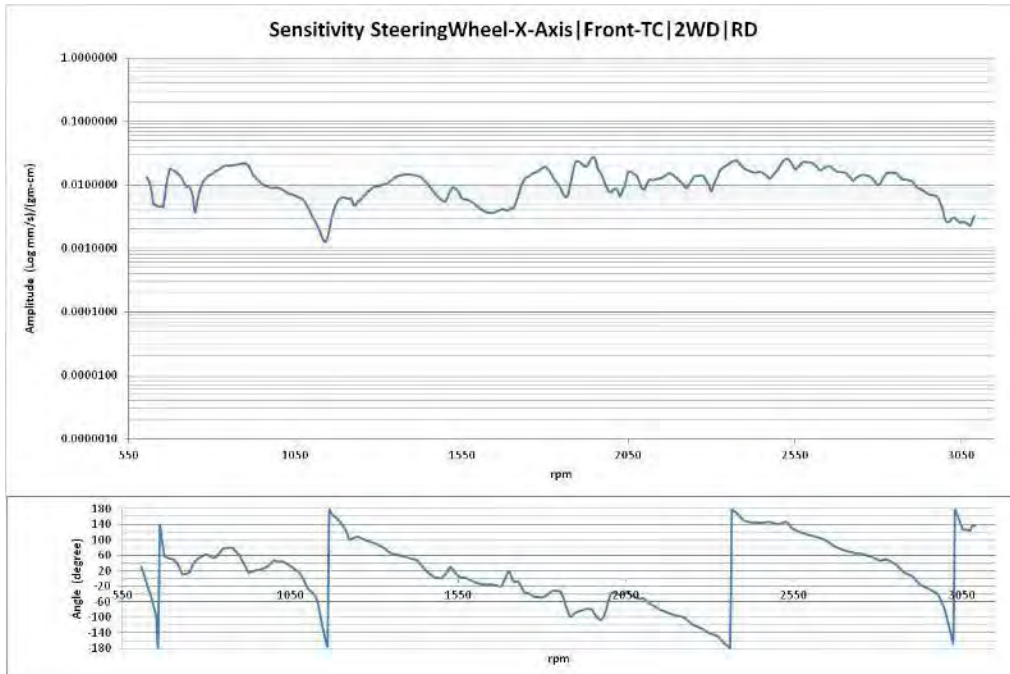


Figure A.45 Sensitivity and phase Steering Wheel-X-Axis| Front-TC | 2WD |RD

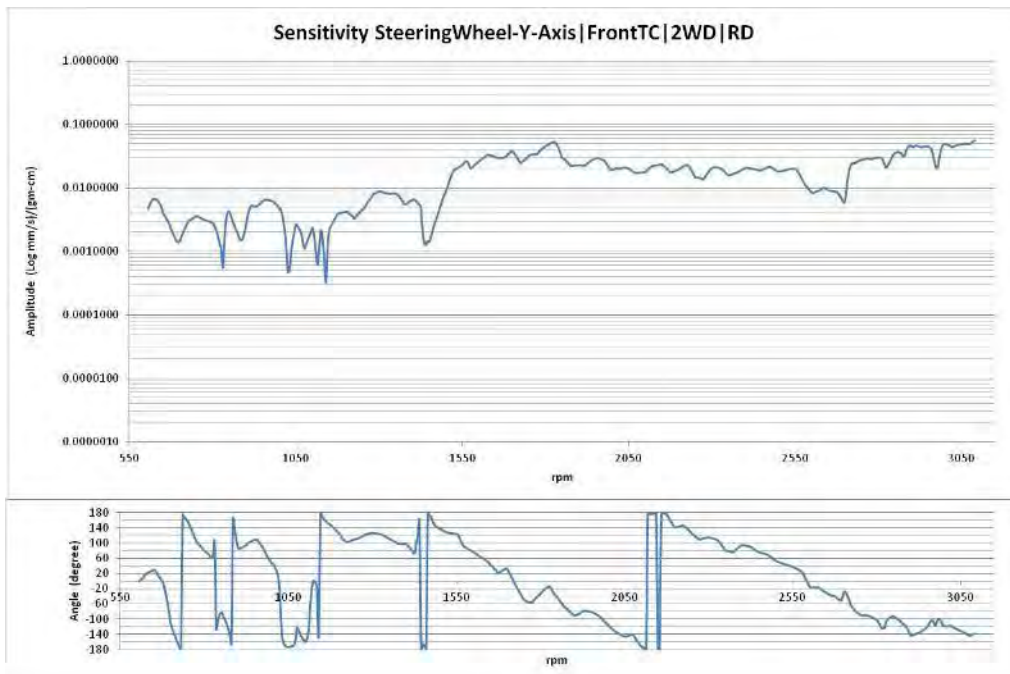


Figure A.46 Sensitivity and phase Steering Wheel-Y-Axis| Front-TC | 2WD |RD

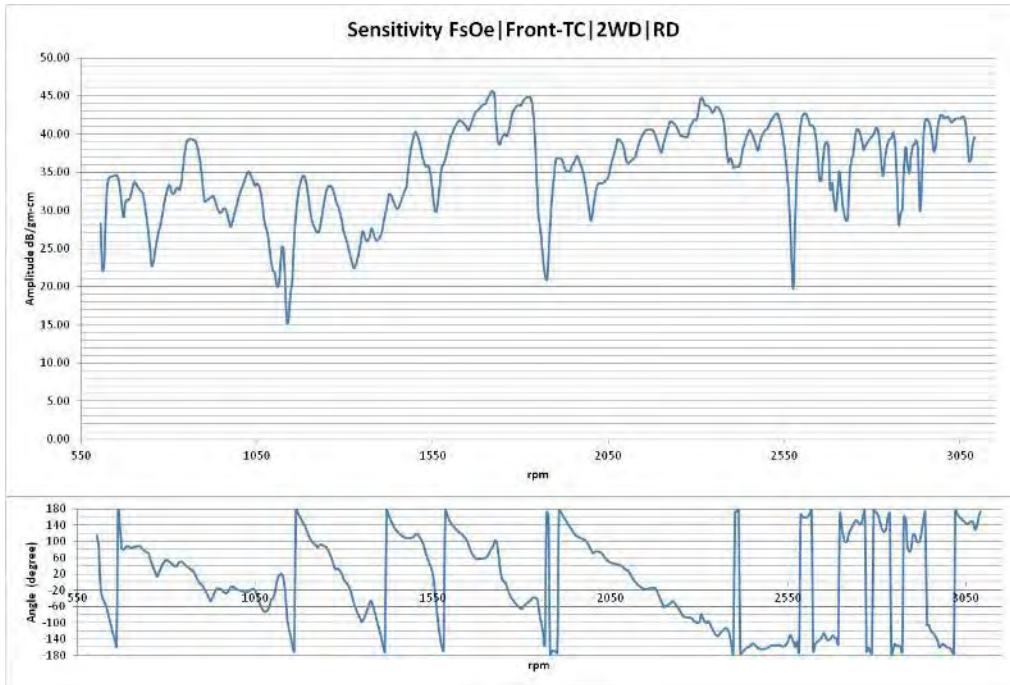


Figure A.47 Sensitivity and phase FsOe | Front-TC | 2WD | RD

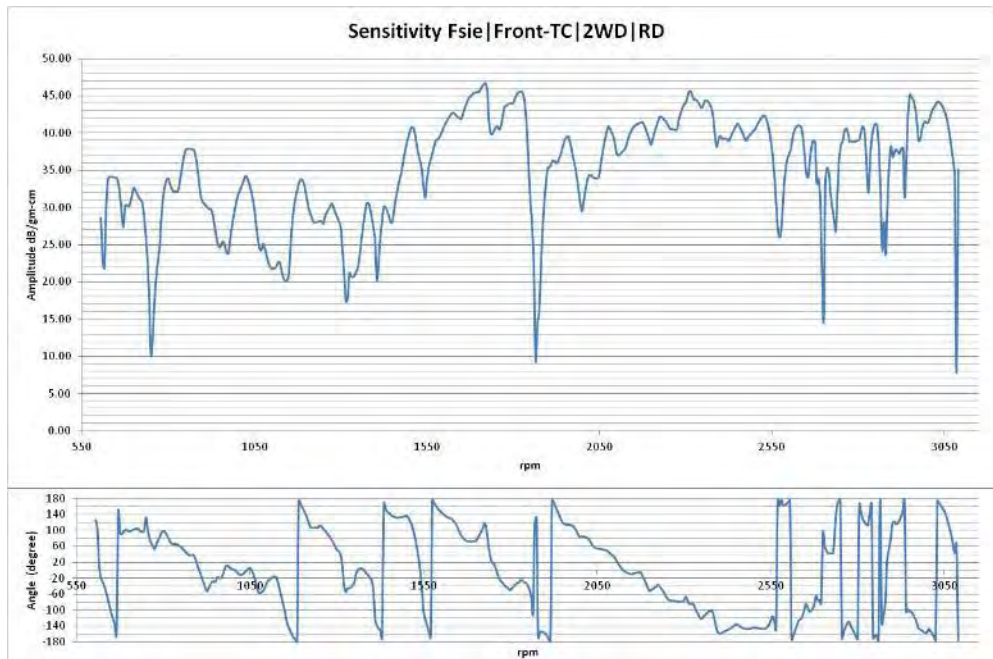


Figure A.48 Sensitivity and phase Fsie | Front-TC | 2WD | RD

Four Wheel Drive (4WD)-Run up (RU) Sensitivity Calculations:

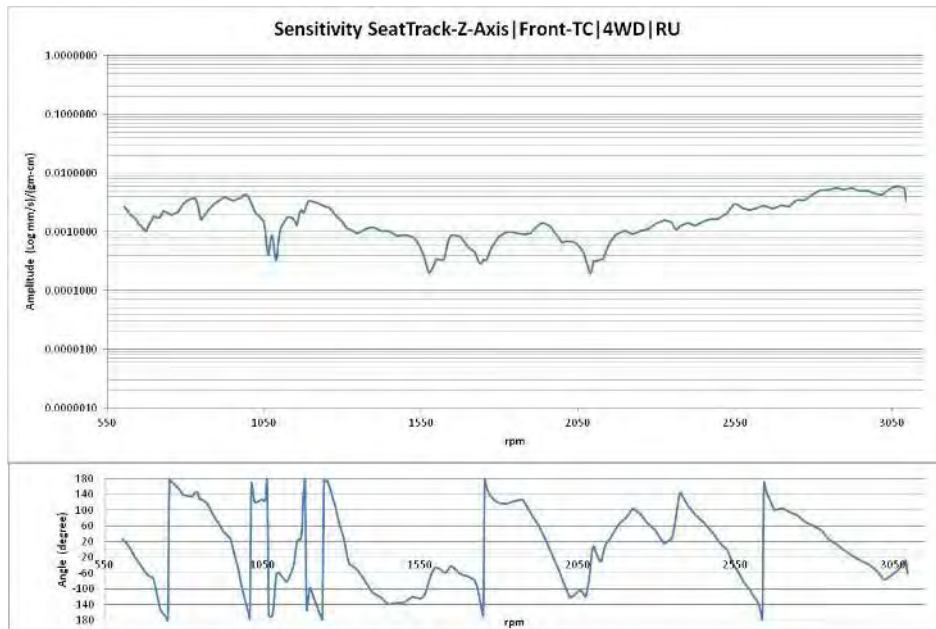


Figure A.49 Sensitivity and phase Seat-Track-Z-Axis| Front-TC | 4WD |RU

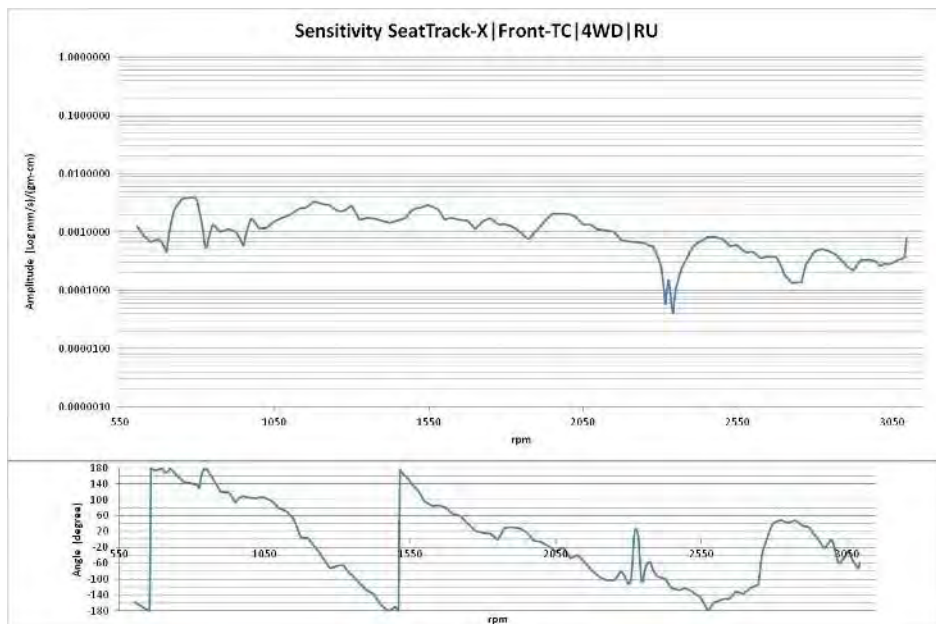


Figure A.50 Sensitivity and phase Seat-Track-X-Axis| Front-TC | 4WD |RU

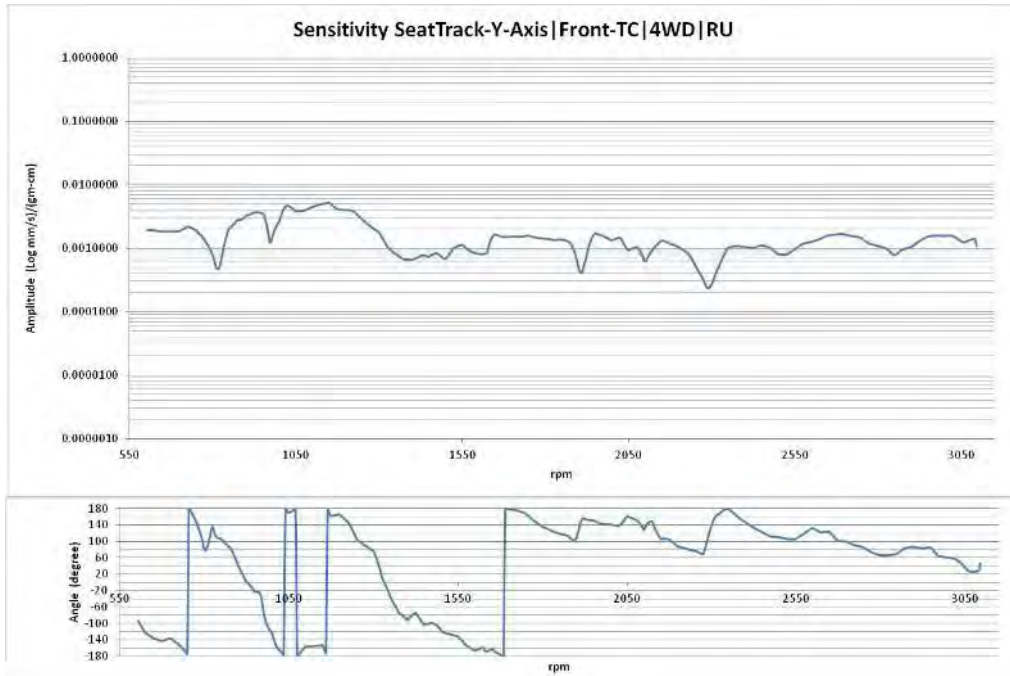


Figure A.51 Sensitivity and phase Seat-Track-Y-Axis| Front-TC | 4WD |RU

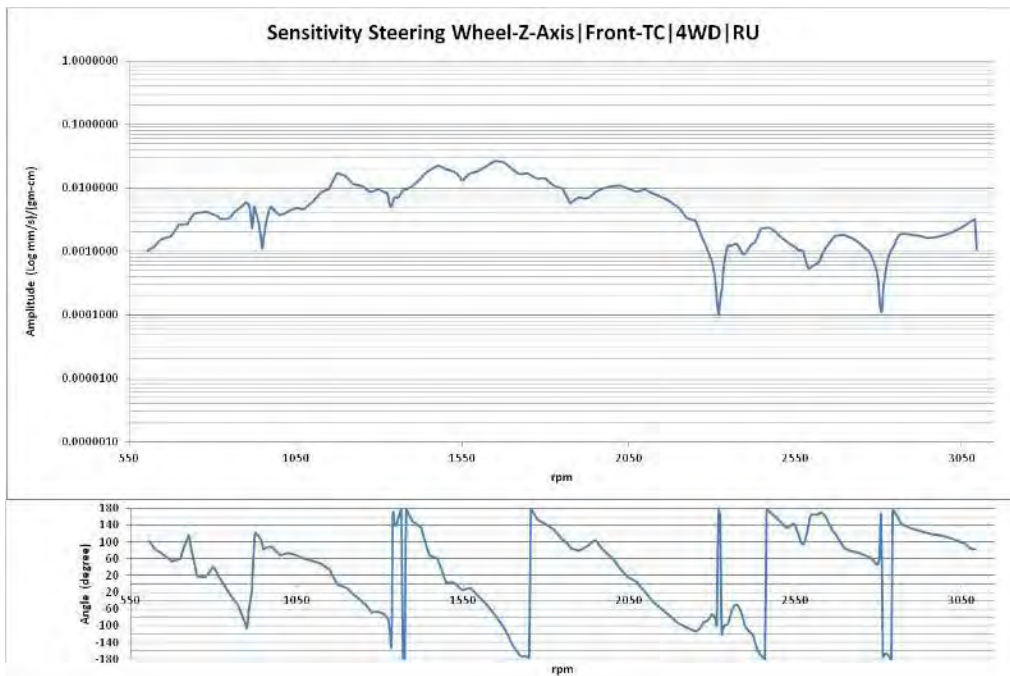


Figure A.52 Sensitivity and phase Steering Wheel-Z-Axis| Front-TC | 4WD |RU

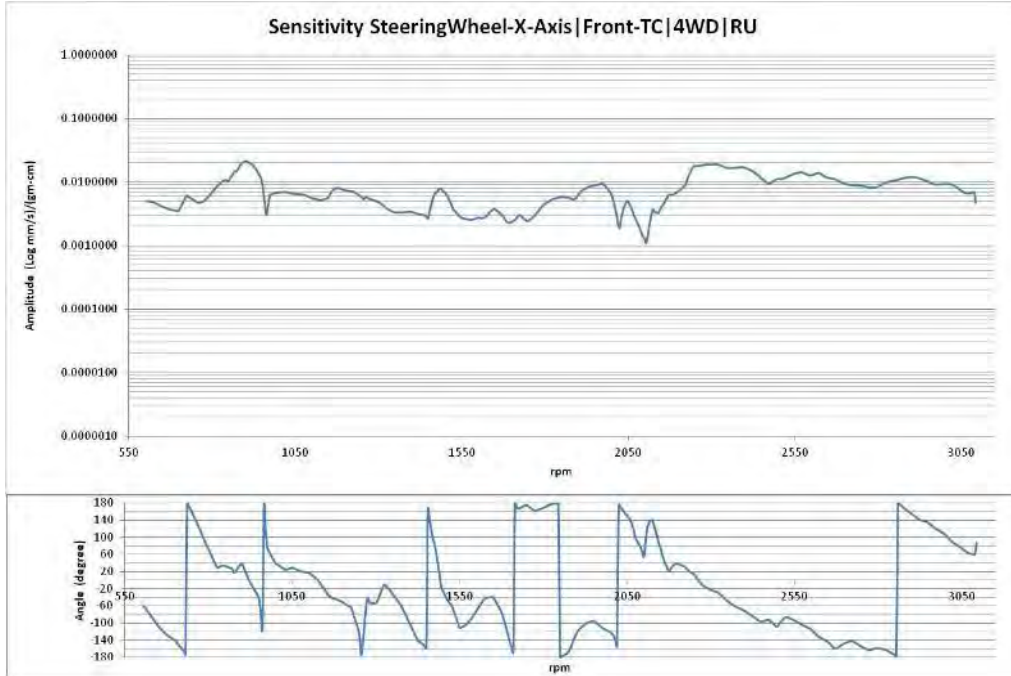


Figure A.53 Sensitivity and phase Steering Wheel-X-Axis| Front-TC | 4WD |RU

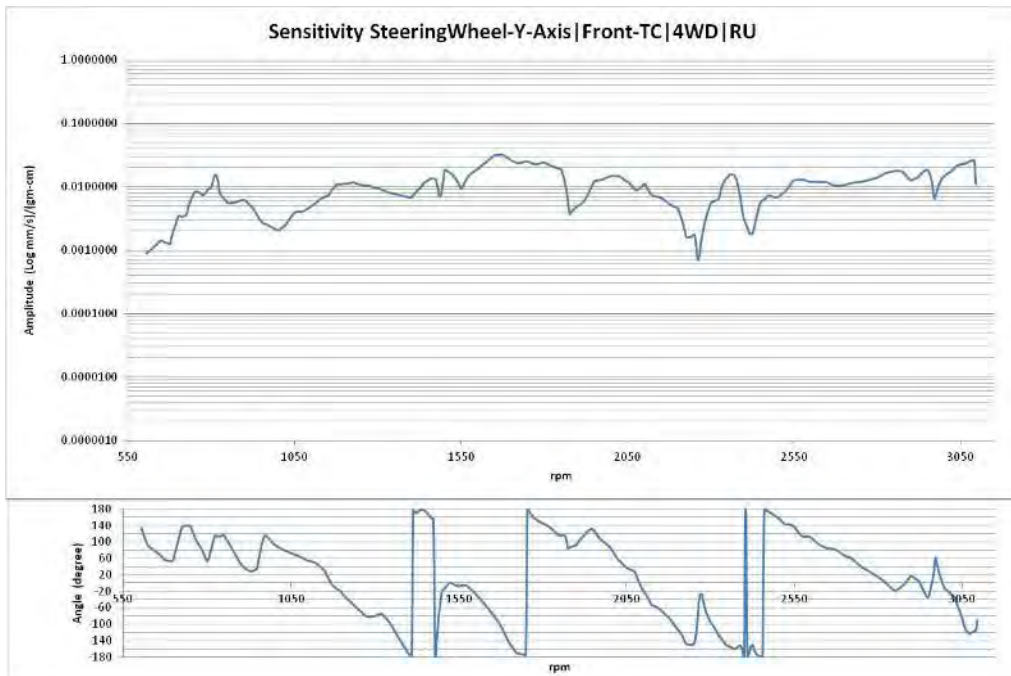


Figure A.54 Sensitivity and phase Steering Wheel-Y-Axis| Front-TC | 4WD |RU

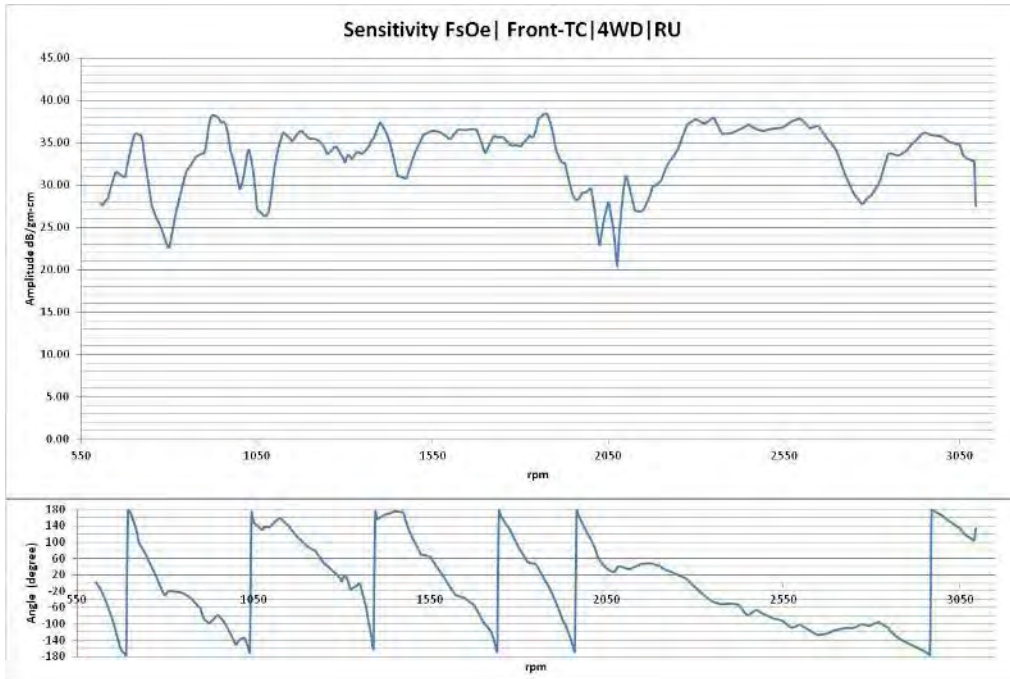


Figure A.55 Sensitivity and phase FsOe | Front-TC | 4WD | RU

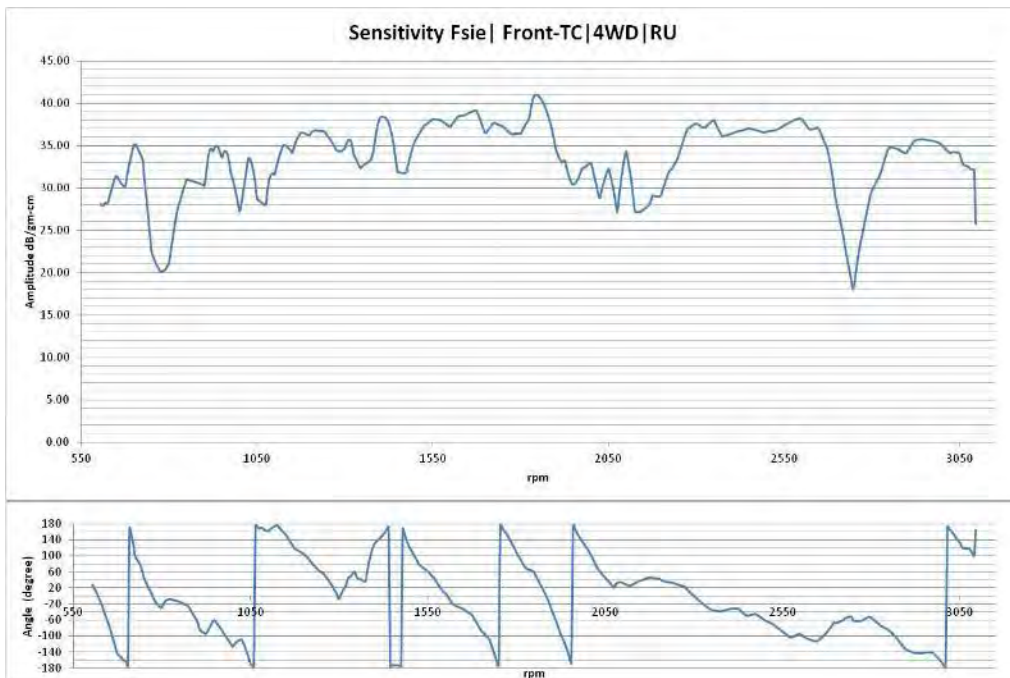


Figure A.56 Sensitivity and phase Fsie | Front-TC | 4WD | RU

Four Wheel Drive (4WD)-Run down (RD) Sensitivity Calculations:

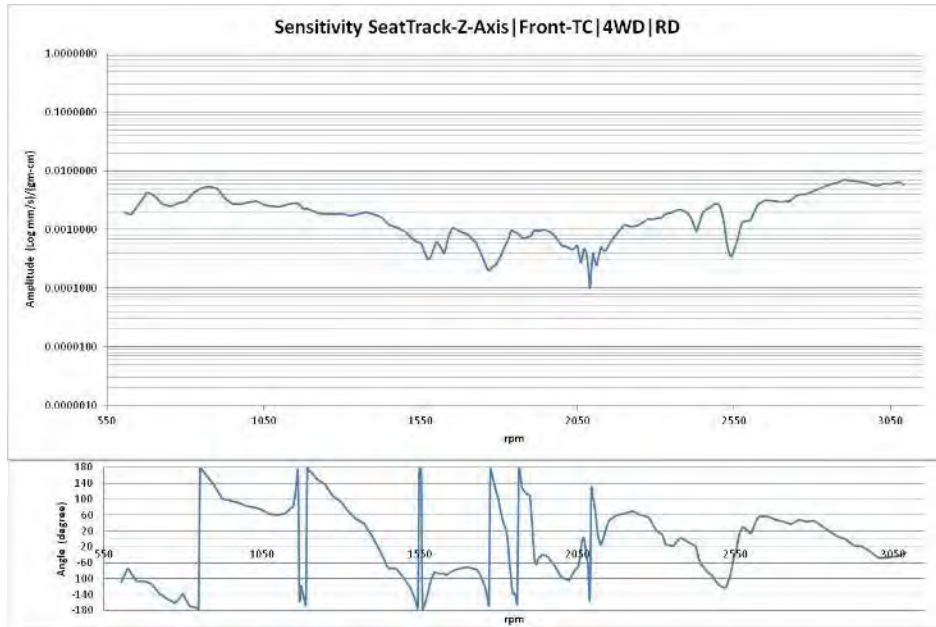


Figure A.57 Sensitivity and phase Seat Track -Z-Axis| Front-TC | 4WD |RD

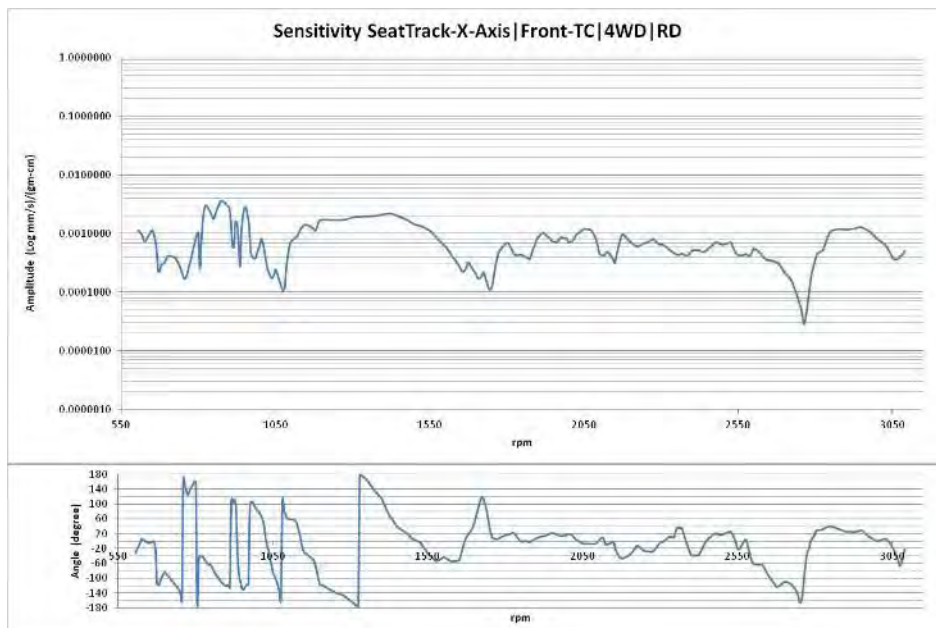


Figure A.58 Sensitivity and phase Seat Track -X-Axis| Front-TC | 4WD |RD

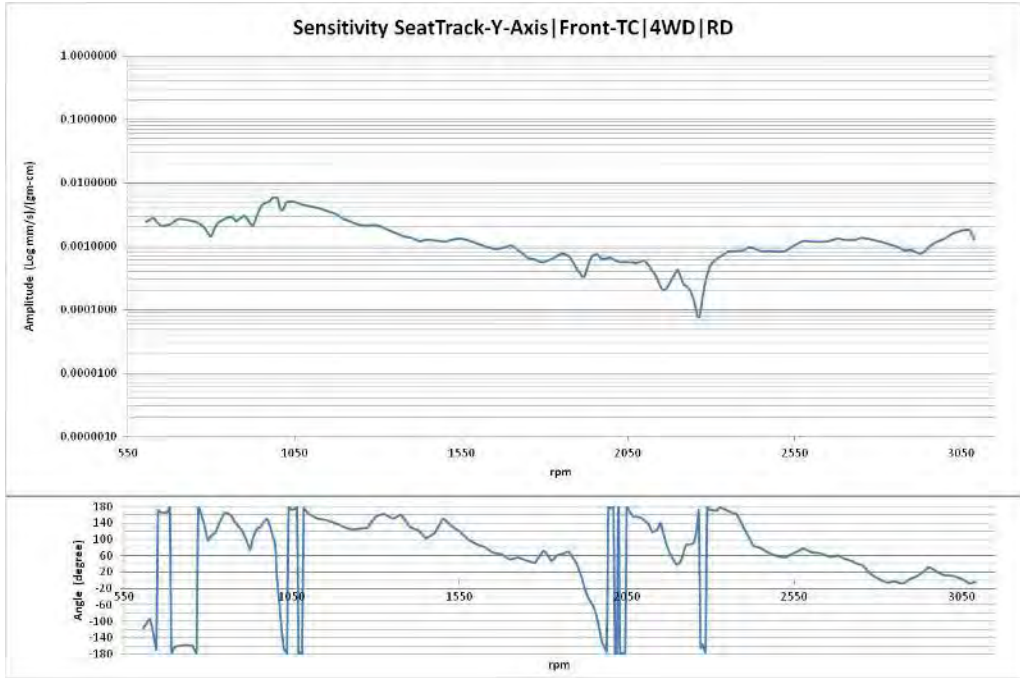


Figure A.59 Sensitivity and phase Seat Track -Y-Axis| Front-TC | 4WD |RD

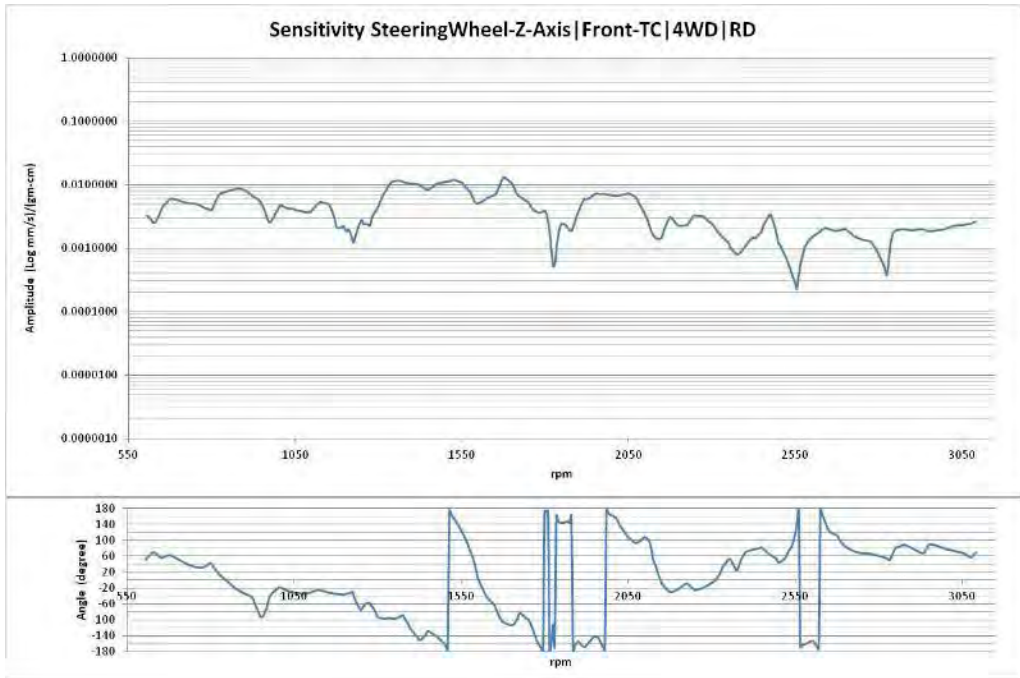


Figure A.60 Sensitivity and phase Steering Wheel-Z-Axis| Front-TC | 4WD |RD

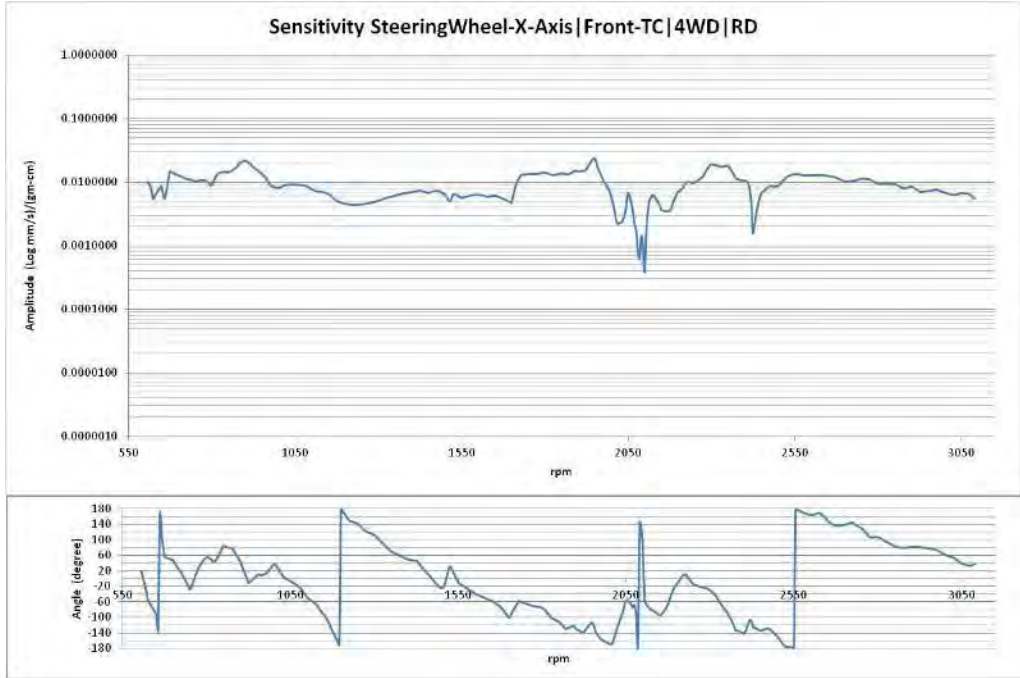


Figure A.61 Sensitivity and phase Steering Wheel-X-Axis | Front-TC | 4WD | RD

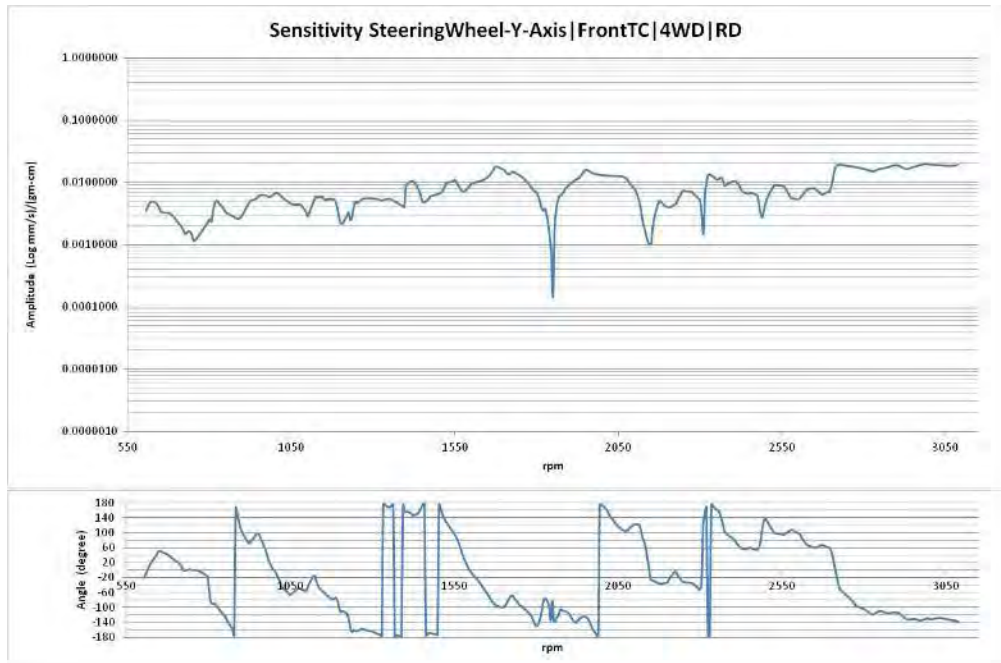


Figure A.62 Sensitivity and phase Steering Wheel-Y-Axis | Front-TC | 4WD | RD

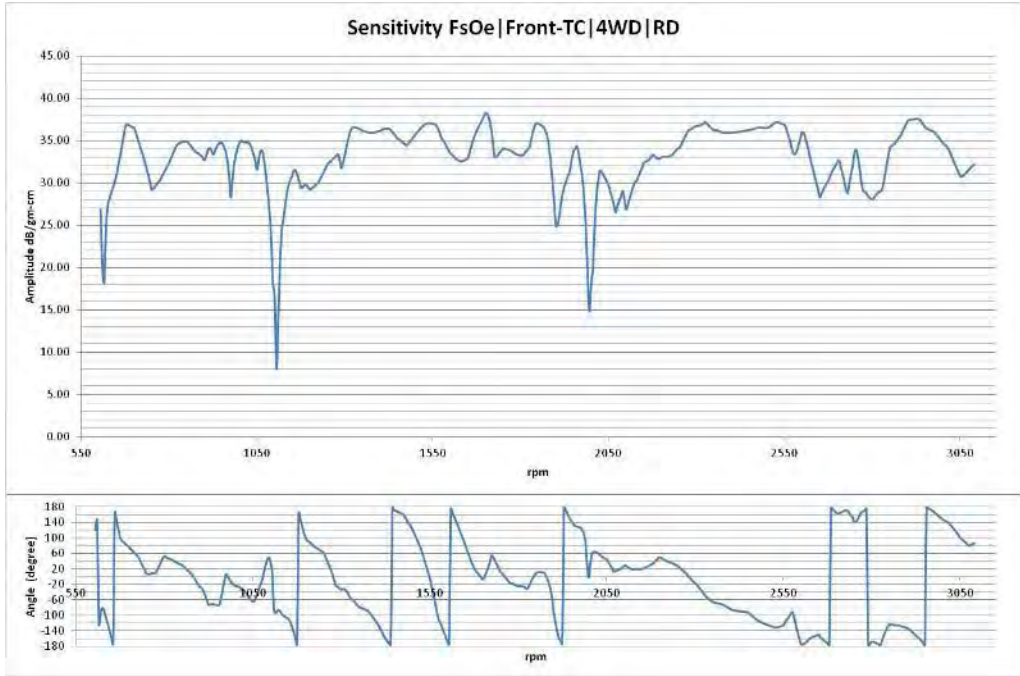


Figure A.63 Sensitivity and phase FsOe | Front-TC | 4WD | RD

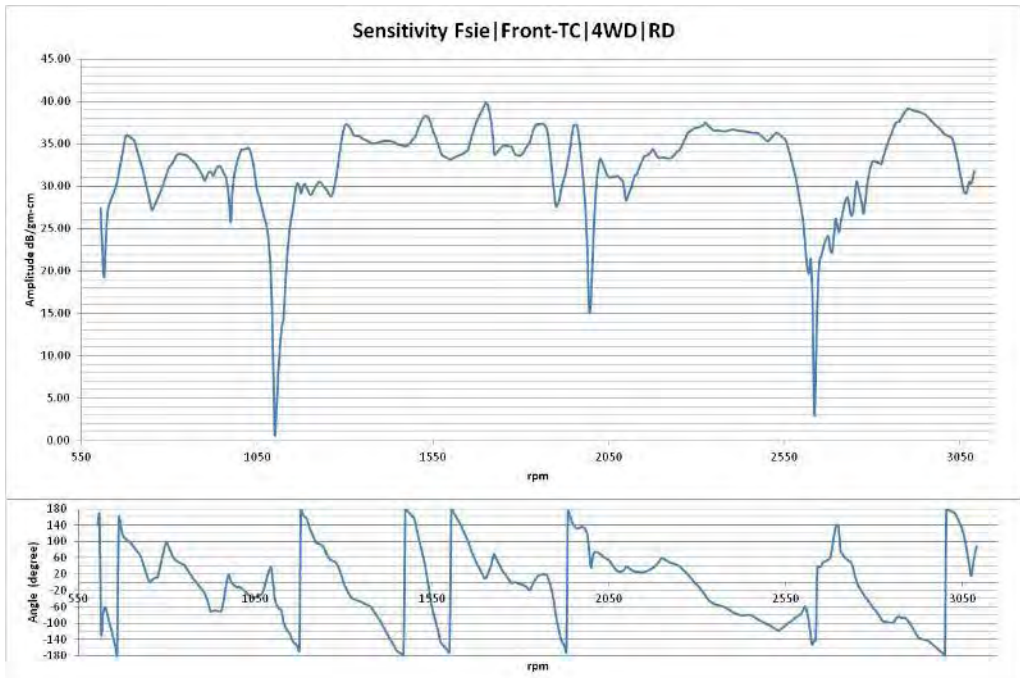


Figure A.64 Sensitivity and phase Fsie | Front-TC | 4WD | RD

Plane C sensitivity curves

Two Wheel Drive (2WD)-Run up (RU) Sensitivity Calculations:

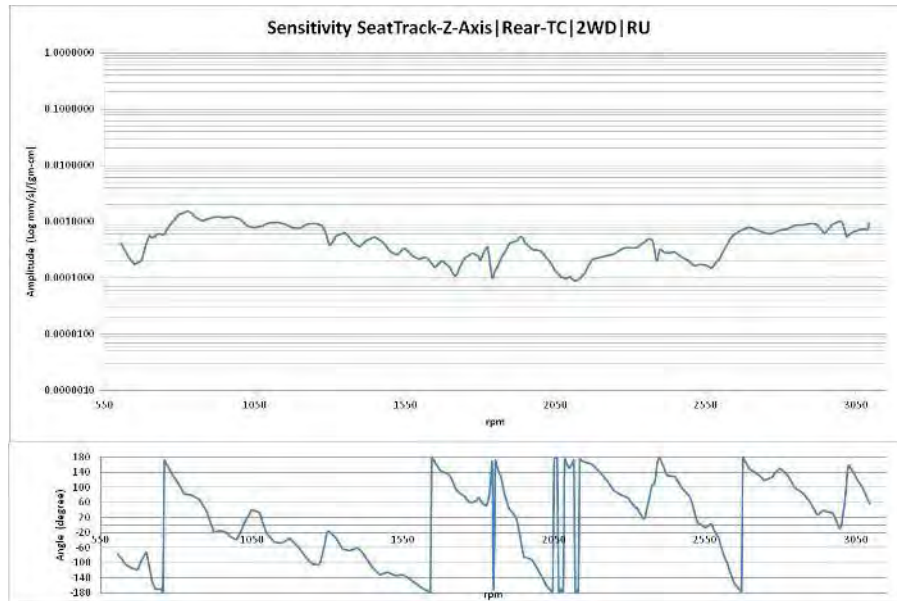


Figure A.65 Sensitivity and phase Seat-Track-Z-Axis | Rear-TC | 2WD |RU

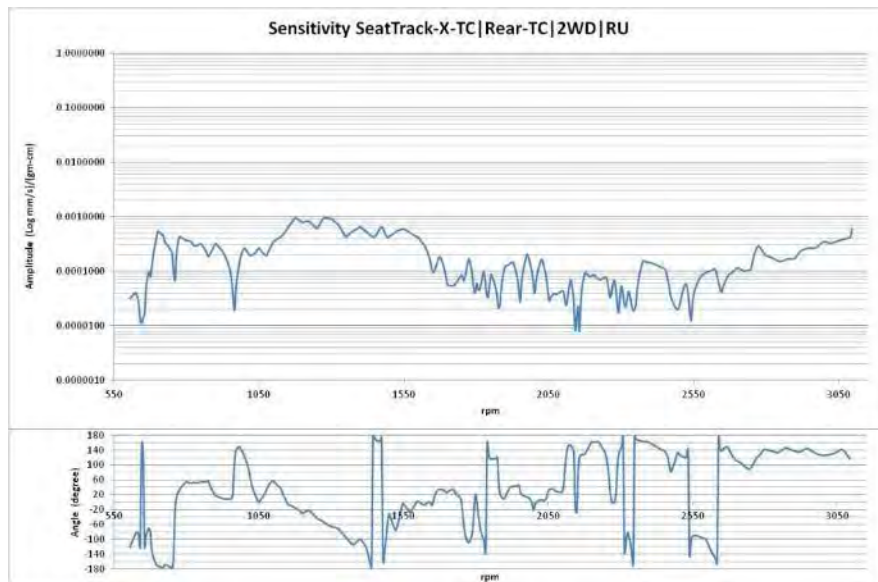


Figure A.66 Sensitivity and phase Seat-Track-X-Axis | Rear-TC | 2WD |RU

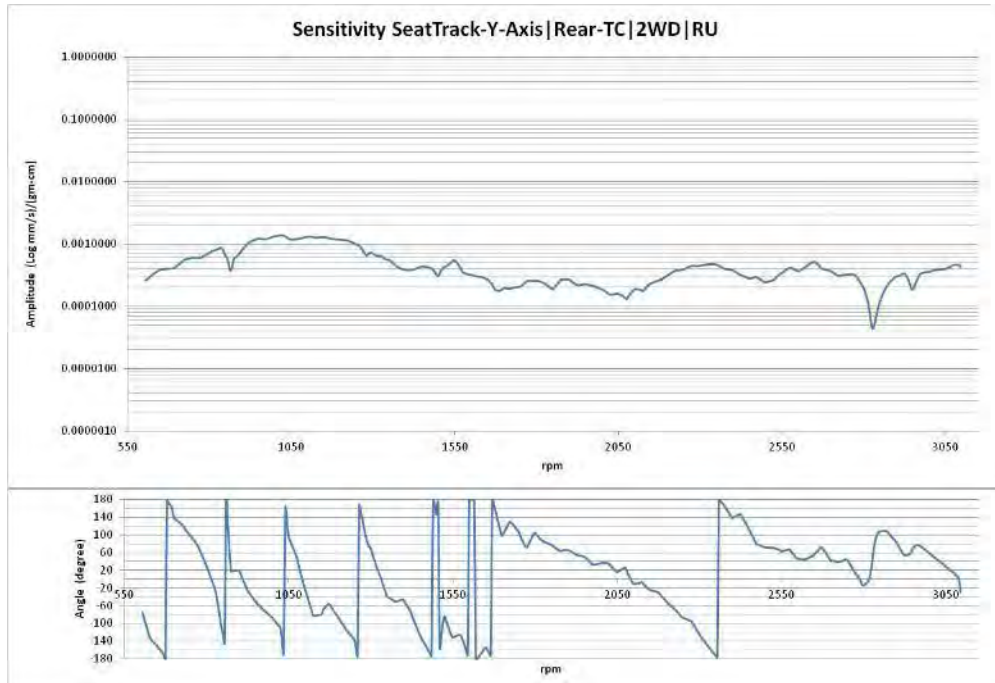


Figure A.67 Sensitivity and phase Seat-Track-Y-Axis| Rear-TC | 2WD |RU

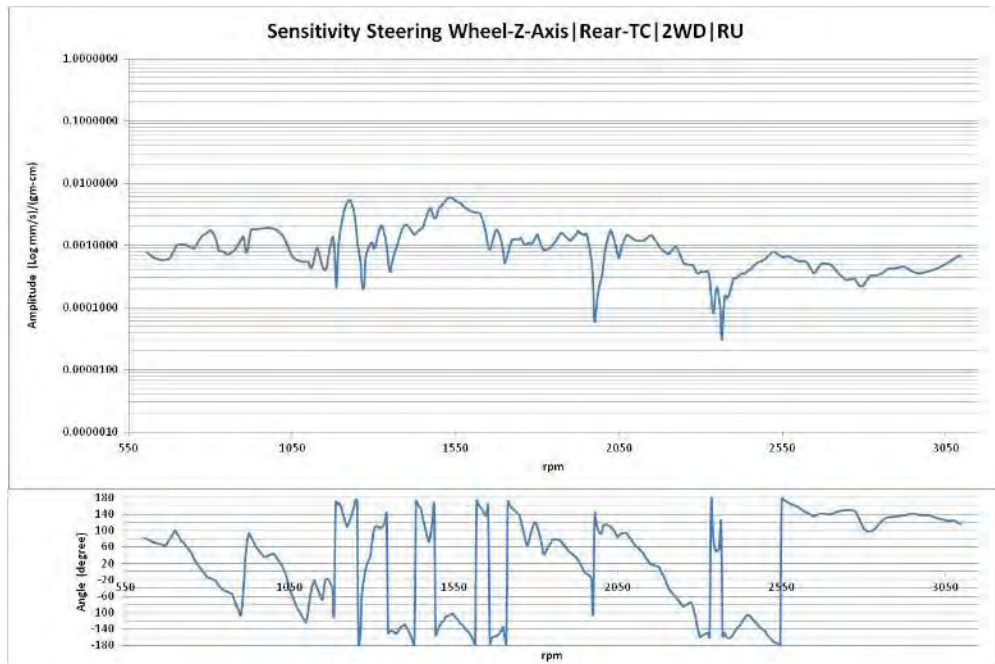


Figure A.68 Sensitivity and phase Steering Wheel-Z-Axis| Rear-TC | 2WD |RU

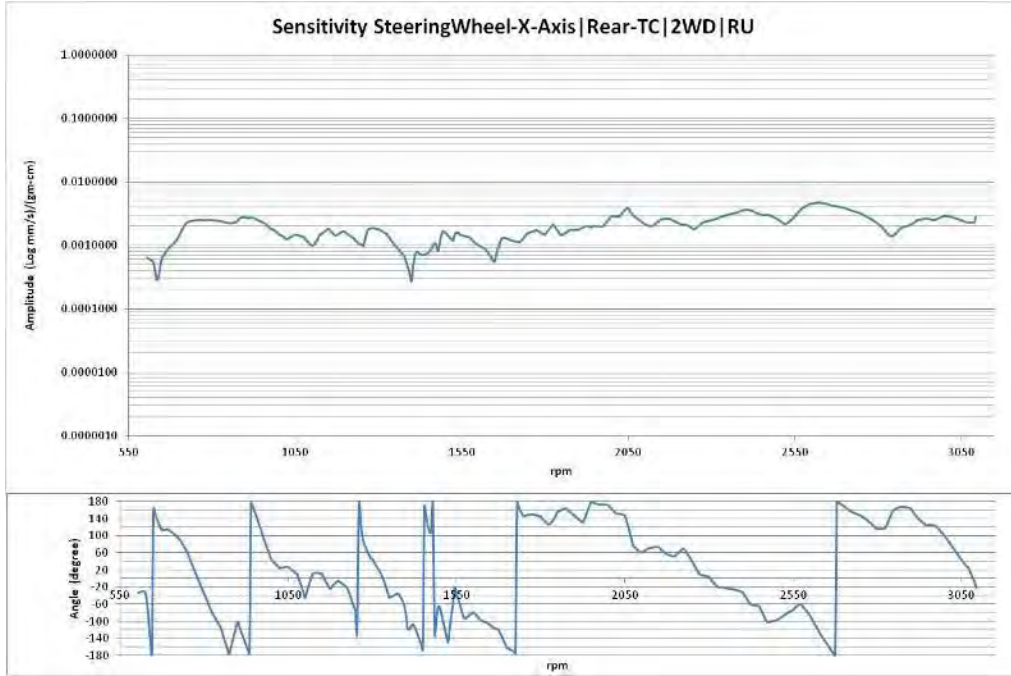


Figure A.69 Sensitivity and phase Steering Wheel-X-Axis| Rear-TC | 2WD |RU

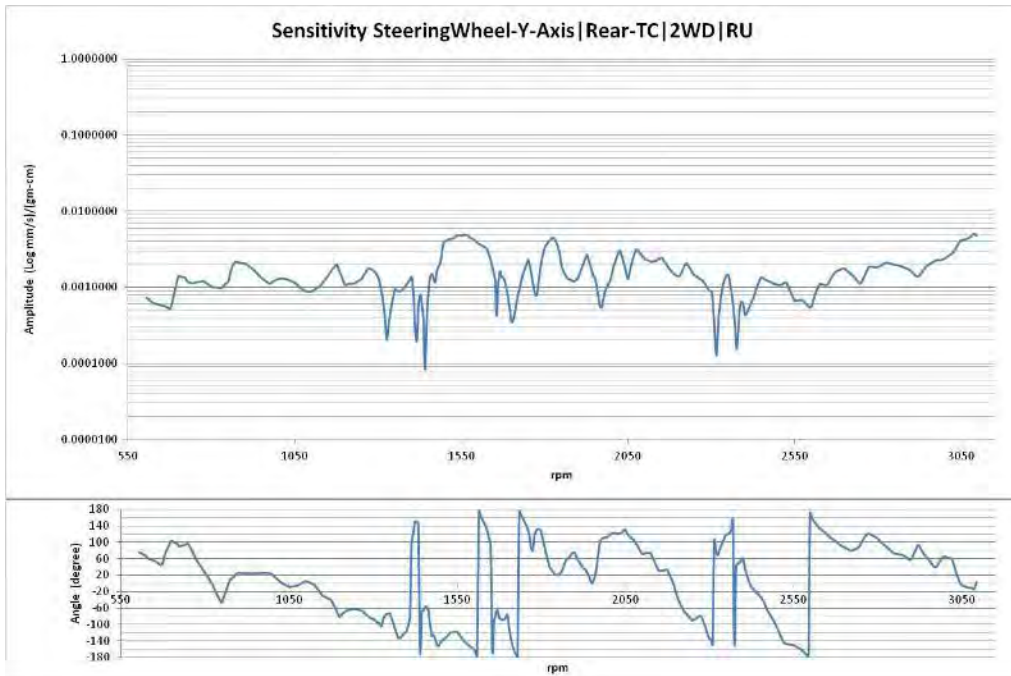


Figure A.70 Sensitivity and phase Steering Wheel-Y-Axis| Rear-TC | 2WD |RU

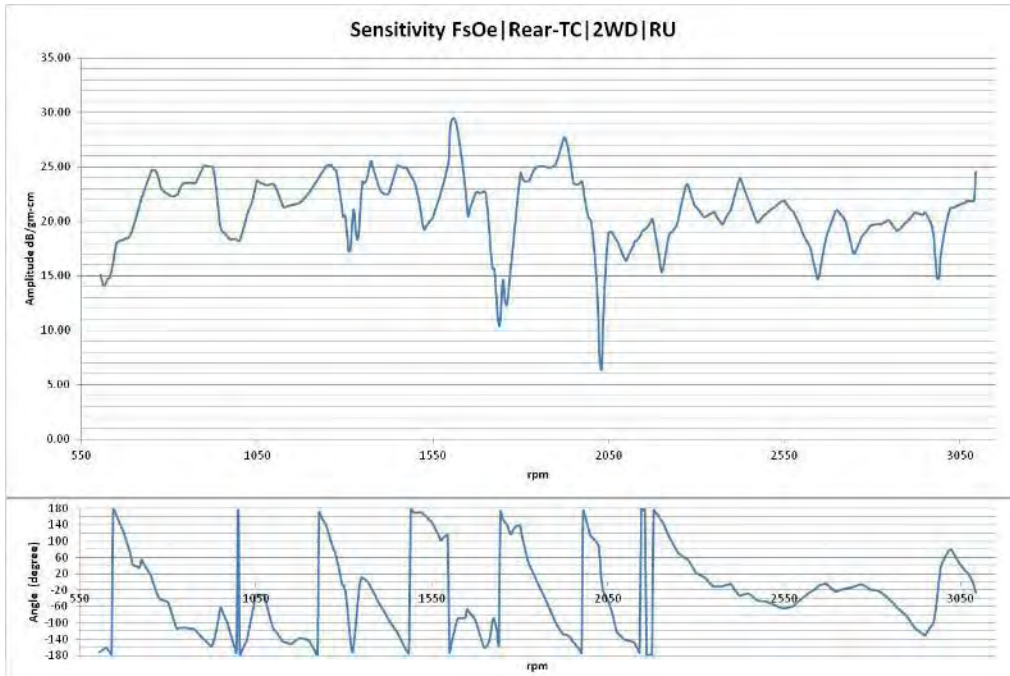


Figure A.71 Sensitivity and phase FsOe | Rear-TC | 2WD | RU

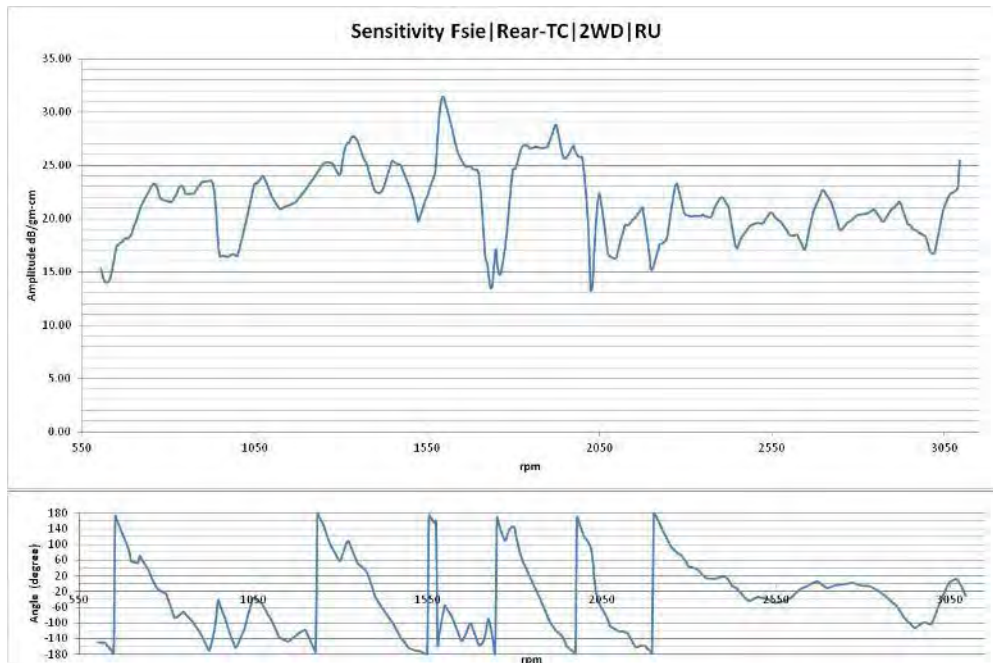


Figure A.72 Sensitivity and phase Fsie | Rear-TC | 2WD | RU

Two Wheel Drive (2WD)-Run down (RD) Sensitivity Calculations:

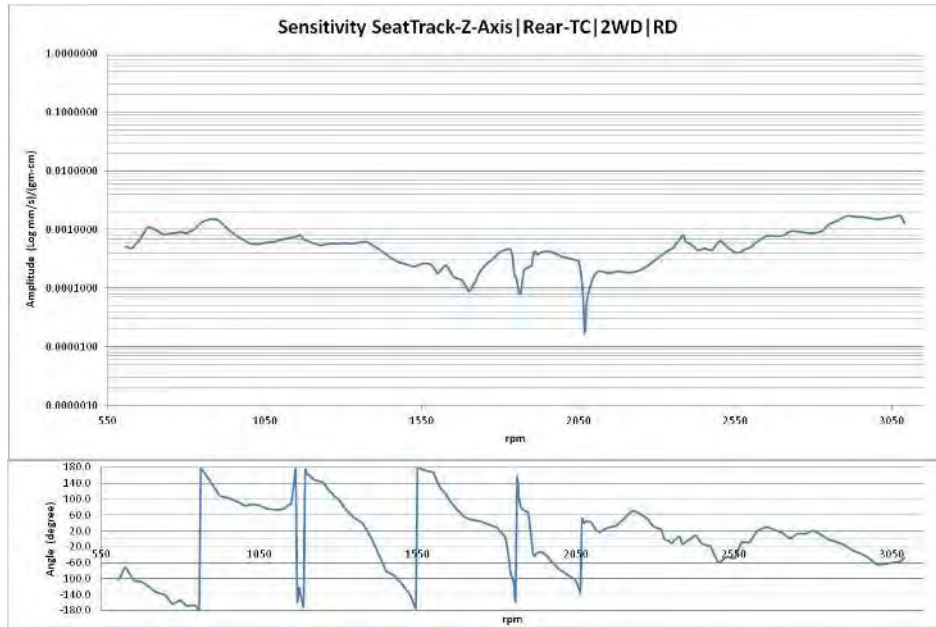


Figure A.73 Sensitivity and phase Seat Track -Z-Axis| Rear-TC | 2WD |RD

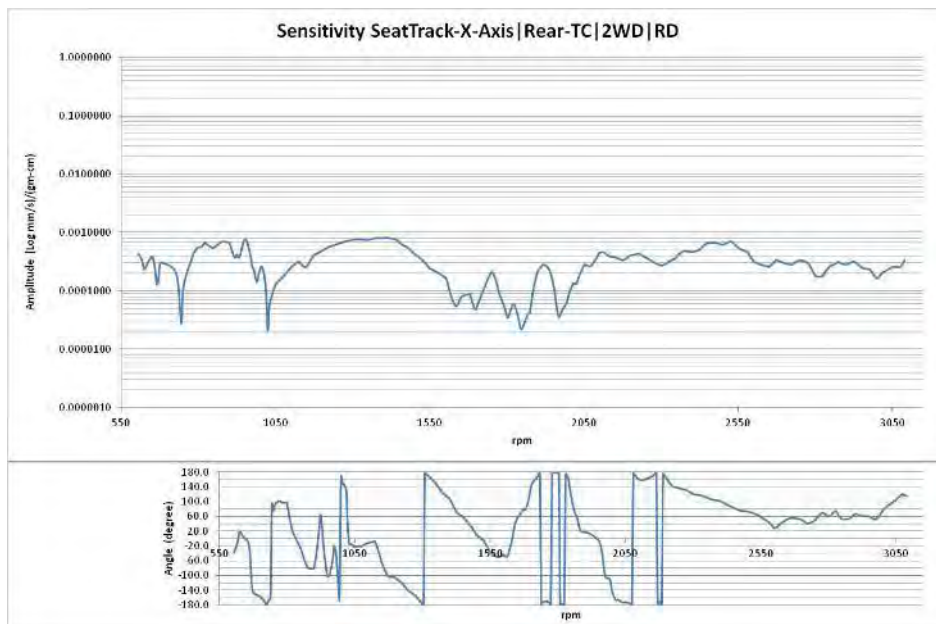


Figure A.74 Sensitivity and phase Seat Track -X-Axis| Rear-TC | 2WD |RD

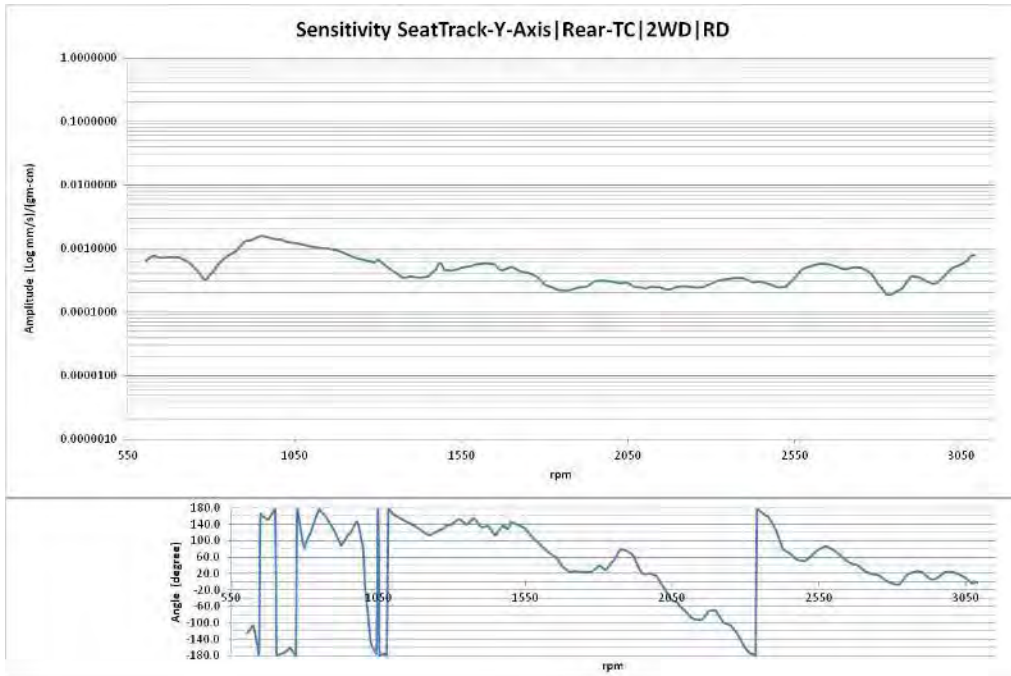


Figure A.75 Sensitivity and phase Seat Track -Y-Axis| Rear-TC | 2WD |RD

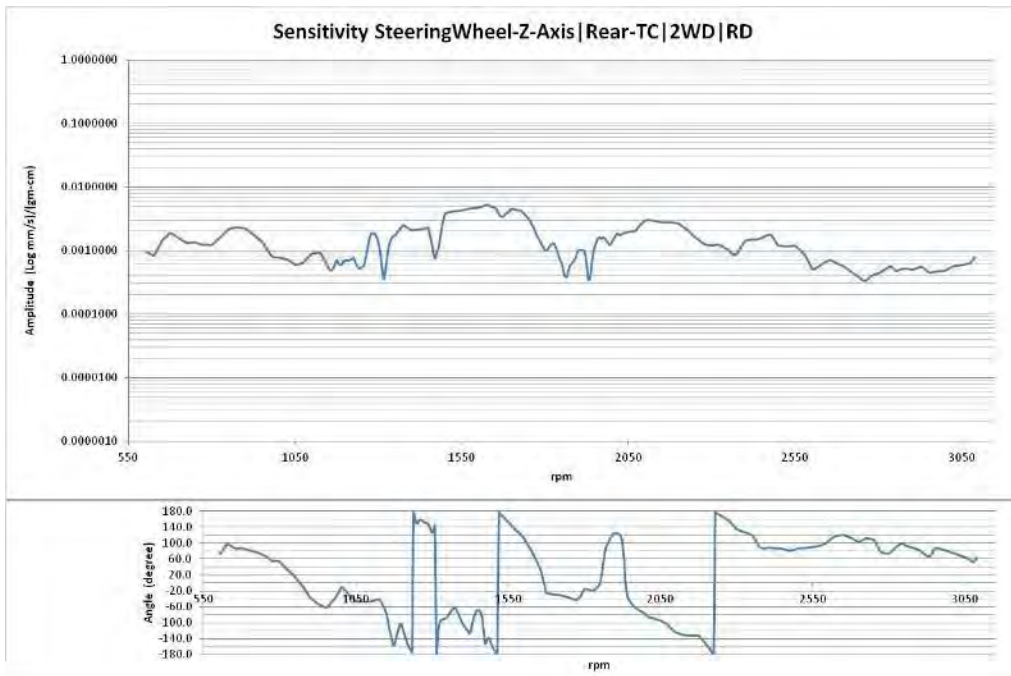


Figure A.76 Sensitivity and phase Steering Wheel-Z-Axis| Rear-TC | 2WD |RD

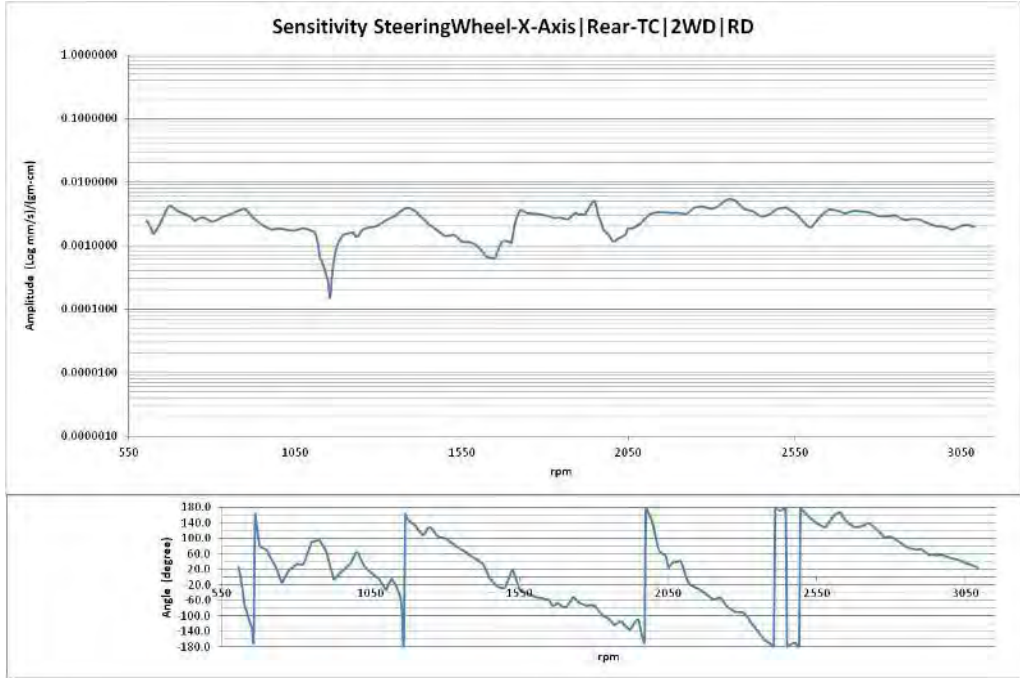


Figure A.77 Sensitivity and phase Steering Wheel-X-Axis| Rear-TC | 2WD |RD

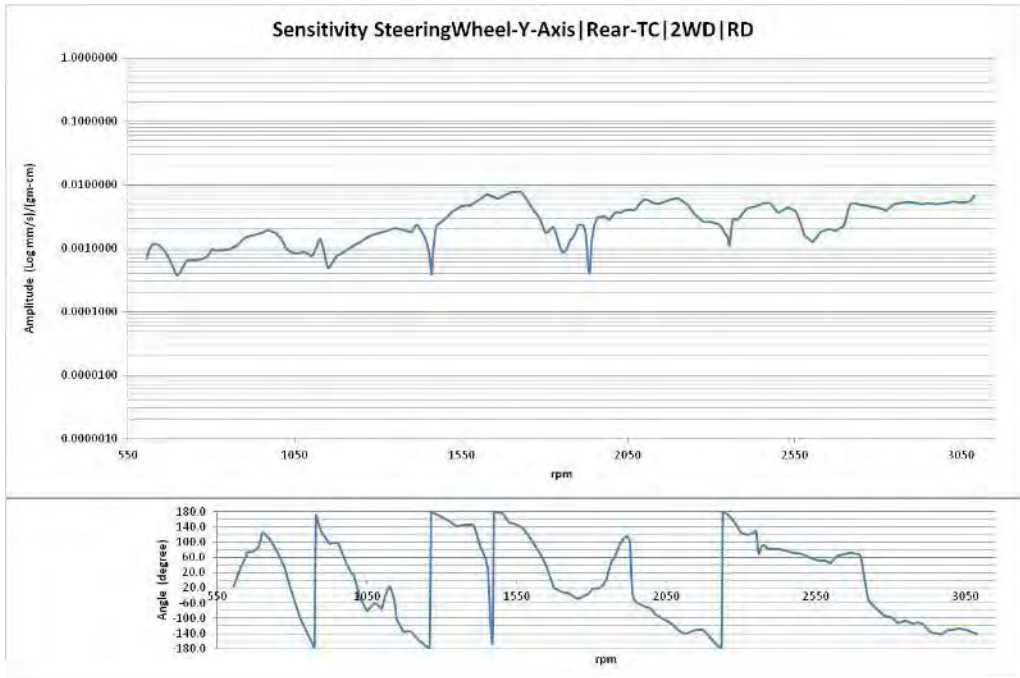


Figure A.78 Sensitivity and phase Steering Wheel-Y-Axis| Rear-TC | 2WD |RD

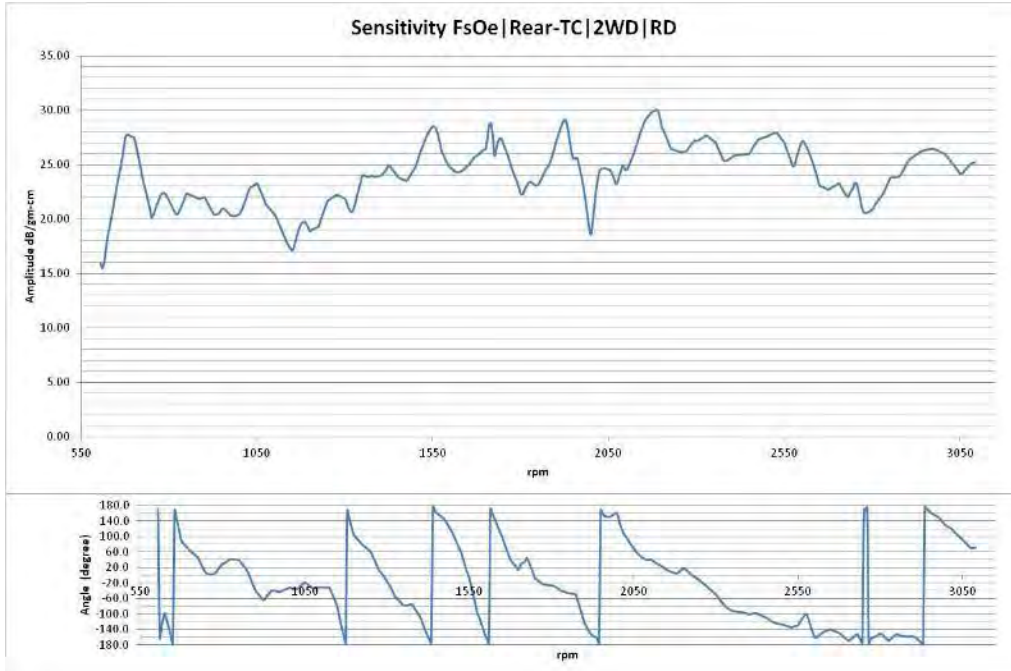


Figure A.79 Sensitivity and phase FsOe | Rear-TC | 2WD | RD

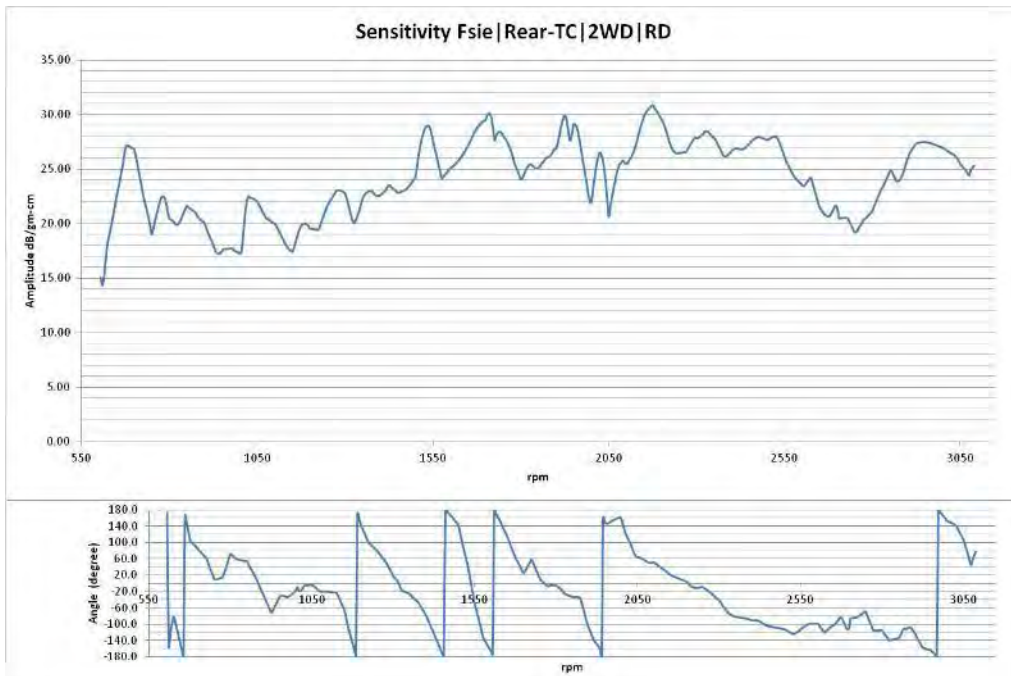


Figure A.80 Sensitivity and phase Fsie | Rear-TC | 2WD | RD

Four Wheel Drive (4WD)-Run up (RU) Sensitivity Calculations:

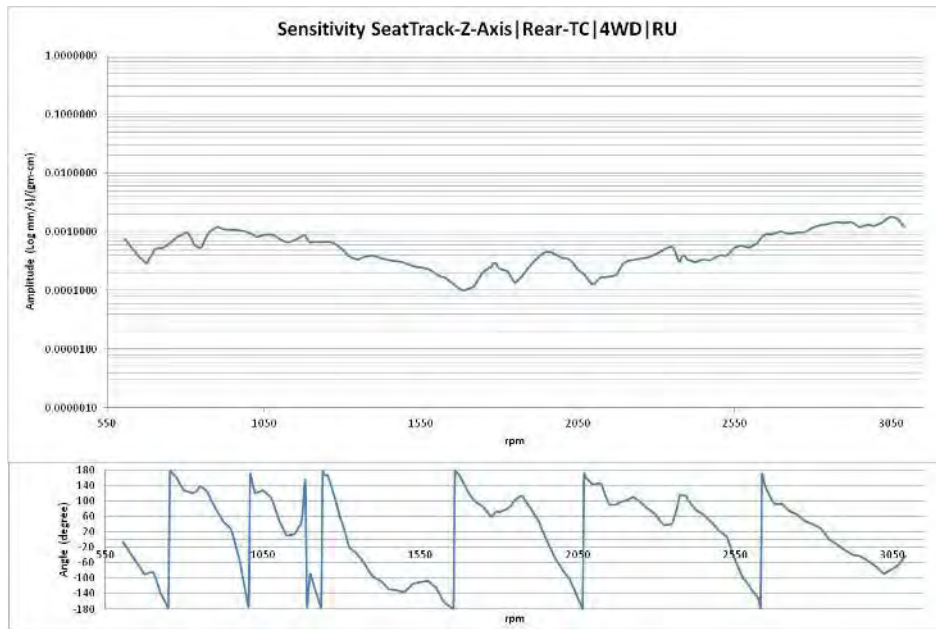


Figure A.81 Sensitivity and phase Seat-Track-Z-Axis | Rear-TC | 4WD |RU

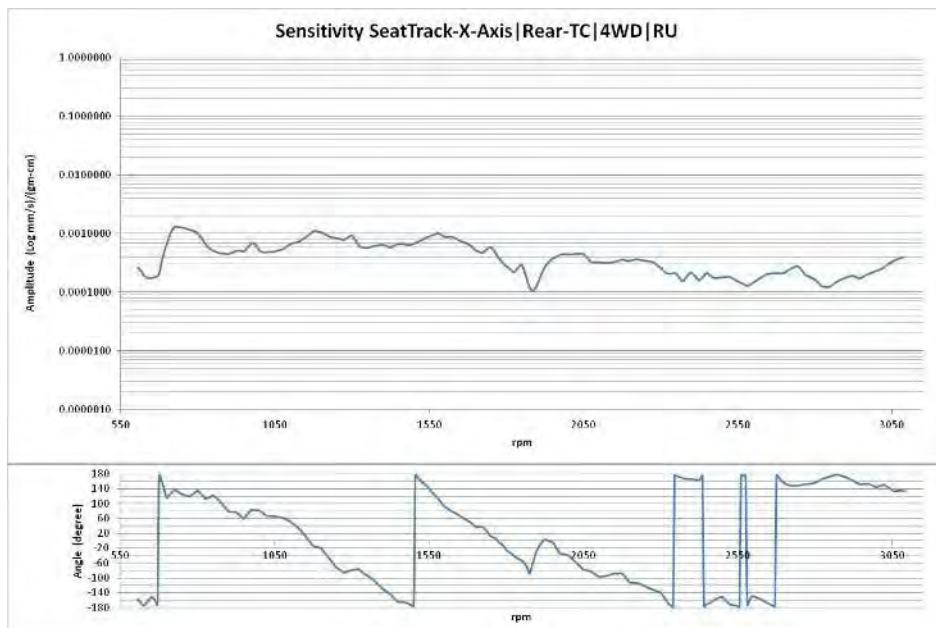


Figure A.82 Sensitivity and phase Seat-Track-X-Axis | Rear-TC | 4WD |RU

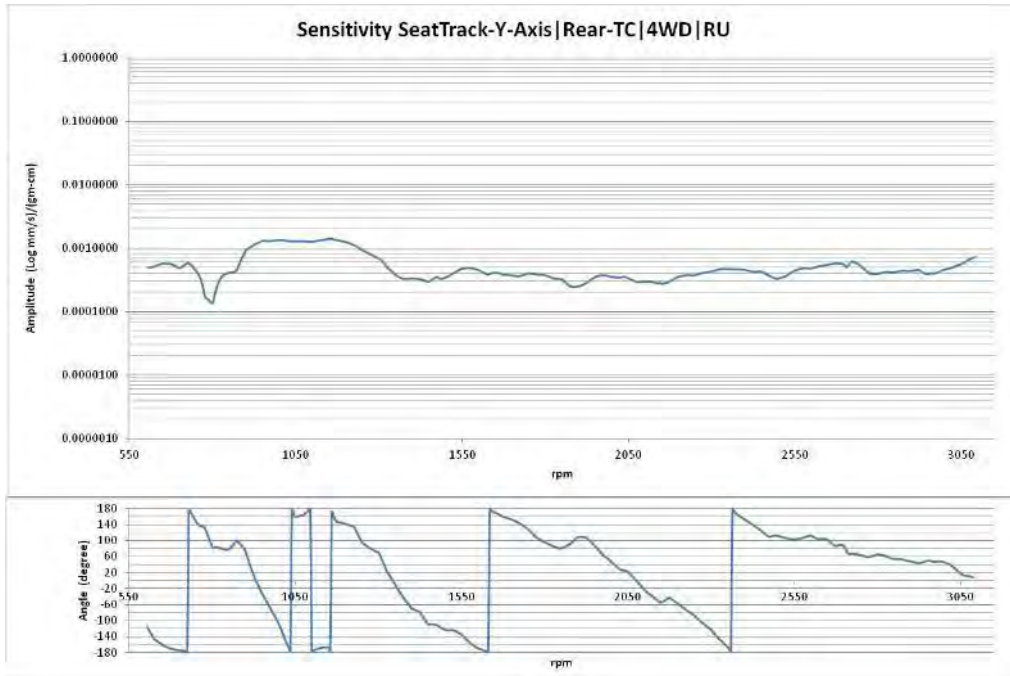


Figure A.83 Sensitivity and phase Seat-Track-Y-Axis| Rear-TC | 4WD |RU

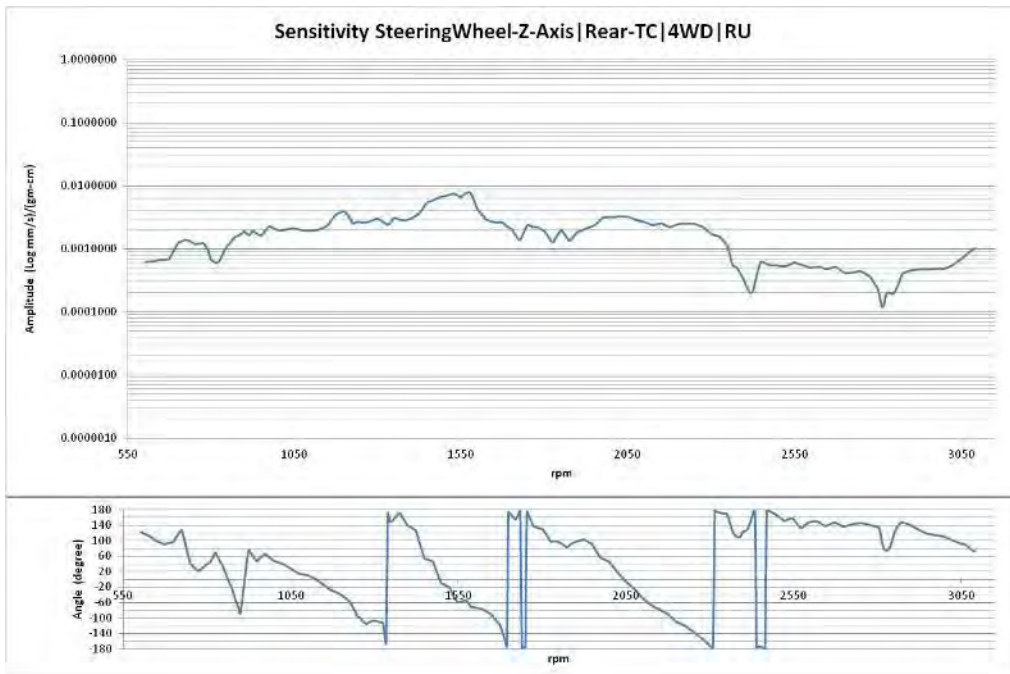


Figure A.84 Sensitivity and phase Steering Wheel-Z-Axis| Rear-TC | 4WD |RU

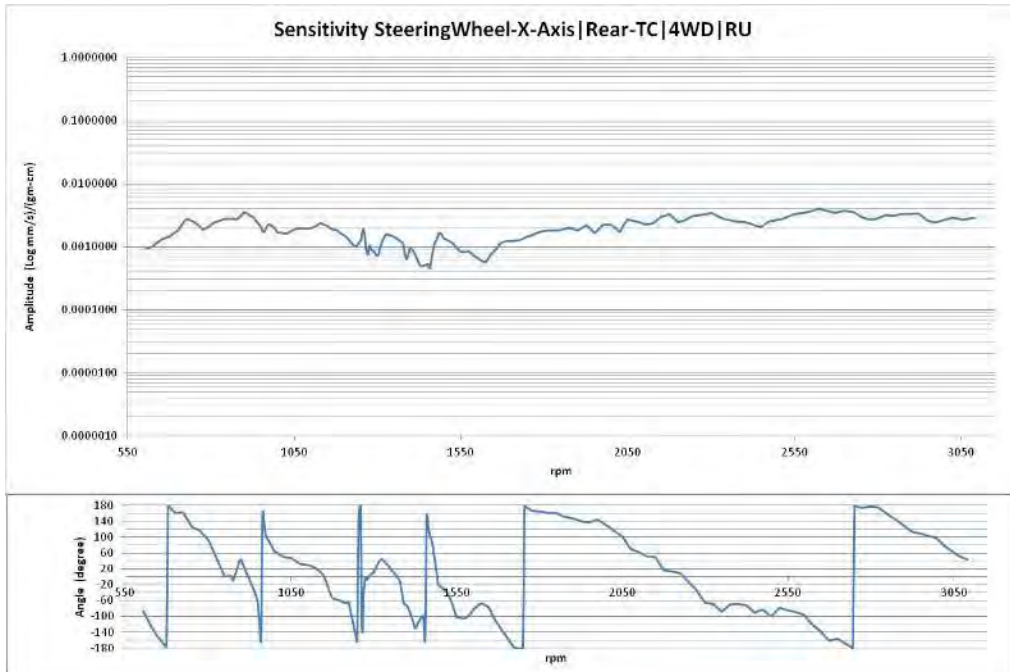


Figure A.85 Sensitivity and phase Steering Wheel-X-Axis| Rear-TC | 4WD |RU

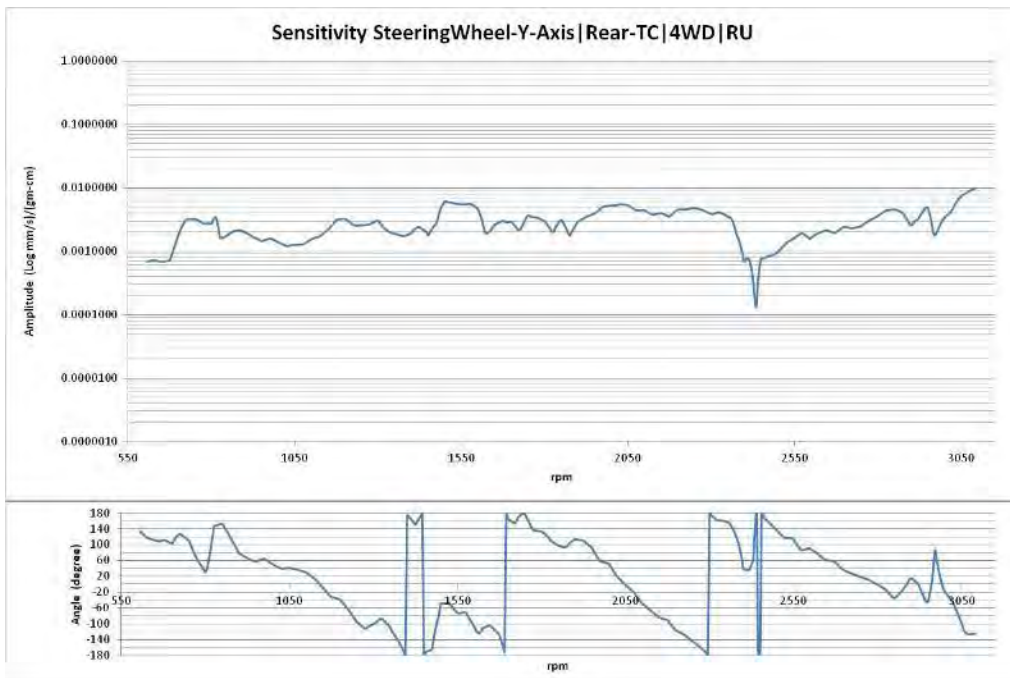


Figure A.86 Sensitivity and phase Steering Wheel-Y-Axis| Rear-TC | 4WD |RU

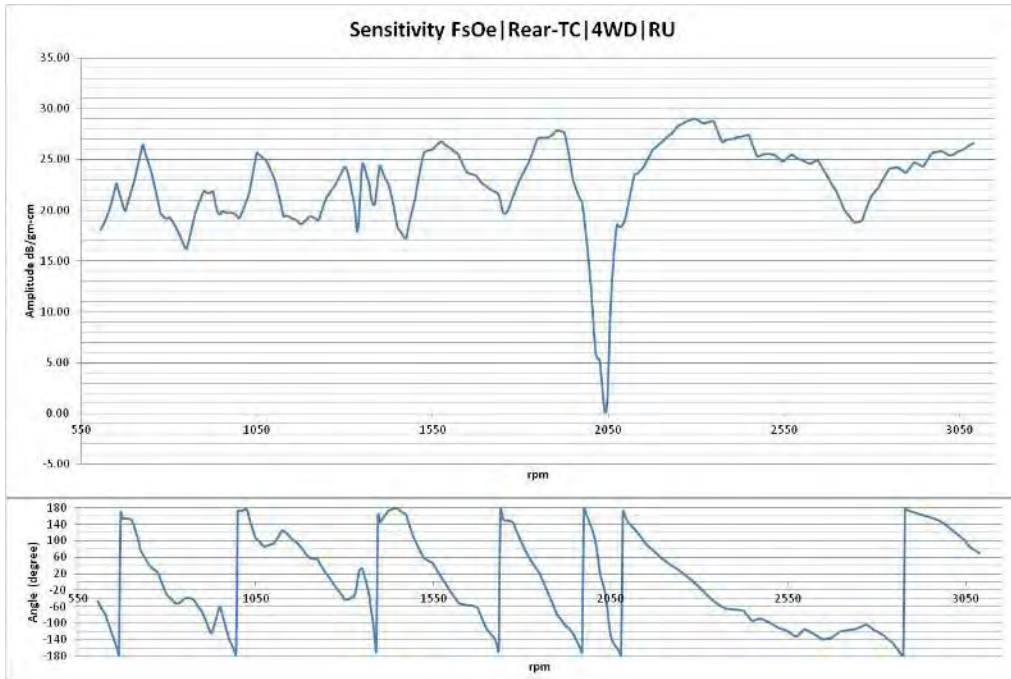


Figure A.87 Sensitivity and phase FsOe | Rear-TC | 4WD | RU

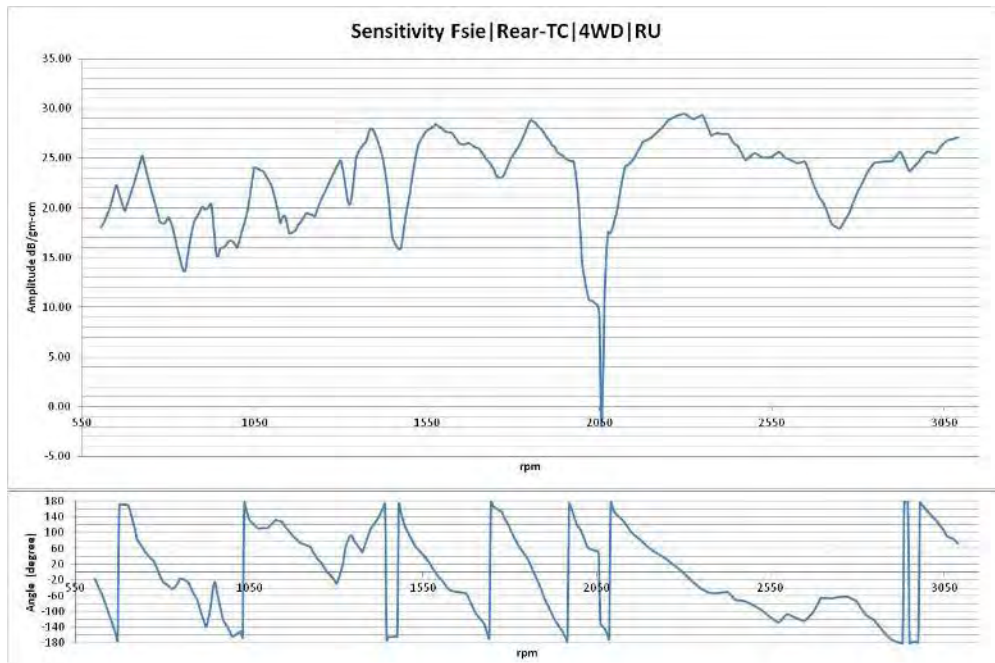


Figure A.88 Sensitivity and phase Fsie | Rear-TC | 4WD | RU

Four Wheel Drive (4WD)-Run down (RD) Sensitivity Calculations:

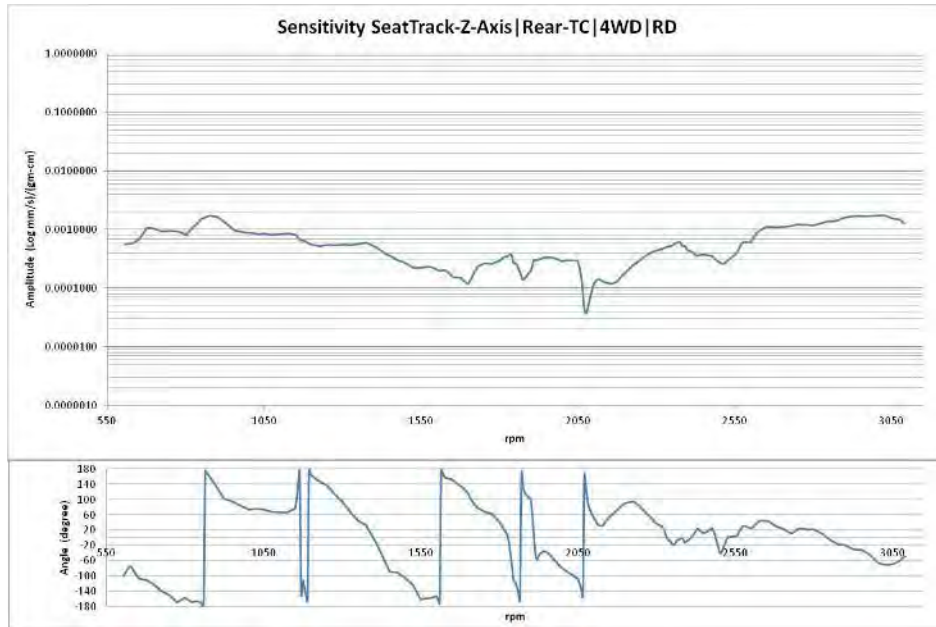


Figure A.89 Sensitivity and phase Seat Track -Z-Axis| Rear-TC | 4WD |RD

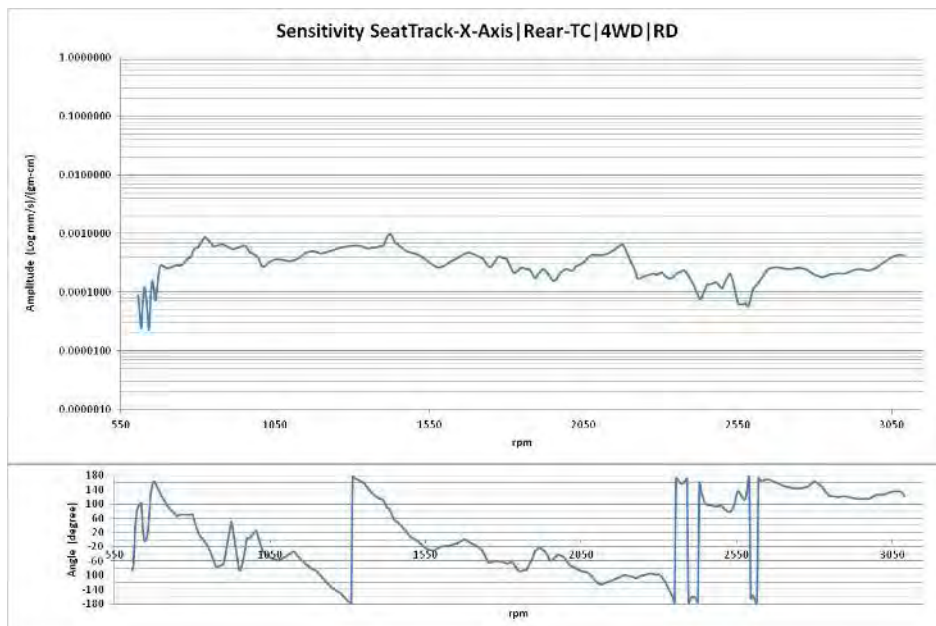


Figure A.90 Sensitivity and phase Seat Track -X-Axis| Rear-TC | 4WD |RD

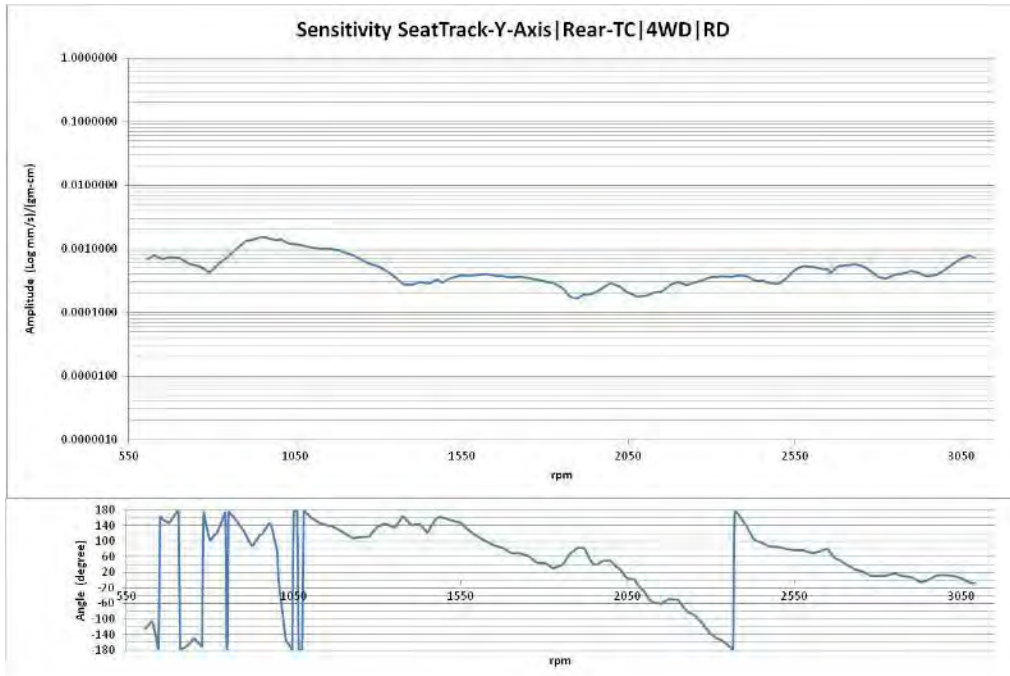


Figure A.91 Sensitivity and phase Seat Track -Y-Axis| Rear-TC | 4WD |RD

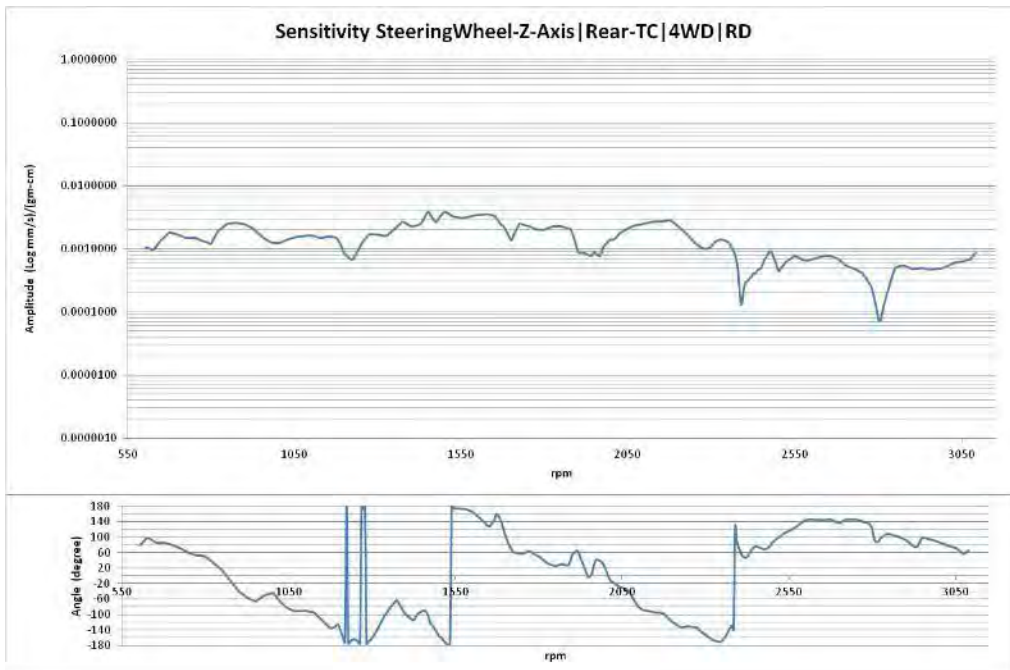


Figure A.92 Sensitivity and phase Steering Wheel-Z-Axis| Rear-TC | 4WD |RD

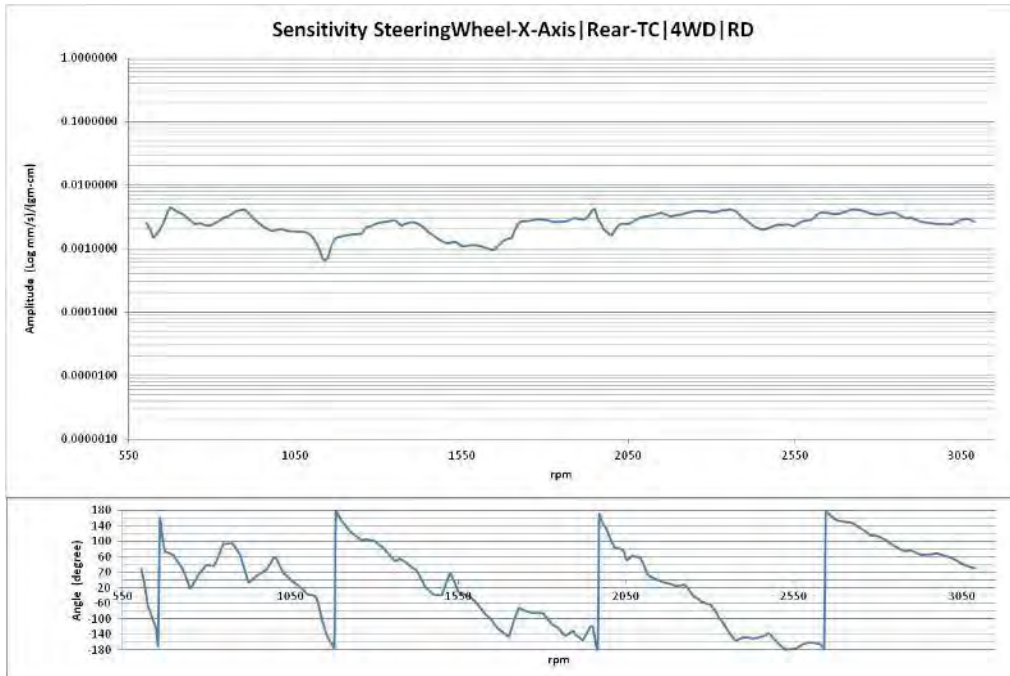


Figure A.93 Sensitivity and phase Steering Wheel-X-Axis| Rear-TC | 4WD |RD

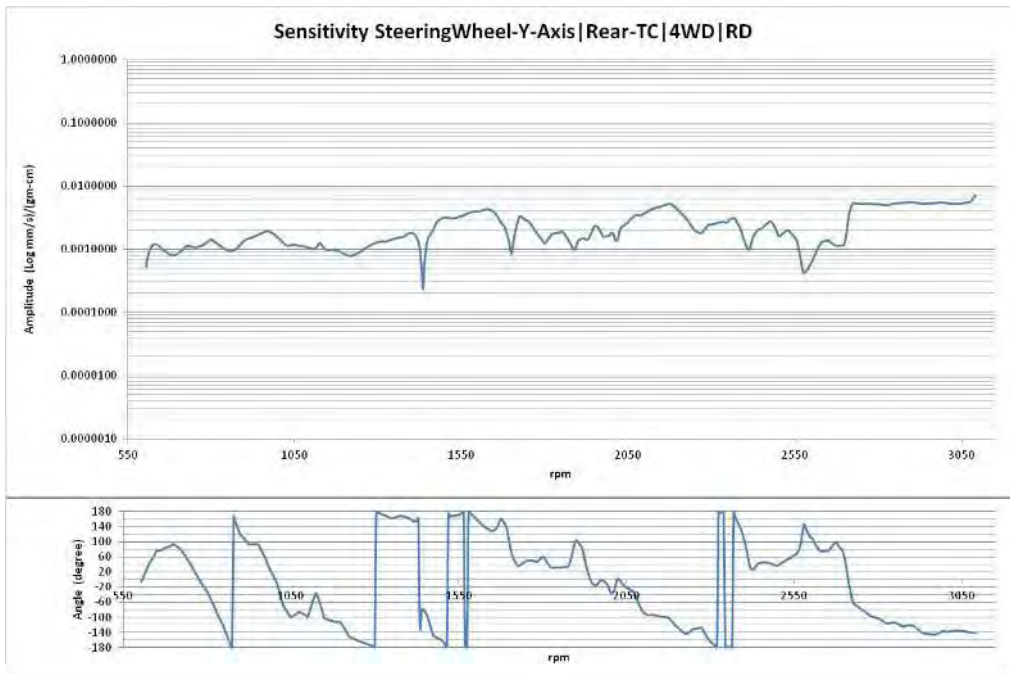


Figure A.94 Sensitivity and phase Steering Wheel-Y-Axis| Rear-TC | 4WD |RD

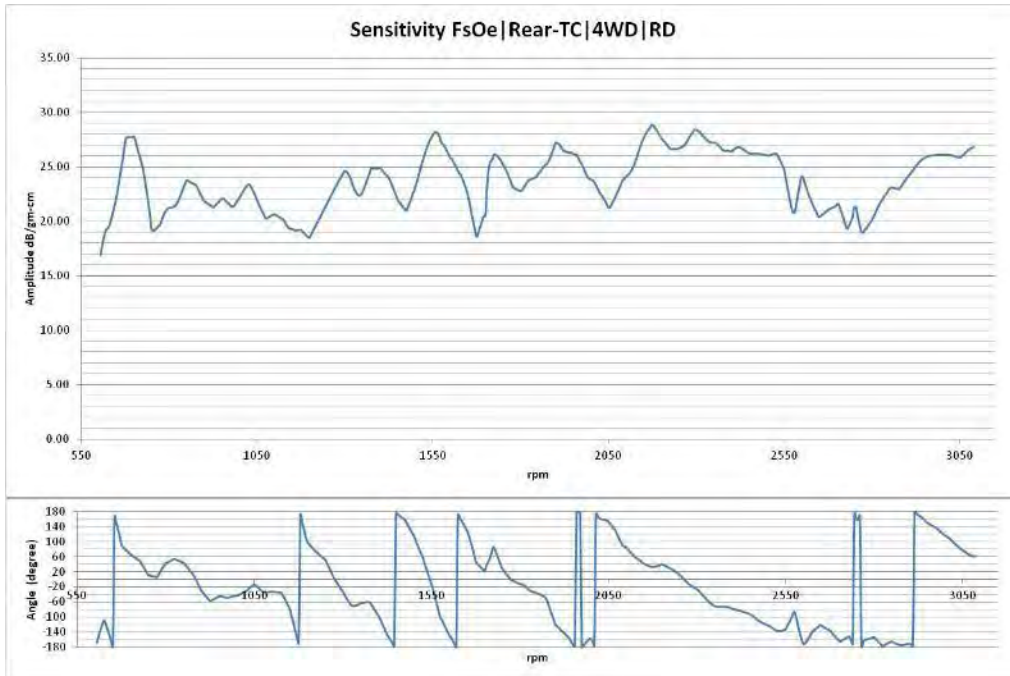


Figure A.95 Sensitivity and phase FsOe | Rear-TC | 4WD | RD

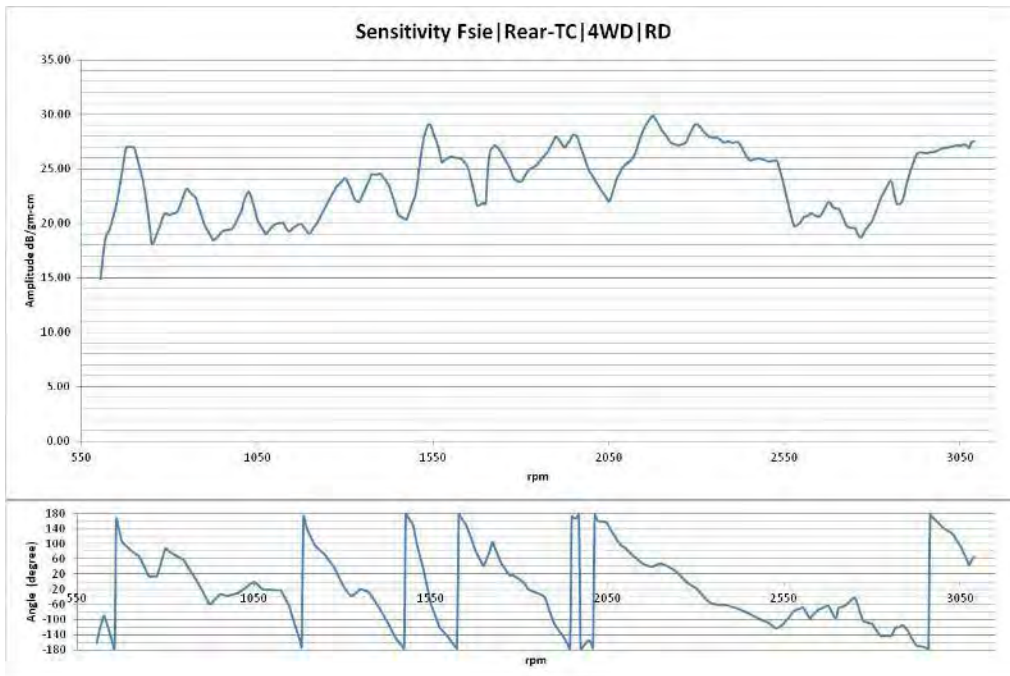


Figure A.96 Sensitivity and phase Fsie | Rear-TC | 4WD | RD

APPENDIX B
SIMULATION RUN OUTPUT CASES

Simulation run output curves for 2WD-RU

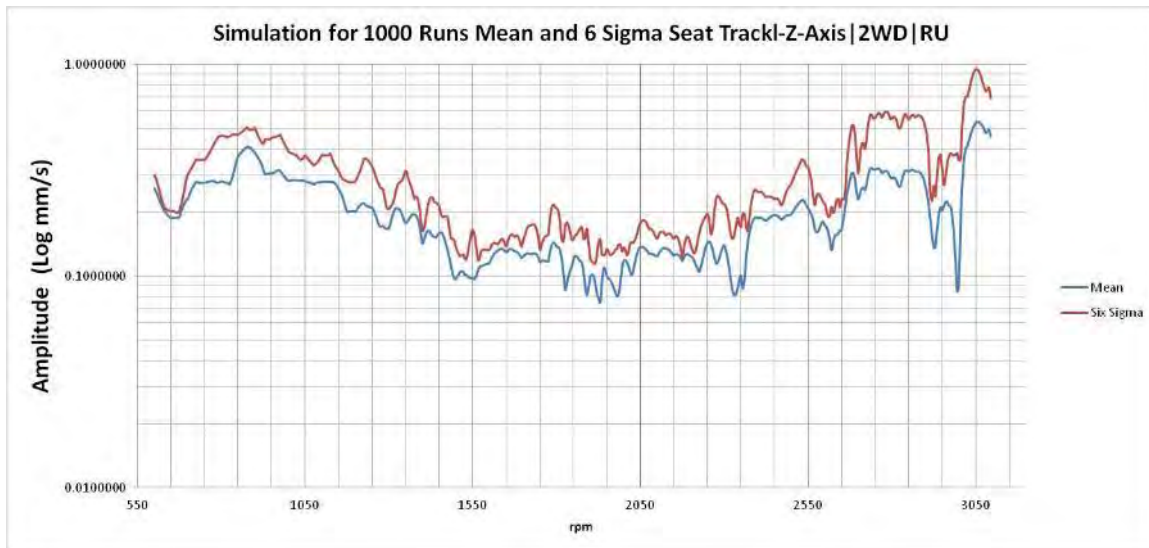


Figure B.1 Simulation run output (mean and 6σ) for Seat Track z-axis 2WD-RU

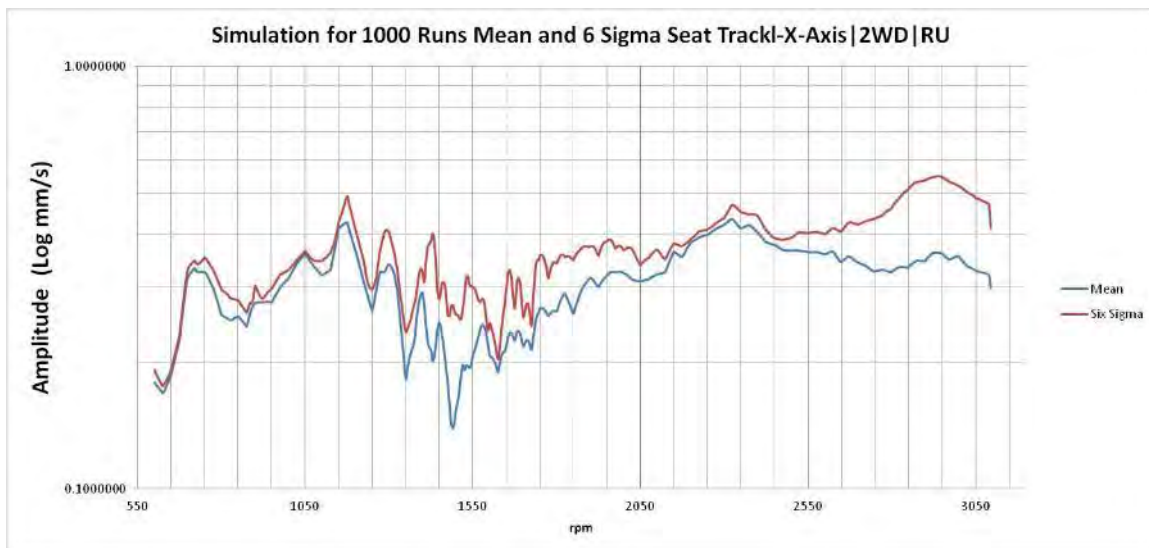


Figure B.2 Simulation run output (mean and 6σ) for Seat Track x-axis 2WD-RU

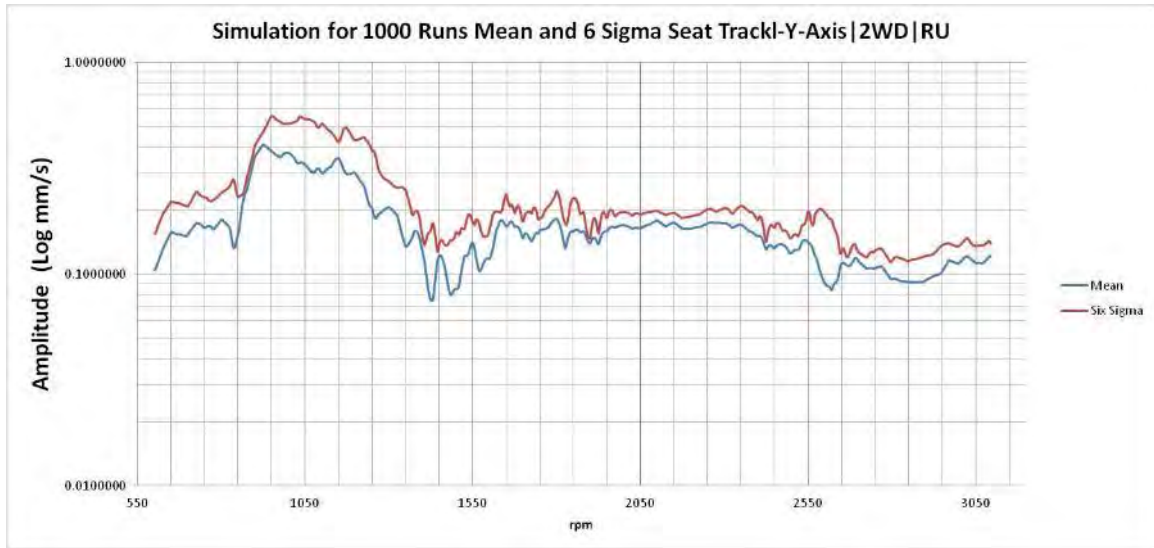


Figure B.3 Simulation run output (mean and 6σ) for Seat Track y-axis 2WD-RU

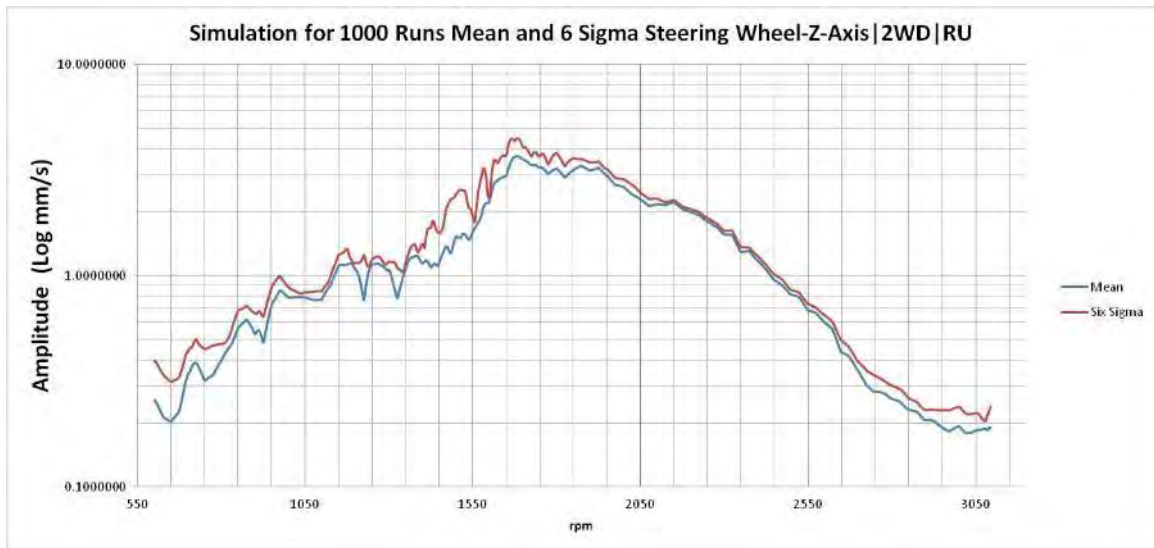


Figure B.4 Simulation run output (mean and 6σ) for Steering Wheel z-axis 2WD-RU

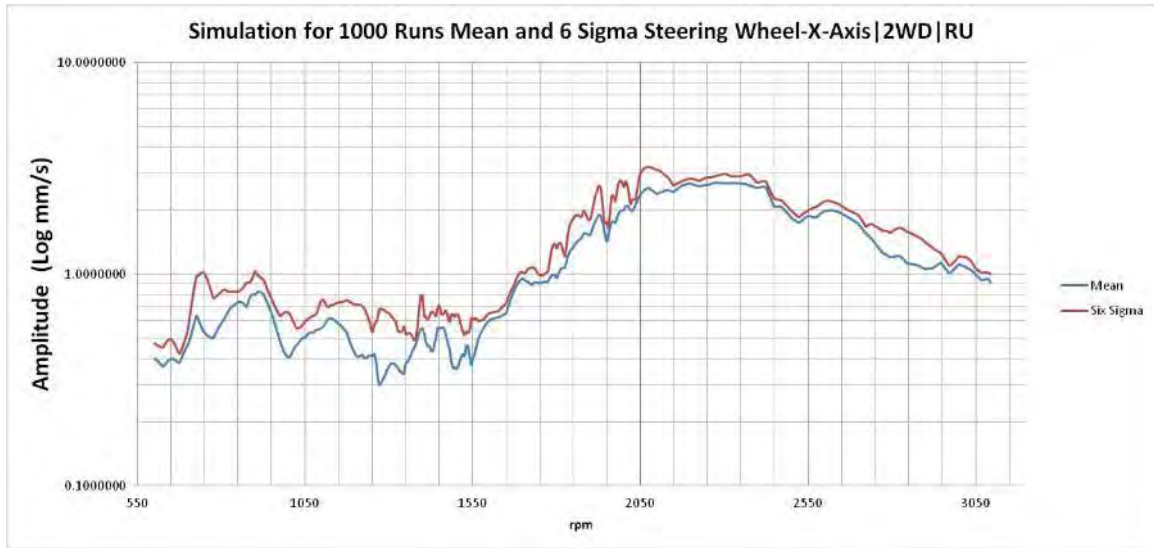


Figure B.5 Simulation run output (mean and 6σ) for Steering Wheel x-axis 2WD-RU

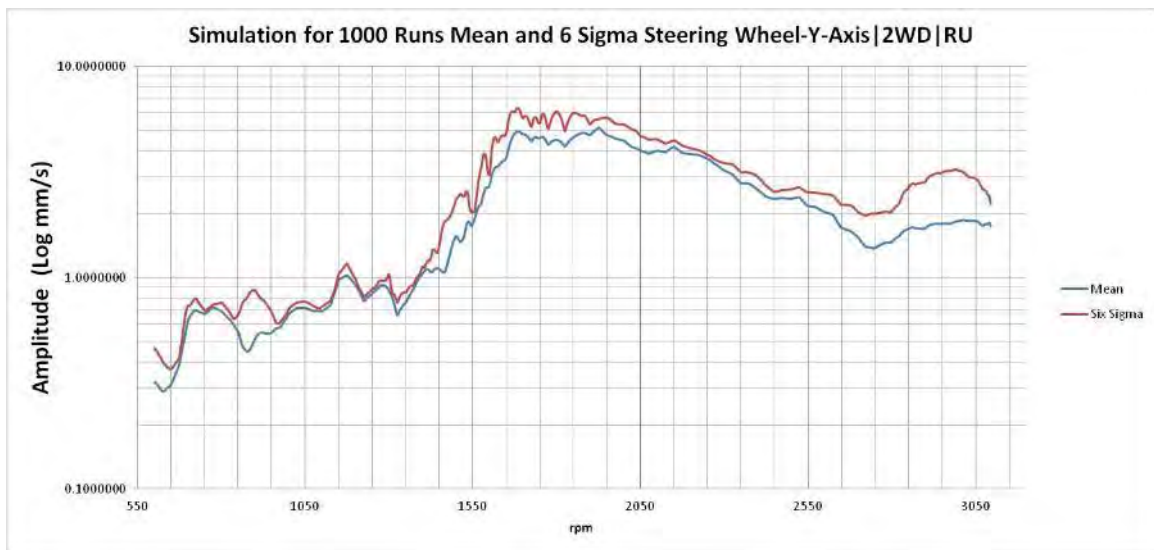


Figure B.6 Simulation run output (mean and 6σ) for Steering Wheel y-axis 2WD-RU

Simulation run output curves for 2WD-RD

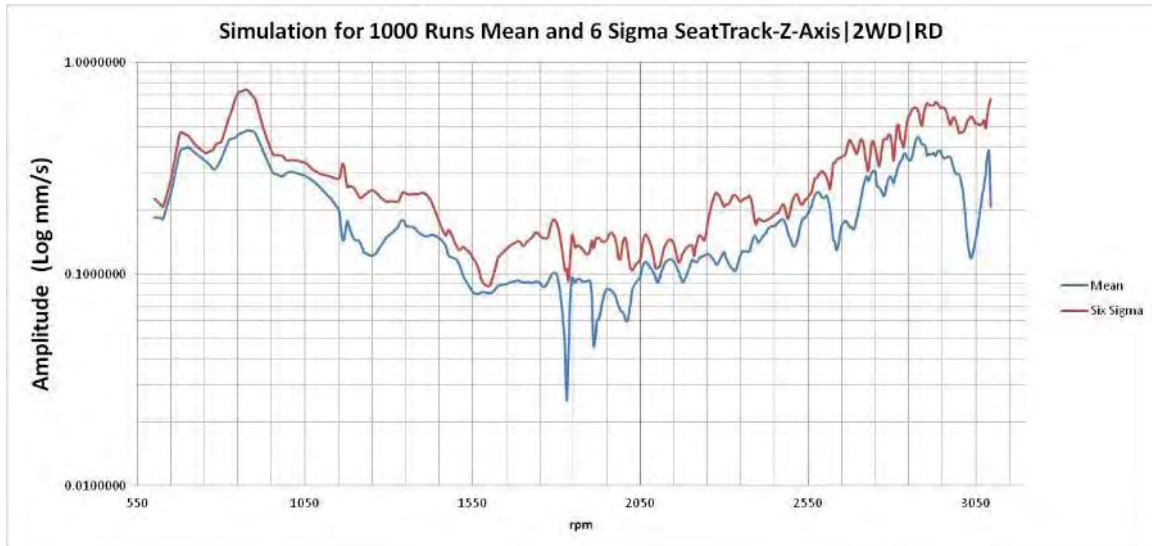


Figure B.7 Simulation run output (mean and 6σ) for Seat Track z-axis 2WD-RD

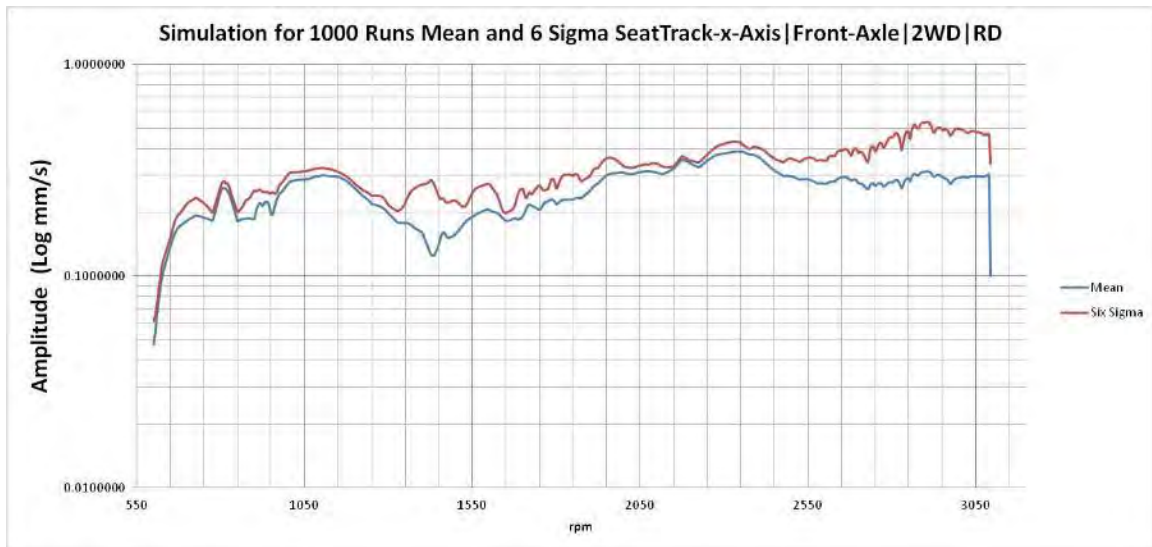


Figure B.8 Simulation run output (mean and 6σ) for Seat Track x-axis 2WD-RD

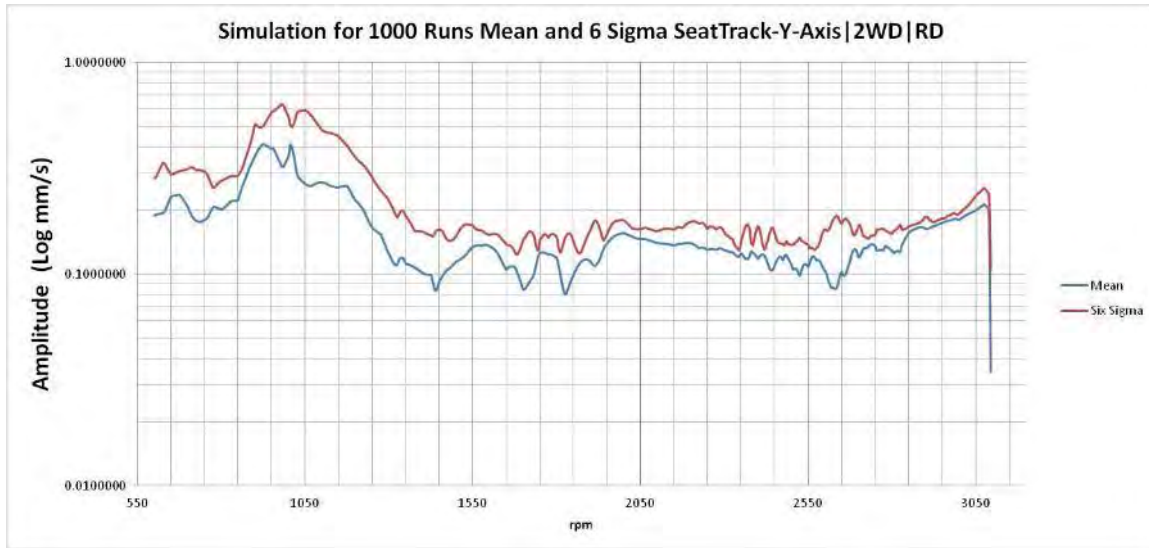


Figure B.9 Simulation run output (mean and 6σ) for Seat Track y-axis 2WD-RD

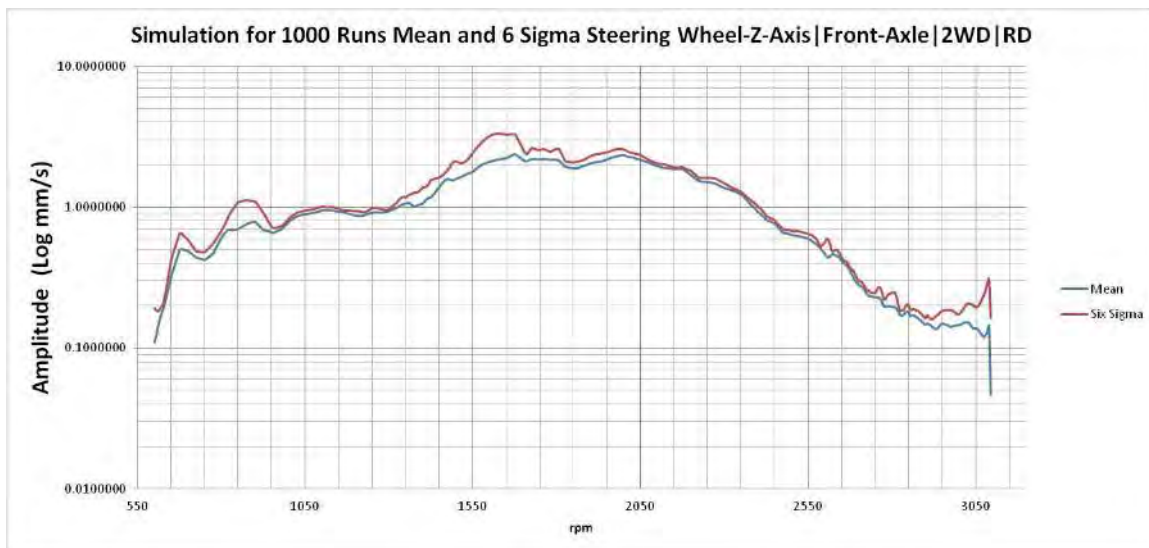


Figure B.10 Simulation run output (mean and 6σ) for Steering Wheel z-axis 2WD-RD

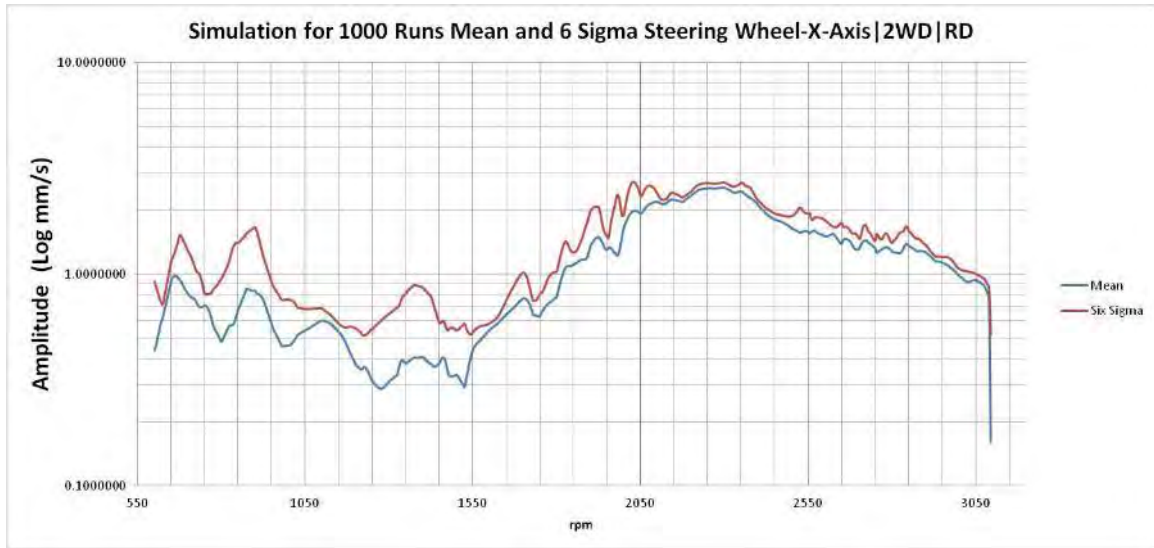


Figure B.11 Simulation run output (mean and 6σ) for Steering Wheel x-axis 2WD-RD

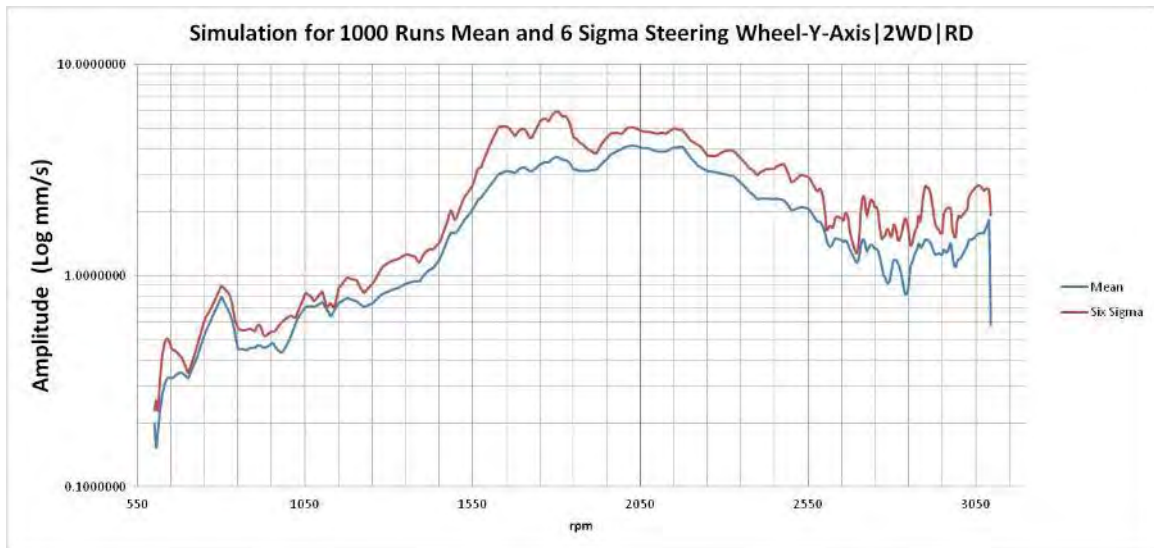


Figure B.12 Simulation run output (mean and 6σ) for Steering Wheel y-axis 2WD-RD

Simulation run output curves for 4WD-RU

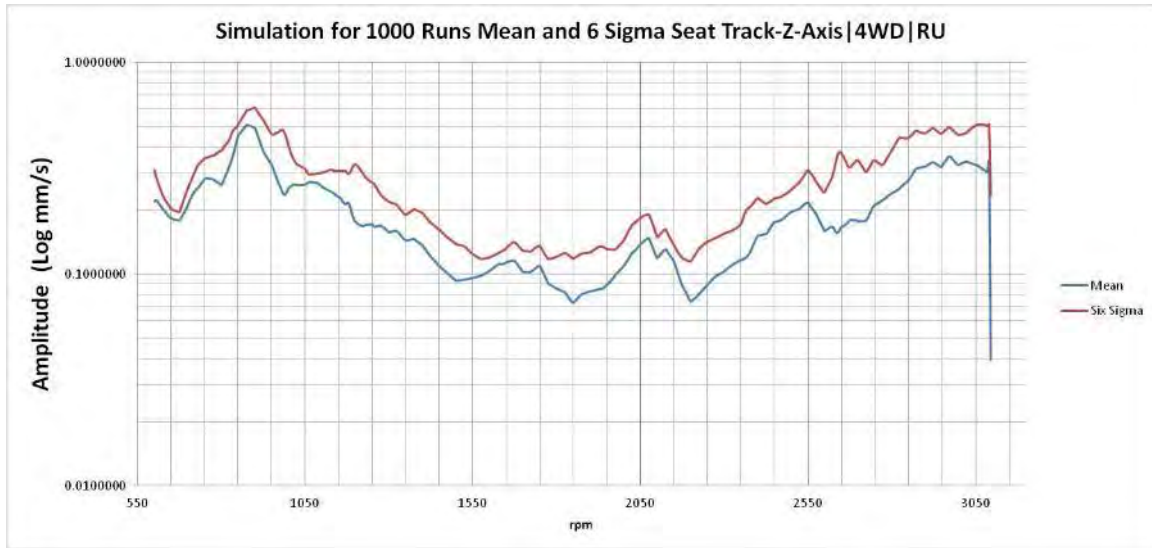


Figure B.13 Simulation run output (mean and 6σ) for Seat Track z-axis 4WD-RU

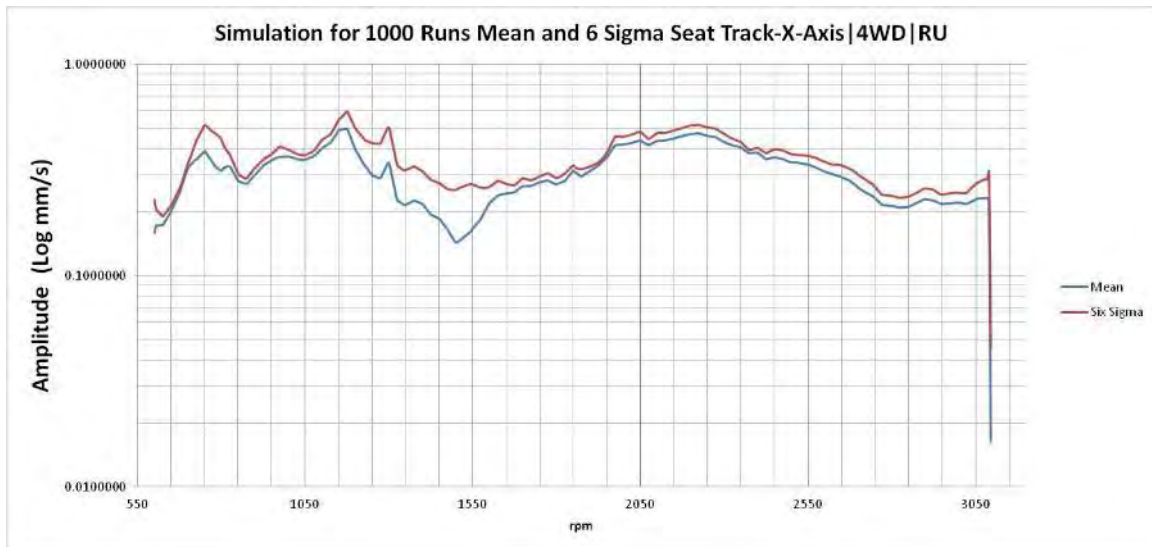


Figure B.14 Simulation run output (mean and 6σ) for Seat Track x-axis 4WD-RU

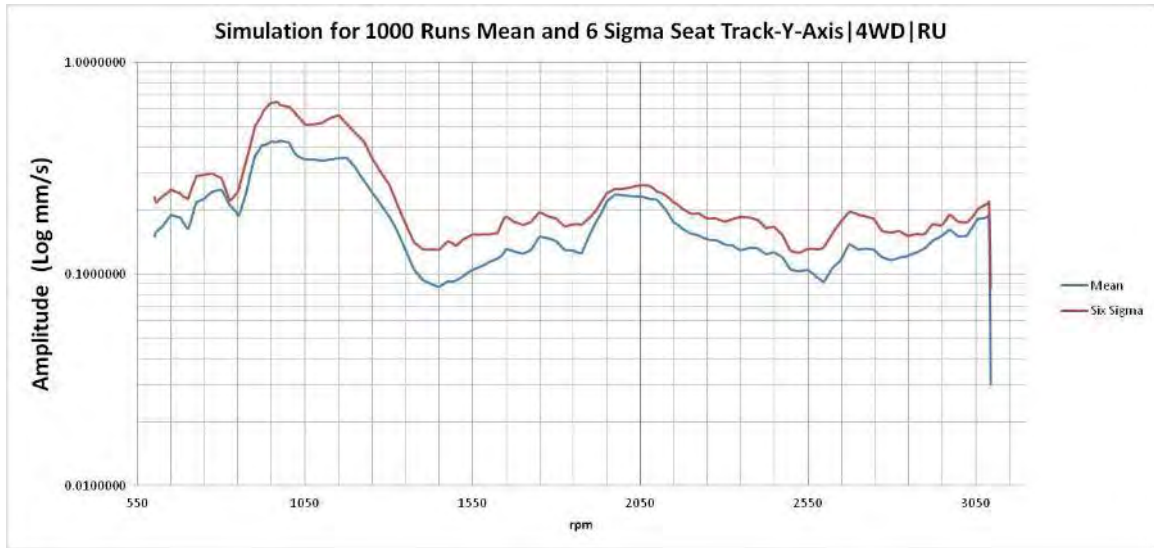


Figure B.15 Simulation run output (mean and 6σ) for Seat Track y-axis 4WD-RU

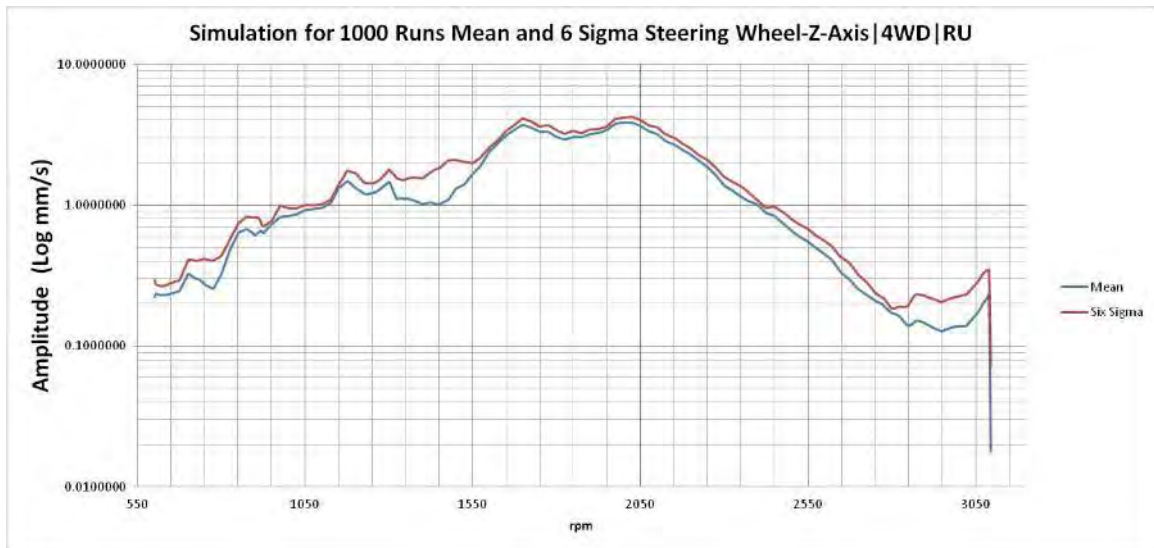


Figure B.16 Simulation run output (mean and 6σ) for Steering Wheel z-axis 4WD-RU

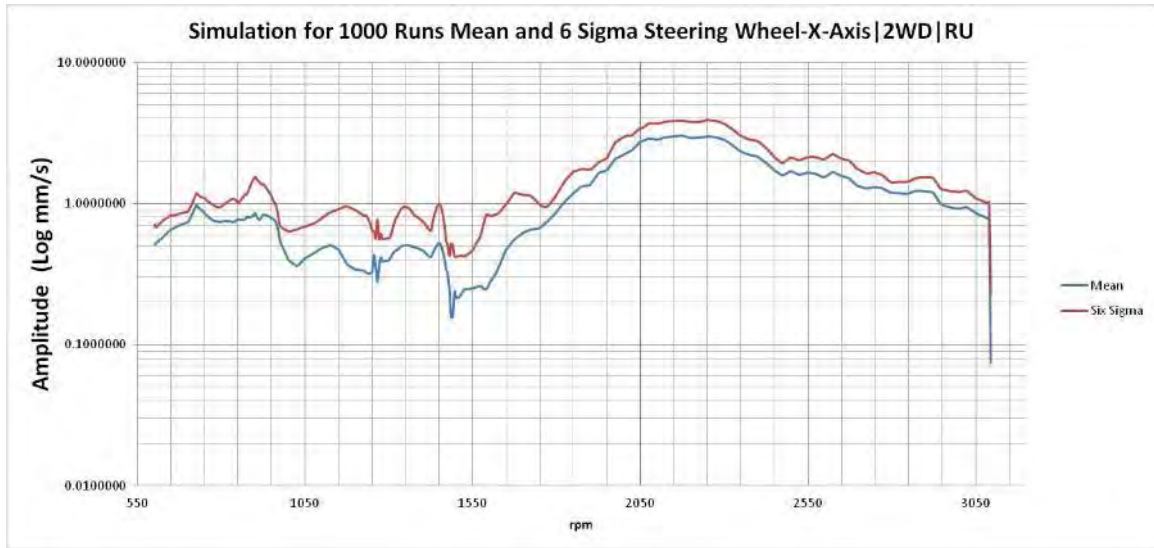


Figure B.17 Simulation run output (mean and 6σ) for Steering Wheel x-axis 4WD-RU

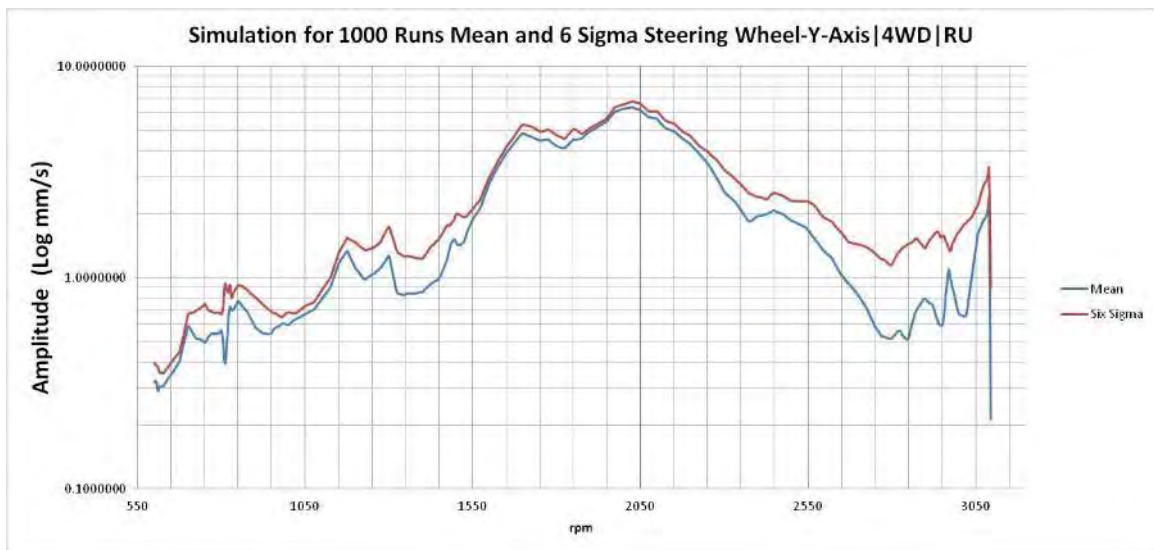


Figure B.18 Simulation run output (mean and 6σ) for Steering Wheel y-axis 4WD-RU

Simulation run output curves for 4WD-RD

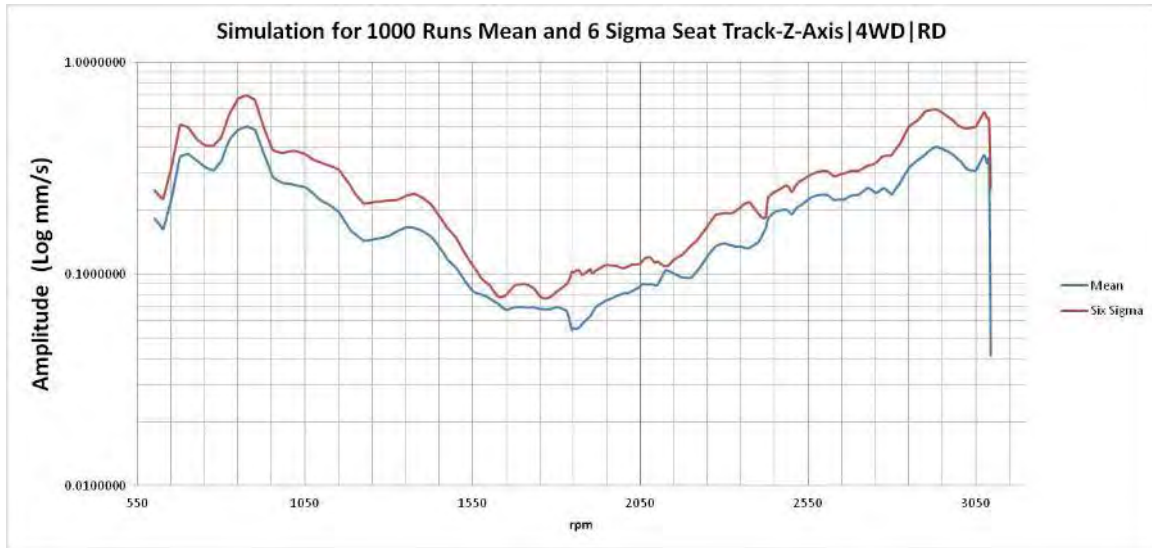


Figure B.19 Simulation run output (mean and 6σ) for Seat Track z-axis 4WD-RD

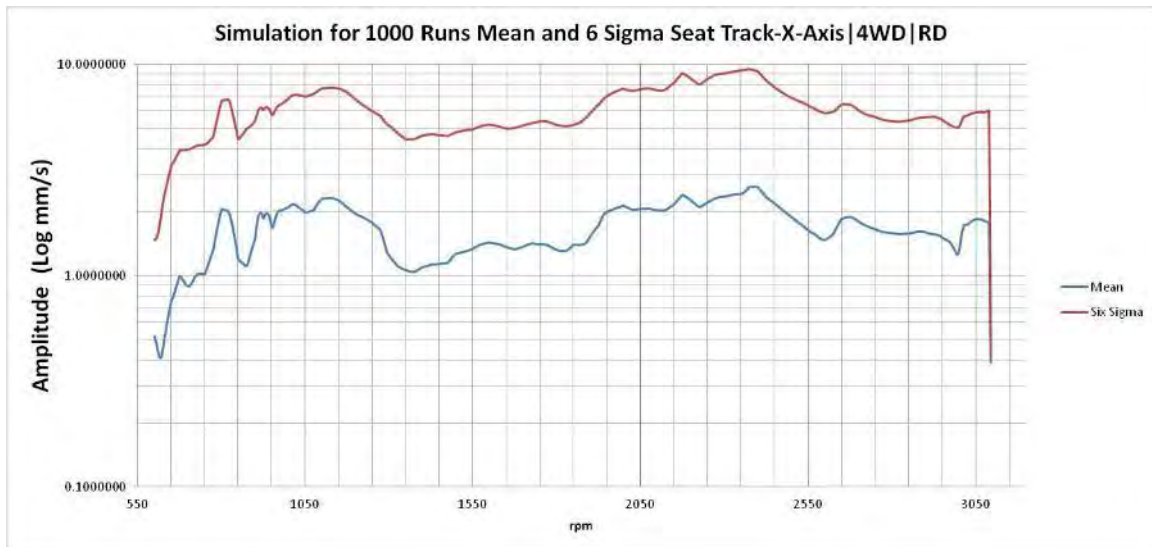


Figure B.20 Simulation run output (mean and 6σ) for Seat Track x-axis 4WD-RD

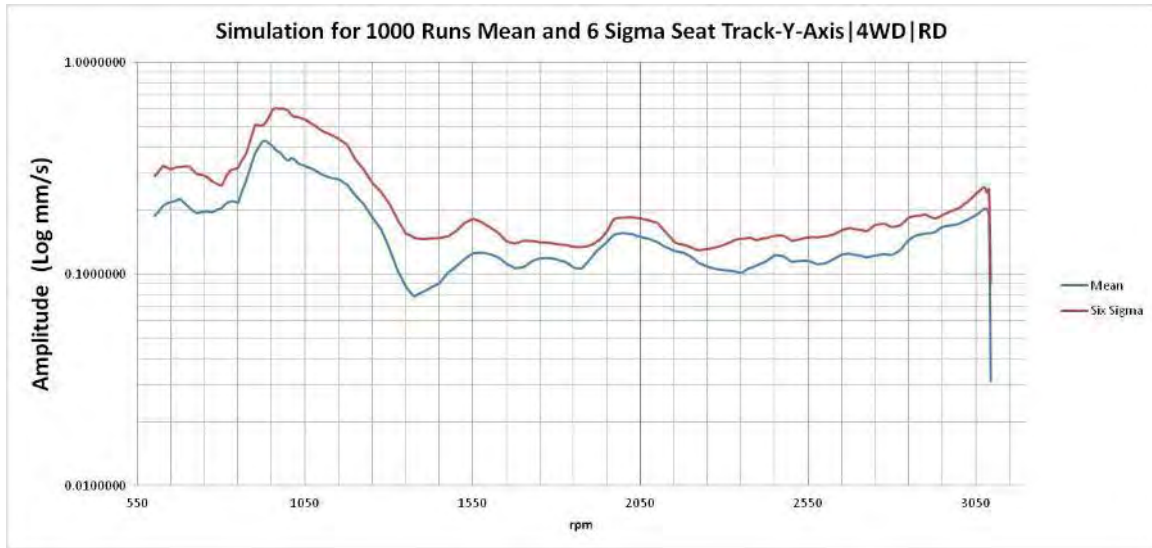


Figure B.21 Simulation run output (mean and 6σ) for Seat Track y-axis 4WD-RD

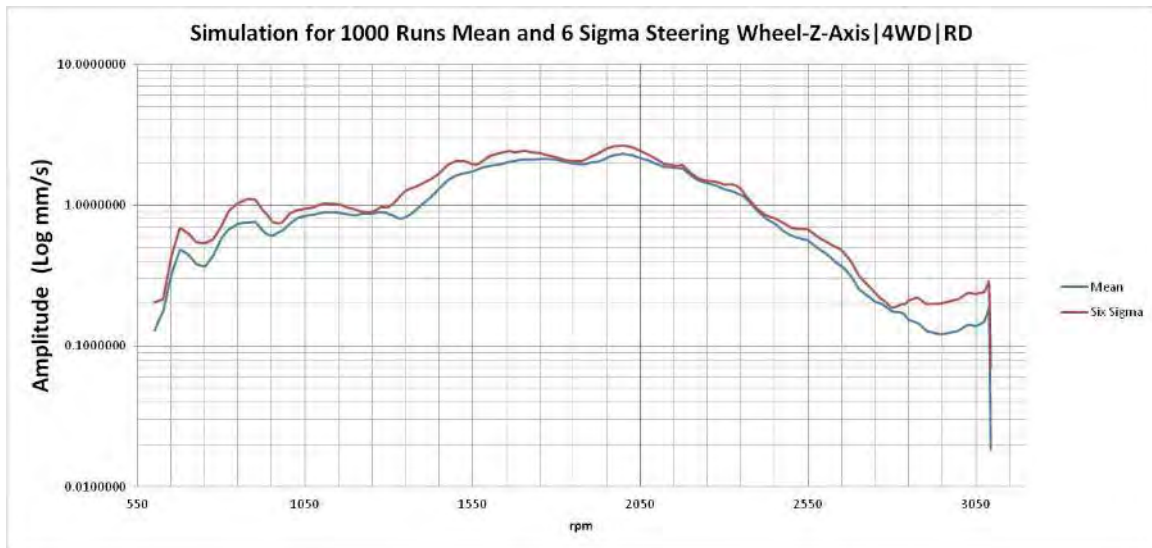


Figure B.22 Simulation run output (mean and 6σ) for Steering Wheel z-axis 4WD-RD

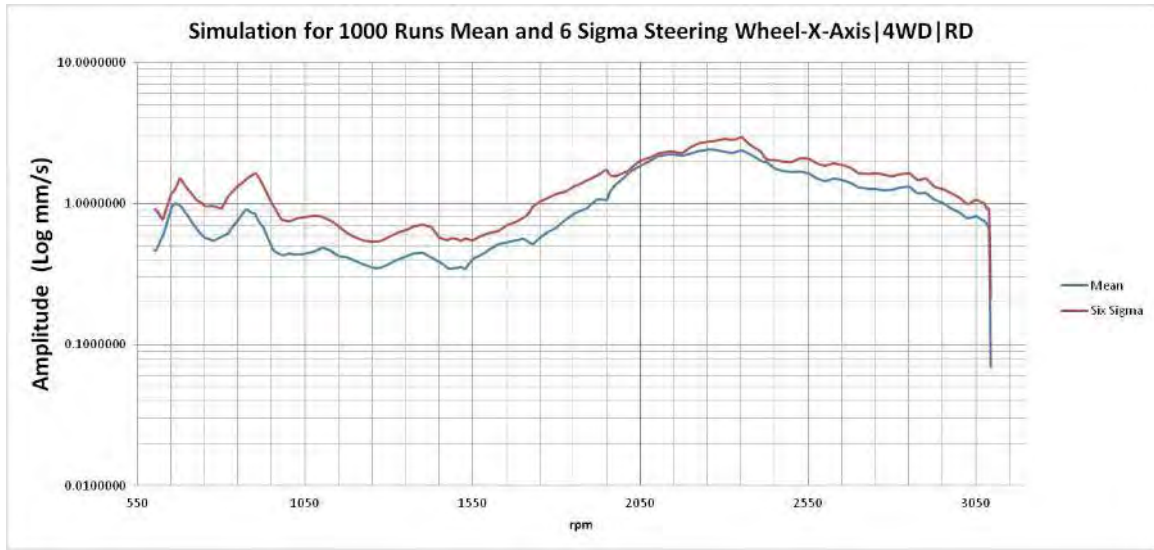


Figure B.23 Simulation run output (mean and 6σ) for Steering Wheel x-axis 4WD-RD

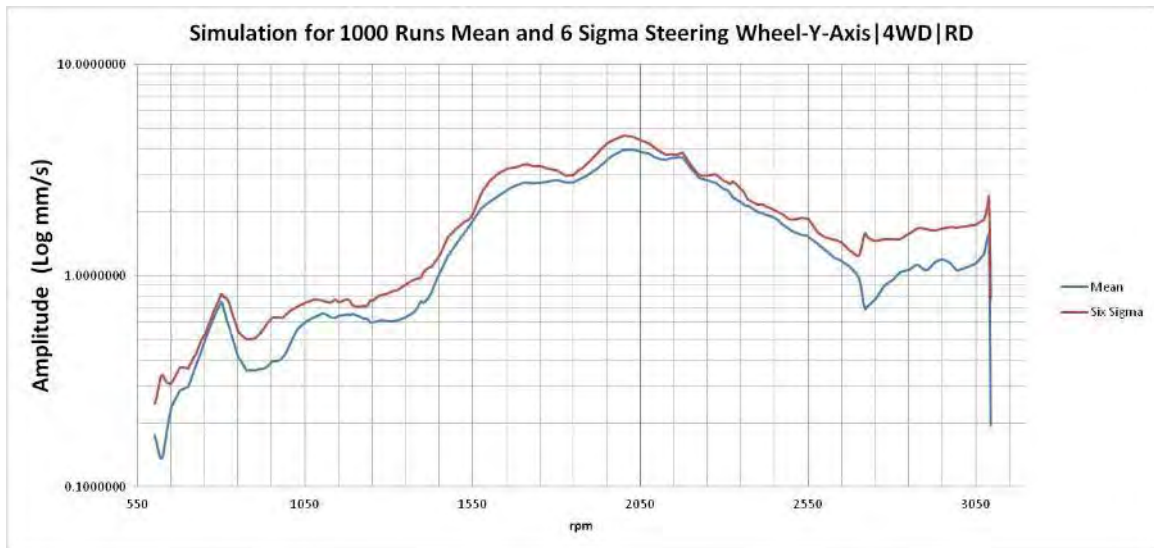


Figure B.24 Simulation run output (mean and 6σ) for Steering Wheel y-axis 4WD-RD

APPENDIX C

MANUAL FOR THE DEVELOPED SIMULATION PROGRAM

Using the developed simulation Java program

The simulation program was developed in Java; a batch program was developed to interface between the program inputs and output.

The software is designed to run 1000 simulation iterations with different imbalance levels at each plane. The different levels of imbalance are drawn from the developed probability distributions, which in their turn have been developed by fitting actual measured imbalance data points. Using the developed sensitivity curves as input with the imbalance level randomly produced; the software will be able to predict the level of vibration at each Customer Touch Point (CTP). By adding the vibration inputs from each plane in complex numbers, the final output for a single iteration will be calculated for the frequency spectrum; in this case the frequency spectrum started at 600 rpm and up to 3100 rpm in steps of 5 rpm.

The software application is straightforward; it utilizes lists and options. The user only needs to read the options and make a choice by numbers, it operates on Windows OS.

The first step is starting the batch program by double clicking on the name is: NVH_Simulatiion_CAVS, see Figure C.1.

Name	Date modified	Type	Size
input	6/12/2013 3:11 PM	File folder	
Simout_G	6/12/2013 3:03 PM	File folder	
Simout_N	6/11/2013 6:34 PM	File folder	
NVH_Simulation_CAVS	6/12/2013 10:30 AM	Windows Batch File	41 KB
program_gamma_noise	6/12/2013 10:31 AM	Executable Jar File	9,069 KB
program_gamma_vib	6/12/2013 10:33 AM	Executable Jar File	9,069 KB
program_normal_noise	6/12/2013 10:33 AM	Executable Jar File	9,069 KB
program_normal_vib	6/12/2013 10:32 AM	Executable Jar File	9,069 KB

Figure C.1 The batch file name.

The batch program will launch the Command Prompt; a black window with a command line will appear. The program will ask you to make a choice from a list of options. The first part of the command line screen will introduce the software; the first choice is regarding the probability distribution the user wishes to use to generate the imbalance random number; Normal or Gamma distribution. A default set of probability distribution parameters, representing imbalance levels for each plane, have been supplied for either probability distribution; another venue is offered to user to enter his/her own probability distribution parameter for each plane. (Figure C.2).

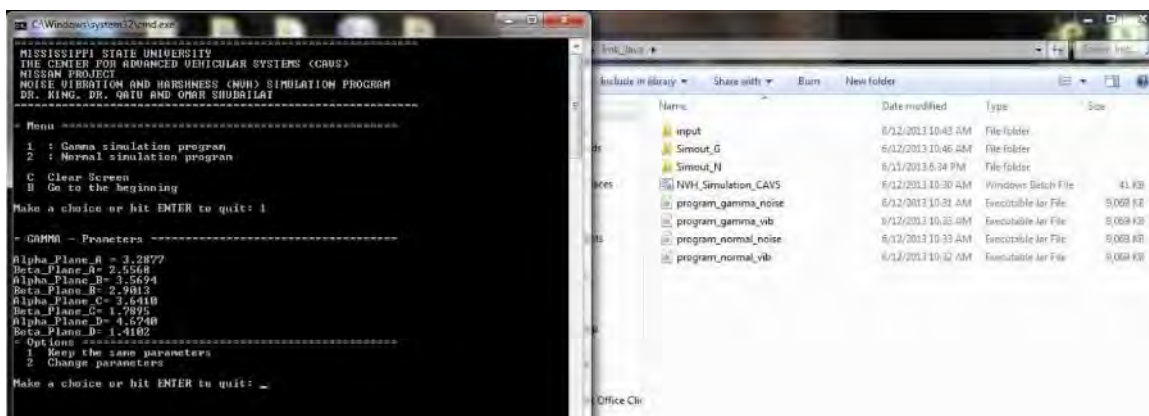
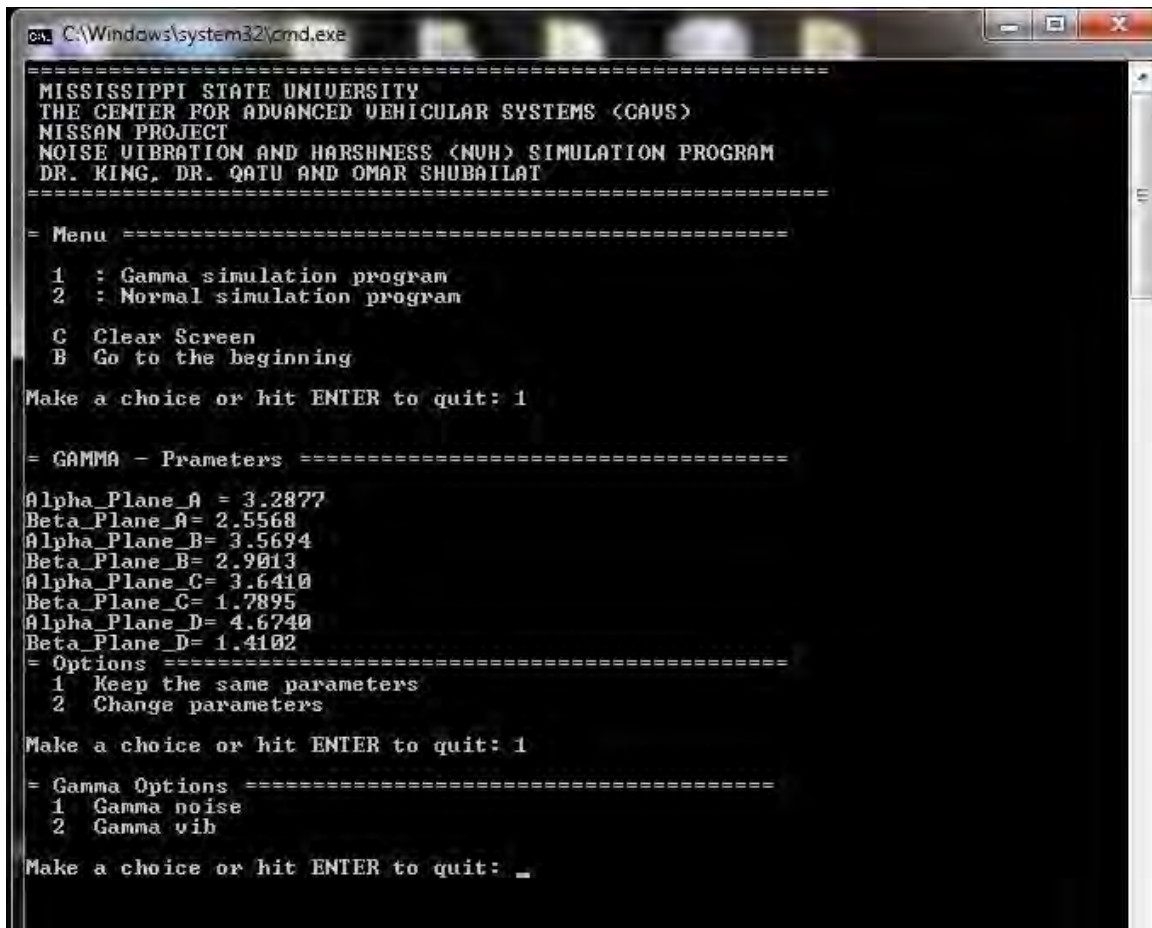


Figure C.2 After launching the batch program with the Command Prompt Screen.

The order of entering the parameters is (see Figure C.3 and Figure C.4):

- Plane A: Front driveshaft-Front axle.
- Plane B: Front driveline-transfer case.
- Plane C: Rear driveline-transfer case.
- Plane D: Rear driveshaft-Rear axle.



```

C:\Windows\system32\cmd.exe
=====
MISSISSIPPI STATE UNIVERSITY
THE CENTER FOR ADVANCED VEHICULAR SYSTEMS (CAVS)
NISSAN PROJECT
NOISE VIBRATION AND HARSHNESS (NVH) SIMULATION PROGRAM
DR. KING, DR. QATU AND OMAR SHUBAILAT
=====

= Menu =====
1 : Gamma simulation program
2 : Normal simulation program

C Clear Screen
B Go to the beginning

Make a choice or hit ENTER to quit: 1

= GAMMA - Parameters =====
Alpha_Plane_A = 3.2877
Beta_Plane_A = 2.5568
Alpha_Plane_B = 3.5694
Beta_Plane_B = 2.9013
Alpha_Plane_C = 3.6410
Beta_Plane_C = 1.7895
Alpha_Plane_D = 4.6740
Beta_Plane_D = 1.4102
= Options =====
1 Keep the same parameters
2 Change parameters

Make a choice or hit ENTER to quit: 1

= Gamma Options =====
1 Gamma noise
2 Gamma vib

Make a choice or hit ENTER to quit: _

```

Figure C.3 Probability distribution default parameters.

```

C Clear Screen
B Go to the beginning
Make a choice or hit ENTER to quit: 1

= GAMMA - Parameters =====
Alpha_Plane_A = 3.2877
Beta_Plane_A= 2.5568
Alpha_Plane_B= 3.5694
Beta_Plane_B= 2.9013
Alpha_Plane_C= 3.6410
Beta_Plane_C= 1.7895
Alpha_Plane_D= 4.6740
Beta_Plane_D= 1.4102
= Options =====
1 Keep the same parameters
2 Change parameters
Make a choice or hit ENTER to quit: 2
Enter Alpha_Plane_A value:2
Enter Beta_Plane_A value:1
Enter Alpha_Plane_B value:2
Enter Beta_Plane_B value:1
Enter Alpha_Plane_C value:2
Enter Beta_Plane_C value:1
Enter Alpha_Plane_D value:2
Enter Beta_Plane_D value:1
= The parameters are: =====
Alpha_Plane_A = 2
Beta_Plane_A= 1
Alpha_Plane_B= 2
Beta_Plane_B= 1
Alpha_Plane_C= 2
Beta_Plane_C= 1
Alpha_Plane_D= 2
Beta_Plane_D= 1
1 Gamma noise
2 Gamma vib
Make a choice or hit ENTER to quit:

```

Figure C.4 User specific probability distribution parameters' entering option.

In the case of Gamma distribution, the parameters are alpha or beta. While in case of Normal distribution they will be mean and standard deviation.

A note in regard to the Normal distribution; as the Normal distribution extends from both sides, the tails, to infinity; there will be a chance to generate negative numbers and very large numbers. The probability of getting a negative number depends on the

fitted normal distribution parameters. If the mean was close to zero while the standard deviation was relatively large; a probability of generating a negative number may become higher. Also there will be always a probability to generate a very large number. In order to compensate for such cases, the program is coded in a manner to set any negative value to zero and to set very large random number to a maximum value of the mean plus eight times standard deviation of the fitted probability distribution. The expected probability of generating such value is almost zero and this will operate as a safe guard. Please see Figure C.5 (prepared by Jeremy Kemp, 2005), in which the area under the curve in relation to the standard deviation and percentage of contribution. The area under the curve extending to six standard deviation length from each side will contribute to 99.9999975 of the curve area.

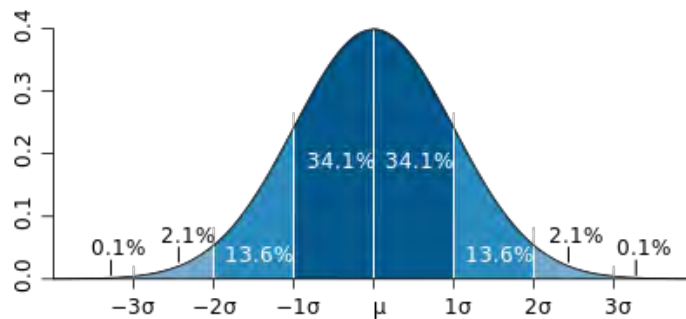


Figure C.5 Normal distribution and the

The menu continues in the same manner after populating the selected probability distribution parameter values or selecting to keep the default parameter values, see Figure C.6.

```

Alpha_Plane_D= 4.6740
Beta_Plane_D= 1.4102
= Options =====
  1 Keep the same parameters
  2 Change parameters
Make a choice or hit ENTER to quit: 2
Enter Alpha_Plane_A value:2
Enter Beta_Plane_A value:1
Enter Alpha_Plane_B value:2
Enter Beta_Plane_B value:1
Enter Alpha_Plane_C value:2
Enter Beta_Plane_C value:1
Enter Alpha_Plane_D value:2
Enter Beta_Plane_D value:1
= The parameters are: =====
Alpha_Plane_A = 2
Beta_Plane_A= 1
Alpha_Plane_B= 2
Beta_Plane_B= 1
Alpha_Plane_C= 2
Beta_Plane_C= 1
Alpha_Plane_D= 2
Beta_Plane_D= 1
  1 Gamma noise
  2 Gamma vib
Make a choice or hit ENTER to quit: 2
= GAMMA - Vib Options =====
  1 4WD
  2 2WD
Make a choice or hit ENTER to quit:

```

Figure C.6 The options after choosing the proper probability distribution

The program allows running simulations for vibrations (vib) or noise. Either choice will be followed by the same options until the last step before running simulation.

Following the vibration option, as in Figure C.6, the simulation program will help you locking on the right sensitivity curve.

By asking the question whether it is a four wheel drive or two wheel drive case. Also next whether it is a runup or run down, see Figure C.7.

```

C:\Windows\system32\cmd.exe
Enter Beta_Plane_C value:1
Enter Alpha_Plane_D value:2
Enter Beta_Plane_D value:1
= The parameters are: =====
Alpha_Plane_A = 2
Beta_Plane_A= 1
Alpha_Plane_B= 2
Beta_Plane_B= 1
Alpha_Plane_C= 2
Beta_Plane_C= 1
Alpha_Plane_D= 2
Beta_Plane_D= 1

1 Gamma noise
2 Gamma vib
Make a choice or hit ENTER to quit: 2
= GAMMA - Uib Options =====
1 4WD
2 2WD
Make a choice or hit ENTER to quit: 2
= GAMMA - Uib - 2WD Options =====
1 Run up
2 Run down
Make a choice or hit ENTER to quit: 1
= GAMMA - Uib - 2WD - Run up Options =====
1 Seat Track X-axis, 2WD, runup: ST-X-2WD-RU.xls
2 Seat Track Y-axis, 2WD, runup: ST-Y-2WD-RU.xls
3 Seat Track Z-axis, 2WD, runup: ST-Z-2WD-RU.xls
4 Steering Wheel X-axis, 2WD, runup: SW-X-2WD-RU.xls
5 Steering Wheel Y-axis, 2WD, runup: SW-Y-2WD-RU.xls
6 Steering Wheel Z-axis, 2WD, runup: SW-Z-2WD-RU.xls
Make a choice or hit ENTER to quit: 2
502
2

```

Figure C.7 The program is locking on the right sensitivity curve through a series of questions.

The last part the program will ask the user about the CTP that the simulation needs to be run for. The options as stated in Figure C.7. The program will start running showing the numbers (502) in a line and (2) in another line (these numbers mean nothing to the user and the user). It will take a short time before the output files are produced in the right folder, see Figure C.8.

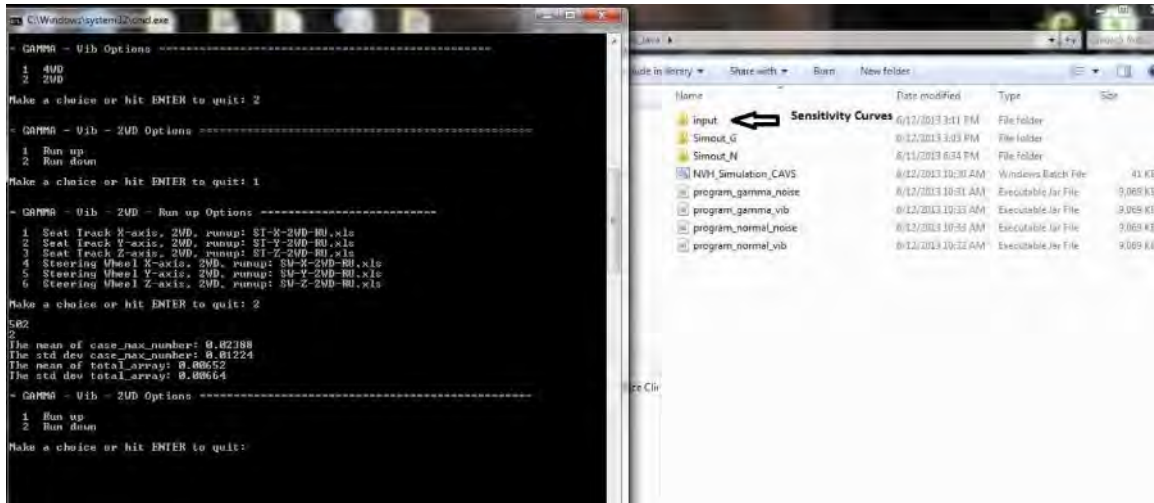


Figure C.8 Three folder available for the user

The three folders are: first for input files (sensitivity curves), second output files for the Gamma simulation run, and the third for output files of the Normal simulation run.

There are three output files stored in the output folder depending on the case; (i.e., Normal distribution simulation or Gamma simulation run), in the our example case here the output files are stored in the folder named (Simulation_G), where G stands for Gamma probability distribution choice.

The first file is the phase angles with a name starts by (atan) the rest of the name of each file will give information on the simulation run case. For example the trial run gave three output files one of them had the name of: atan2wdrusty. The first part (atan) denotes that this is the phase angles result file. The other part (2wdrusty) each set of symbols means something, see Figure C.9:

- Two wheel drive case: 2wd (the other option is four wheel drive: 4wd).
- Run up: ru (the other option is Run down: rd).
- Seat track: st (the other option is steering wheel: sw).
- The Y-axis: y (the other options are: x-axis or z-axis).

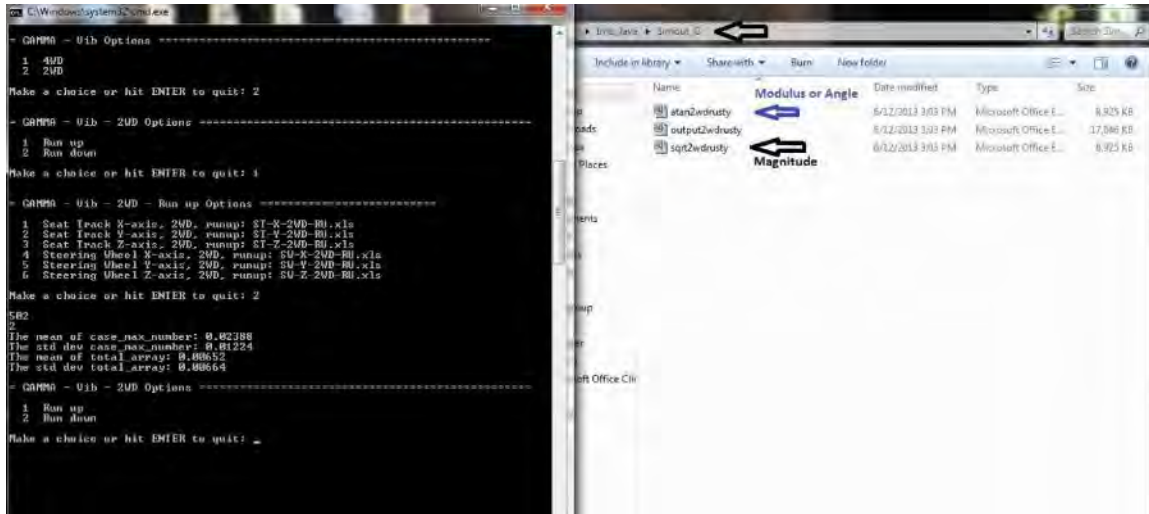


Figure C.9 Three output files with coded name to help identify the simulation run

The Excel will be filled with numbers, see Figure C.10.

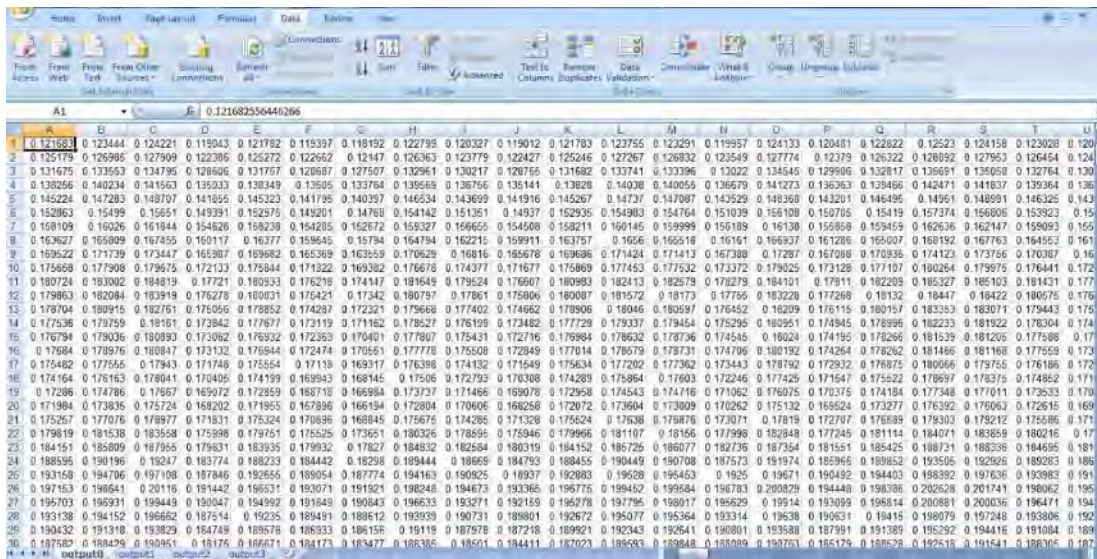


Figure C.10 Output file

The Excel file will contain multiple sheets (tabs), with each column representing simulation iteration with a random imbalance at each plane. Excel program has limitation to 256 columns; this is why we have multiple sheets to compensate for this limitation per sheet.

The sheets will have 500 rows representing the chosen frequency spectrum; (i.e., from 600 up to 3100 rpm). Creating another sheet to find the mean and standard deviation at each frequency has been done and a graph has been produced like the ones you find in APPENDIX B.